UNIVERSITY OF CALIFORNIA, SAN DIEGO

Investigating the Biosynthesis of Halogenated Meroterpenoid Natural Products from Marine Actinomycetes

A dissertation submitted in partial satisfaction of the requirements for the degree Doctor of Philosophy

in

Oceanography

by

Jaclyn Marie Winter

Committee in charge:

Professor Bradley Moore, Chair
Professor Lihini Aluwihare
Professor William Fenical
Professor Tadeusz Molinski
Professor Joseph Noel

2010

ProQuest LLC
789 East Eisenhower Parkway
P.O. Box 1346
Ann Arbor, MI 48106-1346

The Dissertation of Jaclyn Marie Winter is approved, and it is acceptable in quality and form for publication on microfilm and electronically:

Chair

University of California, San Diego

2010

For Grandma Bert, Grandpa Eugene, Mom, Dad, Chris,

AND MY FURRY “CHILDREN” Pita and Pelle

EPIGRAPH

If it wasn't for the last minute, nothing would every get done.

Anonymous

You must do the things you think you cannot do.

Eleanor Roosevelt

God, give us grace to accept with serenity the things that cannot be changed, Courage to change the things which should be changed, and the Wisdom to distinguish the one from the other.

Reinhold Niebuhr

It always seems impossible until it's done.

Nelson Mandela

Choose a job you love, and you will never have to work a day in your life.

Confucius

Success consists of getting up just one more time than you fall.

Oliver Goldsmith

A man's got to do what a man's got to do. A woman must do what he can't.

Rhonda Hansome

TABLE OF CONTENTS

LIST OF ABBREVIATIONS

bp	base pair
BLAST	basic local alignment search tool
BSA	bovine serum albumin
cDNA	complementary strand DNA
CoA	Coenzyme A
CDP	cytidine diphosphate
Da	Daltons
DH	dehydratase
DMAPP	dimethylallyl diphosphate
DNA	deoxyribonucleic acid
ER	enoylreductase
fnq	furaquinocin biosynthetic cluster
fur	furanonaphthoquinone biosynthetic cluster
gDNA	genomic DNA
GST	glutathione sulfur transferase
HMG-CoA	beta-hydroxy-beta-methylglutaryl-Coenzyme A
HR	beta-hydroxy-beta-methylglutaryl-Coenzyme A reductase
HS	beta-hydroxy-beta-methylglutaryl-Coenzyme A synthase
II	type II isopentenyl diphosphate isomerase
IPP	isopentenyl diphosphate
kb	kilobase (10^3 base)
KR	ketoreductase
KS	ketosynthase

LB	Luria-Bertani
MEP	2C-methyl-D-erythritol-4-phosphate
MD	mevalonate diphosphate
MK	mevalonate kinase
mRNA	messenger RNA
nap	napyradiomycin biosynthetic cluster
ORF	open reading frame
PCR	polymerase chain reaction
PK	phosphomevalonate kinase
PKS	polyketide synthase
rRNA	ribosomal RNA
RNA	ribonucleic acid
RT-PCR	reverse transcription PCR
ter	terpentecin biosynthetic cluster
THN	1,3,6,8-tetrahydroxynaphthalene
THNS	1,3,6,8-tetrahydroxynaphthalene synthase
U	unit
V-BrPO	vanadium-dependent bromoperoxidase
V-ClPO	vanadium-dependent chloroperoxidase
V-HPO	vanadium-haloperoxidase

LIST OF FIGURES

LIST OF TABLES

LIST OF SCHEMES

ACKNOWLEDGEMENTS

The process of acquiring a PhD has been a long and stressful journey and would not have been possible without the help of some wonderful people along the way. Thank you to everyone who has supported me during my graduate studies and who have been there to hold my hand during the scary parts. In particular, I would like to thank and acknowledge:

Professor Bradley Moore, for guidance, supervision, advice, encouragement, and unconditional support during this adventure. Thank you for trusting my judgment and for supplying me with endless resources to explore my outrageous ideas. You have always being enthusiastic about this project, which encouraged me to keep pushing the bar higher. I can't thank you enough for always having an open door policy and your willingness to listen and offer advice whether science related or other. Finally, thank you for allowing me to join your lab and for providing me with the tools to develop into the scientist I am today.

Professors William Fenical and Paul Jensen, for providing me with organisms to work with. Without you this dissertation would not exist. I would also like to thank Drs. Irma Soria-Mercado, Alejandra Prieto-Davo, Ji Young Cho, Philip Williams, and Hak Cheol Kwon who provided me with samples, skills, many laughs, and knowledge for a complete understanding of this project. Thank you for all your help.

Professor Joseph Noel, for allowing me to work in his lab at the Salk Institute. Without such an opportunity, much of Chapter 3 would not have been possible. Thank you also to the members of the Noel lab for their kindness and

late night laughs and for answering all of my many questions. In particular, I would like to thank Marianne for taking me under her wing and providing me with extensive knowledge, skills and general understanding about structural biology.

Professor Ted Molinski, for all your advice, constant encouragement, and all your great ideas and experiments for exploring and understanding the nitrogen biochemistry in azamerone biosynthesis.

Professor Lihini Aluwihare, for helping with my understanding of nitrogen chemistry which was required for a complete understanding of azamerone's biosynthesis.

The members of the Moore lab both past and present. You have all made working in the lab a pleasure. The endless laughs; the countless "that's what she said" jokes; the afternoon coffees; group meeting cocktails; mid-day cocktails; afternoon cocktails; and group outings skiing, camping and shooting each other with paintballs will be truly missed. Each one of you holds a special place in my heart and I am thankful for your friendship and support during the past 5 years. In particular I would like to thank (in order of appearance) Michelle, Laura, John, Qian, Longkuan, Dan, Yuan, Lisa, Drew, Ale, Markus, Mike, Ryan, Anna, Kale, Tobi, Alex, Amy, Kaity, Aki, Taylor, and Roland. I would also like to thank Michelle Hook who was a summer scholarship student who picked more colonies than anyone should ever have to pick, but had a smile on her face the entire time.

Drs. Ariane Jansma and Anthony Mrse, for their NMR technical support and extreme kindness.

My family, for their love and support. To Mom and Dad, thank you for all the encouragement during this adventure. It must not have been easy to let your only child move across the country, but thank you for supporting my decision and for letting me discover who the real me is. I can't express how grateful and thankful I am for everything you have given me. To Grandma Bert and Grandpa Eugene, for always there for me through thick and thin and providing me with the encouragement and strength to keep going when I wanted to give up. Words can't describe how appreciative I am for everything you have done for me and how much I miss you both.

Chris Kauffman, for his unconditional love and support. You are my rock and my sunshine and I treasure every moment I get to spend with you. Thank you for inspiring me to be a better person.

Chapter 1, in full, is a reprint of the material as it appears in Formation of the Pyridazine Natural Product Azamerone by Biosynthetic Rearrangement of an Aryl Diazoketone (2009). Winter, Jaclyn M; Jansma, Ariane L.; Handel, Tracy M.; Moore, Bradley S., Angewandte Chemie International Edition, 48, 767–70. The dissertation author was the primary investigator and author of this paper.

Chapter 2, in full, is a reprint of the material as it appears in Molecular Basis for Chloronium-mediated Meroterpene Cyclization: Cloning, Sequencing, and Heterologous Expression of the Napyradiomycin Biosynthetic Gene Cluster

(2007). Winter, Jaclyn M; Moffitt, Michelle; Zazopoulos Emmanuel; McAlpine James; Dorrestein, Pieter C.; Moore, Bradley S., Journal of Biological Chemistry, 282, 16362–68. The dissertation author was the primary investigator and author of this paper.

Chapter 3, in full, is a reprint of the material as it appears in Exploring the Chemistry and Biology of Vanadium-Dependent Haloperoxidases. (2009). Winter, Jaclyn M.; Moore, Bradley S., Journal of Biological Chemistry, 284, 18577–81. The dissertation was the primary investigator and author of this material.

VITA

2004	Bachelor of Science, State University of New York College at Fredonia
2004-2005	Research Assistant, University of Arizona
2005-2009	Research Assistant, University of California, San Diego
2010	Doctor of Philosophy, University of California, San Diego

PUBLICATIONS

Cifuentes M., Schilling, B., Ravindra, R., Winter, J., Janik, M. E. (2006). Synthesis and Biological Evaluation of B-ring Modified Colchicines and Isocholchicine Analogs. *Bioorganic Medicinal Chemistry Letters* 16: 2761-2764.

Winter, J. M., Moffitt, M. C., Zazopoulos, E., McAlpine, J., Dorrestein, P. C., Moore, B.S. (2007). Molecular Basis for Chloronium-mediated Meroterpene Cyclization: Cloning, Sequencing, And Heterologous Expression of the Napyradiomycin Biosynthetic Gene Cluster. *J. Biol. Chem.* 282:16362-16368.

Winter, J. M., Jansma, A. L., Handel, T. M., Moore, B. S. (2009). Formation of the Pyridazine Natural Product Azamerone by Biosynthetic Rearrangement of an Aryl Diazoketone. *Angew. Chem. Int. Ed.* 48: 767-770.

Winter, J. M., and Moore, B. S. (2009) Exploring the Chemistry and Biology of Vanadium-Dependent Haloperoxidases. *J. Biol. Chem.* 284:18577-18581.

FIELD OF STUDY

Major Field: Biosynthesis of Marine Derived Natural Products

ABSTRACT OF THE DISSERTATION

Investigating the Biosynthesis of Halogenated Meroterpenoid Natural Products from Marine Actinomycetes

by

Jaclyn Marie Winter

Doctor of Philosophy in Oceanography

University of California, San Diego, 2010

Professor Bradley Moore, Chair

The marine sediment-derived *Streptomyces* spp. CNQ-525 and CNQ-766 were recently characterized by the Fenical laboratory as a new group of marine sediment-derived actinomycetes, tentatively named the MAR4s. These bacteria are prolific producers of hybrid isoprenoids, including the meroterpenoid (polyketide-terpene) antibiotics that are rarely encountered from bacteria. Structural inspection of the meroterpenoid antibiotics belonging to the

napyradiomycin family of chlorinated dihydroquinones suggests that the biosynthetic cyclization of their terpenoid subunits is initiated via a chloronium ion, which exists as hypochlorous acid. The vanadium-dependent haloperoxidases that are known to catalyze such reactions are distributed in fungi and marine algae and have yet to be characterized from bacteria.

The MAR4 strain *Streptomyces* sp. CNQ-525 was used as a source for identifying novel halogenating enzymes. The cloning and sequence analysis of the 43-kb napyradiomycin biosynthetic cluster yielded an unprecedented arrangement of biosynthetic genes including a $FADH_2$-dependent halogenase and three putative vanadium-dependent chloroperoxidases. Heterologous expression of the CNQ-525-based *nap* biosynthetic cluster in a surrogate host produced at least seven napyradiomycins, including the new analog 2-deschloro-2-hydroxy-A80915C. These data revealed the molecular basis behind the biosynthesis of these novel meroterpenoid natural products, and also resulted in the first identification of vanadium-dependent haloperoxidases from a prokaryote. Preliminary biochemical data suggests both NapH1 and NapH3 from the napyradiomycin biosynthetic cluster are vanadium-dependent chloroperoxidases and inactivation of the *nap*H1 gene resulted in the first *in vivo* verification of a vanadium-dependent haloperoxidase.

The phthalazinone meroterpenoid azamerone was isolated by the Fenical-Jensen lab from the marine sediment-derived bacterium *Streptomyces* sp. CNQ-766. Given the structural novelty of azamerone and its relation to the chlorinated meroterpenoids, a variety of feeding experiments with ^{13}C and ^{15}N-labeled

molecules were used to explore the formation of its phthalazinone core. These experiments confirmed that azamerone's phthalazinone core is derived from a naphthoquinone precursor such as in the chlorinated dihydroquinones and progresses through a diazo intermediate.

Introduction

I.1: Natural products

In all living organisms, the metabolism and modification of molecules that are vital for life, e.g., carbohydrates, nucleic acids, proteins and fatty acids, are universally conserved.[1] Secondary metabolites (natural products), on the other hand, are molecules with limited organismal distribution that provide many distinguishing features (pigmentation, odor, toxicity) to life.[1] In most cases, secondary metabolites are only produced under certain environmental conditions, during different stages of growth, or when challenged with another species. These molecules have evolved over time to interact with diverse biological targets, and from a human health perspective, natural products have dramatically improved our quality of life. Some important compounds that are used clinically include the antibiotics penicillin G[2] and vancomycin,[3] the anticancer agent paclitaxel,[4] the analgesic morphine,[5] the antimalarial agent artemisinin,[6] and the hypolipidemic agent lovastatin[7] (Figure I.1).

More than 60% of known antibiotics and bioactive microbial compounds are produced by Gram-positive soil bacteria of the order Actinomycetales.[8, 9] *Streptomyces* is the largest genus of the order Actinomycetales with over 500 species being reported,[10] and is responsible for over two-thirds of clinically used antibiotics.[11] It has been calculated that roughly 3% of all antibacterial agents synthesized by streptomycetes have been reported to date,[11] which opens the door to the biosynthetic potential of these bacteria and the large number of possible drugs yet to be discovered.

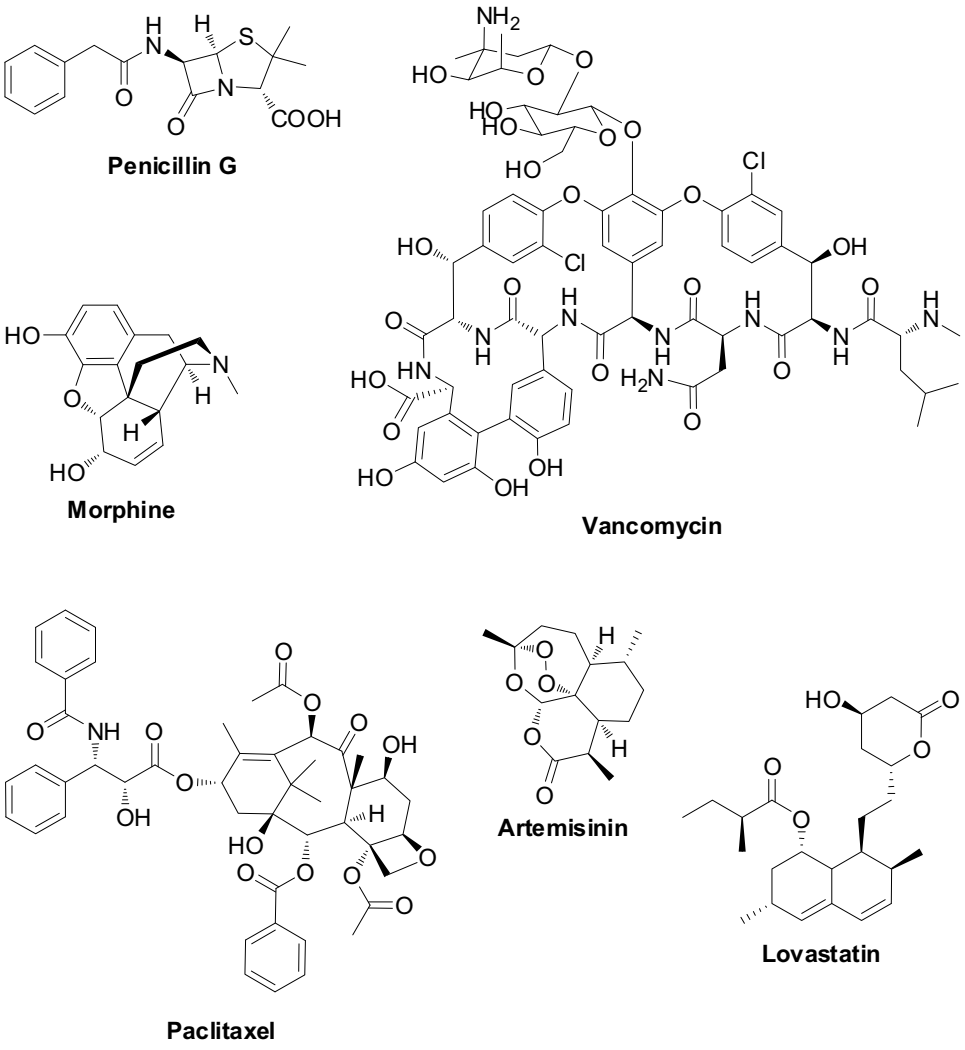

Figure I.1: Medicinal natural products isolated from plants, bacteria and fungi.

I.2: Hybrid isoprenoid natural products

Isoprenoids, which include antibiotics, steroids, plant hormones, plant oils, insecticides, carotenoids, and flavors, form one of the largest and structurally diverse family of natural products with over 24,000 isolated metabolites.[1, 8, 12] Hybrid natural products containing terpene units comprise a diverse group of molecules that serve as important drugs; e.g., the fungal immunosuppressant mycophenolic acid,[13] the plant antimalarial agent quinine,[14] and the plant anticancer agent vincristine[15] (Figure I.2).

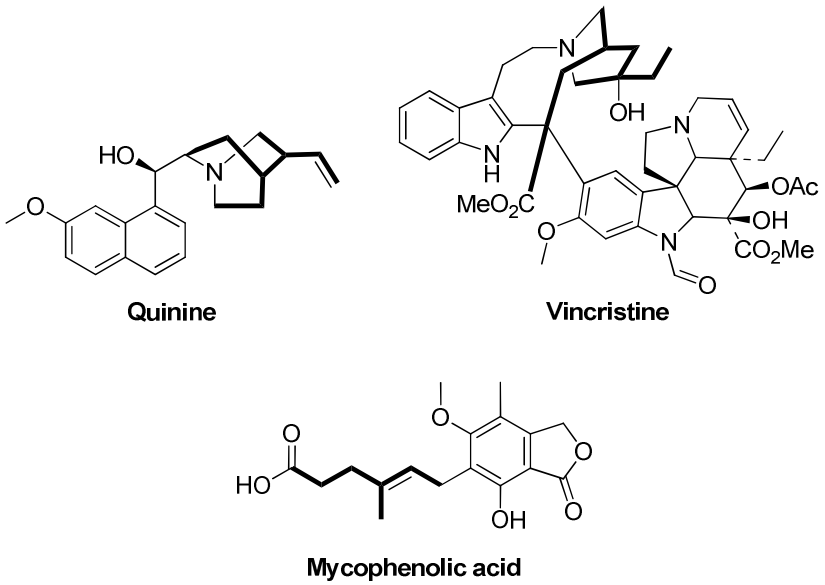

Figure I.2: Hybrid isoprenoids isolated from plants and fungi. Isoprenoid units are highlighted in bold.

The vast majority of hybrid isoprenoids are derived from eukaryotes, particularly plants and fungi,[16] and to date, only a few hybrid isoprenoids have been isolated from actinomycetes.[17] Due to technical difficulties in purifying

isoprenoid enzymes from plants and fungi and the inability to clone all of the biosynthetic genes, only a limited number of isoprenoid biosynthetic enzymes have been charazterized.[8] In plants and fungi, biosynthetic genes required for the assembly of a natural product are typically scattered throughout the genome making it difficult to identify and isolate all of the corresponding biosynthetic genes. On the other hand, it is generally observed in actinomycetes that the corresponding biosynthetic genes are clustered together, making the organism desirable for characterizing biosynthetic enzymes.[18, 19] However, while actinomycetes tend to be metabolically rich bacteria producing many important classes of natural products, e.g., polyketides, nonribosomal peptides, aminoglycosides, etc.,[18, 19] the isoprenoids are scarce.[20] The antibiotic novobiocin was the first streptomycete natural product characterized with an isoprene side chain,[21] and since its discovery, hybrid isoprenoids have been identified from streptomycetes including prenylated phenazines (lavanducyanin[22] and aestivophoenin B[23]), naphthoquinones (the meroterpenoids naphterpin,[24] furaquinocin,[25] and the napyradiomycins[26]), and shikimate-derived quinones (Figure I.3).

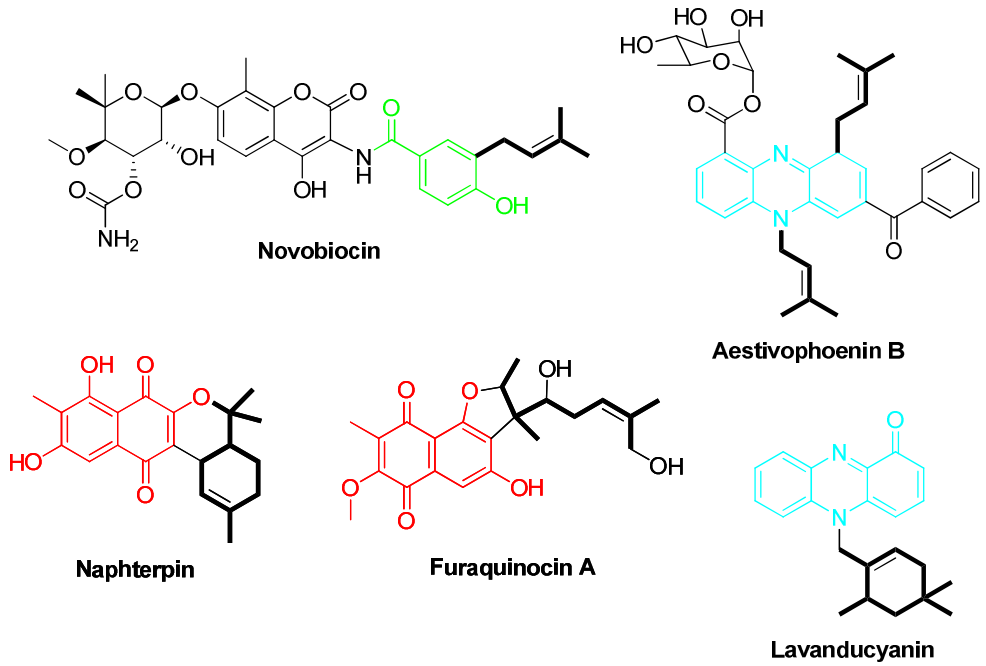

Figure I.3: Hybrid isoprenoids isolated from actinomycetes. Isoprenoid units are highlighted in bold and are attached to phenols (highlighted in green), phenazine (highlighted in blue), and naphthoquinone (highlighted in red).

I.3: Meroterpenoids

The term meroterpenoid was first described in 1968 as "compounds containing terpenoid elements along with structures of different biosynthetic origin."[27] However, meroterpenoids were re-defined in 1987 as "compounds of mixed polyketide-terpenoid origin." [28] These hybrid polyketide-terpenoids are commonly isolated from fungi and higher plants and only a small group of prenylated naphthoquinones have been identified from actinomycetes.[16, 17]

I.3.1: Meroterpenoids from terrestrial actinomycetes

In 1986, the napyradiomycins, which are halogenated meroterpenoids, were first reported from the terrestrial actinomycete *Chainia rubra* MG802-AF1 (Figure I.4).[26, 29-31] They were shown to possess antibacterial activity toward Gram-positive bacteria including multiple drug-resistant strains such as *Staphylococcus aureus* MS8710 and MS9610, but are not active against most Gram-negative bacteria and fungi.[29] Biological evaluations have also shown that napyradiomycin A and B1 are non-steroidal estrogen-receptor antagonists.[32] To date, napyradiomycins and related analogs have been isolated from a handful of terrestrial streptomycetes including *S. antimycoticus* NT17[33] (Figure I.5), *S.* sp. 9558[32] (Figure I.5), and *S. aculeolatus* NRRL 18422[34-36] (Figure I.6). Additional prenylated naphthoquinones have been isolated from streptomycetes and include the anti-oxidant agent naphterpin,[37] furaquinocin A and D,[25] furanonaphthoquinone I,[38] naphthomevalin,[39] and the tyrosine phosphatase inhibitors phosphatoquinones A and B[40](Figure I.7).

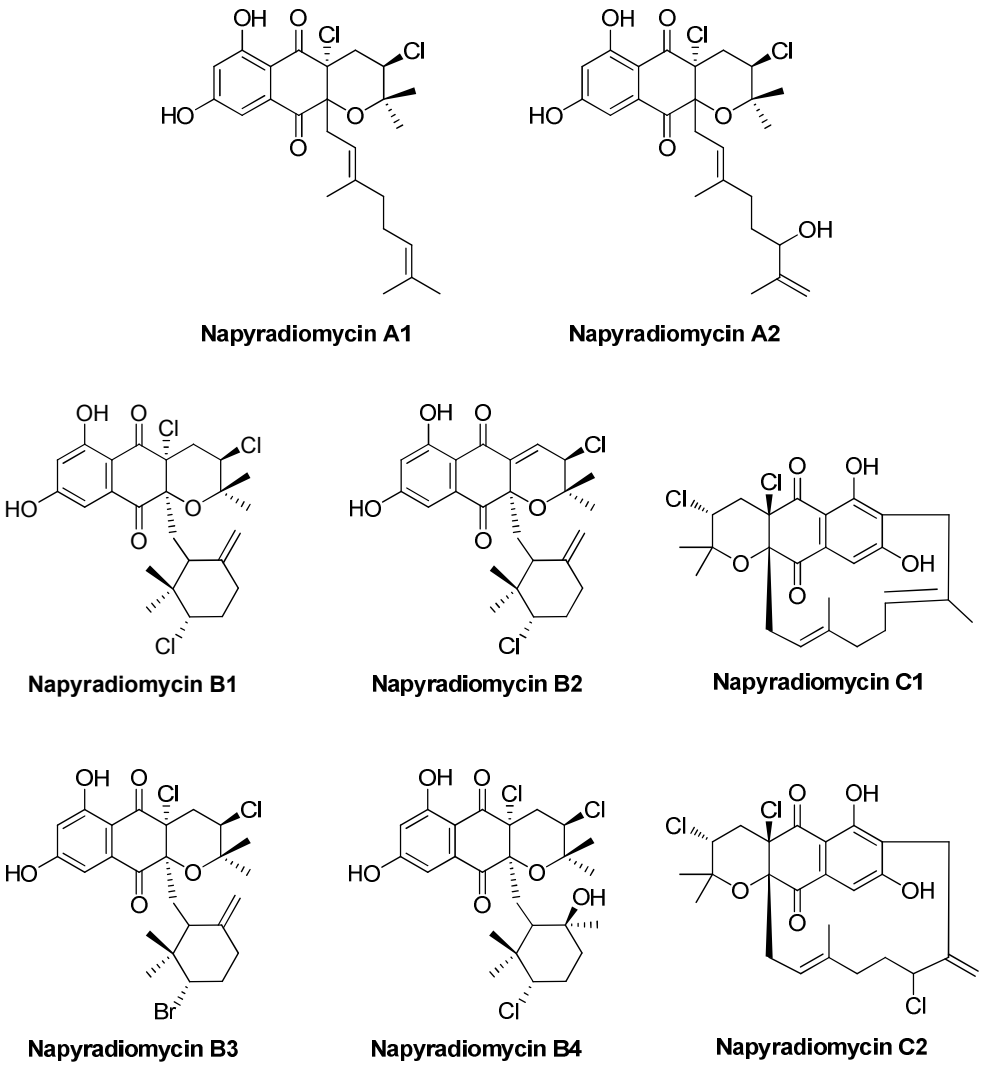

Figure I.4: Halogenated meroterpenoids. Napyradiomycins A1, A2, B1, B2, B3, B4, C1, and C2, isolated from *Chainia rubra* MG802-AF1.

A.

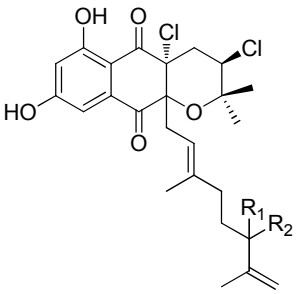

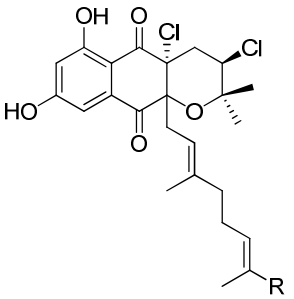

	R_1	R_2
16-oxonapyradiomycin A2	=O	-
Napyradiomycin A2a	OH	H
Napyradiomycin A2b	H	OH

	R
18-hydroxynapyradiomycin A_1	CH_2OH
18-oxonapyradiomycin A1	CHO

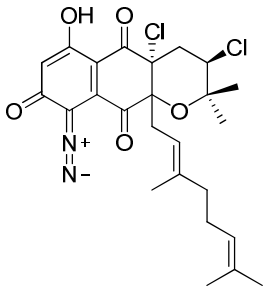

7-desmethyl SF2415A3

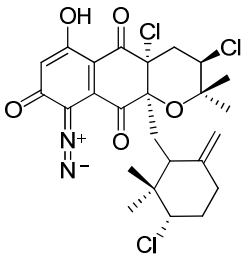

7-desmethyl A80915B

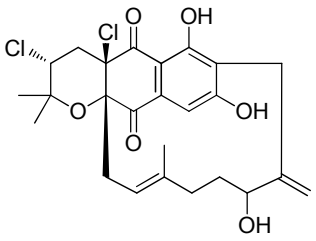

16-deschloro-16-hydroxy-napyradiomycin C2

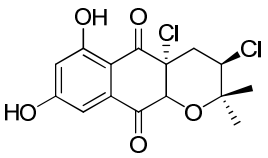

(*R*)-3-chloro-6-hydroxy-8-methoxy-α-lapachone

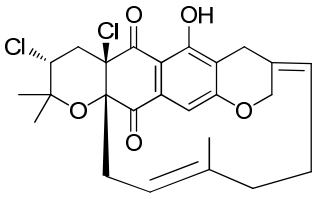

Napyradiomycin SR

B.

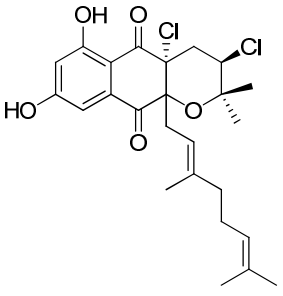

Napyradiomycin A1

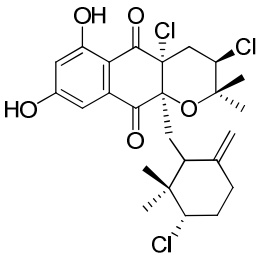

Napyradiomycin B1

Figure I.5: Halogenated meroterpenoids from actinomycetes. A) Napyradiomycins analogs isolated from *S. antimycoticus* NT17. B) Napyradiomycins isolated from *S.* sp. 9558.

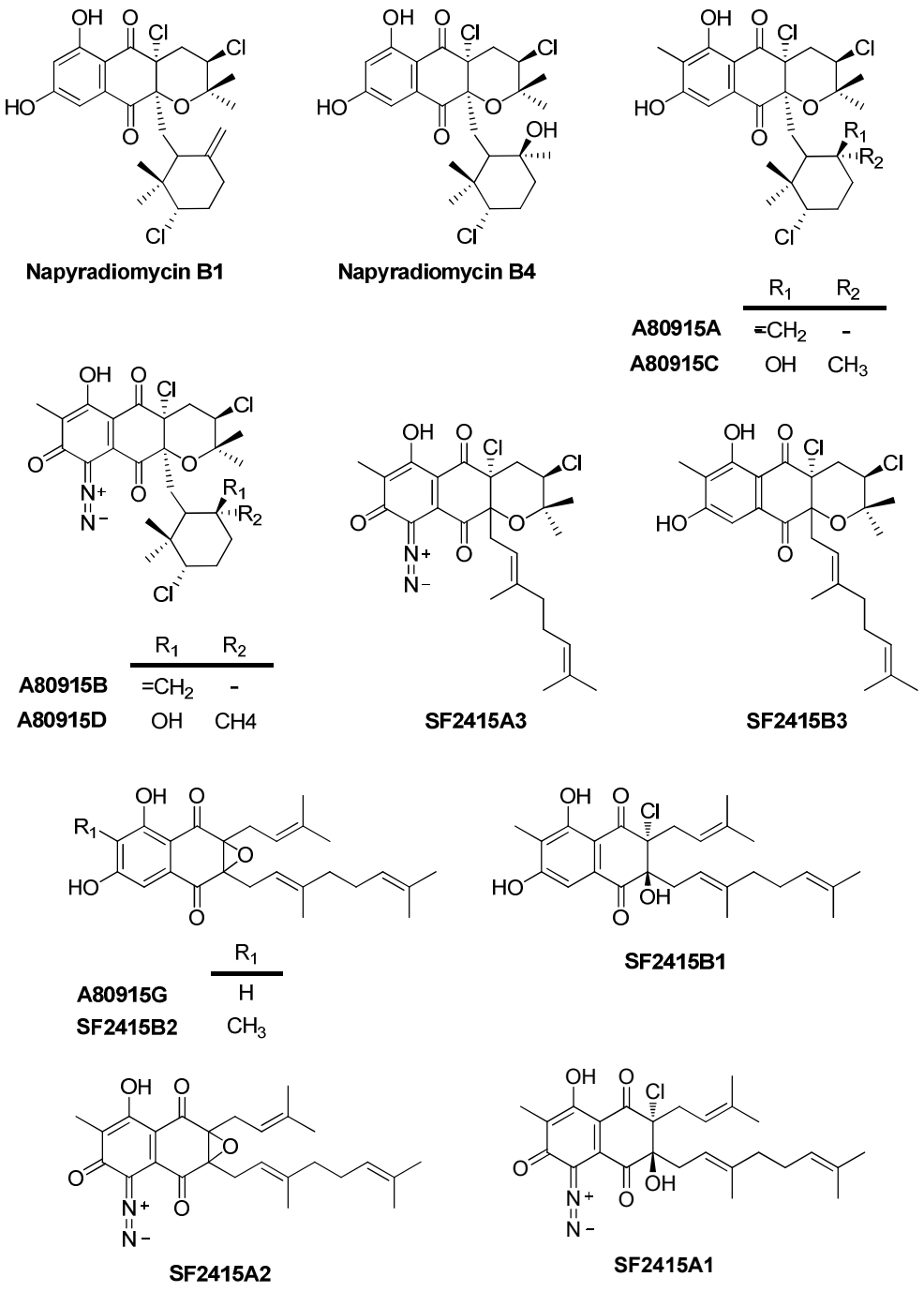

Figure I.6: Napyradiomycins and analogs. Isolated from *S. aculeolatus* NRRL 18422.

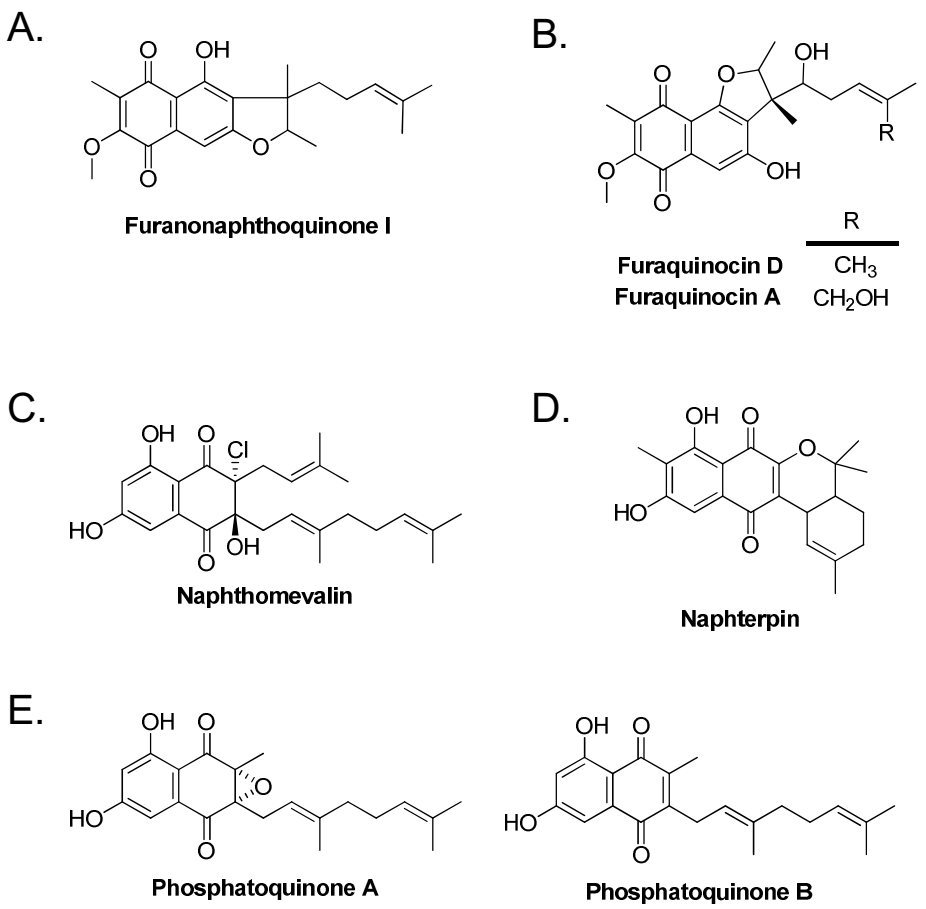

Figure I.7: Prenylated dihydroquinones from actinomycetes. A) Furanonaphthoquinone I isolated from *S. cinnamonensis* DSM 1042. B) Furaquinocin A and D isolated from *S.* sp. KO-3988. C) Naphthomevalin isolated from *S.* sp. Gö 28. D) Naphterpin isolated from *S.* sp. CL190. E) Phosphatoquinone A and B isolated from *S.* sp. TA-0363.

I.3.2: Biosynthesis of meroterpenoids

I.3.2.1: Polyketide biosynthesis

Polyketides are one of the largest classes of natural products and are produced by bacteria, fungi, and plants in a manner reminiscent to fatty acid

biosynthesis. These metabolites are biosynthesized by polyketide synthases (PKS) through successive decarboxylative Claisen condensation reactions of acyl thioesters, which are generally derived from malonyl-coenzyme A (CoA) (Figure I.8)[16, 41] Unlike fatty acid biosynthesis, which reduces each β-keto position to saturation,[42] polyketide intermediates generally retain some or all of their polar β-keto groups by varying the ketoreduction (KR), dehydration (DH), and enoylreduction (ER) reactions, leading to greater product diversity.[43-45] In addition to these reactions, polyketide synthases also dictate the selection of starter and extender units, carbon chain length, and cyclizations, which further adds to the chemical diversity. Post modification events after the assembly of the polyketide backbone such as glycosylation, acylation, methylation, oxidation, halogenation and prenylation increases the polyketides structural diversity, which may lead to important biological features of the metabolite.[46]

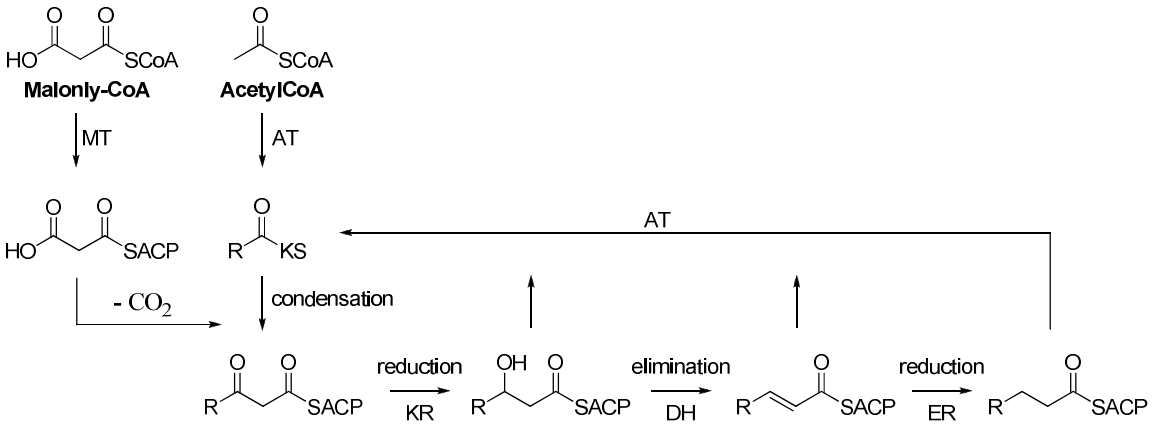

Figure I.8: Assembly of polyketides by polyketide synthases. CoA = coenzyme A, ACP= acyl carrier protein, AT= acyl transferase, , MT = malonyl transferase, KR = ketoreduction, DH = dehydration, and ER = enoylreduction.

On the basis of molecular genetics, structural biology and biochemistry, polyketide synthases isolated from bacteria are divided into three classes.[41, 45, 47] The type I polyketide synthases are large modular enzymes consisting of one or more multifunctional proteins and contain a different active site for each enzyme-catalyzed polyketide chain elongation and modification.[45] Type I polyketide synthases typically produce macrolides such as 6-deoxyerythronolide B, the non-glycosylated parent macrolide core of the antibiotic erythromycin[48] (Figure I.9). The type II polyketide synthases are an enzyme complex containing a single set of iteratively used individual proteins, which is minimally comprised of two ketosynthases and an acyl carrier protein. Type II polyketide synthase typically produce aromatic molecules, e.g. tetracycline (Figure I.9).[49] Finally, the type III polyketide synthases are homodimers and use free CoA thioesters as substrates without the involvement of acyl carrier proteins.[50, 51] These enzymes synthesize small aromatic molecules such as 1,3,6,8-tetrahydroxynaphthalene (THN), which is similar to those found in plants and fungi (Figure I.9).[52]

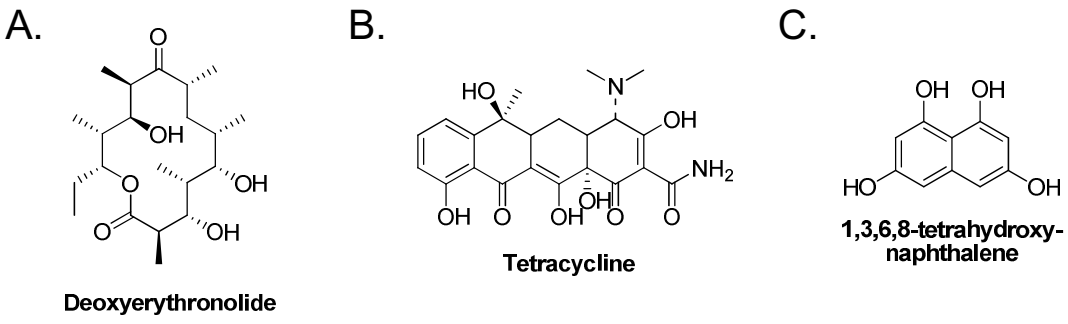

Figure I.9: Polyketide synthase products from microbes. A) Deoxyerythronolide B (Type I polyketide). B) Tetracycline (Type II polyketide). C) THN (Type III polyketide).

In the biosynthesis of the meroterpenoids, the naphthoquinone core is derived from the symmetrical pentaketide intermediate THN, which is the product of the type III polyketide synthase THN synthase (THNS). THNSs are common among *Streptomyces* spp. and synthesize THN by catalyzing Claisen and aldol cyclizations of a linear polyketide assembled from five molecules of malonyl-CoA.[50 51] After THN or its oxidation product flaviolin is assembled, a prenyltransferase involved in meroterpenoid biosynthesis transfers an isoprenoid subunit to the aromatic scaffold.

I.3.2.2: Isoprenoid (terpene) biosynthesis

To date, all living organisms synthesize the 5-carbon isoprenoid building block isopentenyl diphosphate (IPP) and its isomer dimethylallyl diphosphate (DMAPP) by either the mevalonate pathway and/or the 2C-methyl-D-erythritol-4-phosphate (MEP) pathway; also known as the nonmevalonate pathway.[53] The classic mevalonate pathway operates in eukaryotes, archaebacteria, and the cytosol of higher plants, while the MEP pathway operates in green algae, the chloroplasts of higher plants, and many eubacteria including actinomycetes.[53] The mevalonate pathway is a well studied and established pathway and was first identified in 1967 in association with cholesterol biosynthesis.[54, 55] The MEP pathway, on the other hand, was recently identified[56] and changed the whole concept of terpenoid biosynthesis.[57]

There are six genes in the mevalonate pathway that code for all the enzymes responsible for the formation of mevalonic acid and its transformation into IPP and DMAPP (Figure I.10).[1, 12] Through a Claisen condensation, two molecules of acetyl-CoA are combined to give acetoacetyl-CoA.[58] This molecule is condensed with a third molecule of acetyl-CoA through an aldol addition giving rise to β-hydroxy-β-methylglutaryl-CoA (HMG-CoA).[59] HMG-CoA is reduced to mevalonate, which is then phosphorylated to phosphomevalonate.[60] A second phosphorylation reaction generates diphosphomevalonate and a decarboxylation of this intermediate yields IPP.[60] Finally, isomerization of IPP gives rise to DMAPP.[61, 62]

A.

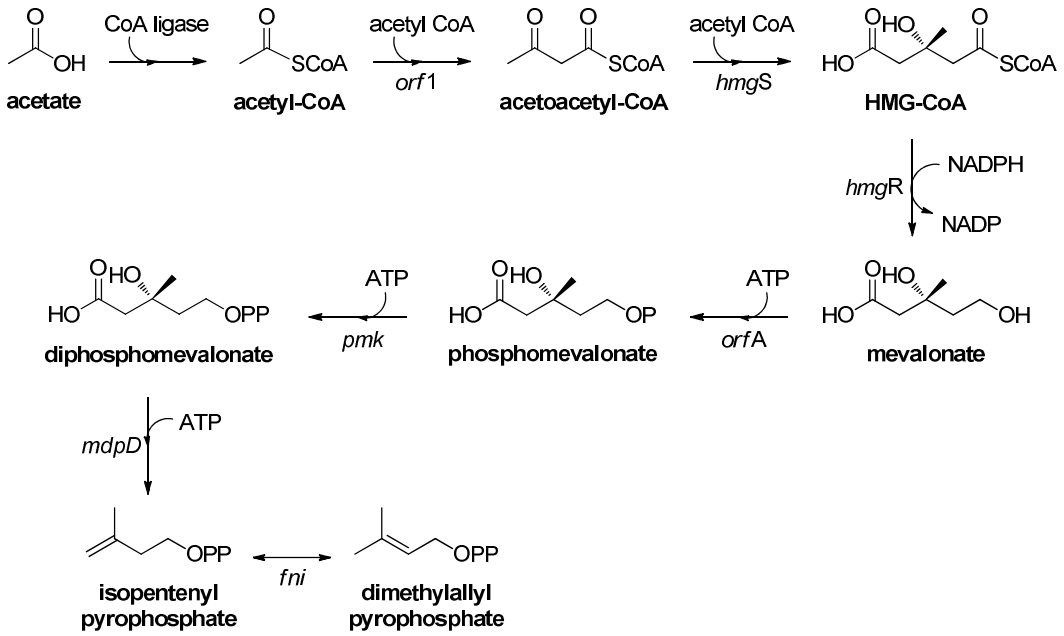

B.

Proposed Function	Gene
Acetyl CoA-acetyl transferase	*Orf*1
HMG CoA synthase	*hmg*S
HMG CoA reductase	*hmg*R
Mevalonate kinase	*orf*A
Phosphomevalonate kinase	*Pmk*
Diphosphomevalonate decarboxylase	*mdp*D
IPP isomerase	*fni*

Figure I.10: Mevalonate biosynthetic pathway. A) Isoprenoid biosynthesis via the mevalonate pathway. B) Deduced function of the mevalonate genes. CoA= coenzyme A; HMG-CoA = β-hydroxy-β-methylglutaryl-coenzyme A.

For many years, it was assumed that the 5-carbon isoprenoid building blocks in all organisms were biosynthesized by the mevalonate pathway. However, acetate feeding experiments in *E. coli,*[63, 64] glucose feeding

experiments in *S.* sp.,[65, 66] and HMG-CoA inhibition studies[63] were inconsistent with the mevalonate pathway, and in 1996 the first reaction step of the MEP pathway was established in *E. coli.*[56] There are seven genes in the MEP pathway (Figure I.11) and most all of them have been characterized from *E. coli*.[67-76] These genes are typically scattered throughout the genome much like those identified in *S. avermitilis'* genome.[18, 77] The first step in the MEP pathway is the condensation of pyruvic acid and D-glyceraldehyde-3-phosphate, which is catalyzed by the *dxs* gene.[68, 69] The *dxr* gene reduces and isomerizes 1-deoxy-D-xylulose-5-phosphate to 2-C-methyl-D-erythritol-4-phosphate and *isp*D transfers cytidine diphosphate (CDP) to this intermediate forming CDP-2-C-methyl-D-erythritol.[70, 72, 78] Phosphorylation catalyzed by *isp*E yields 2-phospho-CDP-2-C-methyl-D-erythritol and *isp*F cyclizes this molecule to 2-C-methyl-D-erythritol-2,4-cyclodiphosphate.[75, 76] Finally, *isp*G converts 2*C*-methyl-D-erythritol 2,4-cyclodiphosphate to 1-hydroxy-2-methyl-2-(*E*)-butenyl 4-diphosphate and *isp*H reduces 1-hydroxy-2-methyl-2-(*E*)-butenyl 4-diphosphate to IPP and DMAPP in a 5:1 ratio.[67, 71, 73, 74, 79, 80]

A.

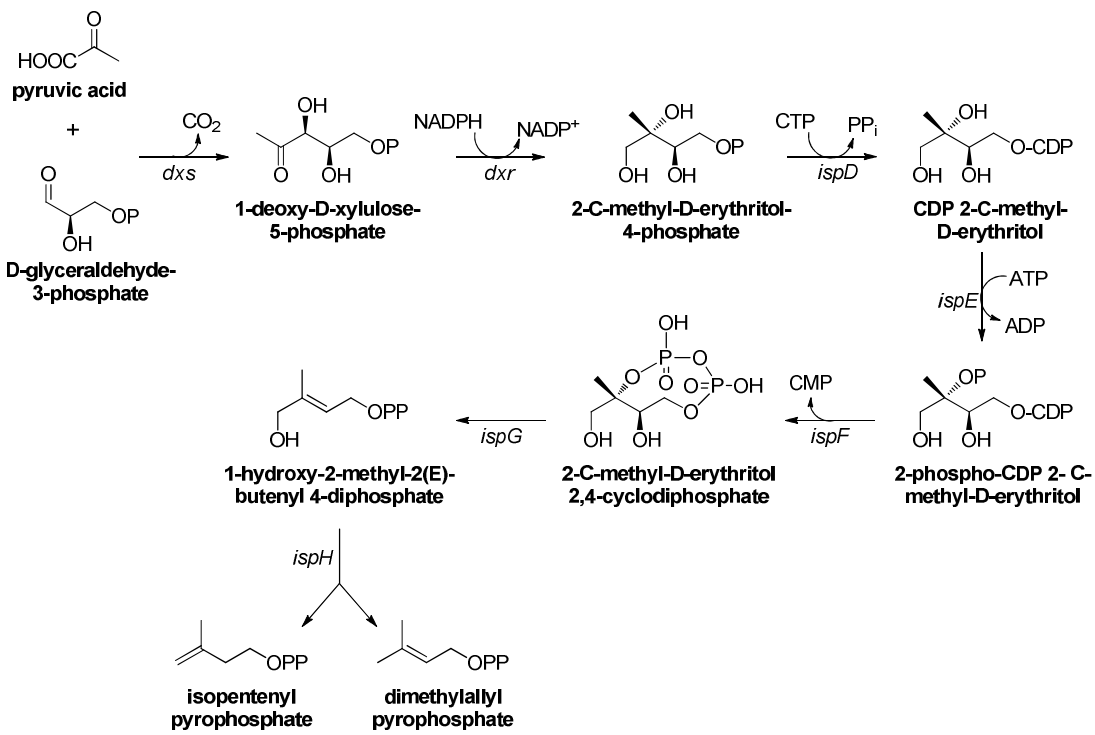

B.

Proposed Function	Gene
1-deoxyxylulose-5-phosphate synthase	*dxs*
1-deoxy-D-xylulose 5-phosphate reductoisomerase	*dxr*
2-C-methyl-D-erythritol 4-phosphate cytidylyltransferase	*ispD*
4-diphosphocytidyl-2-C-methyl-D-erythritol kinase	*ispE*
2-C-methyl-D-erythritol 2,4-cyclodiphosphate synthase	*ispF*
1-hydroxy-2-methyl-2-(*E*)-butenyl-4-diphosphate synthase	*ispG*
1-hydroxy-2-methyl-2-(*E*)-butenyl-4-diphosphate reductase	*ispH*

Figure I.11: Nonmevalonate biosynthetic pathway. A) Isoprenoid biosynthesis via the nonmevalonate pathway. B) Deduced function of the nonmevalonate genes. CDP = cytidine diphosphate.

After the formation of the 5-carbon building blocks IPP and DMAPP, the second step in isoprenoid biosynthesis is the formation of linear polyprenyl diphosphates. These polyprenyl diphosphates, which are typically joined in a head-to-tail fashion, are produced by the condensation of IPP into allylic diphosphates and are classified by the number of IPP units they contain (Figure I. 12).[1, 8] Following their formation, most isoprenoids undergo a variety of modifications, including cyclization, oxidation, rearrangement, reduction, halogenation, and methylation, giving rise to a vast number of chemically and functionally diverse metabolites.

A.

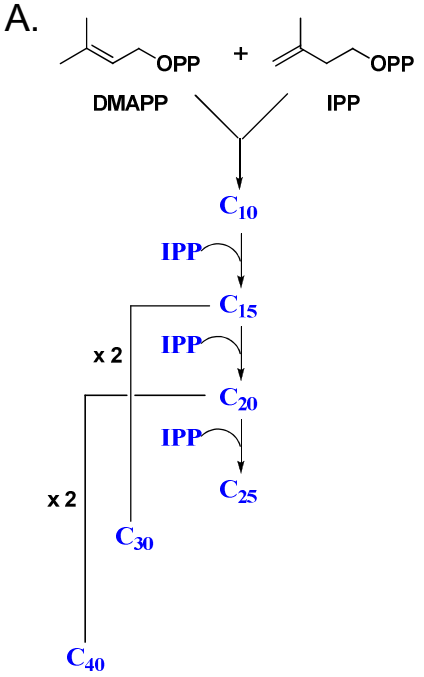

B .

Classification	Carbon Units
Hemiterpene (DMAPP or IPP)	5
Monoterpene (geranyl diphosphate)	10
Sesquiterpene (farnesyl diphosphate)	15
Diterpenes (geranylgeranyl diphosphate)	20
Sesterterpenes (geranylfarnesyl diphosphate)	25
Triterpenes (farnesylfarnesyl diphsophate)	30
Tetraterpenes (geranylgeranyl diphosphate x 2)	40

Figure I.12: Isoprenoid biosynthesis catalyzed by polyprenyl diphosphate synthases. A) Production of linear polyprenyl diphosphates by condensation of IPP into allylic diphosphates. B) Classification of linear polyprenyl diphosphates and their specific chain lengths.

I.3.2.2.1: Isprenoid biosynthesis in streptomycetes

Although most streptomycetes possess the MEP pathway for the formation of the 5-carbon building blocks IPP and DMAPP used in primary metabolism, some strains also contain the mevalonate pathway for the biosynthesis of secondary metabolites.[8, 17, 81, 82] Feeding studies have shown that the isoprenoid moieties in meroterpenoids produced by the genus *Streptomyces* such as longestin,[83] brasilicardin A,[84] novobiocin,[85] marinone,[86] pentalenolactone,[65] and neomarinone[86] are synthesized by the MEP pathway (Figure I.13), wheras isoprenoid moieties in naphterpin,[24] furaquinocin,[87] naypradiomyicin A,[31] BE-40644,[88] furanonaphthoquinone I,[38] and terpentecin[89] are products of the mevalonate pathway (Figure I.14).[53]

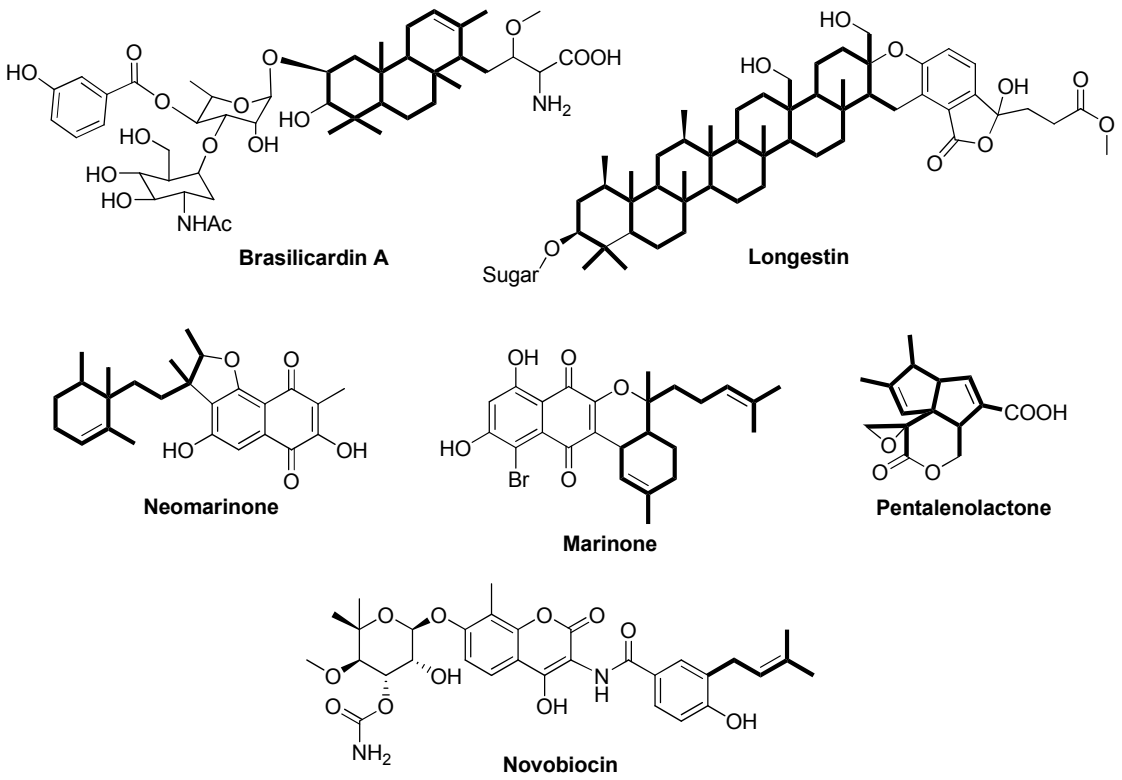

Figure I.13: Isoprenoids produced by actinomycetes that are biosynthesized by the MEP pathway. Isoprene units are highlighted in bold.

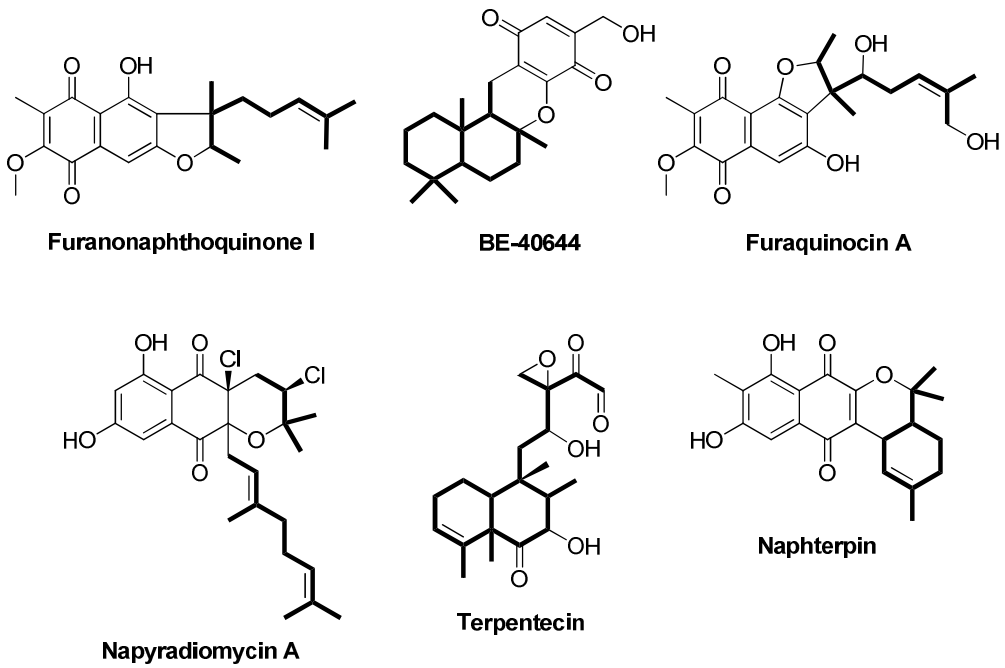

Figure I.14: Isoprenoids produced by actinomycetes that are biosynthesized by the mevalonate pathway. Isoprene units are highlighted in bold.

Although most streptomycetes are only equipped with the MEP pathway for the production of IPP, some strains also possess the mevalonate pathway for the synthesis of this 5-carbon building block. Interestingly, the strains that possess both pathways biosynthesize the isoprenoid subunits of hybrid isoprenoids mainly by the mevalonate pathway suggesting that the mevalonate pathway is closely related to the production of secondary metabolites. Labeling experiments with the naphterpin producer *S. aeriouvifer* proved that the organism used the MEP pathway for the formation of primary metabolites during the initial stages of growth and switches over to the mevalonate pathway during later stages of growth, which is when naphterpin production begins.[81] Growth-phase expression experiments with the terpentecin producer *S. griseolosporeus*

MF730-N6 showed that transcription of the genes associated with the mevalonate pathway were not detected at early growth of the organism, but were transcribed when terpentecin production started.[82] Together, these results suggest that the regulation of the mevalonate pathway gene cassette is closely related to the biosynthesis of isoprenoids in *Streptomyces* strains.

The complete six gene operon coding for all enzymes of the mevalonate pathway was first cloned and sequenced from the terpentecin producer, *S. griseolosporeus*,[90] and *a*dditional mevalonate gene cassettes have been identified in the naphtherpin producer *S.* sp. CL190,[91] the BE-40644 producer *Actinoplanes* sp. A40644,[88] and the furaquinocin A producer *S.* sp. KO-3988[92] (Figure I.15). When aligned, the mevalonate gene cassettes are conserved among strains in which the types of genes, their order and orientation are practically identical.[8] Further investigation of these cassettes also revealed that they exist directly upstream or downstream of the natural product biosynthetic clusters (Figure I.15).[88, 92, 93]

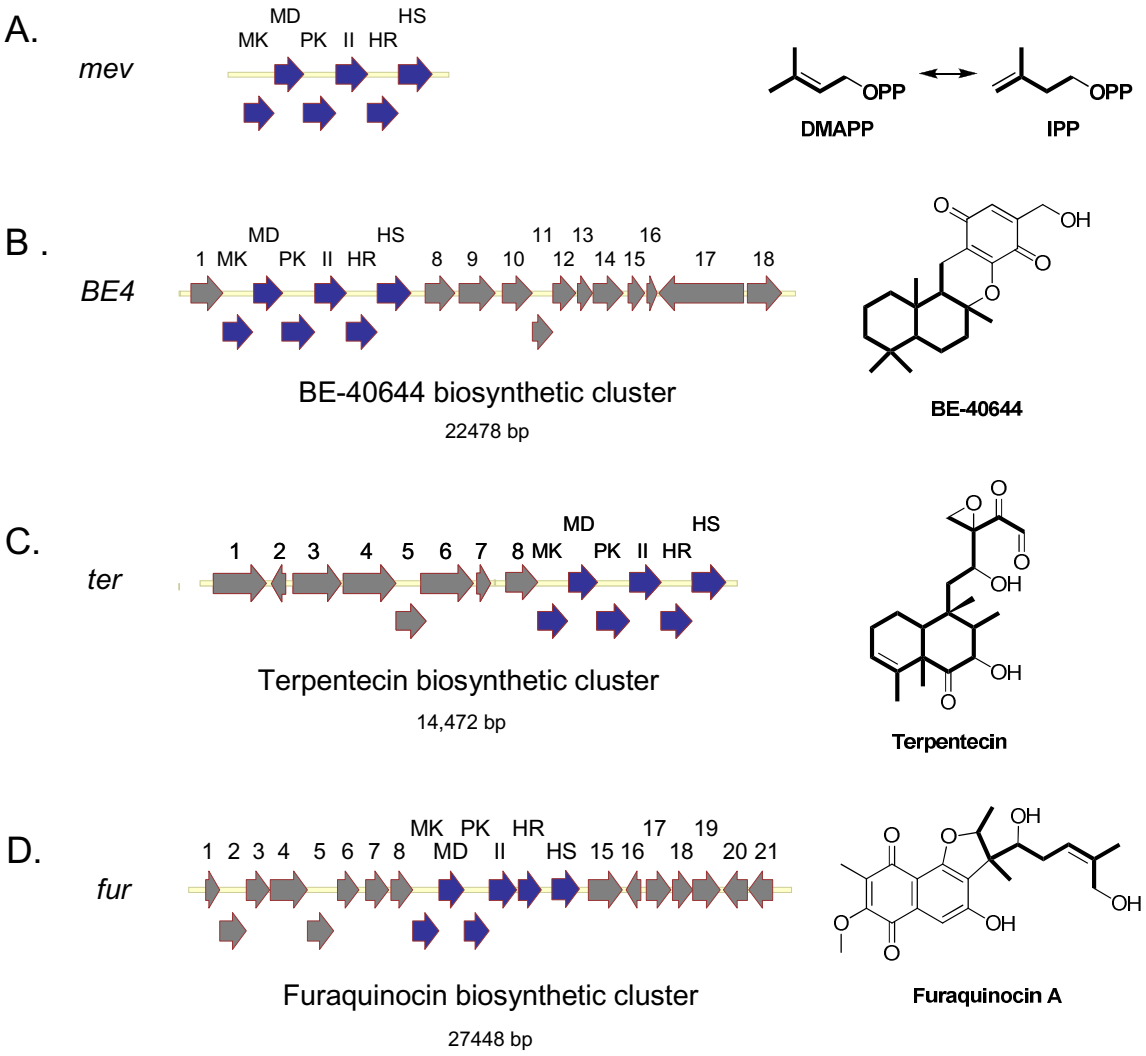

Figure I.15: Isoprenoids produced by actinomycetes via the mevalonate pathway. A) Mevalonate biosynthetic gene cassette. B) BE-40644 (*BE4*) biosynthetic cluster. C) Terpentecin (*ter*) biosynthetic cluster. D) Furaquinocin A (*fur)* biosynthetic cluster. Isoprenoid units are highlighted by bold lines. MK = mevalonate kinase, MD = mevalonate diphosphate decarboxylase, PK = phosphomevalonate kinase, II = Type 2 isopentenyl diphosphate isomerase, HR = HMG-CoA reductase, HS = HMG-CoA synthase. Deduced functions of the open reading frames can be found in Appendix Tables IA.1-IA.3.

I.3.3: Meroterpenoid biosynthetic clusters

Currently, the furanonaphthoquinone I (*fnq*)[94] from *S. cinnamonensis* DSM 1043 and furaquinocin A (*fur*)[92] from *S.* sp. KO-3988 are the only two hybrid meroterpenoid biosynthetic clusters isolated from actinomycetes (Figure I.16). Sequence analysis of the two biosynthetic clusters revealed a clustering of genes responsible for the naphthoquinone core, which included the type III polyketide synthase 1,3,6,8-tetrahydroxynaphthalene synthase and a monooxygenase. In addition to these genes, both clusters contained prenyltransferases for the attachment of the monoterpene GPP to the naphthoquinone core. The *fur* biosynthetic cluster also contained the six gene operon coding for the mevalonate pathway, which was located in the middle of the cluster, whereas the *fnq* biosynthetic cluster only contained the mevalonate kinase gene. Feeding studies with [$^{13}C_2$]acetate and [2-^{13}C]glycerol showed that the isoprenoid building blocks of furanonaphthoquinone I are produced by both the mevalonate and MEP pathways, with the mevalonate pathway being the predominat producer at ~80% compared to ~20% from the MEP pathway.[38] This study is the first example of a *Streptomyces* using both the MEP and mevalonate pathway for the formation of a single secondary metabolite.

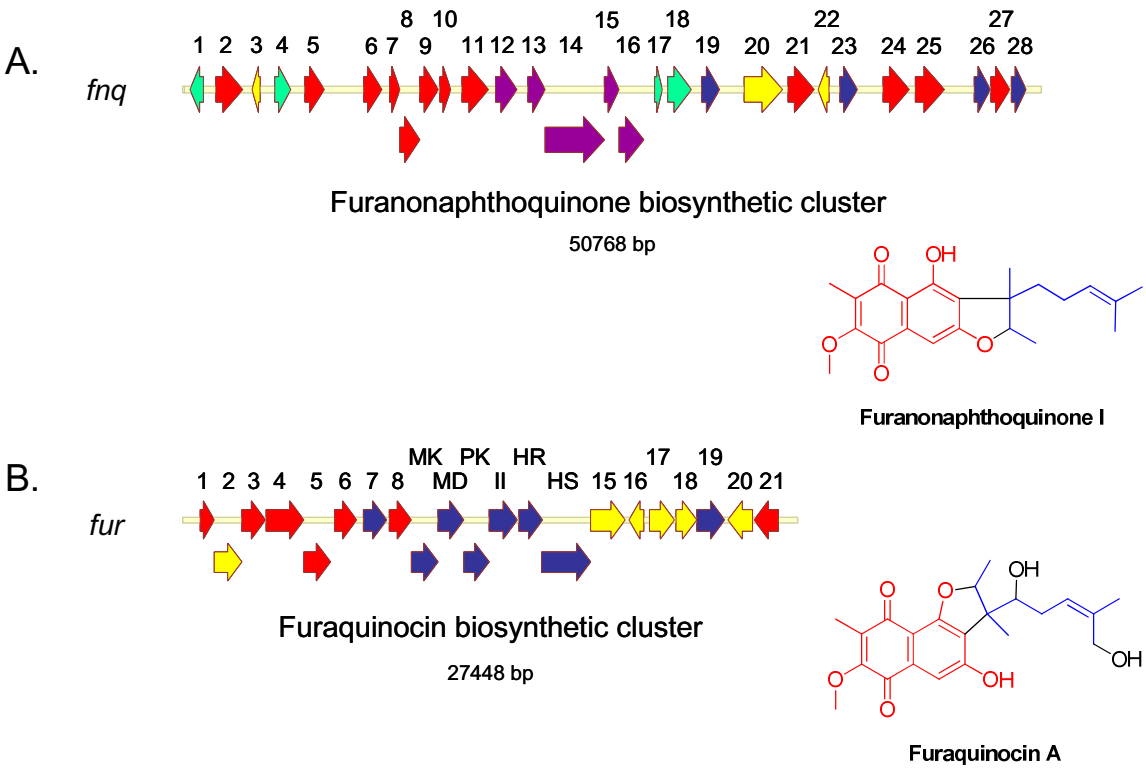

Key:

- Naphthoquinone biosynthesis
- Isoprenoid biosynthesis
- Generation of S-adenosylmethionine
- Regulatory and resistance genes
- Unknown

Figure I.16: Organization of meroterpenoid biosynthetic clusters isolated from actinomycetes. A) Furanonaphthoquinone I biosynthetic cluster isolated from *S. cinnamonensis*. B) Furaquinocin A biosynthetic cluster isolated from *S.* sp. KO-3988. Each arrow represents the direction of transcription of an open reading frame. Deduce function of the open reading frames of the *fur* biosynthetic cluster and the *fnq* biosynthetic cluster can be found in Appendix Table IA.3 and IA.4, respectively.

I.3.4: Total synthesis of microbial meroterpenoids

In addition to the total syntheses of α-pyrone meroterpenoids,[95] the total synthesis of napyradiomycin A1[96, 97] and 80915G[98] have been reported. Unlike the α-pyrones and A80915G, napyradiomycin A1 contains two chlorine atoms that may be responsible for its biological activity. The first total synthesis of napyradiomycin A1 was achieved in 17 steps and yielded a racemic mixture of napyradiomycin A1.[96] Recently, a 15 step asymmetric total synthesis of (–)-napyradiomycin A1 was reported and represented the first asymmetric chlorination of an isolated alkene.[97]

Many biologically active natural products that benefit human health are chlorinated and include the anticancer agent rebeccamycin[99] and the antibiotics griseofulvin[100] and chloramphenicol.[101] It is now known that the introduction of a chlorine atom into one or more specific positions of a molecule may substantially improve, or be required for, biological activity. Although synthetic chemistry has been successful at introducing halogen atoms into specific locations on molecules, the harsh conditions used to do so and the low yields of compounds can make this approach costly and environmentally unfriendly. For this reason, there is a great need for new efforts to introduce chlorine atoms into specific locations on existing molecules. One possible solution is using enzymes as biocatalysts. The advantage of this approach over traditional chemical synthesis is that biocatalysts are renewable and environmentally friendly. Hence, the

discovery and characterization of new chlorinating enzymes is an important step in making these enzymes available for biotechnology applications.

I.3.5: Meroterpenoids from marine bacteria

Oceans cover over 70% of the earth's surface and represent an ideal source for isolating unique and unexplored populations of marine bacteria.[9, 102] Marine sediments are a nutrient-rich microhabitat and differ greatly from terrestrial soil. It has been shown that microorganisms inhabiting these sediments have developed unique metabolic capabilities that allow them to survive and adapt to the constant changing conditions affiliated with the marine environment, i.e., nutrient levels, pressure, salinity and temperature.[9 102] Therefore, marine bacteria represent a novel resource for the identification and isolation of novel enzymes and bioactive molecules that would not be encountered from terrestrial microorganisms.[102]

Recently, Professors William Fenical and Paul R. Jensen (University of California at San Diego) identified and characterized a phylogenetically distinct group of marine sediment-derived actinomycetes belonging to the group MAR4, which is related to the genus Streptomyces. Although hybrid isoprenoids are uncommon actinomycetes natural products, the MAR4s predominantly produce assorted hybrid isoprenoids, including the prenylated pyrroles CNQ-509.366,

CNQ-509.364 and CNQ-509.332; the prenylated phenazines lavanducyanin and CNQ-509.364; and the meroterpenoids naphterpin, marinone,[103] neomarinone,[103] azamerone,[104] and a suite of napyradiomycin analogs (Figure I.17).[105, 106]

Figure I.17: Structures of hybrid isoprenoids from marine sediment-derived actinomycetes belonging to the MAR4s. Isoprene units are highlighted in blue, naphthoquinone cores are highlighted in red, phenazine moieties are highlighted in powder blue, and pyrrole units are highlighted in green.

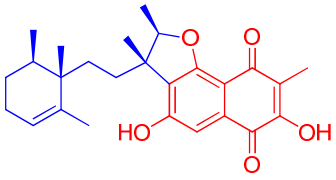

Neomarinone

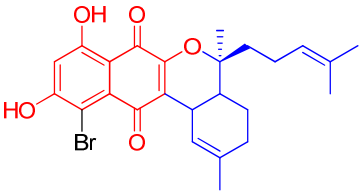

Marinone

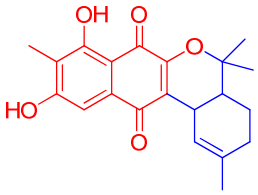

Naphterpin

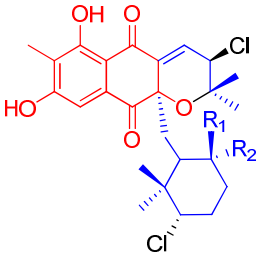

	R_1	R_2
7-methylnapyradiomycin B2	$=CH_2$	-
3''-hydroxy-7-methylnapyradiomycin B2	OH	CH_3

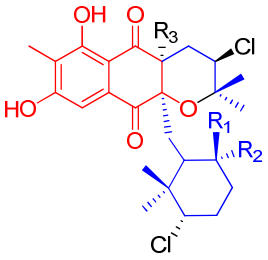

	R_1	R_2	R_3
A80915A	$=CH_2$	-	Cl
A80915C	OH	CH_3	Cl
2-deschloro-A80915C	OH	CH_3	H

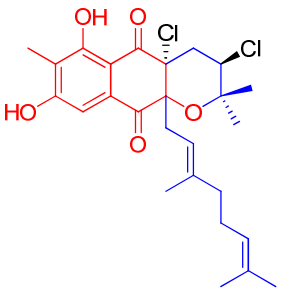

SF2415B3

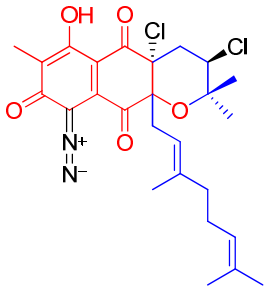

SF2415A3

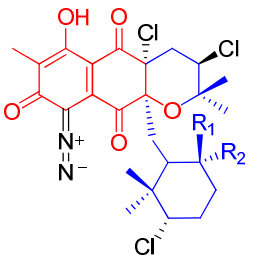

	R_1	R_2
A80915B	$=CH_2$	-
A80915D	OH	CH_3

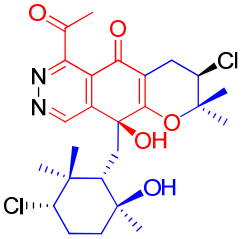

Azamerone

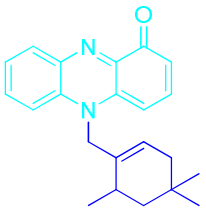

Lavanducyanin

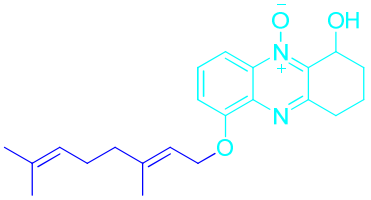

CNQ-509.364

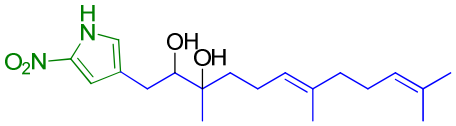

CNQ-509.350

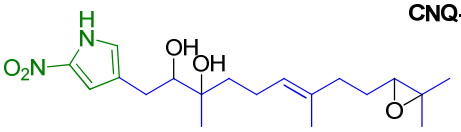

CNQ-509.366

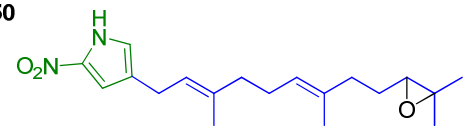

CNQ-509.332

The marine sediment-derived *S.* spp. CNQ-525 and CNQ-766 are prolific producers of meroterpenoids, which include the family of napyradiomycin analogs,[105, 106] the diazo chlorinated dihydroquinones, and the phthalazinone containing meroterpenoid azamerone.[104] Understanding how these chlorinated meroterpenoids are assembled will help facilitate the identification of unique biosynthetic enzymes with unique halogenating capabilites, which in turn can be used to generate new secondary metabolite diversity and enhance the inherent biological activity of natural products.

I.4: Appendix

Table IA.1: Deduced functions of the ORFs in the *BE4* biosynthetic cluster.[88]

ORF's from *Actinoplanes* sp. A40644	**Proposed function**
BE4_1	Polyprenyl diphosphate synthase
MK/BE4_2	Mevalonate kinase
MD/BE4_3	Mevalonate diphosphate decarboxylase
PK/BE4_4	Phosphomevalonate kinase
II/BE4_5	Type 2 IPP isomerase
HR/BE4_6	HMG-CoA reductase
HS/BE4_7	HMG-CoA synthase
BE4_8	3-oxacyl synthase
BE4_9	2-*epi*-5-*epi*-valiolone synthase
BE4_10	Alcohol dehydrogenase
BE4_11	Hypothetical protein
BE4_12	Oxidoreductase
BE4_13	Hypothetical protein
BE4_14	1,4-dihydroxy-2-naphthoate octaprenyltransferase
BE4_15	Drug efflux protein
BE4_16	Hypothetical protein
BE4_17	Transcriptional regulator
BE4_18	Hexosyl transferase

Table IA.2: Deduced functions of the ORFs in the *ter* biosynthetic cluster.[93]

ORF's from *S. Griseolosporeus* MF730-N6	**Proposed function**
ter1	Efflux protein
ter2	Hypothetical protein
ter3	Cytochrome P450
ter4	Cyclase
ter5	Pentalenolactone synthase
ter6	Cytochrome P450
ter7	Ferredoxin
ter8	Geranylgeranyl diphosphate synthase
MK/ter9	Mevalonate kinase
MD/ter10	Mevalonate diphosphate decarboxylase
PK/ter11	Phosphomevalonate kinase
II/ter12	Type 2 IPP isomerase
HR/ter13	HMG-CoA reductase
HS/ter14	HMG-CoA synthase

Table IA.3: Deduced functions of the ORFs in the *fur* biosynthetic cluster.[92]

ORF's from *S.* sp. KO-3988	**Proposed function**
fur1	THN synthase
fur2	Hypothetical protein
fur3	Aminotransferase
fur4	*C*-methyltransferase
fur5	Fatty acid-CoA ligase
fur6	*O*-methyltransferase
fur7	Prenyltransferase
fur8	P450
MK/fur9	Mevalonate kinase
MD/fur10	Mevalonate diphosphate
PK/fur11	Phosphomevalonate kinase
II/fur12	Type 2 IPP isomerase
HR/fur13	HMG-CoA reductase
HS/fur14	HMG-CoA synthase
fur15	3-oxacyl synthase
fur16	Hypothetical protein
fur17	3-carboxy-*cis*, *cis*-muconate cycloisomerase
fur18	Hypothetical protein
fur19	Polyprenyl diphosphate synthase
fur20	Hypothetical protein
fur21	Methyl transferase

Table IA.4: Deduced functions of the ORFs in the *fnq* biosynthetic cluster.[94]

ORF's from *S. cinnamonensis*	**Proposed function**
fnq1	Transcriptional regulator MerR
fnq2	Methylmalonyl-Co-A-decarboxylase-A-subunit
fnq3	Hypothetical protein
fnq4	SARP regulator
fnq5	Polyketide cyclase/aromatase
fnq6	THN synthase
fnq7	Monooxygenase MomA
fnq8	Aminotransferase
fnq9	SAM-dependent O-methyltransferase
fnq10	NAD(P)H:quinone oxidoreductase
fnq11	Fatty acid CoA-ligase
fnq12	S-adenosylmethionine synthase
fnq13	Adenosice kinase
fnq14	Methionine synthase
fnq15	5,10-methylene-tetrahydrofolate reductase
fnq16	Adenosylhomocysteinase
fnq17	Transcriptional regulator
fnq18	Transmembrane transporter
fnq19	Mevalonate kinase
fnq20	Hypothetical protein
fnq21	Carboxymuconate cycloisomerase
fnq22	Hypothetical protein
fnq23	Trans-polyprenyl diphosphate synthetase
fnq24	Monooxygenase
fnq25	Cytochrome B subunit
fnq26	Prenyltransferase
fnq27	SAM-dependent methyltransferase
fnq28	Prenyltransferase

I.5: References

1. Dewick, P. M., *Medicinal natural products a biosynthetic approach*. Second ed.; John Wiley & sons, LTD: West Sussex, 2005.

2. Fleming, A., On the antibacterial action of cultures of a *Penicillium*, with special reference to their use in the isolation of *B . influenzae. Br. J. Exp. Pathol.* **1929,** 10, 226-36.

3. McCormick, M. H.; McGuire, J. M.; Pittenger, G. E.; Pittenger, R. C.; Stark, W. M., Vancomycin, a new antibiotic. I. Chemical and biological properties. *Antibiot. Annu.* **1955,** 3, 606-11.

4. Wani, M.; Taylor, H.; Wall, M.; Coggon, P.; A., M., Plant antitumor agents VI. The isolation and structure of taxol, a novel antileukemic and antitumor agent from *Taxus brevifolia*. *J. Am. Chem. Soc.* **1971,** 93, 2325-27.

5. Seibert, R. A.; Williams, C. E.; Huggins, R. A., The isolation and identification of bound morphine. *Science* **1954,** 120, 222-23.

6. Klayman, D. L., Qinghaosu (artemisinin): an antimalarial drug from China. *Science* **1985,** 228, 1049-55.

7. Gunde-Cimerman, N.; Cimerman, A., Pleurotus fruiting bodies contain the inhibitor of 3-hydroxy-3-methylglutaryl-coenzyme A reductase-lovastatin. *Exp. Mycol.* **1995,** 19, 1-6.

8. Dairi, T., Studies on biosynthetic genes and enzymes of isoprenoids produced by actinomycetes. *J. Antibiot.* **2005,** 58, 227-43.

9. Fenical, W., Chemical studies of marine bacteria: developing a new resource. *Chem. Rev.* **1993,** 93, 1673-83.

10. Kieser, T.; Bibb, M. J.; Buttner, M. J.; Chater, K. F.; Hopwood, D. A., *Practical Streptomyces Genetics*. The John Innes Foundation: Norwich, 2000.

11. Watve, M. G.; Tickoo, R.; Jog, M. M.; Bhole, B. D., How many antibiotics are produced by the genus Stretpomyces? *Arch. Microbiol.* **2001,** 176, 386-90.

12. Chappell, J., Biochemistry and molecular-biology of the isoprenoid biosynthetic-pathway in plants. *Ann. Rev.Plant Physiol. Plant Mol. Biol.* **1995,** 46, 521-47.

13. Collier, S. J., Immunosuppressive drugs. *Curr. Opin. Immunol.* **1989-1990,** 2, 854-8.

14. Douglas, B. D.; Jacomb, R. G.; Dermack, W. O., Attempts to find new antimalarials: Further derivatives of *p*-phenanthroline. *J. Chem. Soc.* **1947,** 1, 1659-61.

15. Costa, G.; Hreshchyshyn, M. M.; Holland, J. F., Initial clinical studies with vincristine. *Cancer Chemother. Rep.* **1962,** 24, 39-44.

16. Geris, R.; Simpson, T. J., Meroterpenoids produced by fungi. *Nat. Prod. Rep.* **2009,** 26, 1063-94.

17. Kuzuyama, T.; Seto, H., Diversity of the biosynthesis of the isoprene units. *Nat. Prod. Rep.* **2003,** 20, 171-83.

18. Omura, S.; Ikeda, H.; Ishikawa, J.; Hanamoto, A.; Takahashi, C.; Shinose, M.; Takahashi, Y.; Horikawa, H.; Nakazawa, H.; Osonoe, T.; Kikuchi, H.; Shiba, T.; Sakaki, Y.; Hattori, M., Genome sequence of an industrial microorganism Streptomyces avermitilis: deducing the ability of producing secondary metabolites. *Proc. Natl. Acad. Sci. USA* **2001,** 98, 12215-20.

19. Bentley, S. D.; Chater, K. F.; Cerdeno-Tarraga, A. M.; Challis, G. L.; Thomson, N. R.; James, K. D.; Harris, D. E.; Quail, M. A.; Kieser, H.; Harper, D.; Bateman, A.; Brown, S.; Chandra, G.; Chen, C. W.; Collins, M.; Cronin, A.; Fraser, A.; Goble, A.; Hidalgo, J.; Hornsby, T.; Howarth, S.; Huang, C. H.; Kieser, T.; Larke, L.; Murphy, L.; Oliver, K.; O'Neil, S.; Rabbinowitsch, E.; Rajandream, M. A.; Rutherford, K.; Rutter, S.; Seeger, K.; Saunders, D.; Sharp, S.; Squares, R.; Squares, S.; Taylor, K.; Warren, T.; Wietzorrek, A.; Woodward, J.; Barrell, B. G.; Parkhill, J.; Hopwood, D. A., Complete genome sequence of the model actinomycete *Streptomyces coelicolor* A3(2). *Nature* **2002,** 417, 141-7.

20. Hohn, T. M., *Comprehensive natural products chemistry: isoprenoids incluldling cartenoids and steroids.* Pergamon: New York, 1999; Vol. 2.

21. Hoeksema, H.; Caron, E. L.; Hinman, J. W., Novobiocin. III. The structure of novobiocin. *J. Am. Chem. Soc.* **1956,** 78, 2019-20.

22. Imai, S.; Furihata, K.; Hayakawa, Y.; Noguchi, T.; Seto, H., Lavanducyanin, a new antitumor substance produced by *Streptomyces* sp. *J. Antibiot.* **1989,** 42, 1196-98.

23. Shin-Ya, K.; Shimizu, S.; Kunigami, T.; Furihata, K.; Hayakawa, Y.; Seto, H., Novel neuronal cell protecting substances, aestivophoenins A and B produced by *Streptomyces purpeofuscus. J. Antibiot.* **1995,** 48, 1378-81.

24. Shin-Ya, K.; Furihata, K.; Hayakawa, Y.; Seto, H., Biosynthetic studies of naphterpin, a terpenoid metabolite of *Streptomyces*. *Tetrahedron Lett.* **1990,** 31, 6025-26.

25. Komiyama, K.; Funayama, S.; Anraku, Y.; Ishibashi, M.; Takahashi, Y.; Omura, S., Novel antibiotics, furaquinocins A and B. Taxonomy, ferementation, isolation and physico-chemical and biological characteristics. *J. Antibiot.* **1990,** 43, 247-52.

26. Shiomi, K.; Nakamura, H.; Iinuma, H.; Naganawa, H.; Isshiki, K.; Takeuchi, T.; Umezawa, H.; Iitaka, Y., Structures of new antibiotics napyradiomycins. *J. Antibiot.* **1986,** 39, 494-01.

27. Cornforth, J. W., Terpenoids biosynthesis. *Chem. Br.* **1968,** 4, 102-06.

28. Simpson, T. J., Applications of multinuclear NMR to structural and biosynthetic studies of polyketide microbial metabolites. *Chem. Soc. Rev.* **1987,** 16, 123-60.

29. Shiomi, K.; Iinuma, H.; Hamada, M.; Naganawa, H.; Manabe, M.; Matsuki, C.; Takeuchi, T.; Umezawa, H., Novel antibiotics napyradiomycins production, isolation, physico-chemical properties and biological activity. *J. Antibiot.* **1986,** 39, 487-93.

30. Shiomi, K.; Nakamura, H.; Iinuma, H.; Naganawa, H.; Takeuchi, T.; Umezawa, H.; Iitaka, Y., New antibiotic napyradiomycins A2 and B4 and stereochemistry of napyradiomycins. *J. Antibiot.* **1987,** 40, 1213-19.

31. Shiomi, K.; Iinuma, H.; Naganawa, H.; Isshiki, K.; Takeuchi, T.; Umezawa, H., Biosynthesis of napyradiomycins. *J. Antibiot.* **1987,** 40, 1740-45.

32. Hori, Y.; Abe, Y.; Shigematsu, N.; Goto, T.; Okuhara, M.; Kohsaka, M., Napyradiomycins A and B1: non-steroidal estrogen-receptor antagonists produced by a *Streptomyces. J. Antibiot.* **1993,** 46, 1890-93.

33. Motohashi, K.; Sue, M.; Furihata, K.; Ito, S.; Seto, H., Terpenoids produced by actinomycetes: napyradiomycins from *Streptomyces antimycoticus* NT17. *J. Nat. Prod.* **2008,** 71, 595-01.

34. Shomura, T.; Gomi, S.; Ito, M.; Yoshida, J.; Tanaka, R.; Amano, S.; Watabe, H.; Ohuchi, S.; Itoh, J.; Sezaki, M., Studies on new antibiotics SF2415. I. Taxonomy, fermentation, isolation, physico-chemical properties and biological activities. *J. Antibiot.* **1987,** 40, 732-39.

35. Fukuda, D. S.; Mynderse, J. S.; Baker, P. J.; Berry, D. M.; Boeck, L. D.; Counter, L. D.; Ensminger, P. W.; Allen, N. E.; Alborn, W. E.; Hobbs, J. N., A80915, A new antibiotic complex produced by *Streptomyces aculeolatus*. Discovery, taxonomy, fermentation, isolation, characterization, and antibacterial evaluation. *J. Antibiot.* **1989,** 63, 623-33.

36. Gomi, S.; Ohuchi, S.; Sasaki, T.; Itoh, J.; Sezaki, M., Studies on new antibiotics SF2415. II. The structural elucidation. *J. Antibiot.* **1987,** 40, 740-49.

37. Shin-Ya, K.; Imai, S.; Furihata, K.; Hayakawa, Y.; Kato, Y.; Vanduyne, G. D.; Clardy, J.; Seto, H., Isolation and structural elucidation of an antioxidative agent, naphterpin. *J. Antibiot.* **1990,** 43, 444-47.

38. Bringmann, G.; Haagen, Y.; Gulder, T. A. M.; Gulder, T.; Heide, L., Biosynthesis of the isoprenoid moieties of furanonaphthoquinone I and endophenazine A in *Streptomyces cinnamonensis* DSM 1042. *J. Org. Chem.* **2007,** 72, 4198-04.

39. Henkel, T.; Zeeck, A., Structure and absolute configuration of naphthomevallin, a new dihydro-naphthoquinone antibiotic from *Streptomyces* sp. *J. Antibiot.* **1991,** 44, 665-69.

40. Kagamizono, T.; Hamaguchi, T.; Ando, T.; Sugawara, K.; Adachi, T.; Osada, H., Phosphatoquinones A and B, novel tyrosine phosphatase inhibitors produced by *Streptomyces* sp. *J. Antibiot.* **1999,** 52, 75-80.

41. Hopwood, D. A., Genetic contributions to understanding polyketide synthases. *Chem. Rev.* **1997,** 97, 2465-97.

42. Rawlings, B. J., Biosynthesis of fatty acids and related metabolites. *Nat. Prod. Rep.* **1998,** 18, 231-81.

43. Shen, B., Polyketide bioysnthesis beyond the type I, II and III polyketide synthase paradigms. *Curr. Opin. Chem. Biol.* **2003,** 7, 285-95.

44. Khosla, C.; Gokhale, R. S.; Jacobsen, J. R.; Cane, D. E., Tolerance and specificity of polyketide synthases. *Annu. Rev. Biochem.* **1999,** 68, 219-53.

45. Staunton, J.; Weissman, K. J., Polyketide biosynthesis: a millennium review. *Nat. Prod. Rep.* **2001,** 18, 380-16.

46. Rix, U.; Fischer, C.; Remsing, L. L.; Rohr, J., Modification of post-PKS tailoring steps through combinatorial biosynthesis. *Nat. Prod. Rep.* **2002,** 19, 542-80.

47. Moore, B. S.; Hopke, J. N., Discovery of a new bacterial polyketide pathway. *Chembiochem* **2001,** 2, 35-8.

48. Rawlings, B. J., Type I polyketide bioysnthesis in bacteria (Part A-erythromycin biosynthesis). *Nat. Prod. Rep.* **2001,** 18, 190-27.

49. Wang, I. K.; Vining, L. C.; Walter, J. A.; McInnes, A. G., Use of carbon-13 in biosynthetic studies: Origin of the malonyl coenzyme A incorporated into tetracycline by *Streptomyces auerofaciens. J. Antibiot.* **1986,** 39, 1281-87.

50. Izumikawa, M.; Shipley, P. R.; Hopke, J. N.; O'Hare, T.; Xiang, L.; Noel, J. P.; Moore, B. S., Expression and characterization of the type III polyketide synthase 1,3,6,8-tetrahydroxynaphthalene synthase from *Streptomyces coelicolor* A3(2). *J. Indust. Microbiol. Biotechnol.* **2003,** 30, 510-15.

51. Austin, M. B.; Izumikawa, M.; Bowman, M. E.; Udwary, D. W.; Ferrer, J. L.; Moore, B. S.; Noel, J. P., Crystal structure of a bacterial type III polyketide synthase and enzymatic control of reactive polyketide intermediates. *J. Biol. Chem.* **2004,** 279, 45162-74.

52. Moore, B. S.; Hertweck, C.; Hopke, J. N.; Izumikawa, M.; Kalaitzis, J. A.; Nilsen, G.; O'Hare, T.; Piel, J.; Shipley, P. R.; Xiang, L.; Austin, M. B.; Noel, J. P., Plant-like biosynthetic pathways in bacteria: from benzoic acid to chalcone. *J. Nat. Prod.* **2002,** 65, 1956-62.

53. Kuzuyama, T.; Takahashi, S.; Dairi, T.; Seto, H., Detection of the mevalonate pathway in *Streptomyces* species using the 3-hydroxy-3-methylglutaryl coenzyme A reductase gene. *J. Antibiot.* **2002,** 55, 919-23.

54. Katsuki, H.; Bloch, K., Studies on the biosynthesis of ergosterol in yeast: formation of methylated intermediates. *J. Biol. Chem.* **1967,** 242, 222-27.

55. Lynen, F., Biosynthetic pathways from acetate to natural products. *Pure Appl. Chem.* **1967,** 14, 137-67.

56. Rohmer, M.; Seemann, M.; Horbach, S.; Bringer-Meyer, S.; Sahm, H., Glyceraldehyde 3-phosphate and pyruvate as precursors of isoprenic units in an alternative non-mevalonate pathway for terpenoid biosynthesis. *J. Am. Chem. Soc.* **1996,** 118, 2564-66.

57. Dubey, V. S.; B, R.; L, R., An overview of the non-mevalonate pathway for terpenoid biosynthesis in plants. *J. Biosci.* **2003,** 28, 637-46.

58. Gondet, L.; Bronner, R.; Benveniste, P., Regulation of sterol content in membrants by subcellular compartmentation of steryl-esters accumulating in a sterol-overproducing tobacco mutant. *Plant Physiol.* **1994,** 105, 509-18.

59. Goldstein, J. L.; Brown, M. S., Regulation of the mevalonate pathway. *Nature* **1990,** 343, 425-30.

60. Gray, J. C., Control of isoprenoid biosynthesis in higher plants. *Adv. Bot. Res.* **1987,** 14, 25-91.

61. Dogbo, O.; Camara, B., Purification of isopentenyl pyrophosphate isomerase and geranylgeranyl pyrophosphate synthase from *Capsicum* chromophasts by affinity chromatography. *Biochem. Biophys. Acta* **1987,** 920, 140-48.

62. Ogura, K.; Nishino, T.; Seto, S., The purification of prenyltransferase and isopentenyl pyrophosphate isomerase of pumpkin fruit and some of their properties. *J. Biochem.* **1968,** 64, 197-203.

63. Zhou, D.; White, R. H., Early steps of isoprenoid biosynthesis in *Escherichia coli*. *Biochem. J.* **1991,** 273, 627-34.

64. Rohmer, M.; Knani, M.; Simonin, P.; Sutter, B.; Sahm, H., Isoprenoid biosynthesis in bacteria: a novel pathway for the early steps leading to isopentenyl diphosphate. *Biochem. J.* **1993,** 295, 517-24.

65. Cane, D. E.; Rossi, T.; Pachlatko, J. P., Biosynthesis of pentalenolactone. *Tetrahedron Lett.* **1979**, 3639-42.

66. Cane, D. E.; Rossi, T.; Tillman, A. M.; Pachlatko, J. P., Stereochemical studies of isoprenoid biosynthesis - biosynthesis of pentalenolactone from [U-C-13(6)]glucose and [6-H-2(2)]glucose. *J. Am. Chem. Soc.* **1981,** 103, 1838-43.

67. Adam, P.; Hecht, S.; Eisenreich, W.; Kaiser, J.; Grawert, T.; Arigoni, D.; Bacher, A.; Rohdich, F., Biosynthesis of terpenes: studies on 1-hydroxy-2-methyl-2-(E)-butenyl 4-diphosphate reductase. *Proc. Natl. Acad. Sci. USA* **2002,** 99, 12108-13.

68. Sprenger, G. A.; Schorken, U.; Wiegert, T.; Grolle, S.; de Graaf, A. A.; Taylor, S. V.; Begley, T. P.; Bringer-Meyer, S.; Sahm, H., Identification of a thiamin-dependent synthase in *Escherichia coli* required for the formation of the 1-deoxy-D-xylulose 5-phosphate precursor to isoprenoids, thiamin, and pyridoxol. *Proc. Natl. Acad. Sci. USA* **1997,** 94, 12857-62.

69. Lois, L. M.; Campos, N.; Putra, S. R.; Danielsen, K.; Rohmer, M.; Boronat, A., Cloning and characterization of a gene from *Escherichia coli* encoding a transketolase-like enzyme that catalyzes the synthesis of D-1-deoxyxylulose 5-phosphate, a common precursor for isoprenoid, thiamin, and pyridoxol biosynthesis. *Proc. Natl. Acad. Sci. USA* **1998,** 95, 2105-10.

70. Takahashi, S.; Kuzuyama, T.; Watanabe, H.; Seto, H., A 1-deoxy-D-xylulose 5-phosphate reductoisomerase catalyzing the formation of 2-C-methyl-D-erythritol 4-phosphate in an alternative nonmevalonate pathway for terpenoid biosynthesis. *Proc. Natl. Acad. Sci. USA* **1998,** 95, 9879-84.

71. Rohdich, F.; Hecht, S.; Gartner, K.; Adam, P.; Krieger, C.; Amslinger, S.; Arigoni, D.; Bacher, A.; Eisenreich, W., Studies on the nonmevalonate terpene biosynthetic pathway: metabolic role of IspH (LytB) protein. *Proc. Natl. Acad. Sci. USA* **2002,** 99, 1158-63.

72. Rohdich, F.; Wungsintaweekul, J.; Fellermeier, M.; Sagner, S.; Herz, S.; Kis, K.; Eisenreich, W.; Bacher, A.; Zenk, M. H., Cytidine 5'-triphosphate-dependent biosynthesis of isoprenoids: YgbP protein of *Escherichia coli* catalyzes the formation of 4-diphosphocytidyl-2-C-methylerythritol. *Proc. Natl. Acad. Sci. USA* **1999,** 96, 11758-63.

73. Rohdich, F.; Zepeck, F.; Adam, P.; Hecht, S.; Kaiser, J.; Laupitz, R.; Grawert, T.; Amslinger, S.; Eisenreich, W.; Bacher, A.; Arigoni, D., The deoxyxylulose phosphate pathway of isoprenoid biosynthesis: studies on the mechanisms of the reactions catalyzed by IspG and IspH protein. *Proc. Natl. Acad. Sci. USA* **2003,** 100, 1586-91.

74. Hecht, S.; Eisenreich, W.; Adam, P.; Amslinger, S.; Kis, K.; Bacher, A.; Arigoni, D.; Rohdich, F., Studies on the nonmevalonate pathway to terpenes: the role of the GcpE (IspG) protein. *Proc. Natl. Acad. Sci. USA* **2001,** 98, 14837-42.

75. Herz, S.; Wungsintaweekul, J.; Schuhr, C. A.; Hecht, S.; Luttgen, H.; Sagner, S.; Fellermeier, M.; Eisenreich, W.; Zenk, M. H.; Bacher, A.; Rohdich, F., Biosynthesis of terpenoids: YgbB protein converts 4-diphosphocytidyl-2C-methyl-D-erythritol 2-phosphate to 2C-methyl-D-erythritol 2,4-cyclodiphosphate. *Proc. Natl. Acad. Sci. USA* **2000,** 97, 2486-90.

76. Luttgen, H.; Rohdich, F.; Herz, S.; Wungsintaweekul, J.; Hecht, S.; Schuhr, C. A.; Fellermeier, M.; Sagner, S.; Zenk, M. H.; Bacher, A.; Eisenreich, W., Biosynthesis of terpenoids: YchB protein of *Escherichia coli* phosphorylates the 2-hydroxy group of 4-diphosphocytidyl-2C-methyl-D-erythritol. *Proc. Natl. Acad. Sci. USA* **2000,** 97, 1062-67.

77. Ikeda, H.; Ishikawa, J.; Hanamoto, A.; Shinose, M.; Kikuchi, H.; Shiba, T.; Sakaki, Y.; Hattori, M.; Omura, S., Complete genome sequence and comparative analysis of the industrial microorganism *Streptomyces avermitilis*. *Nat. Biotechnol.* **2003,** 21, 526-31.

78. Kuzuyama, T.; Takahashi, S.; Takagi, M.; Seto, H., Characterization of 1-deoxy-D-xylulose 5-phosphate reductoisomerase, an enzyme involved in isopentenyl diphosphate biosynthesis, and identification of its catalytic amino acid residues. *J. Biol. Chem.* **2000,** 275, 19928-32.

79. Altincicek, B.; Duin, E. C.; Reichenberg, A.; Hedderich, R.; Kollas, A. K.; Hintz, M.; Wagner, S.; Wiesner, J.; Beck, E.; Jomaa, H., LytB protein catalyzes the terminal step of the 2-C-methyl-D-erythritol-4-phosphate pathway of isoprenoid biosynthesis. *FEBS Lett.* **2002,** 532, 437-40.

80. Hsieh, M. H.; Goodman, H. M., The arabidopsis IspH homolog is involved in the plastid nonmevalonate pathway of isoprenoid biosynthesis. *Plant Physiol.* **2005,** 138, 641-53.

81. Seto, H.; Watanabe, H.; Furihata, K., Simultaneous operation of the mevalonate and non-mevalonate pathways in the biosynthesis of isopentenyl diphosphate in *Streptomyces aeriouvifer*. *Tetrahedron Lett.* **1996,** 37, 7979-82.

82. Hamano, Y.; Dairi, T.; Yamamoto, M.; Kuzuyama, T.; Itoh, N.; Seto, H., Growth-phase dependent expression of the mevalonate pathway in a terpenoid antibiotic-producing *Streptomyces* strain. *Biosci. Biotechnol. Biochem.* **2002,** 66, (4), 808-19.

83. Hayashi, Y.; Hiroyasu, O.; Nobuya, I.; Seto, H.; Dairi, T., Cloning of the gene cluster responsible for biosiynthesis of KS-505a (longestin), a unique tetraterpenoid. *Biosci. Biotechnol. Biochem.* **2007,** 71, 3072-81.

84. Shigemori, H.; Komaki, H.; Yazawa, K.; Mikami, Y.; Nemoto, A.; Tanaka, Y.; Kobayashi, J., Biosynthesis of diterpenoid moiety of brasilicardin A *via* non-mevalonate pathway in *Nocardia brasiliensis*. *Tetrahedron Lett.* **1999,** 40, 4353-54.

85. Orihara, N.; Kuzuyama, T.; Takahashi, S.; Furihata, K.; Seto, H., Studies on the biosynthesis of terpenoid compounds produced by actinomycetes. 3. Biosynthesis of the isoprenoid side chain of novobiocin via the non-mevalonate pathway in *Streptomyces niveus*. *J. Antibiot.* **1998,** 51, 676-78.

86. Kalaitzis, J. A.; Hamano, Y.; Nilsen, G.; Moore, B. S., Biosynthesis and structural revision of neomarinone. *Org. Lett.* **2003,** 5, 4449-52.

87. Funayama, S.; Ishibashi, M.; Komiyama, K.; Omura, S., Biosynthesis of furaquinocin-A and furaquinocin-B. *J. Org. Chem.* **1990,** 55, 1132-33.

88. Kawasaki, T.; Kuzuyama, T.; Furihata, K.; Itoh, N.; Seto, H.; Dairi, T., A relationship between the mevalonate pathway and isoprenoid production in actinomycetes. *J. Antibiot.* **2003,** 56, 957-66.

89. Isshiki, K.; Tamamura, T.; Sawa, T.; Naganawa, H.; Takeuchi, T.; Umezawa, H., Biosynthetic studies of terpentecin. *J. Antibiot.* **1986,** 39, 1634-35.

90. Hamano, Y.; Dairi, T.; Yamamoto, M.; Kawasaki, T.; Kaneda, K.; Kuzuyama, T.; Itoh, N.; Seto, H., Cloning of a gene cluster encoding enzymes responsible for the mevalonate pathway from a terpenoid-antibiotic-producing *Streptomyces* strain. *Biosci. Biotechnol. Biochem.* **2001,** 65, 1627-35.

91. Takagi, M.; Kuzuyama, T.; Takahashi, S.; Seto, H., A gene cluster for the mevalonate pathway from *Streptomyces* sp. Strain CL190. *J. Bacteriol.* **2000,** 182, 4153-57.

92. Kawasaki, T.; Hayashi, Y.; Kuzuyama, T.; Furihata, K.; Itoh, N.; Seto, H.; Dairi, T., Biosynthesis of a natural polyketide-isoprenoid hybrid compound, furaquinocin A: identification and heterologous expression of the gene cluster. *J. Bacteriol.* **2006,** 188, 1236-44.

93. Dairi, T.; Hamano, Y.; Kuzuyama, T.; Itoh, N.; Furihata, K.; Seto, H., Eubacterial diterpene cyclase genes essential for production of the isoprenoid antibiotic terpentecin. *J. Bacteriol.* **2001,** 183, 6085-94.

94. Haagen, Y.; Glueck, K.; Fay, K.; Kammerer, B.; Gust, B.; Heide, L., A gene cluster for prenylated naphtoquinone and prenylated phenazine biosynthesis in *Streptomyces cinnamonensis* DSM 1042. *Chembiochem* **2006,** 7, 2016-2027.

95. Sunazuka, T.; Omura, S., Total synthesis of alpha-pyrone meroterpenoids, novel bioactive microbial metabolites. *Chem. Rev.* **2005,** 105, 4559-80.

96. Tatsuta, K.; Tanaka, Y.; Kojima, M.; Ikegami, H., The first total synthesis of (+/-)-napyradimycin A1. *Chem. Lett.* **2002**, 14.

97. Snyder, S. A.; Tang, Z.; Gupta, R., Enantioselective total synthesis of (-)-napyradiomycin A1 via asymmetric chlorination of an isolated olefin. *J. Am. Chem. Soc.* **2009,** 131, 5744-45.

98. Takemura, S.; Hirayama, A.; Tokunaga, J.; Kawamura, F.; Inagaki, K.; Hashimoto, K.; Nakata, M., A concise total synthesis of (+/-)-A80915G, a

member of the napyradiomycin family of antibiotics. *Tetrahedron Lett.* **1999,** 40, 7501-05.

99. Bush, J. A.; Long, B. H.; Catino, J. J.; Bradner, W. T.; Tomita, K., Production and biological activity of rebeccamycin, a novel antitumor agent. *J. Antibiot.* **1987,** 40, 668-78.

100. Oxford, A. E.; Raistrick, H.; P., S., Studies in the biochemistry of micro-organisms: griseofulvin, C(17)H(17)O(6)Cl, a metabolic product of *Penicillium griseo-fulvum Dierckx. Biochem. J.* **1939,** 33, 240-8.

101. Bartz, Q. R., Isolation and characterization of chlormycetin. *J. Biol. Chem.* **1948,** 172, 445-50.

102. Jensen, P. R.; Fenical, W., Marine bacterial diversity as a resource for novel microbial products. *J. Indust. Microbiol.* **1996,** 17, 346-51.

103. Hardt, I. H.; Jensen, P. R.; Fenical, W., Neomarinone, and new cytotoxic marinone derivatives, produced by a marine filamentous bacterium (actinomycetales). *Tetrahedron Lett.* **2000,** 41, 2073-76.

104. Cho, J. Y.; Kwon, H. C.; Williams, P. G.; Jensen, P. R.; Fenical, W., Azamerone, a terpenoid phthalazinone from a marine-derived bacterium related to the genus *Streptomyces* (actinomycetales). *Org. Lett.* **2006,** 8, 2471-4.

105. Soria-Mercado, I. E.; Jensen, P. R.; Fenical, W.; Kassel, S.; Golen, J., 3,4a-dichloro-10a-(3-chloro-6-hydroxy-2,2,6-trimethylcyclohexylmethyl)-6,8-dihydroxy-2,2,7-trimethyl-3,4,4a,10a-tetrhydro-2H-benzo[g]chromene-5,10-dione. *Acta Crystallogr., Sect. E* **2004,** 60, 1627-1629.

106. Soria-Mercado, I. E.; Prieto-Davo, A.; Jensen, P. R.; Fenical, W., Antibiotic terpenoid chloro-dihydroquinones from a new marine actinomycete. *J. Nat. Prod.* **2005,** 68, 904-10.

CHAPTER 1

Formation of the Pyridazine Natural Product Azamerone by Biosynthetic Rearrangement of an Aryl Diazoketone

1.1: Introduction

1.1.1: Nitrogen containing compounds

Compounds containing N–N bonds have been made synthetically for over a hundred years. However, it wasn't until 1951 that the first naturally occurring compound containing a dinitrogen group, the azoxy-containing toxin macrozamin, was reported (Figure 1.1).[1, 2] Since that time, natural products containing hydrazine, nitramine, azoxy, pyrazole, diazo and other N–N bonded functional groups have been identified (Figure 1.1). The enzymes responsible for N–N bond formation could make valuable biocatalysts, however, the biosynthesis of this structural unit is still poorly understood.

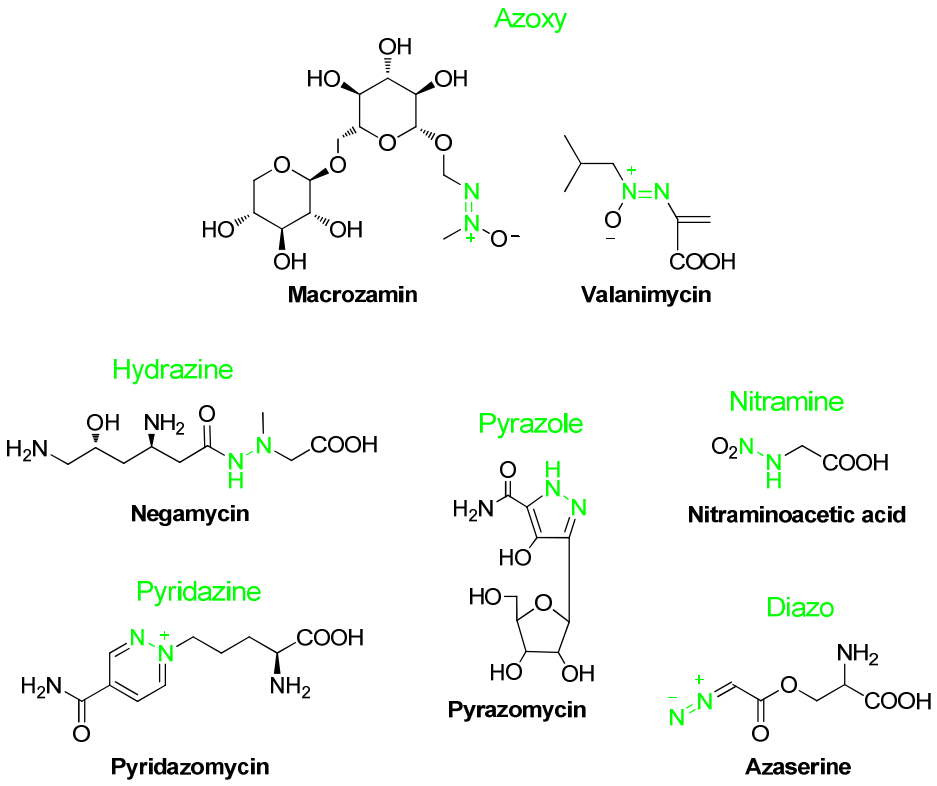

Figure 1.1: Selected natural products containing a N–N bonded functional group (highlighted in green).

1.1.2: Biosynthesis of N–N bonds

1.1.2.1: Biosynthesis of valanimycin and pyridazomycin

Biosynthetic investigations of the azoxy-containing antibiotic valanimycin[3-5] and the antifungal antibiotic pyridazomycin[6] have shown that both of these natural products are derived from the condensation of two amino acids (Figure 1.2). Enzymatic and chemical studies have shown that valanimycin is derived from L-valine and L-serine, and a class II seryl-tRNA synthetase is used to transfer the seryl residue to the hydroxyl group of the isobutylhydroxylamine intermediate.[5, 7] Feeding studies revealed that pyridazomycin originates from glycine and ornithine, and it is spectulated that oxaloacetate is the remaining building block.[6] While these studies revealed the origins of the nitrogen atoms in valanimycin and pyridazomycin, the mechanism and identification of genes responsible for N–N bond formation is still unknown.

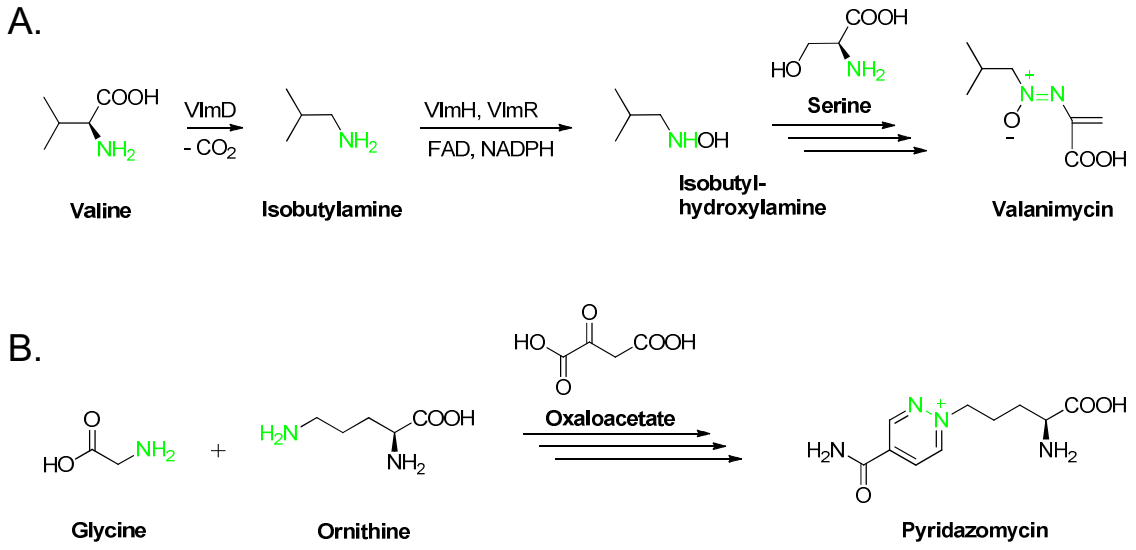

Figure 1.2: Predicted biosynthesis of N–N containing compounds. A) Valanimycin. B) Pyridazomycin.

1.1.2.2: Biosynthesis of kinamycin D

Feeding studies with synthetic and natural intermediates revealed that the diazonium group in kinamycin D is assembled from the stepwise addition of two nitrogen donors. Nitrosobenzo[*b*]fluorene and the related natural product stealthin C were synthesized with deuterium atoms at C6 and C8 and fed to the producing strain *Streptomyces murayamaensis* to probe the biosynthesis of kinamycin D.[8] ^{2}H NMR spectroscopy revealed that stealthin C was incorporated into kinamycin D, whereas the nitrosobenzo[*b*]fluorine precursor was not (Figure 1.3).[8] To determine if a ketobenzo[*b*]fluorene quinone was an early intermediate in the kinamycin pathway, deuterium-labeled kinobscurinone was similarly synthesized and fed to *S. murayamaensis*.[9] Its incorporation was also determined by ^{2}H NMR, suggesting that the diazonium group in kinamycin D is formed from a ketobenzo[*b*]fluorene precursor (Figure 1.3). These results support the theory that a ketobenzo[*b*]fluorene precursor is converted to an aminobenzo[*b*]fluorene intermediate through a transamination reaction, which further reacts with a second nitrogen source yielding the diazonium moiety. Together with the studies on valanimycin and pyridazomycin, a picture has emerged that natural product N_2 groups derive from two nitrogen donors versus from a dinitrogen source.

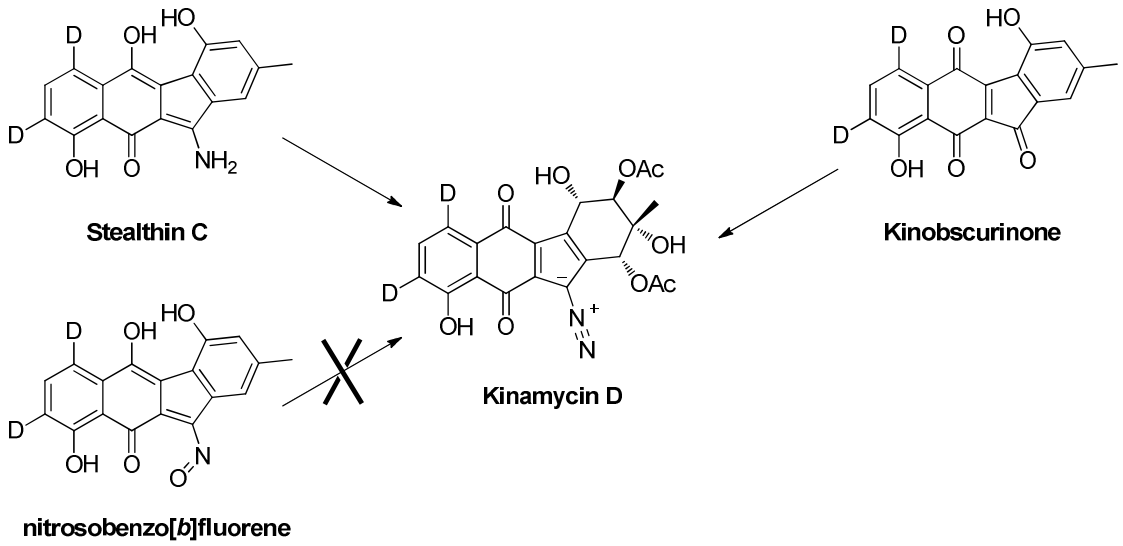

Figure 1.3: Incorporation of the natural products kinobscurinone and stealthin C into kinamycin D.

1.1.3: Specific Aim

Until the phthalazinone meroterpenoid azamerone (Figure 1.4) was isolated from the marine sediment-derived *Streptomyces* sp. CNQ-766,[10] pyridazomycin[11] was the only natural product containing a pyridazine ring and it was speculated that the pyridazine ring moiety in azamerone was also derived from the cyclization of amino acid residues. However, identification of co-produced chlorinated dihydroquinones and diazo meroterpenoids belonging to the SF2415 and A80915 series[12, 13] suggested otherwise that azmerone is biosynthetically linked to the nitrogenated compounds and that its phthalazinone core may be derived from a naphthoquinone precursor. Given the structural novelty of azamerone and its relation to the diazo meroterpenoids, a variety of

feeding experiments with ^{13}C and ^{15}N-labeled molecules were used to explore the formation of its phthalazinone core.

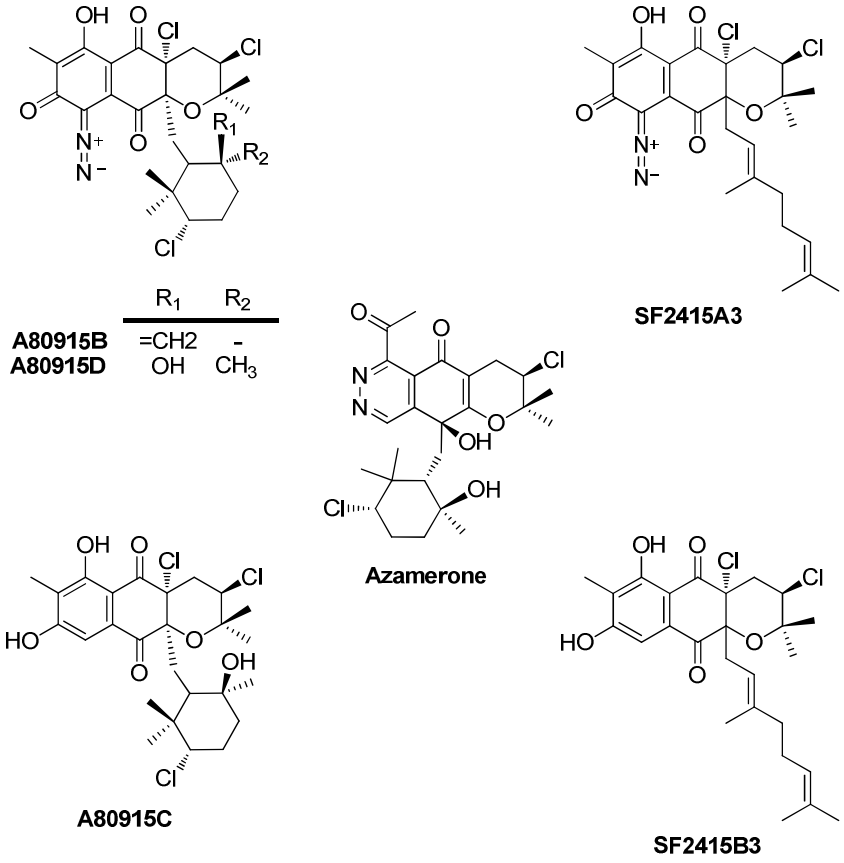

Figure 1.4: Meroterpenoids produced by *S.* sp. CNQ-766: azamerone, the A80915 and SF2415A3 series of chlorinated dihydroquinones, and the A80915 and SF2415 series of diazo containing meroterpenoids.

1.2: Materials and Methods

1.2.1: Bacterial strains and cultural conditions

Streptomyces sp. CNQ-766 was obtained from Professors William Fenical and Paul R. Jensen (University of California at San Diego)[10]. The strain was cultured in 1 L M1 medium in 2.8 L Fernback flasks (Appendix Table 1A.1). Cultivation was carried out at 30^{o} C at 200 rpm for 5–15 days. Inoculation of the 1 L culture was achieved with 5% of a 30 mL seed culture grown in M1 medium for 7 days at 30 ^{o}C.

1.2.2: Feeding experiments

For the L-[methyl-^{13}C]methionine, [1,2-$^{13}C_2$]acetate, [^{15}N]nitrite, [^{15}N]nitrate, [$^{15}N_2$]ammonium sulfate and [$^{15}N_2$]hydrazine sulfate feeding studies, 100 mg of labeled precursor was added to a 1 L culture at the time of inoculation. [2-^{15}N, 9-^{13}C]SF2415A3 (15 mg/ml) was biosynthetically prepared from a fermentation supplemented with 100 mg L-methyl-^{13}C]methionine and 100 mg [^{15}N]nitrite and purified as described below. Feeding studies with [2-^{15}N, 9-^{13}C]SF2415A3 were carried out in 100 ml M1 medium in 500 mL Erlenmeyer flasks at 30^{o} C at 200 rpm for 15 days. At days 3, 5, 7, and 10, two mg of [2-^{15}N, 9-^{13}C]SF2415A3 dissolved in 200 µl of DMSO was administered to the 100 ml culture of *S.* sp. CNQ-766.

1.2.3: Chemicals

Labeled precursors and NMR solvents were purchased from Cambridge Isotope Laboratories, Inc. Authentic azamerone was kindly provided by J. Y. Cho and W. Fenical (University of California at San Diego). All solvents and other chemicals used were of analytical grade.

1.2.4: HPLC analysis of chlorinated dihydroquinone analogs

All cultures were extracted with ethyl acetate, the ethyl acetate was dried over anhydrous $MgSO_4$ and concentrated *in vacuo*. From the 1 L culture feeding studies, the crude extracts were fractionated by reversed-phase C18 flash column chromatography (Fisher Scientific, PrepSep C18 1g/6ml) with a flow rate of 10 ml/min. The fractions were collected in 20 ml aliquots using the following conditions: 40 ml of 20% acetonitrile:water, 60 ml of 40% acetonitrile:water, 60 ml of 60% acetonitrile:water, 60 ml of 80% acetonitrile:water, 40 ml of 100% acetonitrile, and 40 ml of 100% methanol. The fractions were analyzed in positive and negative mode on a Hewlett Packard 1100 series high performance liquid chromatography system linked to an Agilent ESI-1100 MSD mass spectrometer (gas flow set to 13 ml/min, drying temperature set to 350^{o} C, capillary voltage set to 4500 V, and nebulizing pressure set to 40 pounds/square inch). A Luna 4.6 x 100 mm C18 column was used at a flow rate of 0.7 ml/min with a linear solvent gradient of 10–100% acetonitrile:water over a period of 20 min. All compounds were isolated using HPLC with a Waters differential

refractrometer R401 detector (chart recorder set to 12cm/h at 50 mV, and the refractive index was set at 4X).

1.2.5: Spectral Analysis

^{1}H and ^{13}C NMR spectra were obtained on Varian Inova 500-MHz and 300-MHz spectrometers. Multiple-bond ^{1}H-^{15}N connectivities were determined by proton-detected HMBC on a 600-MHz Bruker spectrometer with a 1.7 mm TCI cryoprobe. ^{15}N NMR spectra were obtained on Varian Inova 300-MHz and JNM-ECA500 spectrometers. The deuterium exchange experiment was conducted on a Varian Inova 300-MHz spectrometer.

1.2.6: Deuterium exchange experiment

SF2415A3 enriched with L-[methyl-^{13}C]methionine (15 mg) was dissolved in 500 µl CD_3CN. Carbon spectra were detected using decoupled NOE after 512 scans. D_2O was added in 0.01% increments using a P2 pipet, and the shims were not adjusted between scans.

1.2.7: Isolation of azamerone

Cultures were extracted after ~15 days growth, which yielded 5–8.5 mg of azamerone per liter. Azamerone eluted in the 40% acetonitrile:water fraction as described in Section 1.2.4 and was purified on a Phenomenex Luna C8 column (250 x 10 mm; 5 µm particle size) employing an isocratic condition of 55% acetonitrile:water with a flow rate of 3.0 ml/min (t_R = 17 minutes).

1.2.8: Isolation of SF2415A3

Cultures were extracted after ~5 days growth, which yielded ~20 mg of SF2415A3 per liter. SF2415A3 eluted in the 80% acetonitrile:water fraction as described in section 1.2.4 and was isolated by purifying first on a Luna C18 column (250 x 10 mm; 5 µm particle size) with an isocratic condition of 93% acetonitrile:water and a flow rate of 3.0 ml/min (t_R = 17–18 minutes), followed by a second purification on a Phenomenex Luna C8 column (250 x 10 mm; 5 µm particle size) using an isocratic condition of 87% acetonitrile:water with a flow rate of 2.2 ml/min (t_R = 23–24 minutes).

1.2.9: Isolation of A80915C

For the L-[methyl-^{13}C]methionine and [1,2-$^{13}C_2$]acetate feeding experiments, the 1 L M1 cultures were extracted after ~ 9 days growth to yield ~5 mg of A80915C per liter. A80915C eluted in the 60% acetonitrile:water fraction

as described in Section 1.2.4 and was initially purified on a Phenomenex Luna C18 column (250 x 10 mm; 5 µm particle size) with an isocratic condition of 80% acetonitrile:water and a flow rate of 2.0 ml/min (t_R = 37 minutes) followed by a second purification on a Phenomenex Luna C8 column (250 x 10 mm; 5 µm particle size) using an isocratic condition of 75% acetonitrile:water with a flow rate of 2.0 ml/min (t_R = 28 minutes).

1.2.10: Isolation of A80915D

Cultures were extracted after 5–7 days of growth to yield ~5 mg of A80915D per liter. A80915D was eluted in the 60% acetonitrile:water fraction as described in Section 1.2.4 and was initially purified on a Phenomenex Luna C18 column (250 x 10 mm; 5 µm partice size) with and isocratic conidition of 75% acetonitrile:water and a flow rate of 3.0 ml/min (t_R = 13 minutes), followed by a second purification using a Phenomenex Luna C8 column (250 x 10 mm; 5 µm particle size) using an isocratic condition of 70% acetonitrile:water with a flow rate of 3.0 ml/min (t_R = 21 minutes).

1.3: Results and Discussion

1.3.1: Increasing azamerone production

The original isolation of azamerone from *S.* sp. CNQ-766 using A1 growth media (Appendix Table 1A.1) generated approximately 0.25 mg/L,[10] which was insufficient for labeling experiments. Therefore, different fermentation conditions were evaluated to improve production yields. M1 medium, which was used in the original cultivation of the A80915 series of compounds by Lilly,[13] resulted in a greater than 30-fold increase in azamerone production at 8.5 mg/L (Appendix Table 1A.2 and Figure 1A.1).

1.3.2: [1,2-$^{13}C_2$]acetate feeding study

In addition to exploring the biosynthesis of azamerone with stable isotopes, the chlorinated dihydroquinones such as A80915C and the diazo meroterpenoids such as SF2415A3 and A80915D were also examined to probe the biosynthetic relationship of this extended structural family (Figure 1.4). Feeding experiments with [1,2-$^{13}C_2$]acetate clearly revealed that the naphthoquinone core of A80915C was derived from the symmetrical pentaketide 1,3,6,8-tetrahydroxynaphthalene (THN) and that the two isoprenoid units originated from the mevalonate pathway (Scheme 1.1, Appendix Table 1A.3 and Appendix Figure 1A.2). These findings were consistent with previous isotopic experiments in this compound series from *Chainia rubra* MG802AF1.[14]

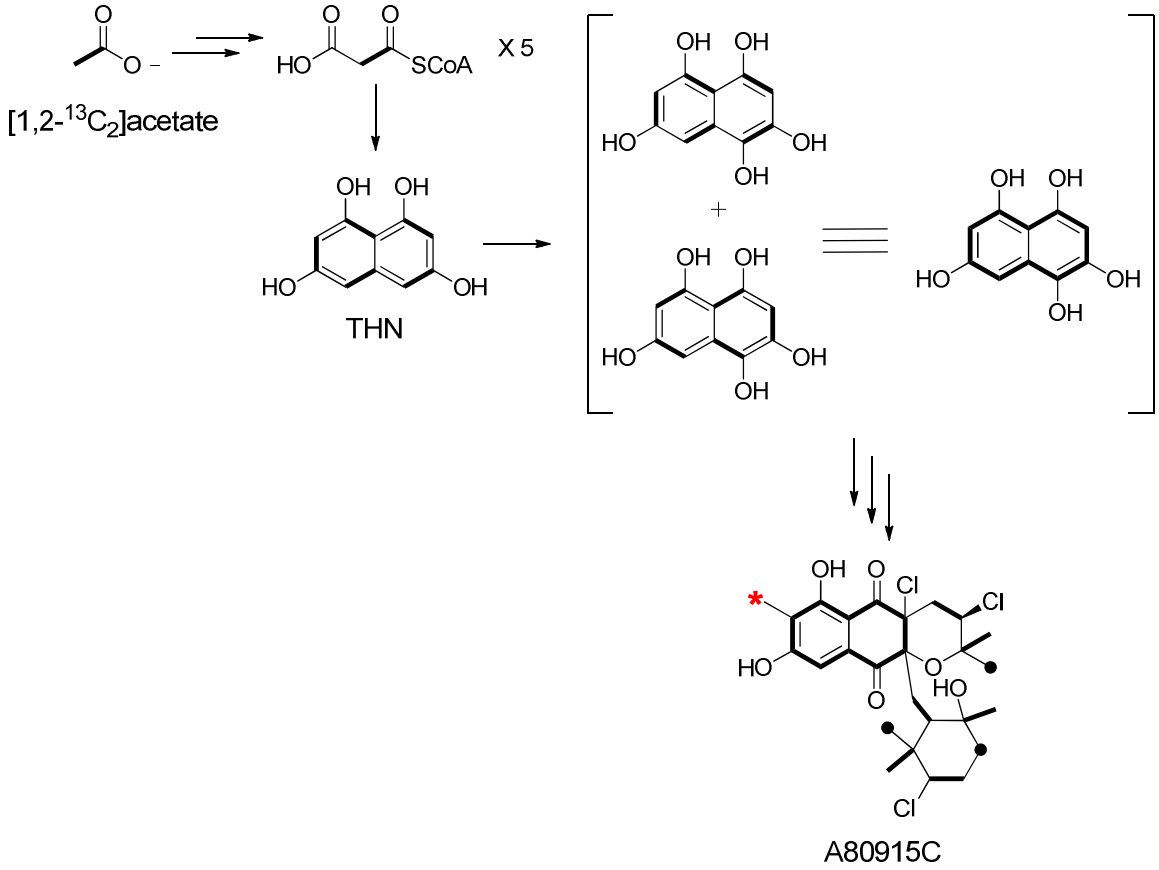

Scheme 1.1: Proposed biosynthetic pathway for the naphthoquinone core of A80915C. A summation of the two [1,2-$^{13}C_2$]acetate-labeling patterns are shown in bold. Lines and dots signify double and single enrichments, respectively. The methyl at C9, which is highlighted with a red asterick, was proven to be methionine-derived.

^{13}C NMR spectroscopic analysis of [1,2-$^{13}C_2$]acetate-enriched azamerone also showed that all carbons except for the C8 methyl group originate from acetate (Figure 1.5, Appendix Table 1A.4 and Appendix Figure 1A.3). The bicyclic phthalazinone unit clearly harbored two distinct ^{13}C-labeling patterns of equal proportions, thereby implying that it too derives from the symmetrical THN unit common to the napyradiomycins.

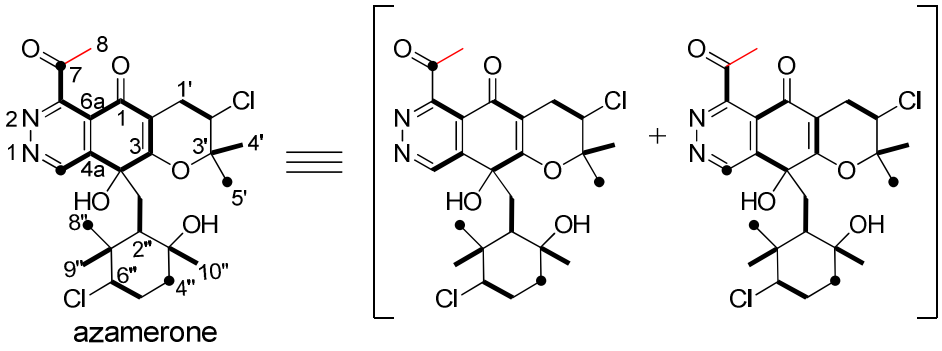

Figure 1.5: ^{13}C labeling of azamerone derived from [1,2-$^{13}C_2$]acetate and L-[methyl-^{13}C]methionine. Two equally independent labeling patterns were evident from the incorporation of [1,2-$^{13}C_2$]acetate (bold lines and dots signify double and single enrichments, respectively). The enrichment from L-[methyl-^{13}C]methionine is shown in red. The numbering scheme has been adopted from references[15, 16].

1.3.3: L-[methyl-^{13}C]methionine feeding study

Feeding experiments with L-[methyl-^{13}C]methionine revealed the C9 methyl group on the naphthoquinone core of A80915C is selectively enriched by 39% (Scheme 1 and Appendix Figure 1A.4). Further analysis of L-[methyl-^{13}C]methionine-enriched azamerone revealed the 26% selective enrichment of C8, confirming that the acetyl methyl group of azamerone is methionine-derived (Figure 1.5 and Appendix Figure 1A.5). Importantly, if labeled materials were administered to *S.* sp. CNQ-766 during the initial production of azamerone, which is roughly five days after inoculation during stationary growth, no enrichment could be detected (Appendix Figure 1A.6). Labeled materials had to be added at the time of inoculation in order for them to be incorporated, thereby suggesting that azamerone originates from a methylated intermediate produced earlier in the fermentation process. Altogether, these data suggest that azamerone is biosynthetically linked to the napyradiomycin family of natural products.

1.3.4: Distinguishing between the diazoketone and diazonium tautomer

Based on previous work with the TW93 series of pyrone containing polyketides from *Streptomyces* spp.,[17] a deuterium exchange experiment was performed to determine if the N–N group in SF2415A3 was being observed as a diazoketone or diazonium substituent. ^{13}C NMR analysis identified a collapse in signal for the C8 phenolic carbon in the hydroquinone core as the amount of D_2O increased. It was proposed that if the N–N moiety in SF2415A3 is being observed as a diazonium group, the resonance for C6 would also disappear as the amount of D_2O increased. However, the resonance for C6 did not disappear after the addition of 0.2% D_2O and instead behaved much like the C1 and C4 ketones of the hydroquinone core, thereby suggesting that SF2415A3 is observed as a diazoketone (Figure 1.6).

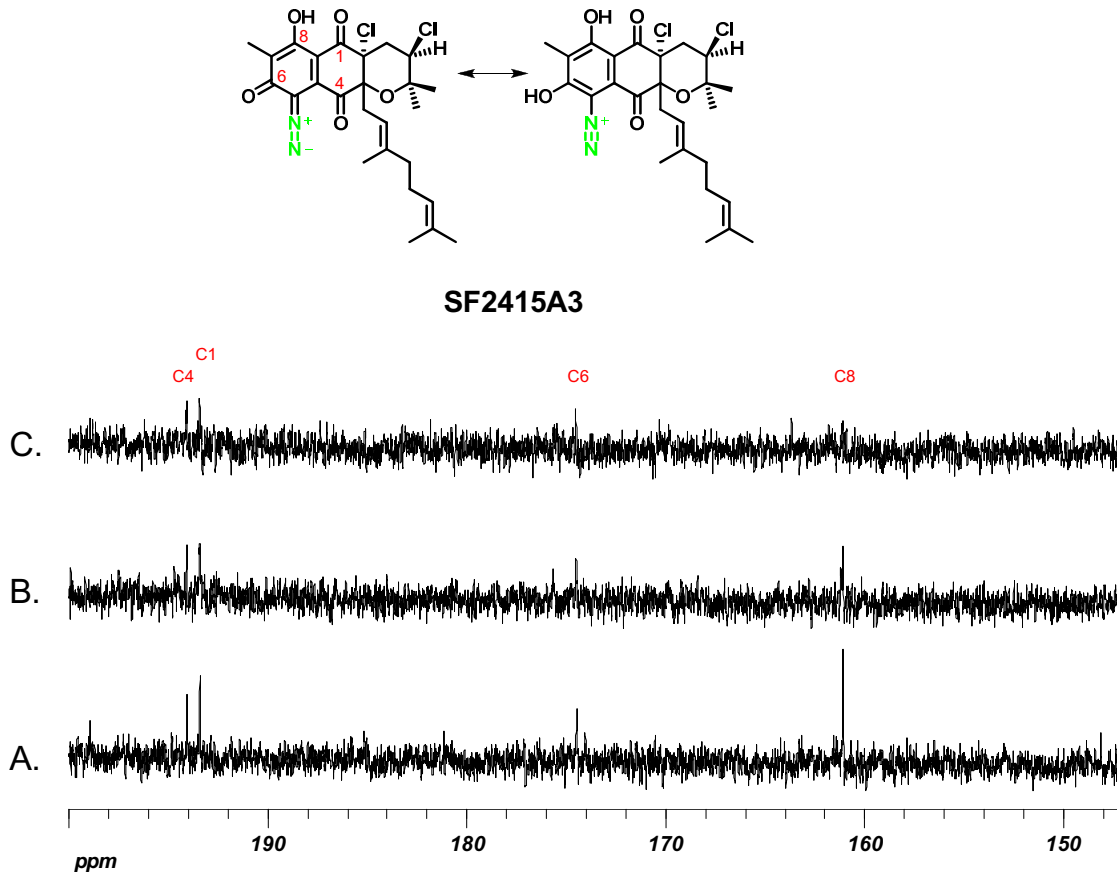

Figure 1.6: A partial ^{13}C NMR spectum of SF2415A3. A) 0 % D_2O. B) 0.1% D_2O. C) 0.2 % D_2O. Carbon atoms analyzed are highlighted in red.

1.3.5: ^{15}N feeding studies

The biosynthetic origin of the diazo functional group, as found in SF2415A3 and A80915D, and its relation to azamerone was addressed by turning to past biosynthetic studies conducted on the natural product kinamycin D (Figure 1.3). Considering a similar scenario, we administered different forms of ^{15}N-enriched substrates; including ammonium sulfate, nitrite, and nitrate, and measured their incorporation into azamerone and A80915D by MS and NMR spectroscopy (Table 1.1).

Table 1.1: ^{15}NMR spectroscopic data of azamerone and A80915D and incororation percentages from nitrogen labeled precursors.

	Enrichment of azamerone[a]		Enrichment of A80915D[a]	
Labeled Precursors	Singly/ Doubly	δ^{15}N ppm [b]	Singly/ Doubly	δ^{15}N ppm [c]
Na[$^{15}NO_2$]	77/6	-2	77/-	-31
Na[$^{15}NO_3$]	74/3	-2	79/-	-31
[$^{15}NH_4$]$_2SO_4$	11/-	-2 & 13	7/-	-[d]
[$^{15}N_2H_4$]SO_4	5/0.3	-2 & 13	0/-	-[d]
[2-^{15}N, 9-^{13}C]-SF2415A3	11/6	-2	6/4	-[d]

[a] Enrichment was calculated by *m*/*z*[18]; [b] ^{1}H-^{15}N HMBC spectra were measured in CD_3OD at 600 MHz and referenced internally to nitromethane (δ 0 ppm); [c] ^{15}N NMR spectra were measured in CD_3CN at 30.4 MHz and referenced externally to nitromethane (δ 0 ppm); [d] chemical shift(s) were not measured due to inadequate sample size and low enrichment levels.

MS analysis revealed that all ^{15}N-labeled precursors were incorporated to different extents, with the oxidized forms having the highest assimilation rates. While [^{15}N]ammonium sulfate singly enriched azamerone and A80915D by 7–11% (Table 1.1), ^{1}H–^{15}N HMBC analysis of azamerone showed that both nitrogen atoms were equally labeled (Appendix Figure 1A.7–1A.8). This result was in stark contrast to the enrichment by [^{15}N]nitrite and [^{15}N]nitrate, which were not only incorporated to a much greater extent at greater than 70% but only labeled one of the two nitrogen atoms in the natural product (Appendix Figures 1A.7 and 1A.9).

In the case of A80915D, ^{15}N NMR spectral analysis showed selective enrichment of the distal diazo nitrogen (δ = –31 ppm)[19, 20] (Appendix Figure 1A.10). ^{15}N-labeling of azamerone gave rise to an enhanced signal at δ = –2 ppm, which was assigned to the C6-bound nitrogen N2 (Figure 1.5) in the

pyridazine ring based upon the $J_{H\text{-}N}$ coupling constants in the $^{1}H–^{15}N$ HMBC experiment (Appendix Figure 1A.7).

Results from the ^{15}N-enrichment studies suggested that the napyradiomycin diazo group is also formed in a stepwise manner. Oxidation of the naphthyl ring at C5 facilitates the introduction of the first nitrogen atom by a transamination reaction. The formation of the N–N bond arises from a nucleophilic attack of the aminodihydroquinone intermediate on nitrous acid (Scheme 1.2).

Scheme 1.2: Proposed biosynthetic pathway for the diazo chlorinated meroterpenoids and their relation to the chlorinated dihydroquinones. A summation of the two [1,2-$^{13}C_2$]acetate-labeling patterns are shown in bold (lines and dots signify double and single enrichments, respectively). Enrichment from L-[methyl-^{13}C]methionine is shown in red, and enrichment from [^{15}N]nitrite or [^{15}N]nitrate is shown in green.

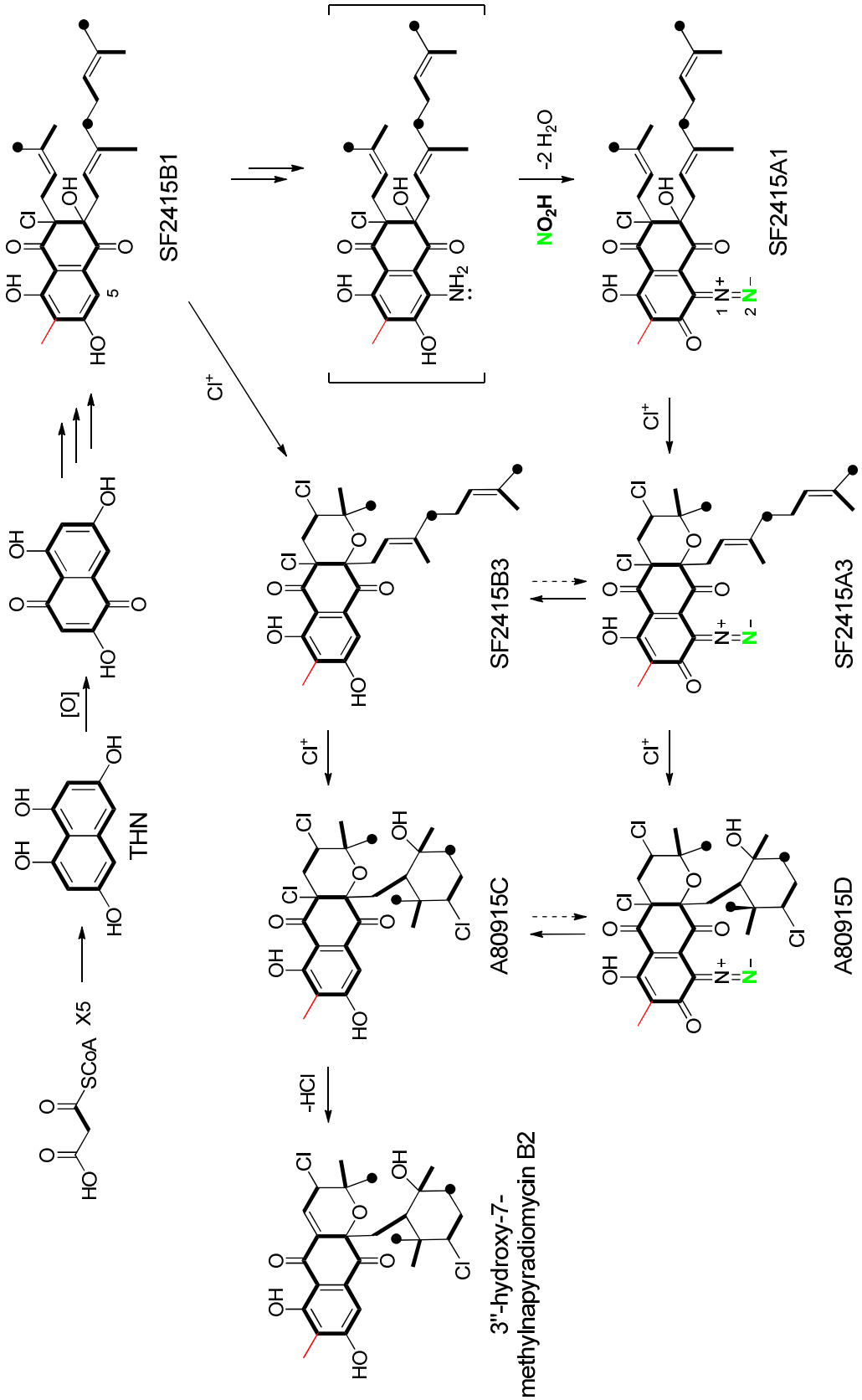
SCoA
X5
THN
[O]
SF2415B1
Cl+
-HCl
SF2415B3
A80915C
3''-hydroxy-7-methylnapyradiomycin B2
NO2H
-2 H2O
SF2415A1
SF2415A3
A80915D

1.3.6: Nitrogen fixation

The direct addition of a dinitrogen precursor was also probed with [$^{15}N_2$]hydrazine to determine if a hydrazine intermediate generated from the nitrogen fixation pathway is attached to the quinone through a transamination reaction. Dinitrogen fixation is a biological process carried out by prokaryotic organisms known as diazotrophs.[21] These organisms are able to reduce molecular nitrogen into ammonia, which is a more readily assimilated form of nitrogen and can be further oxidized to nitrite and nitrate (Figure 1.7). The nitrogenase complex, encoded by the *nif*HDK operon, catalyzes the conversion of molecular nitrogen to two molecules of ammonia. The complex consists of two metalloproteins that are highly conserved in sequence and structure and universal in all diazotrophs (Figure 1.7).[22] Oligotrophic oceans are commonly important niches for diazotrophs, and early work on nitrogen fixation usually focused on the filamentous cyanobacterium *Trichodesmium*.[21] Recently, discrepancies between geochemical estimates of nitrogen fixation and measured nitrogen fixation rates from field population *Trichodesmium* led to the realization that the diversity and abundance of oceanic diazotrophs were underestimated.[21]

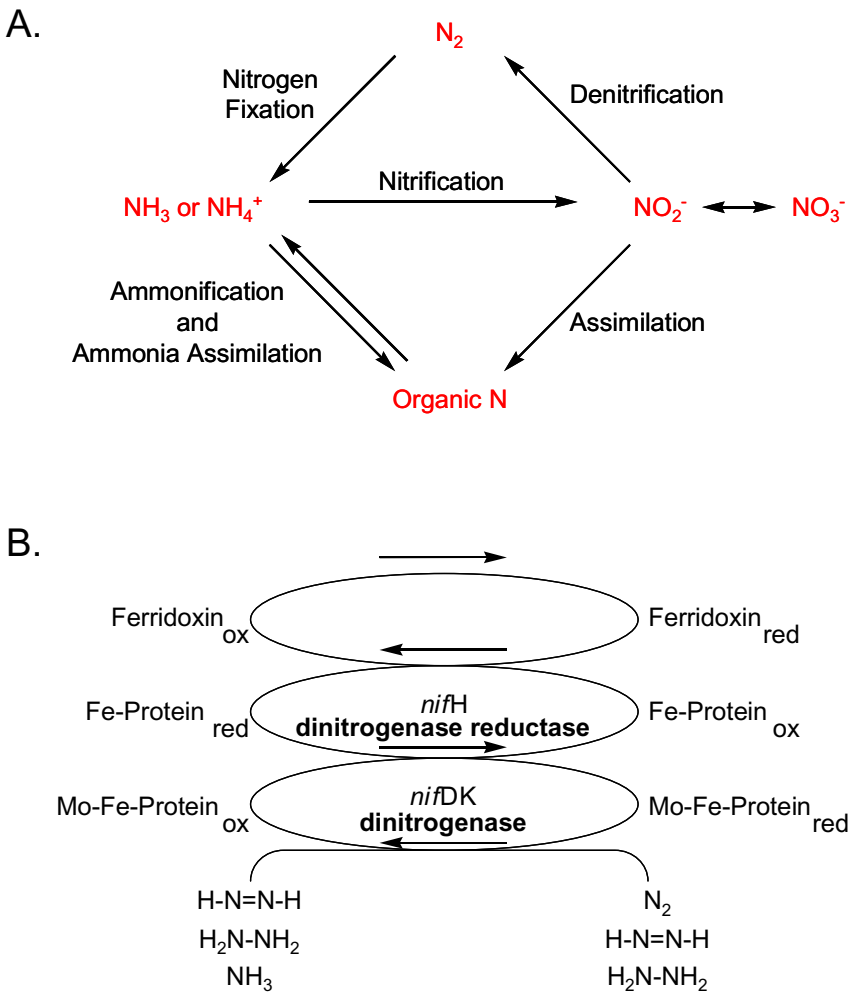

Figure 1.7: A) The nitrogen cycle. B) The nitrogenase complex.

MS analysis revealed that [$^{15}N_2$]hydrazine was only incorporated singly and at a low level into azamerone (Table 1.1). Furthermore, ^{1}H–^{15}N HMBC analysis showed that both nitrogen atoms in azamerone were labeled (Appendix Figure 1A.7). Yet, unlike the [^{15}N]ammonium–labeled product, N2 was enriched to a slightly higher extent than N1, suggesting that metabolism of hydrazine in *S.* sp. CNQ-766 results in nonequivalent forms of single nitrogen species (Appendix Figure 1A.11).

1.3.7: Biotransformation of the aryl diazoketone SF2415A3

The ^{15}N labeling studies indirectly supported that the diazo group, such as those in SF2415A3 and A80915D, is a biosynthetic precursor to the pyridazine unit in azamerone based on their similar isotope characteristics. To unequivocally link the aryl diazoketones to azamerone, we biosynthetically prepared [2-^{15}N, 9-^{13}C]SF2415A3 from [^{15}N]nitrite and L-[methyl-^{13}C]methionine (Appendix Table 1A.5 and Figures 1A.12–1A.14) and fed the labeled natural product back to *S.* sp. CNQ-766. HPLC-MS analysis of the other napyradiomycin derivatives indicated that SF2415A3 was converted into A80915D and azamerone with retention of both isotopes in the same molar ratio as in the substrate. The chlorinated dihydroquinones A80915C and 3”-hydroxy-7-methylnapyradiomycin B2 also showed a single enrichment indicating that SF2415A3 was converted into these analogs after loss of the diazo group. Isolation and characterization by NMR spectroscopy of [2-^{15}N, 9-^{13}C]SF2415A3-enriched azamerone showed ^{13}C enrichment at C8 (Appendix Figure 1A.15) and ^{15}N enrichment at N2 (Appendix Figure 1A.7), thereby confirming that not only is SF2415A3 a precursor of azamerone, but the diazo N2 atom is biosynthetically equivalent with N2 of the pyridazine group in azamerone.

These stable isotope experiments link azamerone to the napyradiomycin family of chlorinated meroterpenoids, in which a Baeyer-Villiger-type oxidation of a diazonaphthoquinone, such as A80915D, may initiate the biosynthetic interconversion (Scheme 1.3). Hydrolysis of the 7-membered heterocyclic

intermediate would open the ring to facilitate both the 1,2-alkyl shift of the monoterpene subunit and the assembly of the pyridazine ring, in which the diazo group forms a new linkage with the C8 diketide. Aromaticity of the ring would be restored by subsequent decarboxylation and dehydration reactions.

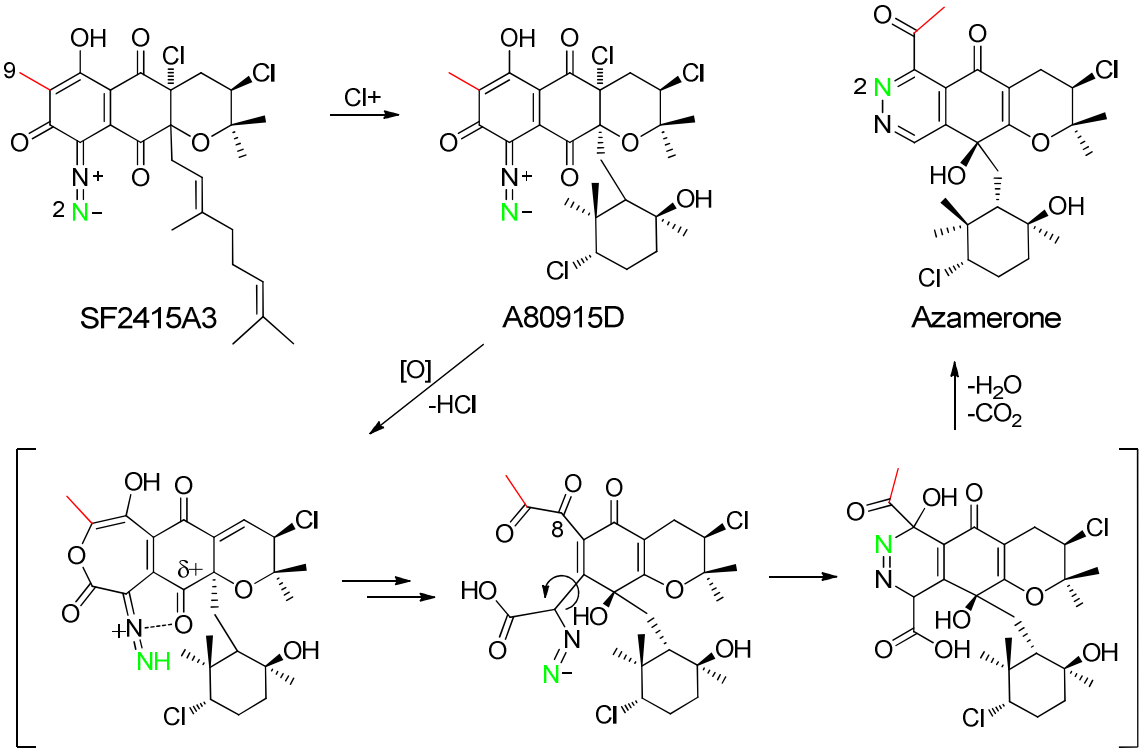

Scheme 1.3: Proposed oxidative rearrangement of the aryl diazoketone SF2415A3 via A80915D to azamerone in *S.* sp. CNQ-766. Isotopically labeled C and N atoms from [2-^{15}N, 9-^{13}C]SF2415A3 are shown in red and green, respectively.

1.4: Conclusion

Using ^{13}C- and ^{15}N-labeled precursors, it was established that azamerone is biosynthesized via SF2415A3 in which the diazo group is derived from the sequential addition of two nitrogen atoms. The aryl diazoketone undergoes a novel rearrangement wherein the aromatic ring is oxidatively cleaved to allow for its rearomatization with a dinitrogen group to give the unique phthalazinone core of azamerone. This unprecedented biochemistry extends our limited knowledge of the biosynthesis of natural products containing N–N bonds and opens the door to exploring and exploiting its molecular basis at the biochemical and genetic levels.

1.5: Appendix

Table 1A.1: Components of A1[22] and M1[13] growth media.

A1 Media	
Starch	10 g
Yeast Extract	4 g
Bacto-peptone	2 g
Real sea H_2O	1 L

M1 Media	
Glucose	10 g
Molasses	20 g
Bacto-peptone	5 g
$CaCO_3$	2 g
KCl	0.2 g
$MgSO_4$ $7H_2O$	0.2 g
$FeSO_4$ $7H_2O$	0.004 g
dd H_2O	1 L
Adjust to pH 7.0 before autoclaving	

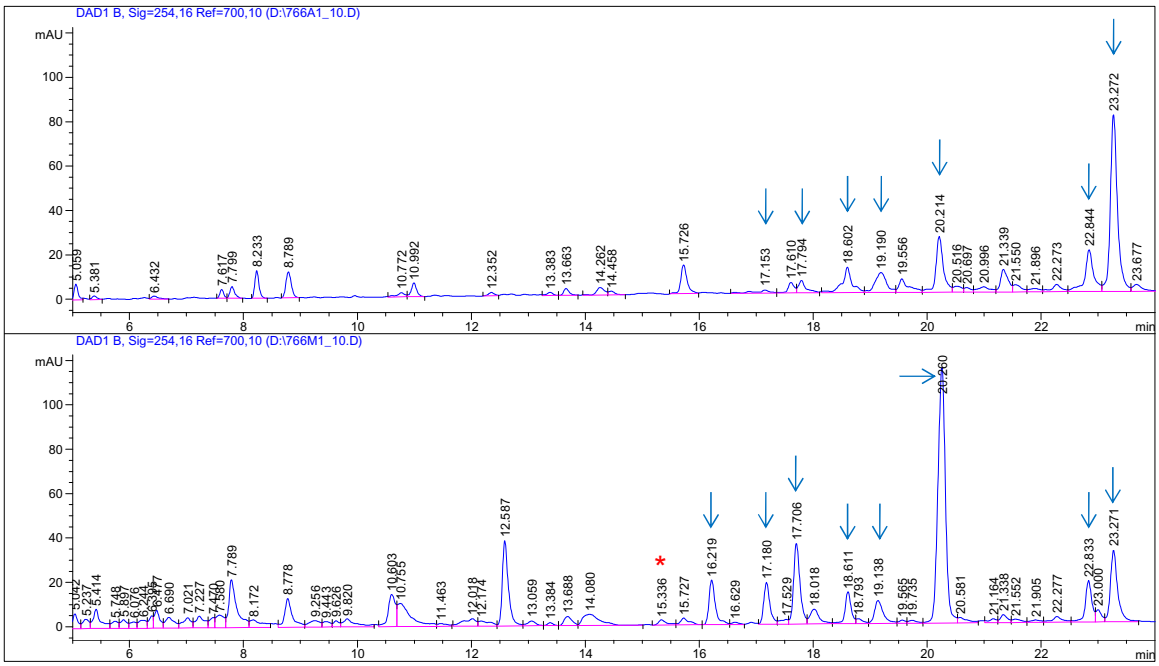

Figure 1A.1: Comparative HPLC analysis of crude extracts from *S.* sp. CNQ-766. A) Grown in A1 growth media. B) Grown in M1 growth media. UV light detection was observed at 254 nm with a linear solvent gradient of 10–100% acetonitrile:water over 20 minutes with a Luna 4.6 x 100 mm C18 column. Azamerone's t_R=15.336 minutes and is highlighted with a red asterick. All napyradiomycin based compounds are denoted with a blue arrow.

Table 1A.2: Production of azamerone.

Media	Mass of crude extract	Amount of Azamerone Isolated
M1 Growth Media	130 mg	8.5 mg/L
A1 Growth Media	60 mg	0.233 mg/L

Table 1A.3: Percent enrichment of L-[methyl-^{13}C]methionine and coupling constants for [1,2-$^{13}C_2$]acetate-enriched A80915C.

		Enrichment Mol (%)[a]	J_{cc} (Hz)
Carbon[b]	δ_C (ppm)[c],[d]	L-[methyl-^{13}C]-methionine[c]	[1,2-$^{13}C_2$]acetate[e]
1	192.67	-	58, 40
2	80.32	-	40, 37
3	85.66	-	39, 37
4	190.91	-	52, 39
4a	131.92	-	64, 52
5	108.7	-	69, 64
6	164.33	-	69, 61
7	120.35	-	69[f]
8	163.35	-	69, 62
8a	107.11	-	62, 58
9	8.45	39	-
1’	42.07	-	34
2’	57.91	-	34
3’	81.53	-	40
4’	23.01	-	40
5’	29.27	-	S[g]
1”	38.25	-	35
2”	52.29	-	35
3”	72.30	-	40
4”	40.53	-	S[g]
5”	29.80	-	35
6”	71.07	-	35
7”	40.82	-	37
8”	28.53	-	S[g]
9”	15.69	-	37
10”	24.40	-	40

[a] Percent enrichment calculated from *m*/*z*;[18] [b] The numbering scheme for A80915C has been adopted from references;[15, 16] [c] ^{13}C NMR spectral data taken at 75 MHz in CD_3OD; [d] δ_C chemical shifts were compared to reported values;[13, 23] [e] ^{13}C NMR spectral data taken at 125 MHz in $CDCl_3$; [f] This signal represents overlapping doublets; [g] enriched singlet based on natural abundance from carbon at 8.45 ppm (C9).

Figure 1A.2: ^{13}C NMR spectrum (125 MHz) of A80915C enriched with [1,2-$^{13}C_2$]acetate in $CDCl_3$.

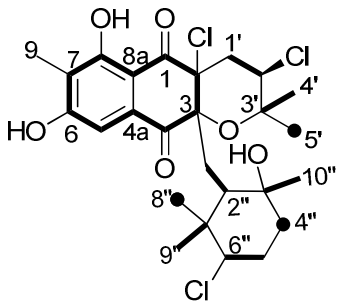

A80915C

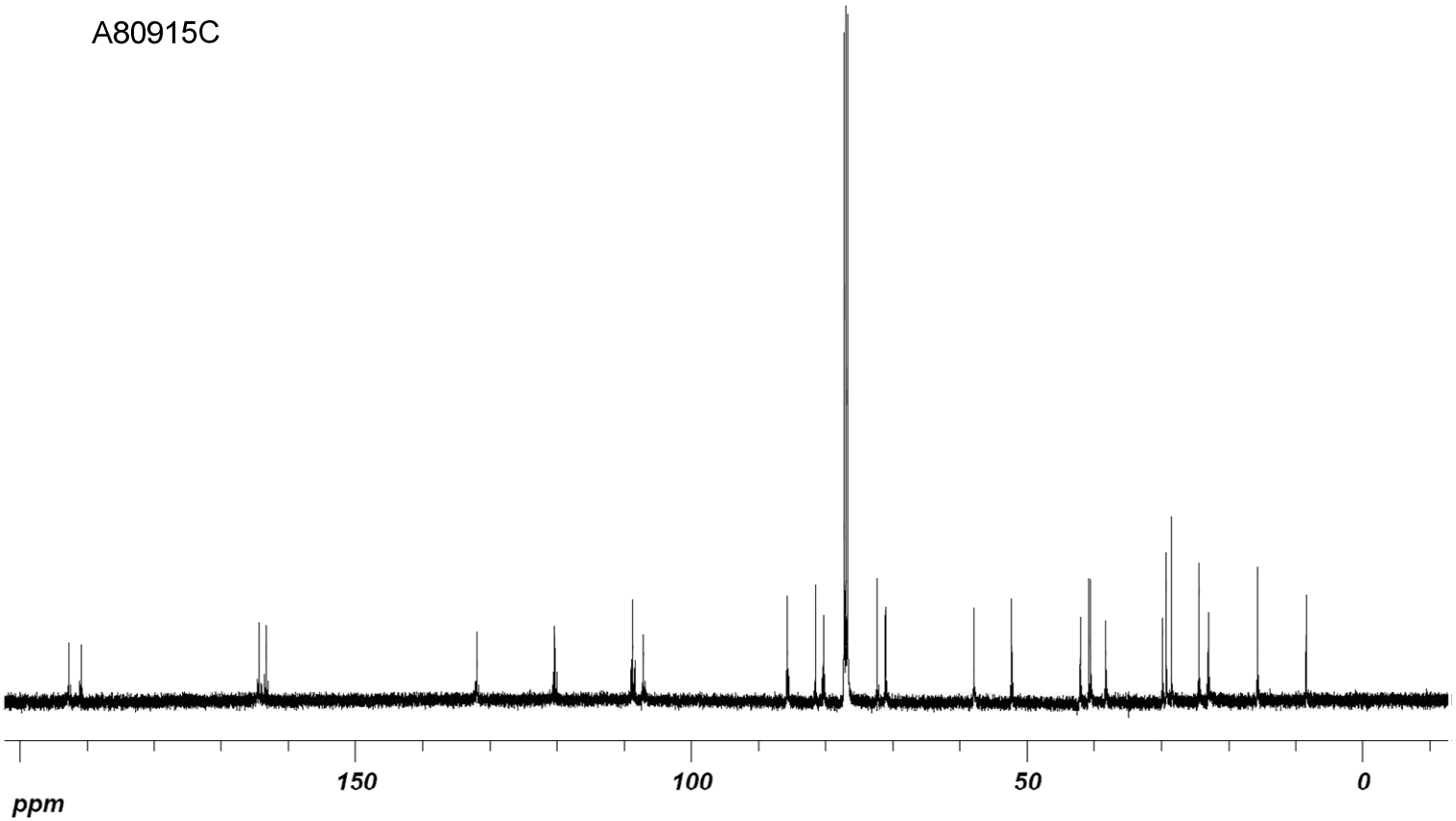

Table 1A.4: Percent enrichment of L-[methyl-^{13}C]methionine and coupling constants for [1,2-$^{13}C_2$]acetate-enriched azamerone.

		Enrichment Mol (%)[a]	J_{cc} (Hz)
Carbon[b]	δ^{13}C ppm[c],[d]	L-[methyl-^{13}C]-methionine[c]	[1,2-$^{13}C_2$]acetate[e]
1	181.6		61, 54
2	110.0		70, 61
3	172.8		70, 54
4	71.4		54, 49
4a	146.5		55, 49
5	152.1		55
6	158.8		59, 57
6a	124.8		57, 54
7	202.5		59
8	30.0	26	–
1’	27.7		36
2’	59.3		36
3’	82.7		41
4’	21.8		40
5’	26.1		S[f]
1“	41.9		37
2“	51.4		37
3“	72.4		39
4“	42.6		S[f]
5“	31.9		35
6“	71.6		35
7“	41.6		35
8“	29.2		S[f]
9“	16.4		35
10“	23.8		39

[a] Percent enrichment calculated from *m*/*z*;[18] [b] The numbering scheme for azamerone has been adopted from references;[15, 16] [c] ^{13}C NMR spectral data taken at 75 MHz in CD_3OD; [d] δ_C chemical shifts were compared to reported values;[10] [e] ^{13}C NMR spectral data taken at 125 MHz in CD_3OD; [f] enriched singlet based on natural abundance from carbon at 30.0 ppm (C8).

Figure 1A.3: ^{13}C NMR spectrum (125 MHz) of azamerone biosynthesized from [1,2-$^{13}C_2$]acetate in CD_3OD.

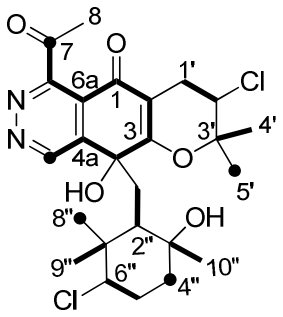

azamerone

Figure 1A.4: ^{13}C NMR spectrum (75 MHz) of A80915C biosynthesized from L-[methyl-^{13}C]methionine in CD_3OD.

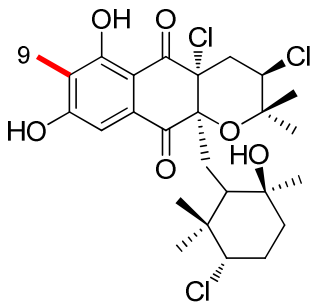

A80915C

Figure 1A.5: ^{13}C NMR spectrum (75 MHz) of azamerone biosynthesized from L-[methyl-^{13}C]methionine that was administered at the time of inoculation. The specturm was taken in CD_3OD.

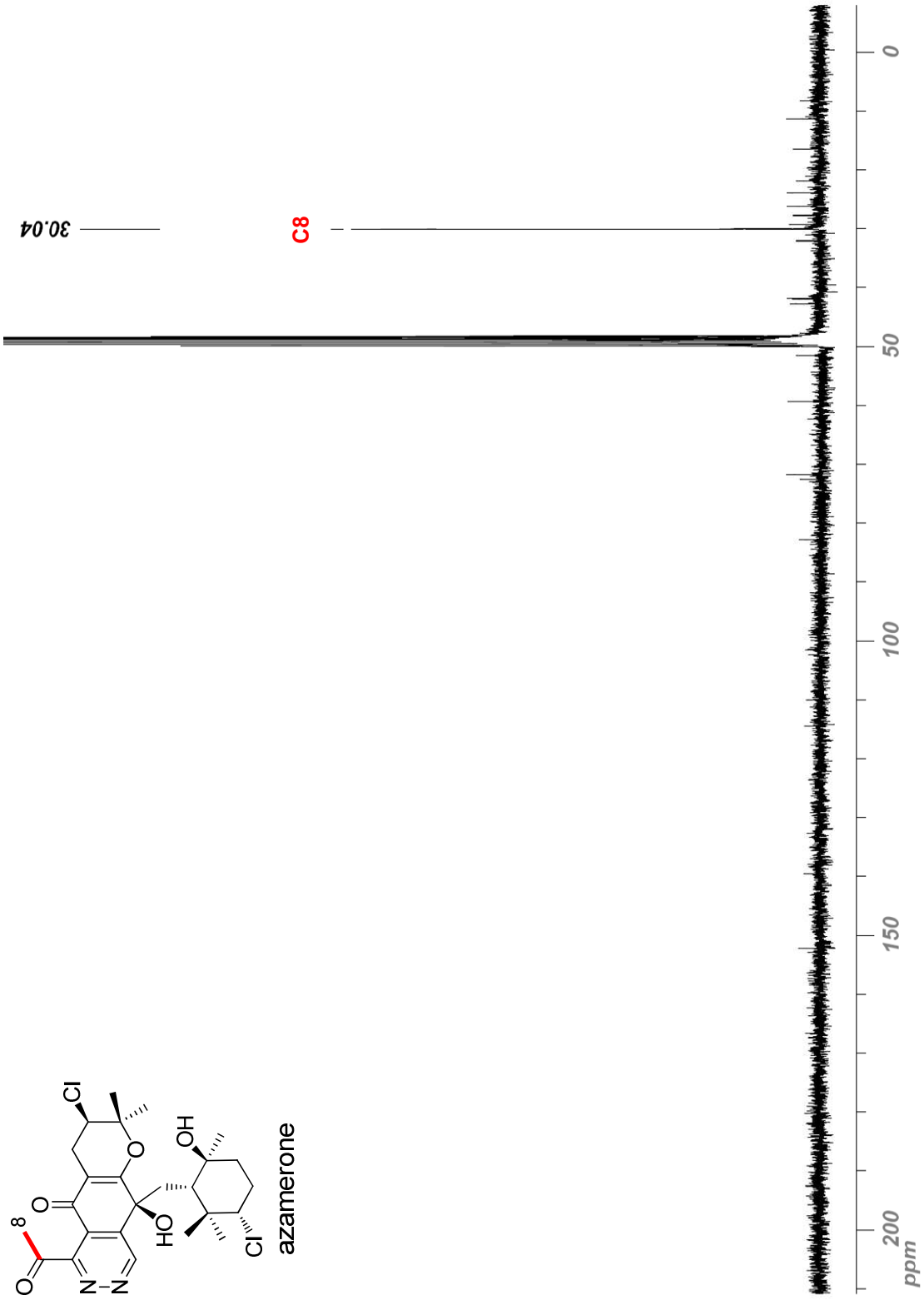
30.04
C8
0
50
100
150
200
ppm
azamerone

Figure 1A.6: ^{13}C NMR spectrum (75 MHz) of azamerone biosynthesized from L-[methyl-^{13}C]methionine that was administered at day 5. The specturm was taken in CD_3OD.

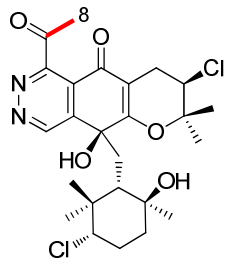

azamerone

Figure 1A.7: ^{1}H-^{15}N NMR spectra of ^{15}N-enriched azamerone in CD_3OD. A) $^{15}NO_2$-enriched and spiked with NO_2CH_3; B) $^{15}NH_4^+$-enriched and spiked with NO_2CH_3; C) [2-^{15}N, 9-^{13}C]SF2415A3-enriched; D) $^{15}N_2H_4$-enriched.

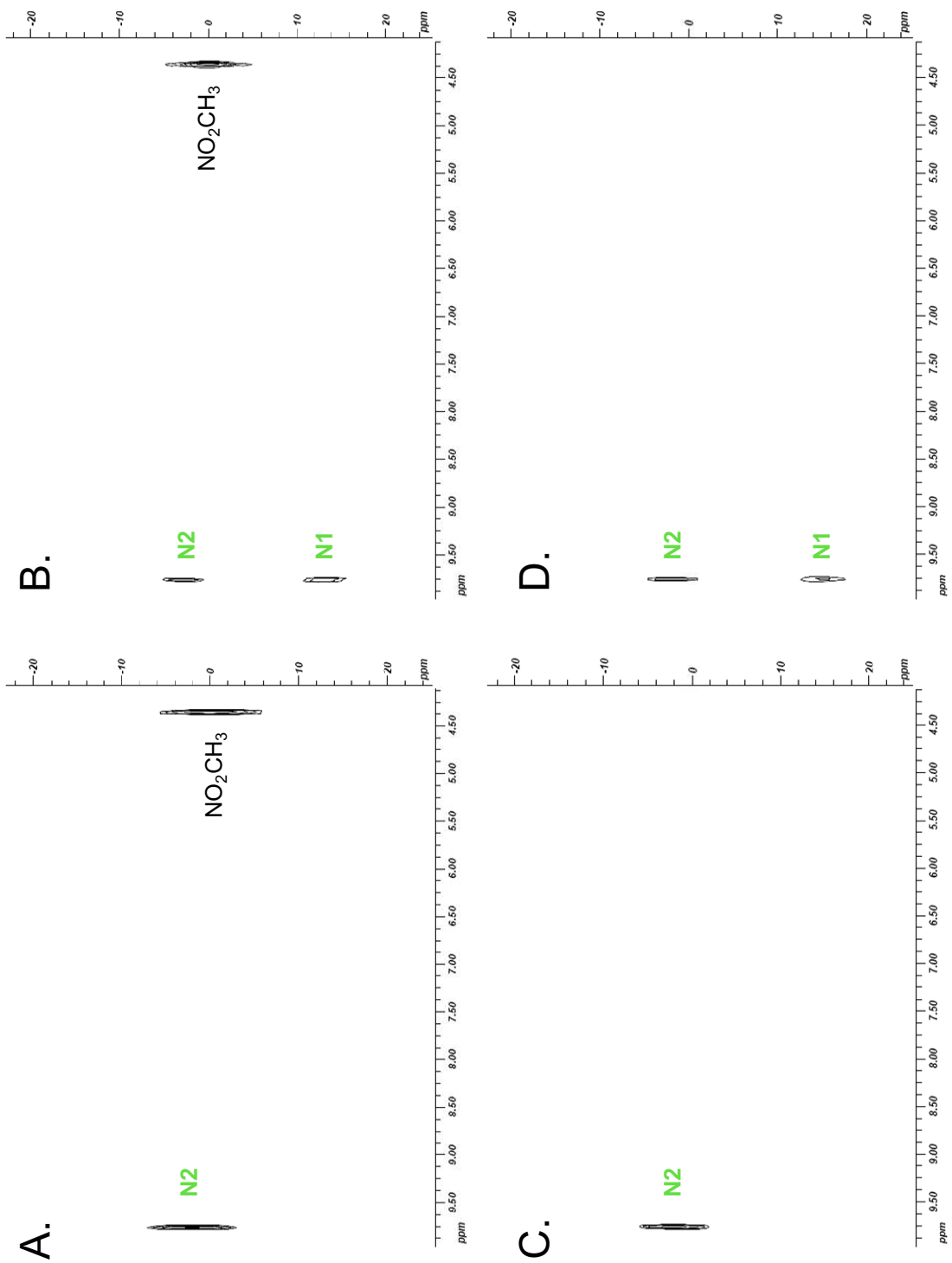
A.
B.
C.
D.
N2
N1
NO_2CH_3
ppm

Figure 1A.8: ^{1}H NMR spectrum (500 MHz) of $^{15}NH_4$-enriched azamerone in CD_3OD. The H5 resonance (shown as a blue asterisk) is blown-up to show that there is no coupling between the proton and nitrogen atoms.

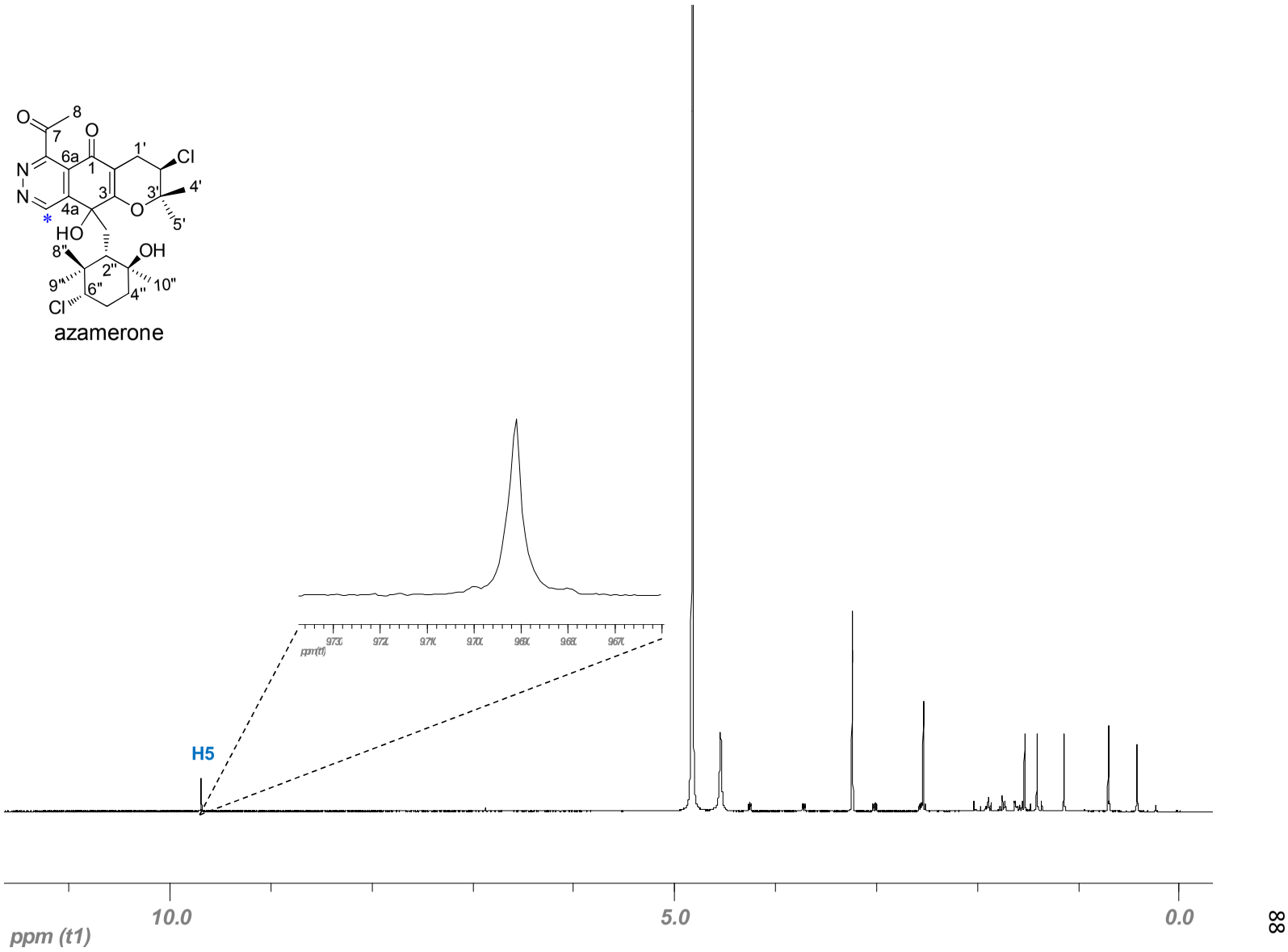
azamerone
H5
10.0
5.0
0.0
ppm (t1)

Figure 1A.9: ^{1}H NMR spectrum (500 MHz) of $^{15}NO_2$-enriched azamerone in CD_3OD. The H5 resonance (shown as a blue asterisk) is blown-up to show the $^{3}J_{HN}$ coupling constant.

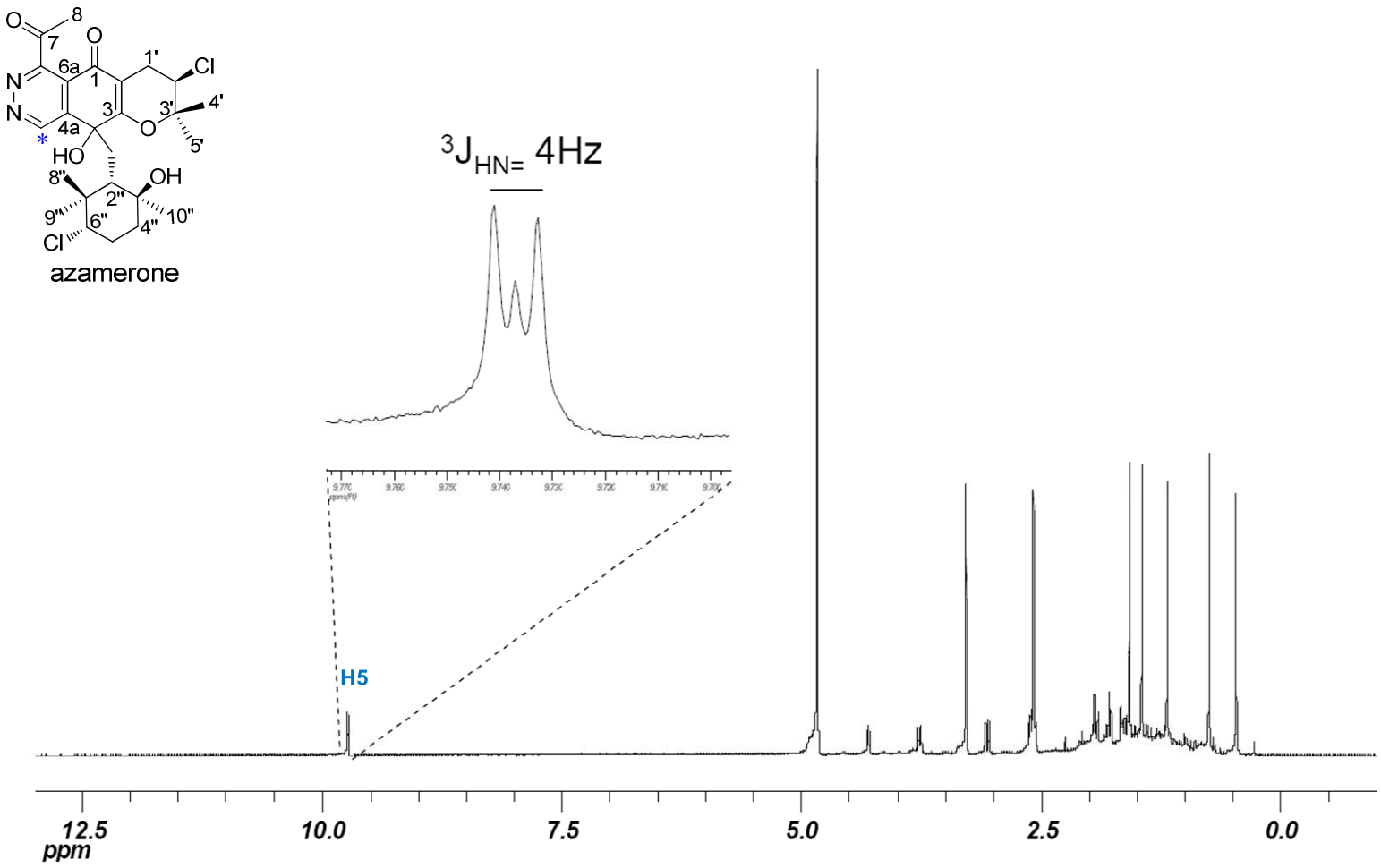
azamerone
$^3J_{HN=}$ 4Hz
H5
12.5
ppm
10.0
7.5
5.0
2.5
0.0

Figure 1A.10: ^{15}N NMR spectrum (30.4 MHz) of $^{15}NO_2$-enriched A80915D in CD_3CN.

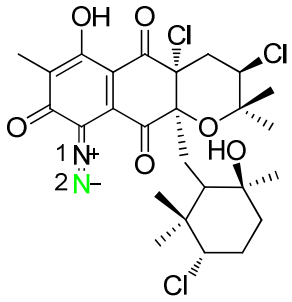
OH
O
Cl
Cl
O
O
1 N+
2 N–
O
HO
Cl

A80915D

-30.90
-135.31
CD3CN
N2
400
300
200
100
0
-100
-200
-300
-400
ppm

Figure 1A.11: ^{1}H-^{15}N NMR spectra of $^{15}N_2H_4$-enriched azamerone in CD_3OD. A) J_{HN}= 4Hz; B) J_{HN}= 20 Hz.

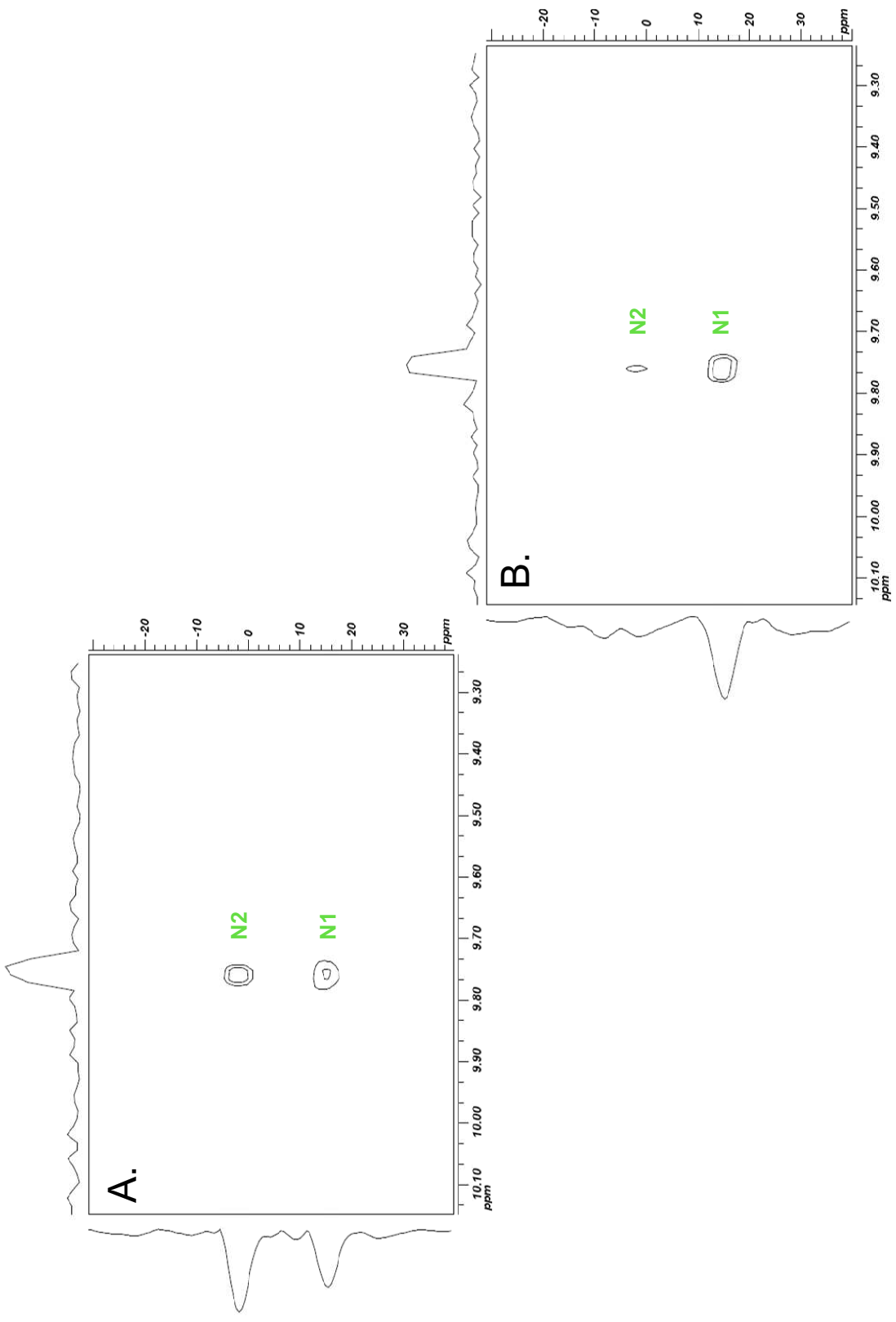
A.
N2
N1
B.
N2
N1
ppm

Table 1A.5: Assignments of ^{13}C and ^{15}N and percent enrichment from L-[methyl-^{13}C]methionine and [^{15}N]nitrite for SF2415A3.

		Percent Enrichment Mol (%)[a]		Percent Enrichment Mol (%)[a]
Carbon[b]	$\delta^{13}C$ ppm[c],[d]	L-[methyl-^{13}C] Methionine[c]	Nitrogen	[$^{15}NO_2$]Na[g]
1	192.8		1	
2	78.3		2	75
3	83.6			
4	193.4			
4a	134.2			
5	79.2[f]			
6	173.7			
7	123.2			
8	160.2			
8a	113.0			
9	9.1	30		
1’	42.8			
2’	58.1			
3’	79.2[f]			
4’	22.3			
5’	28.7			
1”	41.6			
”	114.6			
3”	143.6			
4”	39.7			
5”	26.2			
6”	123.3			
7”	132.0			
8”	25.6			
9”	17.5			
10”	16.5			

[a] Percent enrichment calculated from *m/z*;[18] [b] The numbering scheme for SF2415A3 has been adopted from references[15, 16]; [c] ^{13}C NMR spectral data taken at 75 MHz in $CDCl_3$; [d] δ_C chemical shifts were compared to reported values[15]; [f] overlapping signals; [g] ^{15}N NMR spectral data taken at 50.7 MHz in $CDCl_3$.

Figure 1A.12: ^{13}C NMR spectrum (75 MHz) of [2-^{15}N, 9-^{13}C]SF2415A3 in $CDCl_3$.

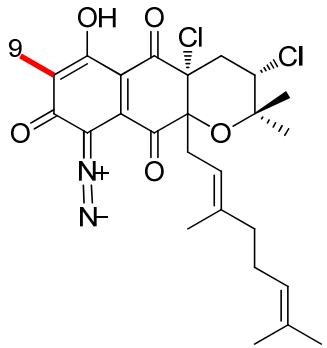

SF2415A3

Figure 1A.13: ^{15}N NMR spectrum (50.8 MHz) of [2-^{15}N, 9-^{13}C]SF2415A3 (**6**) in $CDCl_3$ referenced externally to NO_2CH_3.

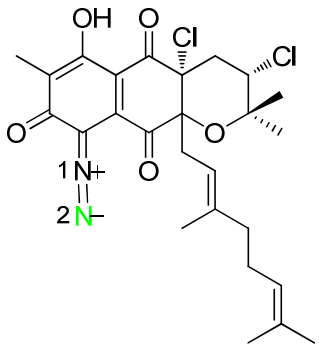

SF2415A3

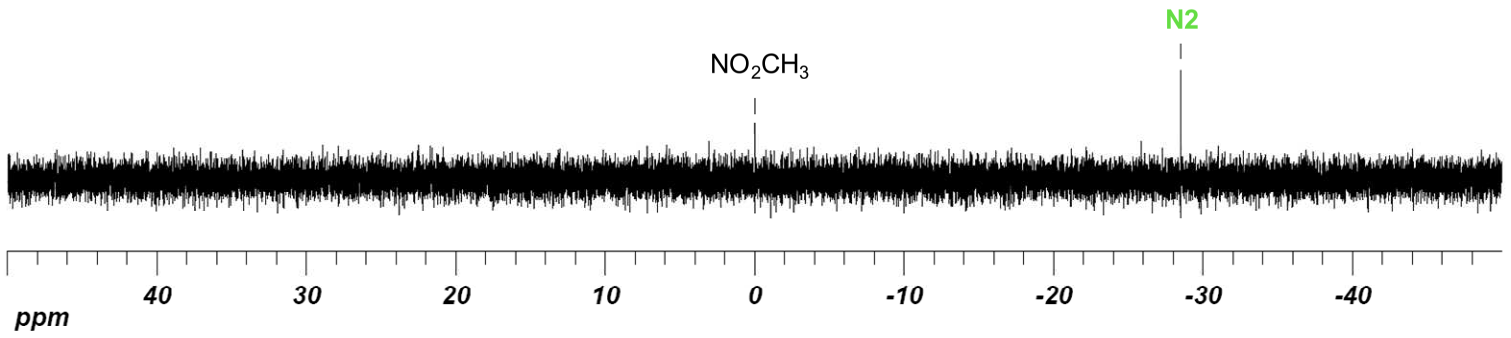

Figure 1A.14: ^{15}N NMR spectrum (50.8 MHz) of [2-^{15}N, 9-^{13}C]SF2415A3 in $CDCl_3$ referenced externally to NH_3.

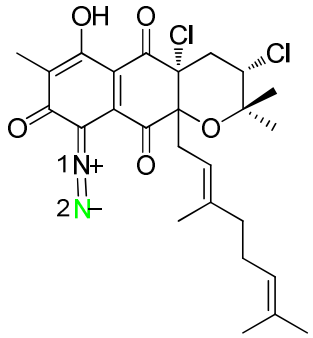
OH
O
Cl
Cl
O
O
O
1N+
2N–

SF2415A3

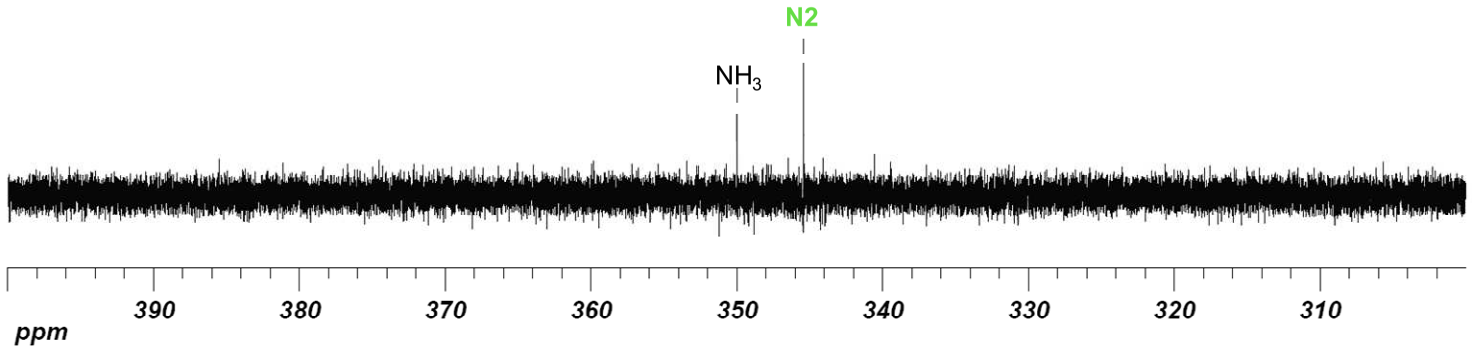
350.00
345.42
N2
NH3
390
380
370
360
350
340
330
320
310
ppm

Figure 1A.15: Portion of ^{13}C NMR spectrum (75 MHz) of azamerone in CD_3OD. A) Unlabeled standard; B) Labeled from [2-^{15}N, 9-^{13}C]SF2415A3. The carbon that is enriched is highlighted in red.

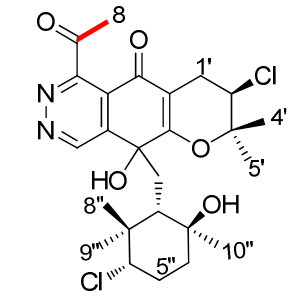
O
8
O
1'
Cl
N
N
4'
O
5'
HO
8"
OH
9"
10"
5"
Cl

azamerone

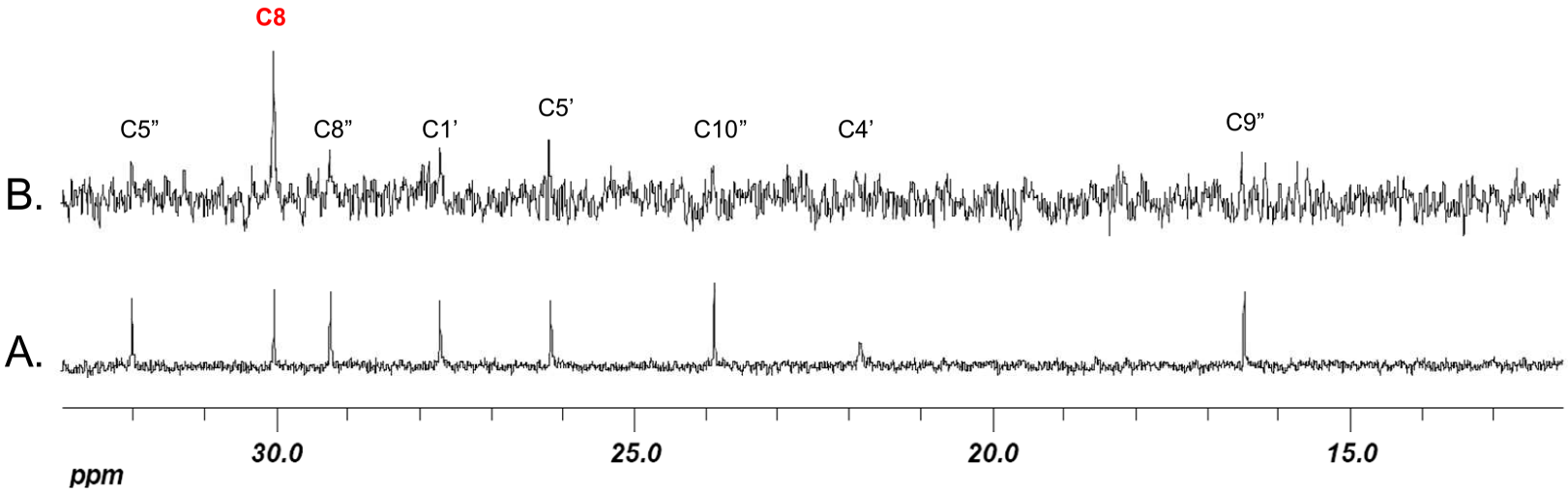
C8
C5”
C8”
C1’
C5’
C10”
C4’
C9”
B.
A.
30.0
25.0
20.0
15.0
ppm

1.6 References

1. LaRue, T. A., Naturally occurring compounds containing a nitrogen-nitrogen bond. *Lloydia* **1977,** 40, 307-21.

2. Langley, B. W.; Lythgoe, B.; Riggs, N. V., Macrozamin. Part II. The aliphatic azoxy structure of the aglycone part. *J. Chem. Soc.* **1951**, 2309-2316.

3. Parry, R. J.; Li, Y.; Lii, F. W., Biosynthesis of azoxy compounds. Investigation of valanimycin biosynthesis. *J. Am. Chem. Soc.* **1992,** 114, 10062-64.

4. Garg, R. P.; Gonzalez, J. M.; Parry, R. J., Biochemical characterization of VlmL, a Seryl-tRNA synthetase encoded by the valanimycin biosynthetic gene cluster. *J. Biol. Chem.* **2006,** 281, 26785-91.

5. Garg, R. P.; Qian, X. L.; Alemany, L. B.; Moran, S.; Parry, R. J., Investigations of valanimycin biosynthesis: elucidation of the role of seryl-tRNA. *Proc. Natl. Acad. Sci. USA* **2008,** 105, 6543-47.

6. Bockholt, H.; Beale, J. M.; Rohr, J., Biosynthetic investigations on pyridazomycin. *Angew. Chem. Int. Ed. Engl.* **1994,** 33, 1648-51.

7. Garg, R. P.; Alemany, L. B.; Moran, S.; Parry, R. J., Identification, characterization, and bioconversion of a new intermediate in valanimyicn biosynthesis. *J. Am. Chem. Soc.* **2009,** 131, 9608-09.

8. Gould, S. J.; Melville, C. R.; Cone, M. C.; Chen, J.; Carney, J. R., Kinamycin biosynthesis. Synthesis, isolation, and incorporation of stealthin C, an aminobenzo[*b*]fluorene. *J. Org. Chem.* **1997,** 62, 320-24.

9. Gould, S. J.; Melville, C. R., Kinamycin biosynthesis. Synthesis, detection, and incorporation of kinobscurinone, a benzo[*b*]fluorenone. *Bioorg. Med. Chem. Lett.* **1995,** 5, 51-4.

10. Cho, J. Y.; Kwon, H. C.; Williams, P. G.; Jensen, P. R.; Fenical, W., Azamerone, a terpenoid phthalazinone from a marine-derived bacterium related to the genus *Streptomyces* (actinomycetales). *Org. Lett.* **2006,** 8, 2471-74.

11. Grote, R.; Chen, Y.; Zeeck, A.; Chen, Z. X.; Zahner, H.; Mischnick-Lubbecke, P.; Konig, W. A., Metabolic products of microorganisms. 243. Pyridazomycin, a new antifungal antibiotic produced by *Streptomyces violaceoniger*. *J. Antibiot.* **1988,** 41, 595-01.

12. Shiomi, K.; Nakamura, H.; Iinuma, H.; Naganawa, H.; Takeuchi, T.; Umezawa, H.; Iitaka, Y., New antibiotic napyradiomycins A2 and B4 and stereochemistry of napyradiomycins. *J. Antibiot.* **1987,** 40, 1213-19.

13. Fukuda, D. S.; Mynderse, J. S.; Baker, P. J.; Berry, D. M.; Boeck, L. D.; Counter, L. D.; Ensminger, P. W.; Allen, N. E.; Alborn, W. E.; Hobbs, J. N., A80915, a new antibiotic complex produced by *Streptomyces aculeolatus*. Discovery, taxonomy, fermentation, isolation, characterization, and antibacterial evaluation. *J. Antibiot.* **1989,** 63, 623-33.

14. Shiomi, K.; Iinuma, H.; Naganawa, H.; Isshiki, K.; Takeuchi, T.; Umezawa, H., Biosynthesis of napyradiomycins. *J. Antibiot.* **1987,** 40, 1740-45.

15. Gomi, S.; Ohuchi, S.; Sasaki, T.; Itoh, J.; Sezaki, M., Studies on new antibiotics SF2415. II. The structural elucidation. *J. Antibiot.* **1987,** 40, 740-49.

16. Winter, J. M.; Moffitt, M. C.; Zazopoulos, E.; McAlpine, J. B.; Dorrestein, P. C.; Moore, B. S., Molecular basis for chloronium-mediated meroterpene cyclization: cloning, sequencing, and heterologous expression of the napyradiomycin biosynthetic gene cluster. *J. Biol. Chem.* **2007,** 282, 16362-68.

17. Yu, T. W.; Shen, Y.; McDaniel, R.; Floss, H. G.; Khosla, C.; Hopwood, D. A.; Moore, B. S., Engineered biosynthesis of novel polyketides from *Streptomyces* spore pigment polyketide synthases. *J. Am. Chem. Soc.* **1998,** 120, 7749-59.

18. Biemann, K., *Mass Spectrometry: Organic Chemical Applications*. McGraw-Hill: Ney York, 1962; Vol. 2.

19. Seaton, P. J.; Gould, S. J., Orgin of the cyanamide carbon of the kinamycin antibiotics. *J. Am. Chem. Soc.* **1988,** 110, 5912-14.

20. Lippmaa, E.; Pehk, T.; Saluvere, T.; Magi, M., Chemical polarisation of ^{15}N and ^{13}C nuclei in diazo coupling reactions. *Org. Magn. Reson.* **1973,** 5, 441-44.

21. Langlois, R. J.; LaRoche, J.; Raab, P. A., Diazotrophic diversity and distribution in the tropical and subtropical Atlantic Ocean. *Appl. Environ. Microbiol.* **2005,** 71, 7910-19.

22. Halbleib, C. M.; Ludden, P. W., Regulation of biological nitrogen fixation. *J. Nutr.* **2000,** 130, 1081-84.

23. Soria-Mercado, I. E.; Prieto-Davo, A.; Jensen, P. R.; Fenical, W., Antibiotic terpenoid chloro-dihydroquinones from a new marine actinomycete. *J. Nat. Prod.* **2005,** 68, 904-10.

1.7: Acknowledgement

Chapter 1, in full, is a reprint of the material as it appears in Formation of the Pyridazine Natural Product Azamerone by Biosynthetic Rearrangement of an Aryl Diazoketone (2009). Winter, Jaclyn M; Jansma, Ariane L.; Handel, Tracy M.; Moore, Bradley S., Angewandte Chemie International Edition, 48, 767–70. The dissertation author was the primary investigator and author of this paper.

Chapter 2

Cloning, Sequencing, and Heterologous Expression of the Napyradiomycin Biosynthetic Gene Cluster

2.1: Introduction

2.1.1: Biological Cyclization of Terpenes

Nature has devised several mechanisms to polarize the terminal olefin of linear terpenes to facilitate the creation of new C–X bonds. For instance, cyclization of the C_{30} hydrocarbon squalene to steroids and hopanoids is initiated, respectively, by epoxidation and protonation of the terminal olefin (Figure 2.1). Although these biosynthetic strategies are widely distributed among organisms, a third mechanism for terpene cyclization has recently emerged in marine macroalgae that involves bromonium ion-induced ring closure by vanadium-dependent bromoperoxidase (V-BrPO) (Figure 2.2).[1-3]

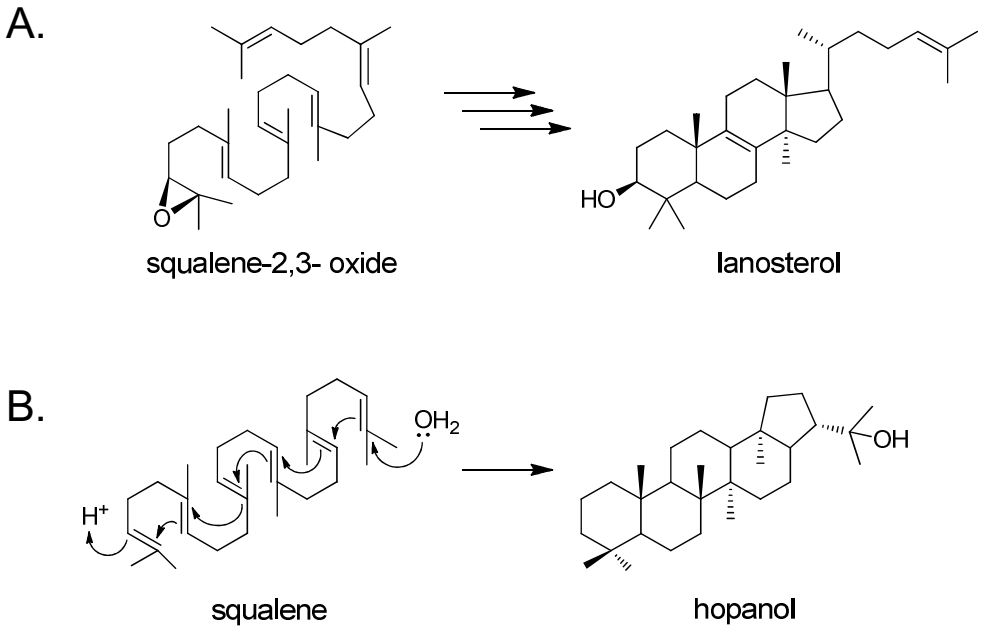

Figure 2.1: Biological cyclization of triterpenes. A) Epoxidation of the terminal olefin to form the steroid lanosterol; B) Protonation of the terminal olefin to form the hopanoid hopanol.

Vanadium-dependent haloperoxidases (V-HPOs) have a limited distribution in nature. These biosynthetic enzymes catalyze the oxidation of halides to their corresponding hypohalous acids at the expense of hydrogen peroxide and are named after the most electronegative halide they are able to oxidize.[4] Because of their ability to halogenate a range of organic compounds in a regio- and stereospecific manner, these enzymes have received increasing attention.[5] V-BrPOs are widely distributed in marine algae, whereas vanadium chloroperoxidases (V-ClPOs) have been isolated primarily from dematiaceous hyphomycete fungi.[1] To date, all known V-HPOs have been characterized *in vitro* from eukaryotic systems,[6] and even though there are numerous chlorinated marine natural products, V-ClPOs have not been functionally characterized from marine organisms.[1, 2, 7] While the biological function of V-ClPOs has yet to be elucidated, marine algal V-BrPOs have been shown through *in vitro* chemoenzymatic conversions to catalyze the cyclization of terpenes and ethers via a bromonium ion mediated mechanism (Figure 2.2). These studies not only demonstrated that the enzymes were able to initiate cyclization of a terpene by a bromonium ion, but also proved that the halogenation reaction occurred with stereochemical control.

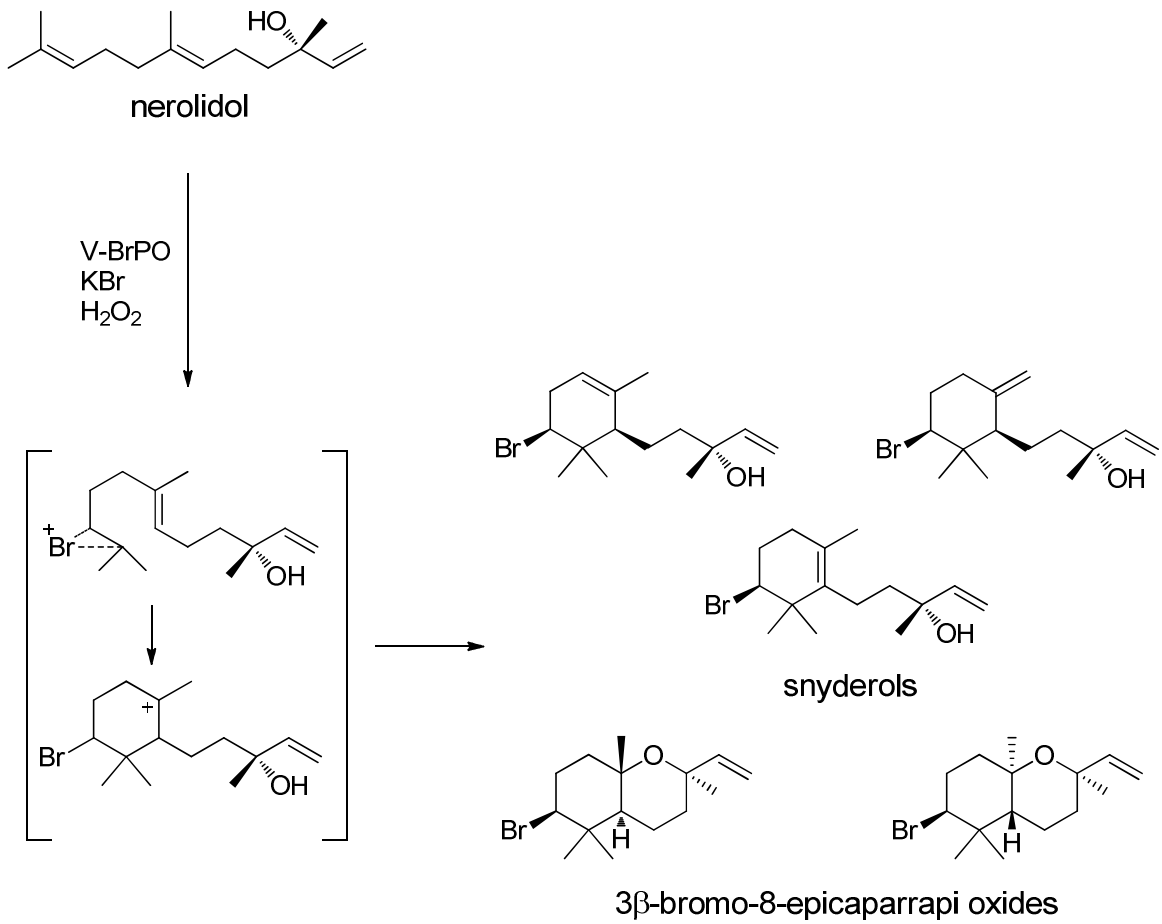

Figure 2.2: V-BrPO chemoenzymatic cyclization of nerolidol to brominated algal natural products.

2.1.2: The Napyradiomycins and Related Analogs

The napyradiomycins are halogenated meroterpenoids (polyketide-terpene hybrids) possessing antibacterial activity toward Gram-positive bacteria.[8] Napyradiomycins A1 and A2, B1–B4, C1 and C2 were first reported from the terrestrial actinomycete *Chainia rubra* MG8092-AF1 in 1986 (Figure 2.3).[8, 9] Since then, similar halogenated naphthoquinones such as A80915A–D,[10, 11] SF2415A3 and B3,[12] 7-methylnapyradiomycin B2,[11] 3"-hydroxy-7-

methylnapyradiomycin B2,[11] 2-deschloro-A80915C,[11] and the semi-naphthoquinones A80915G,[10] SF2415A1–A2 and B1–B2[12] were reported from the terrestrial actinomycete *Streptomyces aculeolatus* NRRL 18442[10, 12] and the marine sediment-derived *Streptomyces* sp. CNQ-525 [11] (Figures 2.3 and 2.4). Further examination of the marine sediment-derived *S.* sp. CNQ-525 revealed that, like the marine sediment-derived *S.* sp. CNQ-755, it too synthesizes azamerone (Figure 2.4) when grown in M1 media (Appendix Figure 2A.1).[13]

Figure 2.3: Structures of the napyradiomycins, diprenylated chlorinated dihydroquinones, and semi-naphthoquinones.

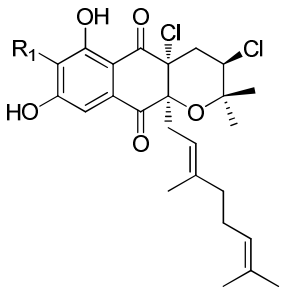

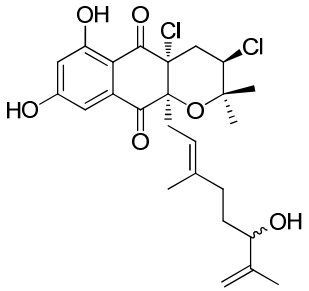

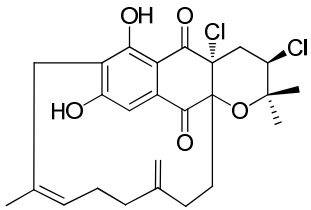

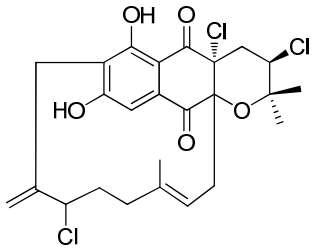

	R_1
Napyradiomycin A1	H
SF2415B3	CH_3

Napyradiomycin A2

Napyradiomycin C1

Napyradiomycin C2

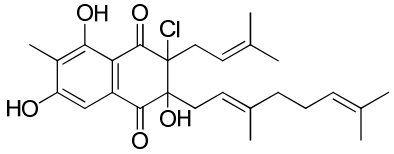

SF2415B1

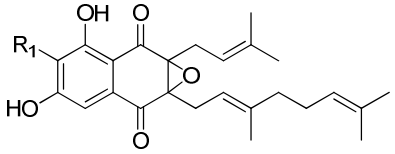

	R_1
A80915G	H
SF2415B2	CH_3

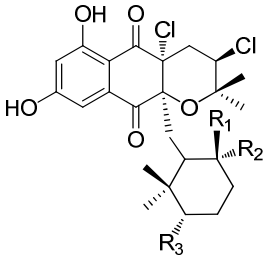

	R_1	R_2	R_3
Napyradiomycin B1	$=CH_2$	-	Cl
Napyradiomycin B2	$=CH_2$	-	Cl
Napyradiomycin B3	OH	CH_3	Br
Napyradiomycin B4	OH	CH_3	Cl

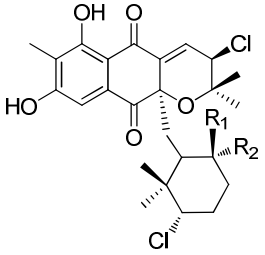

	R_1	R_2
7-methylnapyradiomycin B2	$=CH_2$	-
3"-hydroxy-7-methylnapyradiomycin B2	OH	CH_3

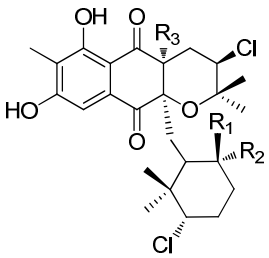

	R_1	R_2	R_3
A80915A	$=CH_2$	-	Cl
A80915C	OH	CH_3	Cl
2-deschloro-A80915C	OH	CH_3	H

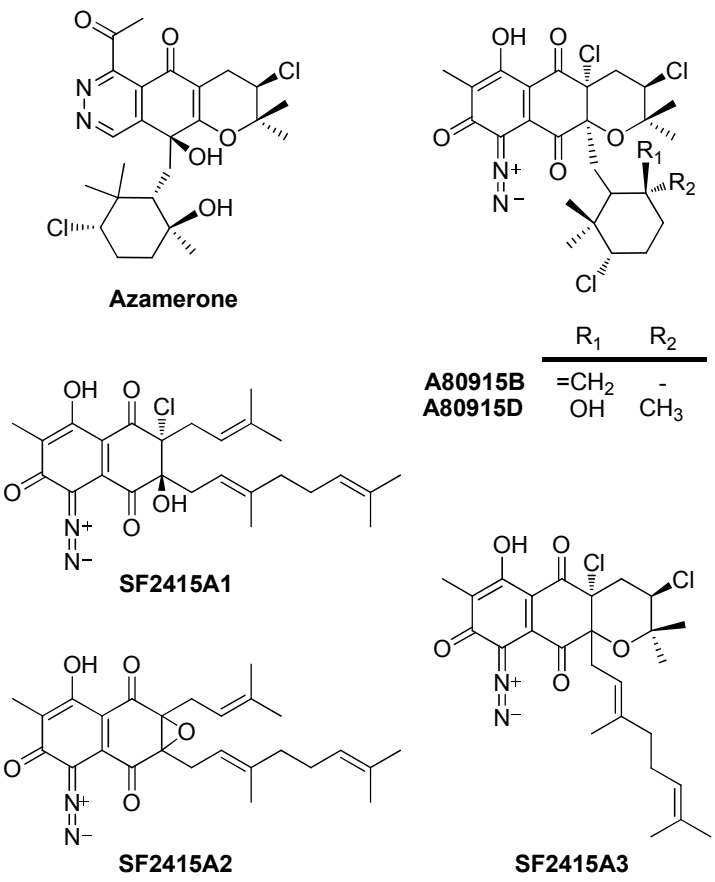

Figure 2.4: Chlorinated dihydroquinones and semi-naphthoquinones possessing a diazo functional group or pyridazine ring.

2.1.3: Chemistry and Biology of the Napyradiomycins and Related Analogs

Stable isotope tracer experiments with [2-^{13}C]- and [1,2-$^{13}C_2$]acetate established that napyradiomycins A1, A2, B1, C1, and C2,[14] the chlorinated dihydroquinones produced by the marine sediment-derived *S.* sp. CNQ-766[13] as well as other meroterpenoids, such as naphterpin,[15] furaquinocin C,[16] neomarinone[17] and furanonaphtoquinone I[18] (Figure 2.5), are biosynthesized from the symmetrical pentaketide 1,3,6,8-tetrahydroxynaphthalene (THN). The

THN core is decorated with isoprenoid units, and in most cases, these building blocks are derived from the mevalonic acid biosynthetic pathway.

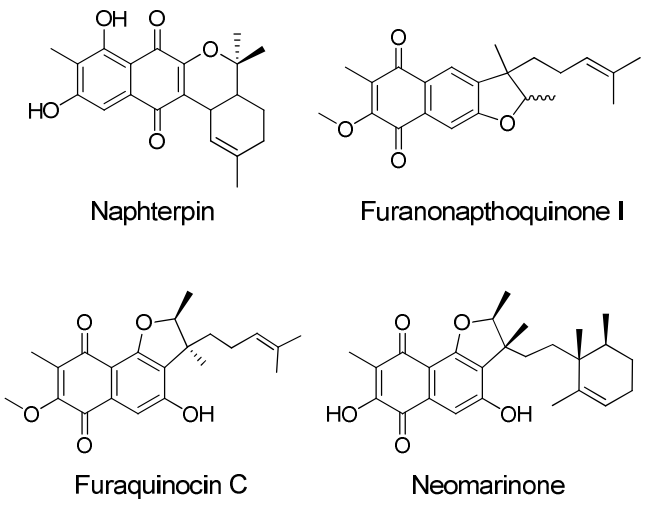

Figure 2.5: Biologically active meroterpenoids possessing a THN core.

Recent biosynthetic gene cluster analysis of the hybrid monoterpene-polyketides furaquinocin from *Streptomyces* sp. strain KO-3988[19] and furanonaphthoquinone I from *Streptomyces cinnamonensis* DSM 1042[18] revealed a clustering of genes coding for the type III polyketide 1,3,6,8-tetrahydroxynaphthalene synthase (THNS), a prenyltransferase, and a complete set of mevalonic acid-specific geranyl diphosphate biosynthetic enzymes. These isoprenoid producing actinomycetes, from which the building blocks are derived from the mevalonic acid biosynthetic pathway, contain a mevalonate biosynthetic gene cassette flanking the natural product biosynthetic cluster. This mevalonate biosynthetic cluster is conserved among strains in which the types of genes, their order, and their orientation are almost identical (Figure 2.6).[20]

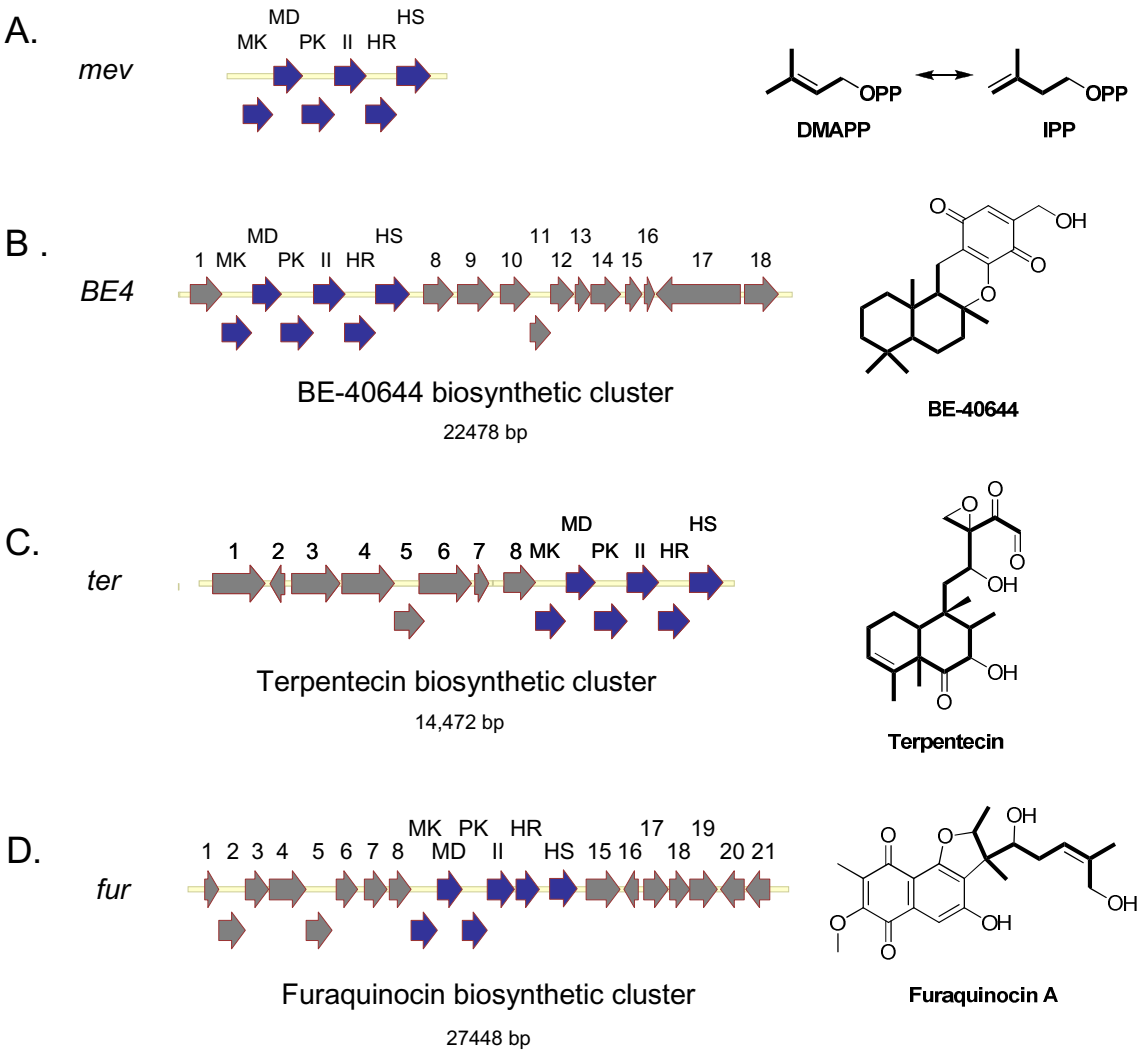

Figure 2.6: Mevalonate biosynthetic gene cassette flanking a natural product biosynthetic cluster. A) Mevalonate biosynthetic gene cassette. B) BE-40644 (*BE4*) biosynthetic cluster.[21] C) Terpentecin (*ter*) biosynthetic cluster.[22] D) Furaquinocin A (*fur*) biosynthetic cluster.[19] Isoprenoid units are highlighted by bold lines. MK= mevalonate kinase, MD= mevalonate diphosphate decarboxylase, PK = phosphomevalonate kinase, II = type 2 isopentenyl diphosphate isomerase, HR = HMG-CoA reductase, HS = HMG-CoA synthase.

2.1.4: Specific Aim

Structural inspections of the bacterial meroterpenoid antibiotics belonging to the napyradiomycin family of chlorinated dihydroquinones suggest that their terpenoid fragments undergo chloronium ion-induced cyclization biochemistry.

The V-HPOs that catalyze such reactions are distributed in fungi and marine algae and have yet to be characterized from bacteria. Given the exclusivity of these enzymes, a cosmid library was constructed to identify the napyradiomycin biosynthetic cluster responsible for the suite of chlorinated dihydroquinones and to verify if V-ClPOs are indeed responsible for the natural product chemistry associated with this suite of halogenated compounds.

2.2: Materials and Methods

2.2.1: Bacterial strains and cultural conditions

Streptomyces sp. CNQ-525 was a gift from Professors William Fenical and Paul R. Jensen (University of California at San Diego).[11] Cultures were grown in 50 ml of A1 growth media (Appendix Figure 2A.1) for nine days at 30 ^{o}C with shaking at 250 revolutions/min. The expressison host *Streptomyces albus* was provided by Professor Joern Piel (University of Bonn). Cultures transformed with the pJW6F11 cosmid were grown in 100 ml of R2YE media (Appendix Figure 2A.2) containing 100 µg/ml apramycin at 30 ^{o}C for 9–14 days by rotary shaking at 250 revolutions/min. *Escherichia coli* cultures (Table 2.1) were grown in Luria Bertani (LB) broth (Appendix Figure 2A.1) at 37 ^{o}C in 15 ml conical tubes for 16 hours at constant shaking. When selecting *E. coli* harboring plasmids, the cultures were grown with the appropriate antibiotics.

Table 2.1: *E. coli* strains used and their corresponding genotypes

***E. coli* strain**	**Genotype**	**Source**
XL1-Blue MRF' Supercompetent cells	Δ(*mcrA*)*183* Δ(*mcrCB-hsdSMR-mrr*)*173 endA1 supE44 thi-1 recA1 gyrA96 relA1 lac* (F´*roAB lacIqZ*Δ*M15*Tn*10* (Tetr))	Stratagene, USA
TOPO One Shot Top10 competent cells	F- *mcr*A Δ(*mrr-hsd*RMS-*mcr*BC) Φ80*lac*ZΔM15 Δ*lac*X74 *rec*A1 *ara*D139 Δ(*araleu*)7697 *gal*U *gal*K *rps*L (StrR) *end*A1 *nup*G	Invitrogen, USA
Subcloning efficiency DH5-α competent cells	F- φ80*lac*ZΔM15 Δ(*lac*ZYA-*arg*F)U169 *rec*A1 *end*A1 *hsd*R17(rk-, mk+) *pho*A*sup*E44 *thi*-1 *gyr*A96 *rel*A1 λ-	Invitrogen, USA

2.2.2: Nucleic acid extraction

2.2.2.1: Genomic DNA extraction

Total genomic DNA of *S.* sp. CNQ-525 was isolated from a 50 ml culture grown in A1 growth media (Appendix Figure 2A.1) for 48 hours at 30 ^{o}C in a 250 ml Erlenmeyer flask with a spring. Inoculation of the 50 ml culture was carried-out with 5% of a 25 ml seed culture grown in A1 growth media for 7 days at 30 ^{o}C. The cells were harvested by centrifugation (3,019 g for 10 minutes at 4 ^{o}C using an Eppendorf 5804 R centrifuge) and washed three times with 10 ml lysis buffer (Appendix Figure 2A.3). After the third wash, the cell pellet was resuspended in 5 ml lysis buffer, lysozyme (MP Biomedicals, LLC) was added to a final concentration of 5 mg/ml, and the mixture was incubated for an hour at 37 ^{o}C. Following the incubation at 37 ^{o}C, 500 µl of 20% SDS and 1 mg of proteinase K (Fisher Bioreagents) were added and the mixture was incubated for an additional 30 minutes at 37 ^{o}C. To ensure complete cell lysis, the reaction mixture was incubated in a 65 ^{o}C water bath for 15 minutes and immediately cooled on ice for 15 minutes. DNA was isolated from the mixture by adding 1.25 ml of 5 M potassium acetate and an equal volume of phenol-chloroform-isoamylalcohol (25:24:1 v/v, pH 8.0) (Fisher Bioreagents). After gently inverting the mixture for six minutes, the aqueous phase was separated from the organic phase by centrifugation at 17,696 g for 15 mintues at 4 ^{o}C (Beckman Coulter Avant J–E centrifuge). A cut-off pipet tip was used to transfer the aqueous layer and an equal volume of chloroform (Sigma) was added. After gently inverting for six minutes, the aqueous phase was isolated by centrifuging as described

previously. DNA was precipitated from the aqueous phase by adding 0.1 volumes of 3 M sodium acetate and two volumes of 100% ethanol. The DNA was spooled and dissolved overnight in 5 ml TE buffer (Appendix Figure 2A.2). RNase (QIAGEN) was added to the dissolved DNA until the final concentration was 50 μg/ml and the reaction was incubated for two hours at 37 ^{o}C. An equal volume of phenol-chloroform-isoamylalcohol (25:24:1 v/v, pH 8.0) was added and after complete mixing of the solution, the aqueous layer was isolated by centrifuging at 3,019 g for 20 minutes at 4 ^{o}C (Eppendorf 5804 R centrifuge). A cut-off tip was used to transfer the aqueous layer, and the DNA was precipitated by adding 0.1 volume 3 M sodium acetate and two volumes of 100% ethanol. The DNA was spooled, dissolved in 1 ml TE buffer (Appendix Figure 2A.2) and stored at -20 ^{o}C.

2.2.2.2: Plasmid extraction

Purification of plasmids from *E. coli* cultures were performed using a QIAprep Spin Miniprep Kit (Qiagen) according to the manufacturer's protocol. The kit isolated up to 20 μg of plasmid DNA from a 1–5 ml culture of *E. coli.* A QIAprep spin column containing a silica membrane bound the DNA in a high-salt buffer. Only DNA is adsorbed on the membrane and was eluted with 30–50 μl EB buffer (Appendix Figure 2A.2) or milli-Q water. The DNA was stored at -20 ^{o}C.

2.2.3: Nucleic acid purification

2.2.3.1: Ethanol precipitation

To remove salt from the DNA sample, two volumes of ice cold 100% ethanol and 0.1 volumes of ice cold 3 M sodium acetate were added. The sample was incubated on ice for 20 minutes before centrifuging at 15,700 g for ten minutes at 4 ^{o}C (Eppendorf 5415 R centrifuge). The supernatant was decanted and the pellet was washed with 500 µl of ice cold 70% ethanol. The resuspended pellet was incubated on ice for 30 minutes, and the DNA was harvested by centrifugation at 15,700 g for eight minutes at 4 ^{o}C. The supernatant was decanted and the pellet was allowed to air dry before being resuspended in sterile milli-Q water.

2.2.4: Cosmid library construction

2.2.4.1: Preparing the vector

The *E.* coli-*Streptomyces* shuttle vector pOJ446[23] was used for library construction and transformed into DH5-α cells for amplification according to standard procedures.[24] To linearize the vector, 9 µg of pOJ446 was digested with 1.5 µl HpaI (New England Biolabs, 5,000 U/mL) in a 100 µl reaction containing 10 µl of NEBuffer 4 (New England Biolabs) and 53.5 µl Milli-Q water and incubated at 37 ^{o}C for one hour. After the digest, 1 µl of calf intestinal phosphatase (Invitrogen, 1,000 U/ml) was added to the digest to de-phosphorylate the ends of the linearized cosmid and the reaction was incubated

for an additional hour at 37 ^{o}C. A QIAGEN gel purification kit was used according to manufacturer's procedures to change the buffer and salt concentrations of the reaction. The digest was split between two columns and the DNA was eluted off each column with 30 µl of EB buffer (Appendix Tabe 2A.3). A second digest with 4 µl of BamH1 (New England Biolabs, 20,000 U/ml), 2 µl bovine serum albumin (BSA) (New England Biolabs, 10 mg/mL), 20 µl of NEBuffer 2 (New England Biolabs), 124 µl of Milli-Q water, and 50 µl of the eluted de-phosphorylated DNA created the site for the *S.* sp. CNQ-525 genomic DNA insert. The reaction was incubated for one hour at 37 ^{o}C and the DNA was purified with a QIAGEN gel elution kit (QIAGEN) according to manufacturer's instructions. DNA was eluted off the column with 50 µl EB buffer (Appendix Figure 2A.3) and was cleaned by ethanol precipitation to remove any remaining salt (Section 2.2.3.1).

2.2.4.2: Preparing the genomic DNA insert

S. sp. CNQ-525's genomic DNA was isolated (Section 2.2.2.1) and partially digested with the restriction enzyme Sau3AI. A serial dilution of the enzyme was used to find optimal conditions required to digest the genomic DNA into fragments of ≥ 35 kilobases (kb), which is the desired size for the bacteria phage packaging reaction. In a 700 µl reaction, 39 µg of genomic DNA was incubated with 70 µl NEBbuffer 4 (New England Biolabs), 7 µl BSA (New England Biolabs, 10 mg/ml) and 473 µl Milli-Q water for an hour at room temperature. Microcentrifuge tubes were placed on ice, and 120 µl of the

genomic DNA mixture was added to tube one while 60 µl of the reaction was added to tubes 2–10. Using a cut-off pipet tip, a 4 µl aliquot of Sau3AI (New England Biolabs, 4,000 U/ml) was added to tube one, mixed, and a 60 µl aliquot was transferred to tube two. After mixing, a 60 µl aliquot was transferred to tube three and so on until tubes 1–9 contained Sau3AI. All reactions were incubated at 37 ^{o}C for one hour, heated to 70 ^{o}C for 15 mintues to inactivate the enzyme, and iced for ten minutes. DNA fragments between 35 and 40 kb were isolated by agarose gel electrophoresis (0.6 % agarose gel run at 100 V) and purified for ligation using a QIAEX II kit (QIAGEN) according to manufacturer's standards.

2.2.4.3: Ligating genomic DNA into pOJ446

A ligation reaction was carried out in a 20 µl reaction using ~100 ng of genomic DNA, 40 ng of doubly digested pOJ446, 1 µl T4 ligase (New England Biolabs, 400,000 U/mL), 2 µl T4 10X ligase buffer (New England Biolabs), and 5 µl Milli-Q water. Before adding the ligase, the mixture containing plasmid and genomic DNA was incubated at 50 ^{o}C for five mintues and then placed on ice for five mintues. Ligation was carried out overnight at 16 ^{o}C.

2.2.4.4: Packaging and titration

Packaging and titration reactions were performed using MaxPlax λ packaging extracts (Epicenter) and XL1-Blue MRF′ supercompetent cells (Stratagene). On ice, 10 µl of the ligation reaction was added to 25 µl of a packaging extract and incubated for 90 minutes at 30 ^{o}C. Following the 90

minute incubation, 25 µl of the remaining packaging extract was added to the reaction and incubated for another 90 minutes at 30 ^{o}C. After the second 90 minute incubation, 500 µl of phage dilution buffer (Appendix Figure 2A.3) was added to the reaction and gently vortexed. A 25 µl aliquot of chloroform was added and the entire reaction was stored at 4 ^{o}C.

XL1-Blue MRF′ cells were prepared according to the manufacturer's instructions. A 1:5 dilution of the packaging reaction was prepared with Milli-Q water and brought to a final volume of 50 µl with phage dilution buffer (Appendix Figure 2A.3). A 50 µl aliquot of the XL1-Blue MRF′ cells (OD_{600} = 0.5) was added to the diluted packaging reaction and incubated at room temperature. After 30 minutes, 200 µl of LB (Appendix Figure 2A.1) was added to the reaction. Incubation was carried out at 37 ^{o}C for an hour and the microcentrifuge tube was gently inverted every 15 minutes to mix the packaging reaction with the XL1-Blue MRF' cells. After the incubation, 300 µl of the reaction was plated on LB agar with apramycin (50 µg/ml) and incubated overnight at 37 ^{o}C. To determine if the ligation of genomic DNA into the pOJ446 cosmid was successful, 10 colonies were grown in 3 ml of LB with apramycin (50 µg/ml) and grown overnight at 37 ^{o}C by constant shaking. The DNA was isolated according to Section 2.2.2.2 and digested with PvuII in a 10 µl reaction containing 4 µl of DNA, 0.2 µl PvuII (10 U/µl, New England Biolabs), 1 µl NEBuffer 2 and 4.8 µl Milli-Q water. The digest was incubated at 37 ^{o}C for one hour, and the entire reaction was analyzed on a 0.8% agarose gel. When it was verified that the 10 cosmids contained genomic DNA inserts that gave different banding patterns after digestion with PvuII, a

2,000 colony library was picked and incubated overnight at 37 ^{o}C in 96-welled plates containing 100 µl LB and apramycin (50 µg/ml).

2.2.5: Transferring DNA from cultures to a nylon membrane for southern hybridization

DNA from liquid cultures were transferred to a Hybond-N membrane (Amersham Biosciences) using a metal stamper (Fisher Scientific). The membranes were grown overnight at 37 ^{o}C on LB agar containing apramycin (50 µg/ml). Protein and cell remnants were washed away from the blots by placing the membranes on whatman paper saturated with 0.5 M NaOH for five minutes at room temperature. Afterward, the blots were washed two times with 5X SSC (Appendix Figure 2A.3). Protein and cell debris were wiped away from the blot using a latex-gloved finger, and the membranes were dried overnight at room temperature.

2.2.6: Transferring DNA from an agarose gel to a nylon membrane for southern hybridization

A 0.8% agarose gel was prepared for hybridization by washing in 0.2 N HCl for seven minutes, rinsing several times with deionized water, washing in a solution of 1.5 M NaCl and 0.5 N NaOH for 15 minutes, and rinally washing with a fresh solution of 1.5 M NaCl and 0.5 NaOH for 20 minutes. A VacuGene Pump (Pharmacia Biotech) was used to fix the DNA to the positively charged Hybond-N

membrane (Amersham Biosciences), which was saturated with deionized water before the agarose gel was placed on top (DNA side up). The vacuum was turned on and adjusted to 50 mbar. The agarose gel was covered with a solution of 1.5 M NaCl and 0.5 M Tris-HCl pH 7.5 for 10 minutes at room temperature. The solution was drained off and the gel was continuously covered in 20X SSC for two hours at room temperature. The membrane was washed with 6X SSC for five minutes and allowed to dry on filter paper overnight.

2.2.7: Designing nucleic acid probes for cosmid library screening

2.2.7.1: Type III polyketide synthase gene

Using the cosmid clone containing the putative neomarinone biosynthetic cluster from *S.* sp. CNH-099 as template DNA (Figure 2.7), the type III polyketide synthase gene was amplified by polymerase chain reaction (PCR) using PKS3 fwd and PKS3 rev primers (Table 2.2). Both primers contain a HindIII restriction site and were diluted with Milli-Q water to a final concentration of 20 µM. For a 50 µl PCR reaction, 1µl of cosmid DNA (22 ng/µl) was mixed with 0.5 µl pfu turbo (2.5 U/µl, Stratagene), 5 µl pfu 10 X buffer, 1 µl PKS3 Fwd (10 pmol/µl), 1 µl of PKS3 Rev (10pmol/µl), 1 µl dNTPs (10 mM), and 38.5 µl Milli-Q water. PCR conditions were 96 ^{o}C for five minutes; 25 cycles of 96 ^{o}C for one minute, 56 ^{o}C for one minute and 72 ^{o}C for 90 seconds, followed by an extra ten minutes at 72 ^{o}C. The entire 50 µl reaction was run on a 0.8% agarose gel, and the 1 kb

amplicon was excised from the gel. DNA was extracted using a QIAGEN gel extraction kit (QIAGEN) according to manufacturer's instructions.

Table 2.2: Primer sequences used to amplify genes from *S.* sp. CNH-099

Primer Name	Primer Sequence (5' to 3')	Target Gene	Tm (°C)
PKS3 Fwd	CAAGCTTATGCCAGGCATGTCGACT	Type III PKS	68
PKS3 Rev	CAAGCTTTCAGCCGACGGCGGCCGC	Type III PKS	79
Prt1 Fwd	CGGATCCATGTTGGCTGAGAAAACC	Prenyltransferase	69
Prt1 Rev	CGCGGCCGCCTACTGGGCATGGTTCTC	Prenyltransferase	77

Restriction sites are underlines

A zero blunt cloning vector (Invitrogen) was used to subclone the PKS fragment in a 10 µl reaction containing 1 µl vector (25 ng/µl), 6 µl purified PCR product (5 ng/µl), 1µl 10X ligation buffer, 1 µl T4 DNA ligase (400,000 U/ml, New England Biolabs), and 1 µl Milli-Q water. The ligation was incubated overnight at 16 ^{o}C. After which, 2 µl of the ligation reaction was transformed into 50 µl of TOPO top 10 cells (Invitrogen) according to manufacturer's instructions. A 50 µl aliquot was plated on LB agar containing kanamycin (50 µg/ml) and incubated overnight at 37 ^{o}C. Colonies were picked and grown overnight by constant shaking at 37 ^{o}C in 5 ml LB containing kanamycin (50 µg/ml). Plasmid DNA was extracted according to Section 2.2.2.2 and eluted off the QIAGEN column with 50 µl EB buffer (Appendix Figure 2A.3).

A HindIII digest was used to excise the PKS fragment from the vector. In a 40 µl reaction, 20 µl of DNA (300 ng/µl) was mixed with 2 µl HindIII (20 U/µl,

New England Biolabs), 4 µl NEBuffer 2, 14 µl Milli-Q water and incubated at 37 ^{o}C for two hours. The entire digest was run on a 0.8% agarose gel, and the fragment was excised from the gel and eluted using a QIAGEN gel extraction kit according to manufacturer's instructions. Eluted DNA was cleaned by ethanol precipitation (section 2.2.3.1), resuspended in 15 µl Milli-Q water and stored at -20 ^{o}C.

2.2.7.2: Prenyltransferase gene

Using the cosmid clone containing the putative neomarinone biosynthetic cluster from *S.* sp. CNH-099 as template DNA (Figure 2.7), the prenyltransferase 1 gene was amplified by polymerase chain reaction (PCR) using Prt1 fwd and Prt1 rev primers (Table 2.2). Prt1 fwd primer contained a BamH1 restriction site, while primer Prt1 rev contained a NotI restriction site. Both primers were diluted with Milli-Q water to a final concentration of 20 µM. The prenyltransferase 1 gene was amplified, subcloned, and transformed into TOPO top 10 cells as described in Section 2.2.7.1.

A BamH1 and NotI double digest was set-up to isolate the prenyltrasferase 1 gene. In a 40 µl reaction, 20 µl of DNA (300 ng/µl) was mixed with 2 µl BamH1 (20 U/µl, New England Biolabs), 2 µl NotI (10 U/µl, New England Biolabs), 0.4 µl BSA (100 µg/ml), 4 µl of NEBuffer 2 and 11.6 µl of Milli-Q water. The digest was incubated for two hours at 37 ^{o}C. After which, the DNA was isolated, and purified as described in Section 2.2.7.1.

2.2.8: Screening the cosmid library

The 2,000 cosmid library was screened using *Streptomyces* sp. CNQ-099-based type III polyketide synthase and prenyltransferase genes as heterologous probes. An ECL direct nucleic acid labeling and detection systems kit (Amersham Pharmacia Biotech), which is based on enhanced chemiluminescence, was used for the labeling and detection of positive cosmid clones according to the manufacturer's instructions. The protocol uses a positively-charged polymer-peroxidase complex to label the probe. This complex loosely binds to the negatively-charged denatured probe, which becomes covalently linked after the addition of glutaraldehyde. The labeled probe is used for hybridization, and detection of labeled positives uses two reagents. Detection reagent 1 creates H_2O_2, which is oxidized by the peroxidase to O_2. This is coupled to detection reagent 2, which contains luminol. Oxidation of luminol by O_2 creates light, which is detected on blue-light sensitive film (Kodak BioMax MR film, Kodak).

2.2.9: Selecting a cosmid clone for sequencing

After screening the library with the PKS and prenyltransferase probes, six cosmid clones were sent off for end sequencing using the primer pOJREV (5' CGCGCTCCAGCGAAAGCGGTCCTCGC). A BLASTP analysis[25] was conducted on the sequence data and cosmid clone pJW6F11's sequencing results showed homology to a mevalonate diphosphate decarboxylase.

pJW6F11 was digested with PstI in 50 µl reaction containing 20 µl DNA (200 ng/µl), 1.5 µl PstI (20 U/µl), 5 µl NEBuffer 3 and 23.5 µl Milli-Q water. The reaction was incubated for an hour at 37 ^{o}C and analyzed on a 0.8% agarose gel. Three bands that hybridized with the PKS and prenyltransferase probes (3.0 kb, 1.8 kb and 1.5 kb) were cut out of the gel. DNA was eluted using a QIAGEN gel extraction kit (QIAGEN) according to manufacturer's instructions. All three fragments were cloned into the pGEM-3Z easy clone vector (Promega) according to manufacturer's instructions and sequenced using the T7 promoter and SP6 promoter sites on the vector (Table 2.3).

Table 2.3: Primer sequences used to analyze subcloned fragments from cosmid clone pJW6F11

Primer Name	Primer Sequence (5' to 3')
T7 promoter	TAATACGACTCACTATAGGG
SP6 promoter	ATTTAGGTGACACTATAGAA

2.2.10: Sequencing and annotating the napyradiomycin biosynthetic cluster

Cosmid clone pJW6F11 was sequenced by the shotgun method (Macrogen Inc., Seoul, Korea). An initial 5x coverage followed by an additional 2x coverage and gap filling was used to sequence the 36-kb insert. The genomic scanning of *S. aculeolatus* NRRL 18422 and identification of the 43-kb *nap* locus

was previously reported.[26] Both sequences were annotated with BLASTP[25] and FRAMEPLOT[27].

2.2.11: Heterologous expression of cosmid clone pJW6F11

Streptomyces albus protoplasts were prepared according to standard procedures.[28] A 100 µl aliquot of protoplasts was incubated at 37 ^{o}C for 10 minutes. To the protoplasts, 5 µl of cosmid clone pJW6F11 (200 ng/µl) was added and mixed immediately by tapping the microcentrifuge tube. To the mixture, 200 µl of 25% PEG1000 in P1 buffer (Appendix Figure 2A.3) was added and mixed with a pipet five times. This mixture was split in half, plated on R2YE agar plates (Appendix Figure 2A.2), and incubated for 20 hours at 30 ^{o}C. After the incubation, 25 µl of apramycin (25 µg/ml) was mixed with 975 µl of Milli-Q water and added to each plate. The plates were allowed to dry in the hood and then incubated at 30 ^{o}C. Spores appeared after six days of incubation and eight colonies were re-plated on fresh R2YE agar plates containing apramycin (25 µg/ml). These plates were incubated for six days at 30 ^{o}C, and when there was sufficient growth on the plates, a 1 cm x 5 mm chunk of agar was cut out and used to inoculate 30 ml of R2YE media containing apramycin (25 µg/ml). These cultures were grown at 30 ^{o}C by rotary shaking at 250 revolutions/min. After four days, 5% of the 30 ml culture was used to inoculate 100 ml of fresh R2YE containing apramycin (25 µg/ml) and grown for 9–14 days by rotary shaking (250 revolutions/min) at 30 ^{o}C.

2.2.12: HPLC analysis of chlorinated dihydroquinone analogs

The 100 ml cultures of *S. albus* transformed with pJW6F11 were harvested by centrifugation at 3,019 g for 15 minutes at 4 ^{o}C (Eppendorf 5804R centrifuge). Cells were lysed by resuspending the cell pellet in 70 ml 80% methanol:water, sonicating for 30 minutes, heating for 30 minutes at 37 ^{o}C, and sonicating for an additional 30 minutes. After the incubation, the samples were centrifuged at 3,019 x g for 15 minutes at 4 ^{o}C. The supernatant was extracted with 1:1 methanol:dichloromethane and concentrated *in vacuo*. Production of *nap*-based compounds were analyzed using a Hewlett Packard 1100 series high performance liquid chromatography system linked to an Agilent ESI-1100 MSD mass spectrometer (gas flow set to 13 ml/min, drying temperature set to 350 ^{o}C, and nebulizing pressure set to 40 pounds/square inch). A Luna 4.6 x 150 mm C18 column was used at a flow rate of 0.7 ml/min with a linear solvent gradient of 10–100 % acetonitrile in water over a period of 20 minutes.

Fourier transform mass spectral analysis was accomplished with a LTQ-FTMS (ThermoFinnigan). Diluted organic extracts from *S. albus* transformed with pJW6F11 were introduced into the spectrometer via direct infusion at 1–3 µl/min. The sheath gas was set to 4 L/min, and the capillary inlet was set to 275 ^{o}C. The signal was optimized at the 509 *m*/*z* peak using the autotuning feature in the LTQ portion of the instrument. All FTMS analyse were performed in the negative ion mode, and the data were collected at 200,000 resolution. All of the theoretical values were obtained by importing the molecular formulas into the Qual browser software (ThermoFinnigan).

2.2.13: Purification of 2-deschloro-2-hydroxy-A80915C

Wild-type *Streptomyces* sp. CNQ-525 was cultured in 1 L A1 growth media in a 2.8 L Fernback flask (Appendix Figure 2A.1). Cultivation was carried out at 30 ^{o}C at 200 rpm for nine days. Inoculation of the 1 L culture was carried-out with 5% of a 30 mL seed culture grown in A1 growth media for 7 days at 30 ^{o}C. The cultures were extracted with ethyl acetate, dried over anhydrous $MgSO_4$ and concentrated *in vacuo*.

The crude extract (310 mg) was fractionated by reversed phase C18 flash column chromatography (Fisher Scientific, PrepSep C18 1g/6ml) with a flow rate of 10 ml/min. The fractions were collected in 20 ml aliquots using the following conditions: 40 ml of 20% acetonitrile:water, 60 ml of 40% acetonitrile:water, 60 ml of 60% acetonitrile:water, 60 ml of 80% acetonitrile:water, 40 ml of 100% acetonitrile, and 40 ml of 100% methanol. Each fraction was analyzed by reversed-phase C18 analytical LC-MS as described above. HPLC with a Waters differential refractrometer R401 detector was used for purification (chart recorder set to 12cm/h at 50 mV, and the refractive index was set at 4X). 2-Descloro-2-hydroxy-A80915C (3 mg) eluted in the 60% acetonitrile:water fraction and was isolated using a Luna 250 x 10 mm C8 column employing an isocratic condition of 67% acetonitrile:water with a flow rate of 2.0 ml/min (t_R = 17–20 min). NMR spectra were recorded on a Varian Inova 500-MHz spectrometer. The acetate feeding study was conducted as described in Section 1.2.2.

2.3: Results and Discussion

2.3.1: Selecting probes for southern hybridization

Based on the chlorinated dihydroquinone's structural similarities to the meroterpenoid neomarinone (Figure 2A 7), the putative neomarinone biosynthetic cluster[29] was used as a source for selecting genes as heterologous probes. The putative type III PKS, which has > 80% similarity to the type III PKS THNS from *S. coelicolor,*[30] is believed to catalyze the condensation of five molecules of malonyl-CoA to yield the pentaketide THN core of neomarinone. A80915C and the other chlorinated dihydroquinones share this same THN structural feature and the THNS gene has been shown to be highly conserved among *Streptomyces* spp. The putative prenyltransferase 1 gene is most similar to the prenyltransferase Orf2 from *S.* sp. CL190.[31] Crystal structure data coupled with *in vitro* experiments have shown that Orf2 attaches the isoprenoids geranyl diphosphate and farnesyl diphosphate to aromatic carbons and phenolic oxygens.[31-33] It is therefore predicted that a gene homologous to Orf2 is responsible for the attachment of geranyl diphosphate to the THN core of the dihydroquinones.

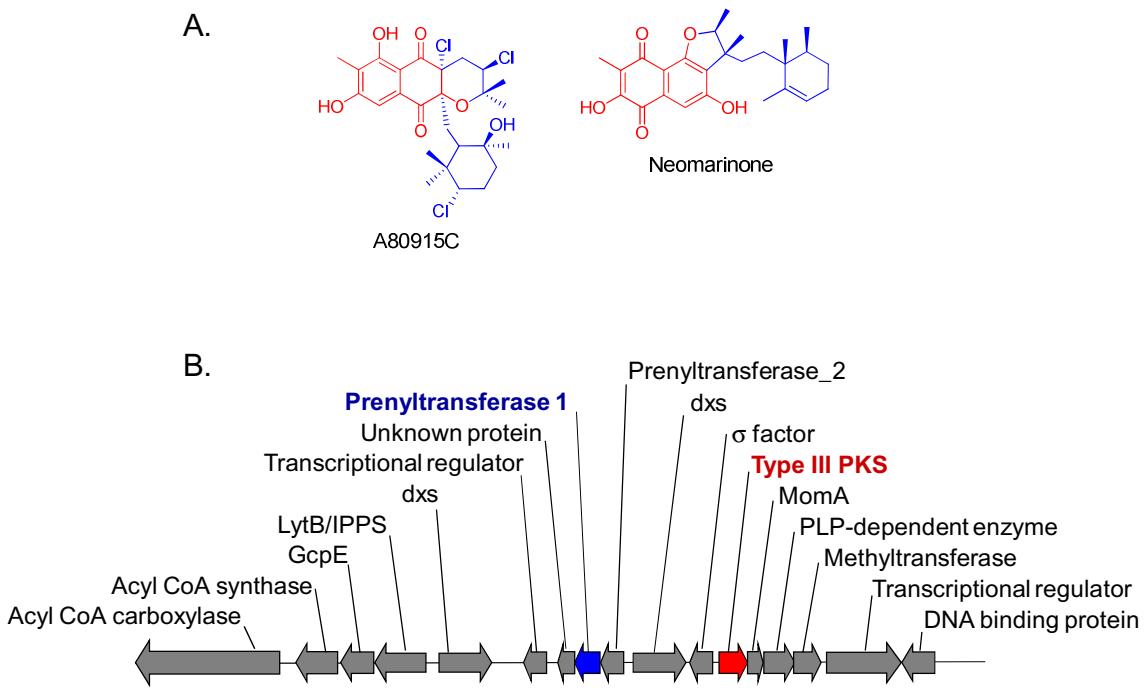

Figure 2.7: Designing probes for screening the *S.* sp. CNQ-525 cosmid library. A) Structural comparision between the meroterpenoids A80915C and neomarinone. The polyketide portion of the molecules is shown in red and the terpene moieties are highlighted in blue. B) Putative neomarinone biosynthetic cluster from *S.* sp. CNH-099).[29] The putative type III polyketide synthase is shown in red and putative prenyltransferase 1 is shown in blue.

2.3.2: Selecting a cosmid clone for sequencing

Based on the equation N = (CG)/L, where N = the number of colonies, C = the desired coverage, G = the size of the genome and L = length of gDNA insert, a 2,000 colony library was selected to ensure at least a 5–10X coverage of *S.* sp. CNQ-525's ~8 Mb genome. After screening the library with the type III PKS and prenyltransferase gene fragments as heterologous probes from the putative neomarinone biosynthetic cluster, 12 colonies showed strong hybridization with both probes. Out of these 12 colonies, six were sent out for end sequencing. Analysis of cosmid clone pJW6F11's sequencing results showed homology to a

mevalonate diphosphate decarboxylase. Biosynthetic gene cluster analysis of the mevalonic acid-derived meroterpenoids furaquinocin from *Streptomyces* sp. strain KO-3988[19] and furanonaphthoquinone I from *Streptomyces cinnamonensis* DSM 1042,[18] revealed a mevalonate gene cluster flanking the isoprenoid biosynthetic cluster. Among isoprenoid producing actinomycetes, this mevalonate biosynthetic cluster is conserved in which the types of genes, their order, and orientation are almost identical. Based on this observation, it was predicted that the gDNA insert in cosmid clone pJW6F11 contained some or all of the genes for the mevalonate gene cluster and this cluster was flanking the genes responsible for the production of the chlorinated dihydroquinones.

Gene fragments from pJW6F11 that hybridized with the type III PKS and prenyltransferases probes (3 kb, 1.8 kb and 1.5 kb) were subcloned and sequenced. Sequence data from the 3 kb fragment using the SP6 promoter showed homology to a mevalonate kinase, while the 1.8 fragment showed homology to a type III PKS from the T7 promoter sequence data and an aminotransferase using the SP6 promote. No sequence data was generated for the 1.5 kb fragment. Cosmid clone pJW6F11 contained a number of genes predicted to be involved in the production of the chlorinated dihydroquinones and was therefore selected to be completely sequenced by the shotgun method.

2.3.3: Analyzing the napyradiomycin biosynthetic cluster

The napyradiomycin biosynthetic cluster (*nap*) was discovered from *Streptomyces aculeolatus* NRRL 18422 and from the undescribed marine sediment-derived *Streptomyces* sp. CNQ-525 using distinct methods. In *S.* sp. CNQ-525, PCR-amplified THN synthase and prenyltransferase gene fragments were used as probes for the identification of a single pOJ446 cosmid clone (pJW6F11) containing a 36-kb genomic insert, which was sequenced by a shotgun approach. Identification of the complete 43-kb *nap* locus was alternatively achieved in *S. aculeolatus* NRRL 18422 by genome scanning.[27] The GenBank™ accession numbers for the *nap* cluster are EF397639 from *Streptomyces* sp. CNQ-525 and EF397638 from *S. aculeolatus*. When aligned, the two clusters are similarly organized and 97% identical at the nucleotide level (Figure 2.8).[34] The DNA sequence in interrupted by a ~350-bp gap between the convergent genes *nap*H2 and *nap*T8 that proved impervious to our sequencing efforts in *S.* sp. CNQ-525. Analysis of the 43-kb *nap* cluster revealed 33 open reading frames, which included five genes putatively involved in the construction of the naphthoquinone polyketide core (*nap*B1–B5), nine genes associated with the biosynthesis (*nap*T1–T7) and attachment (*nap*T8–T9) of the terpenoid units, four halogenases (*nap*H1–H4), nine putative regulatory and resistance proteins (*nap*R1–R9), four open reading frames of unknown function (*nap*U1–U4), and two transposases that suggest this cluster may have been acquired via horizontal gene transfer (Table 2.4 and Figure 2.8). Of the four *nap* halogenases, three

show striking similarity to fungal V-ClPOs and a hypothetical protein TioM from *Micromonospora* sp. ML1[35], which is unprecedented in prokaryotic gene clusters.

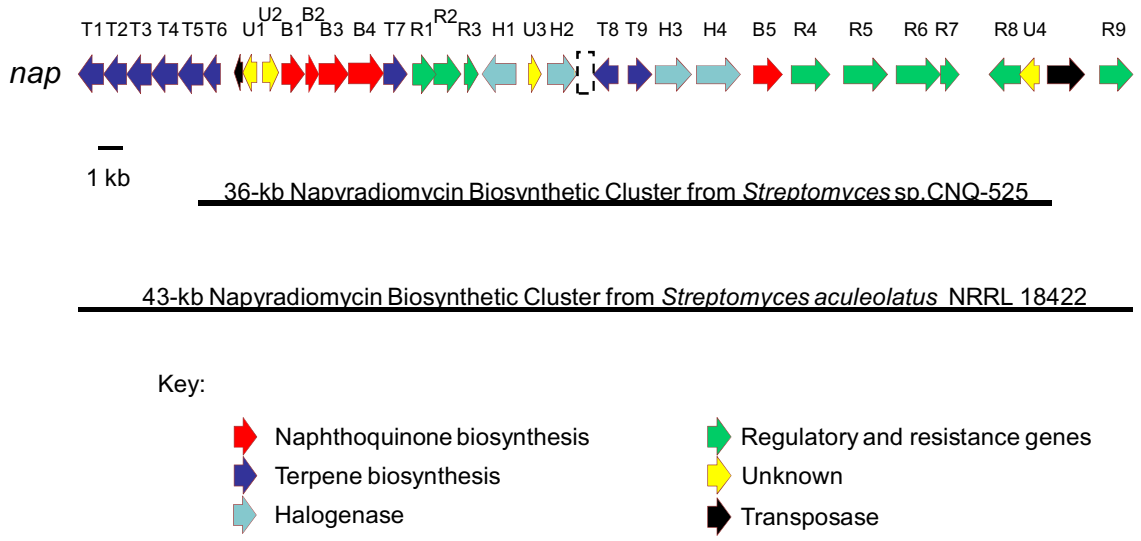

Figure 2.8: Organization of the napyradiomycin biosynthetic cluster (*nap*) in *Streptomyces* sp. CNQ-525 and *Streptomyces aculeolatus* NRRL 18422. Each arrow represents the direction of transcription of an open reading frame. The dashed box between *nap*H2 and *nap*T8 represents a ~350-bp unsequenced gap in *S.* sp. CNQ-525, which correlates to a similarly sized gap in *S. aculeolatus.*

Table 2.4: Deduced function of the open freading frames in Figure 2.8.

Gene Product	Amino acids (no)	Proposed function	Sequence similarity (protein, origin)	Similarity/ identity (%)	Protein accession number
NapB1	355	THN synthase	SarppA, *S. antibioticus*	92/84	BAD89289
NapB2	184	MomA	MomA, *S. antibioticus*	86/74	BAD89290
NapB3	386	Aminotransferase	Fur3, *Streptomyces* sp.	85/76	BAE78971
NapB4	529	Acyl-CoA synthase	Fur5, *Streptomyces* sp.	85/74	BAE78973
NapB5	337	Methyltransferase	Fur4, *Streptomyces* sp.	85/69	BAE78974
NapH1	509	V-ClPO	TioM, Micromonospora sp.	33/21	CAJ34369
NapH2	425	$FADH_2$ dependent halogenase	CalO3, *M. echinospora*	63/43	AAM70353
NapH3	441	V-ClPO	TioM, *Micromonospora* sp.	38/25	CAJ34369
NapH4	523	V-ClPO	TioM, *Micromonospora* sp.	37/27	CAJ34369
NapT1	389	HMG-CoA synthase	HmgS, *Streptomyces* sp.	86/78	BAB07795
NapT2	353	HMG-CoA reductase	HmgR, *Streptomyces* sp.	93/87	BAA70975
NapT3	380	Type 2 IPP isomerase	Fni, *Streptomyces* sp.	89/82	Q9KWG2
NapT4	412	Phosphomevalonate kinase	Pmk, *Streptomyces* sp.	68/62	BAD86802
NapT5	385	Mevalonate decarboxylase	MdpD, *Streptomyces* sp.	83/77	BAD86801
NapT6	262	Mevalonate kinase	OrfA, Streptomyces sp.	81/70	BAB07790
NapT7	310	Polyprenyl synthase	Fur19, *Streptomyces* sp.	82/71	BAE78987
NapT8	297	Prenyltransferase	CloQ, *Streptomyces* sp.	65/46	BAE78975
NapT9	287	Prenyltransferase	Orf2,	54/35	BAE00106

Table 2.4 continued.

Gene product	Amino acids (no)	Proposed function	Sequence similarity (protein, origin)	Similarity/ Identity (%)	Protein accession number
			Streptomyces sp.		
NapR1	268	Regulatory protein	Orf41, *S. globisporus*	52/38	AAL06696
NapR2	423	Sodium transporter	Orf1, *S. carzinostaticus*	68/52	BAD38870
NapR3	220	Transcription regulator	TcmR, *S. coelicolor*	53/43	CAD30962
NapR4	464	Transporter	PcaK, *B. mallei*	52/33	AAU45502
NapR5	535	Efflux protein	Sco0375, *S. coelicolor*	80/68	CAD55439
NapR6	535	Efflux protein	MonT, *S. avermitilis*	70/52	NP_824465
NapR7	219	Transcription regulator	TcmR, *S. coelicolor*	62/45	NP_629129
NapR8	383	Regulatory protein	MarR, *R. palustris*	47/37	NP_947139
NapR9	401	Efflux transporter	AraJ, *S. avermitilis*	71/56	NP_823779
NapU1	225	Unknown	OvmZ, *Streptomyces* sp.	63/46	BAE78986
NapU2	255	Unknown	InfB, *N. farcinica*	35/29	YP_120279
NapU3	206	Hypothetical protein	Sru1144, *S. ruber*	50/33	YP_445270
NapU4	237	Hypothetical protein	Nfa6880, *N. farcinica*	40/27	BAD55533
Transposase 1	67	Transposase	Tra8, *C. glutamicum*	46/38	NP_599434

2.3.4: Comparitive analysis of the meroterpenoid clusters

Before the identification of the napyradiomycin biosynthetic cluster, furanonaphthoquinone I (*fnq*)[18] from *S. cinnamonensis* DSM 1043 and furaquinocin A (*fur*)[19] from *S.* sp. KO-3998 were the only other meroterpenoid biosynthetic clusters isolated from actinomycetes. Sequence analysis of these

three clusters reveals a grouping of genes responsible for the assembly of the naphthoquinone core, which includes the type III polyketide synthase 1,3,6,8-tetrahydroxynaphthalene synthase and a monooxygenase (Figure 2.9). Interestingly, all three clusters also contain a putative aminotransferase and an acyl-CoA synthase within close proximity of the 1,3,6,8-tetrahydroxynaphthalene synthase. It is still unclear what role these putative genes have in the biosynthesis of the naphthoquinone core or if they are even involved in the biosynthesis of these meroterpenoids. In addition to having a similar clustering of genes responsible for the synthesis of their naphthoquinone cores, each cluster contains at least one prenyltransferase for the attachment of an isoprenoid subunit. The *fur* biosynthetic cluster contains one gene coding for a prenyltransferase that is responsible for the attachment of the monoterpene GPP, whereas the *fnq* and *nap* biosynthetic cluster contain two genes coding for prenyltransferases. While the napyradiomycin analogs contain two isoprenoid subunits, which most likely require two independent prenyltransferases for their attachment, furanonaphthoquinone I is only monoprenylated and the function of the second prenyltransferase is unclear.[18] Feeding studies have also proven that all three clusters produce isoprenoids via the mevalonate pathway and both the *fur* and *nap* biosynthetic clusters contain the full mevalonate biosynthetic gene cassette.[13, 16, 36] However, unlike the *fnq* and *fur* biosynthetic clusters, the *nap* biosynthetic cluster contains four halogenating genes encoding for a $FADH_2$-dependent halogenase and three vanadium-dependent chloroperoxidases, which have never been identified in a prokaryote.

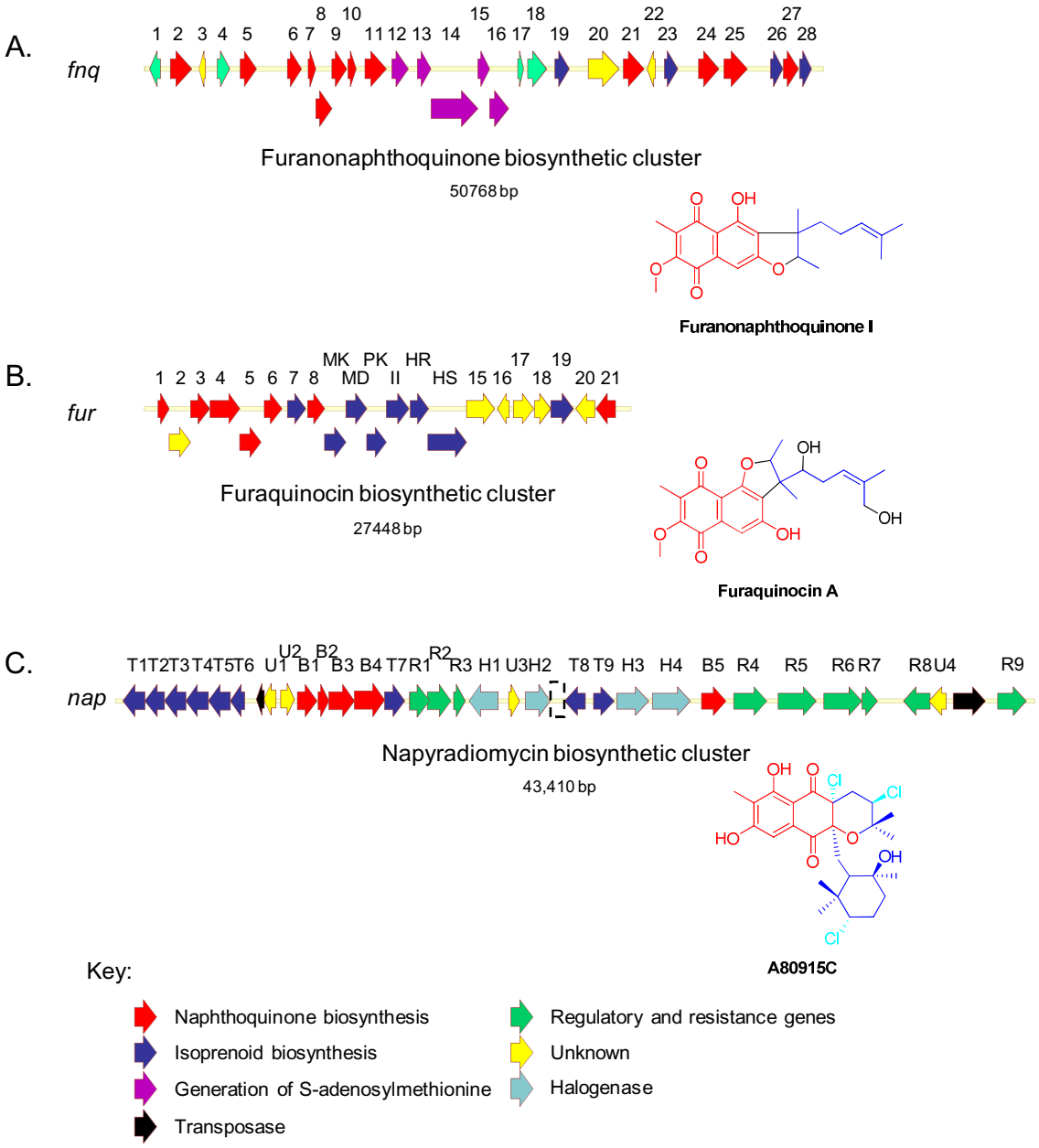

Figure 2.9: Organization of meroterpenoid biosynthetic clusters isolated from actinomycetes. A) Furanonaphthoquinone I biosynthetic cluster isolated from *S. cinnamonensis*. B) Furaquinocin A biosynthetic cluster isolated from *S.* sp. KO-3988. C) Napyradiomycin biosynthetic cluster isolated from *S.* sp. CNQ-525 and *S. aculeolatus* NRRL 18422. Each arrow represents the direction of transcription of an open reading frame. Deduce function of the open reading frames of the *fur* biosynthetic cluster and the *fnq* biosynthetic cluster can be found in Appendix Table IA.3 and IA.4, respectively.

2.3.5: Heterologous expression of the napyradiomycin biosynthetic cluster

To verify that all of the genetic information for the production of chlorinated dihydroquinones, such as A80915C, 3”-hydroxy-7-methylnapyradiomycin B2, and 2-deschloro-A80915C, is contained on the *nap* gene cluster, the *S.* sp. CNQ-525 cosmid clone pJW6F11, containing the truncated 36-kb *nap* cluster, was heterologously expressin in *S. albus*. Although the mevalonic acid pathway genes *nap*T1–T4 and part of *nap*T5 are absent in pJW6F11, the host strain was reasoned to provide the isopentenyl pyrophosphate and dimethylallyl pyrophosphate building blocks from primary metabolism. Co-injection with authentic napyradiomycin standards, high performance liquid chromatography-mass spectrometry, and FTMS analysis of the organic extracts from *S. albus*/pJW6F11 unequivocally demonstrated that the transformant yielded the *nap*-based chlorinated dihydroquinones A80915C, 3”-hydroxy-7-methylnapyradiomycin B2, and 2-deschloro-A80915C. In addition to known chlorinated dihydroquinones, a series of related analogs that exhibited the characteristic napyradiomycin chromophore[11] with high UV light absorption at 258, 300, and 356 nm were also identified (Figure 2.10). The observed masses for two of these dichlorinated analogs at *m*/*z* 527 (2-deschloro-2-hydroxy-A80915C) and 509 (negative ion mode) were observed in both the wild type strain *S.* sp. CNQ-525 and the *S. albus*/pJW6F11 transformant. However, a monochlorinated analog with a *m*/*z* 473 and a dichlorinated analog *m*/*z* 525 (negative ion mode) were only identified in the transformant (Figure 2.10).

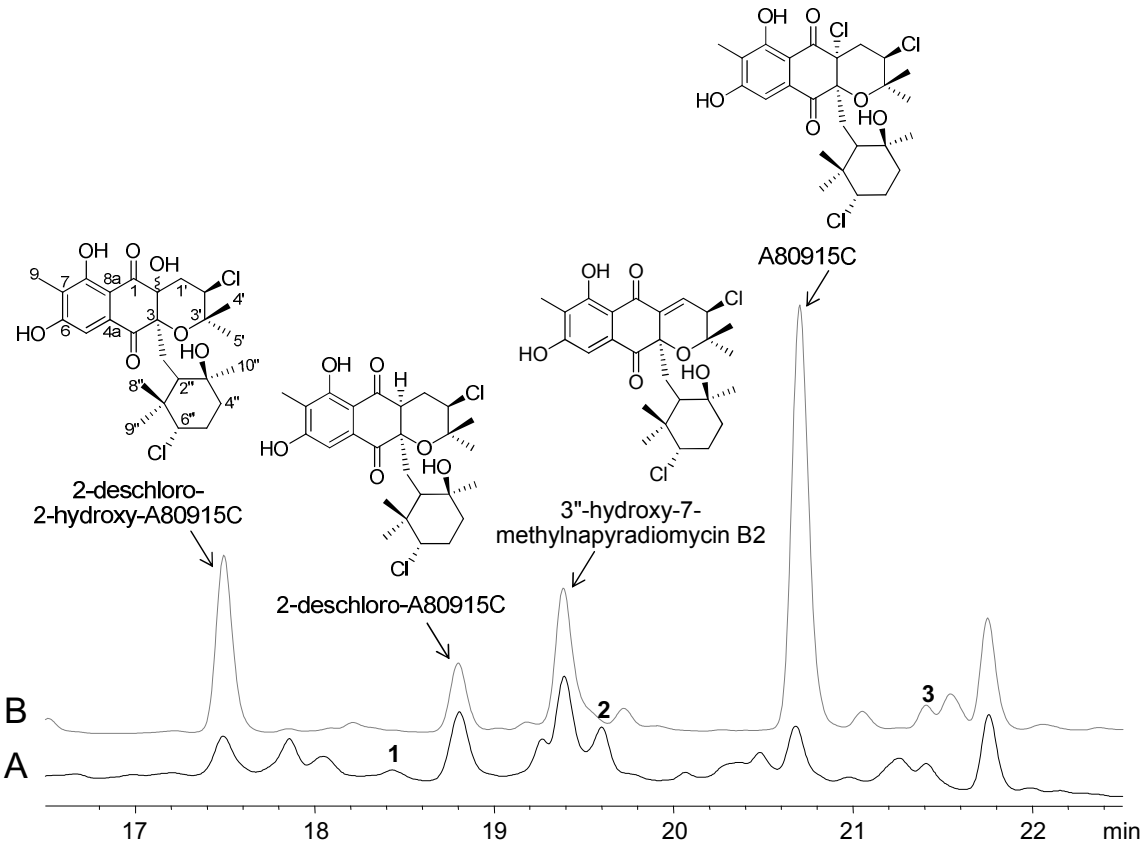

Figure 2.10: LC-MS analysis of the napyradiomycin fraction of *S. albus*/pJW6F11 (trace A) and *S.* sp. CNQ-525 wild type (trace B). UV light detection was carried out at 254 nm. Uncharacterized napyradiomycin analogs **1**, 18.4 min, *m*/*z* 525; **2**, 19.6 min, *m*/*z* 473; **3**, 21.4 min, *m*/*z* 509 (negative ion mode).

2.3.6: FTMS analysis of the *S. albus*/pJW6F11 crude extract

High resolution FTMS analysis of the organic extracts from the transformant verified exact masses for napyradiomycins A80915C (calculated for $[M - H]^+$: *m*/*z* 545.1259, observed: 545.1279), 3"-hydroxy-7-methylnapyradiomycin B2 (calculated for $[M - H]^+$: *m*/*z* 511.1649, observed: 511.1654), and 2-deschloro-A80915C (calculated for $[M - H]^+$: *m*/*z* 509.1429,

observed: 509.1429) (Figure 2.11). FTMS analysis further provided molecular composition data of three new napyradiomycin analogs namely the dichlorinated 525 species (**1**) (calculated for $C_{26}H_{30}Cl_2O_7^-$: *m*/*z* 525.1447, observed 525.1423), the dichlorinated 527 species 2-deschloro-2-hydroxy-A80915C (calculated for $C_{26}H_{33}Cl_2O_7^-$: *m*/*z* 527.1598, observed: 527.1514), and the monochlorinated 473 species (**2**) (calculated for $C_{26}H_{30}ClO_6^-$: *m*/*z* 473.1725, oserved: 473.1734) (Figures 2.10 and 2.11). The unknown dichlorinated 509 species (**3**) observed by high performance liquid chromatography-mass spectrometry analysis (Figure 2.10) likely has the same molecular formula as 3”-hydroxy-7-methylnapyradiomycin B2 ($C_{26}H_{31}Cl_2O_6^-$), so its exact mass could not be distinguished by FTMS.

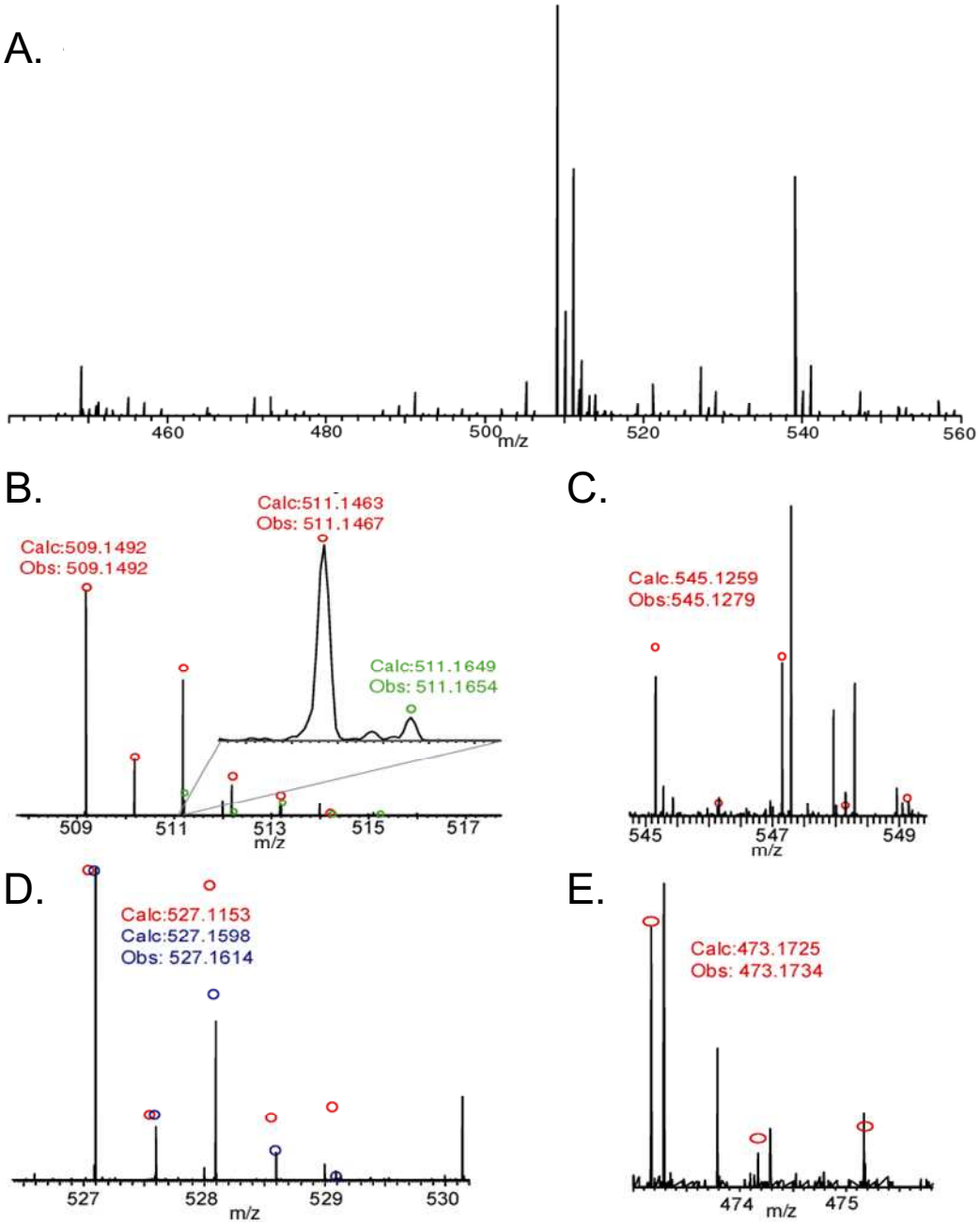

Figure 2.11: FTMS analysis of the crude extract from *S. albus*/pJW6F11. A) FTMS broadband mass spectrum of the organic extract from 440 to 560 *m*/*z* (negative ion mode). B) FTMS trace for 3"-hydroxy-7-methylnapyradiomycin B2 and 2-deschloro-A80915C. The red circles are theoretical isotopic distribution for 3"-hydroxy-7-methylnapyradiomycin B2, whereas the green circles correspond to the theoretical isotopic distribution of 2-deschloro-A80915C. C) FTMS trace for A80915C. The red circles indicate the theoretical mass and isotopic distribution. D) FTMS signal for the 527 species 2-deschloro-2-hydroxy-A80915C. The red circles indicate the theoretical mass and isotopic distribution. E) The observed FTMS signal for the 473 species **2**. The theoretical distribution for the molecular ions associated with $C_{26}H_{30}ClO_6^-$ is indicated with red circles.

2.3.7: Isolation and structure of elucidation of 2-deschloro-2-hydroxy-A80915C

Fermentation of *S.* sp. CNQ-525 followed by extraction and chromatography provided the dichlorinated 527 species 2-deschloro-2-hydroxy-A80915C in 4.3 mg/l (Appendix Table 2A.1). Analysis of the proton and carbon NMR spectra (Appendix Figures 2A.4 and 2A.5, respectively), with the aid of gradient-enhanced heteronuclear multiple bond correlation and heteronuclear single quantum coherence data (Appendix Figure 2A.6 and 2A.7, respectively), clearly established that 2-deschloro-2-hydroxy-A80915C contained the chlorocyclohexyl monoterpenoid unit common to A80915C, 3"-hydroxy-7-methylnapyradiomycin B2, and 2-deschloro-A80915C. NMR comparison with structurally related compounds A80915C and 2-deschloro-A80915C indicated that they only differed in the substitution at C-2. The presence of a broad singlet at δ 4.16 in the ^{1}H spectrum for 2-deschloro-2-hydroxy-A80915C (Appendix Figure 2A.4) indicated an additional hydroxyl signal not observed in A80915C and 2-deschloro-A80915C, which was confirmed by high resolution FTMS. This new C-2 hydroxyl substitution resulted in subtle differences in the NMR spectra of 2-deschloro-2-hydroxy-A80915C in comparison to that of the chloro analog A80915C at C-1', in which the methylene protons shift from δ 2.62 and 2.45 to δ 2.15 in 2-deschloro-2-hydroxy-A80915C. The relative stereochemistry of 2-deschloro-2-hydroxy-A80915C was assigned by comparing nulcear Overhauser effect spectroscopy correlations (Appendix Figure 2A.8) to those previously described for A80915C.[11, 37] Feeding experiments with [1,2-$^{13}C_2$]acetate also

revealed similar labeling patterns in the naphthoquinone core and isoprenoid units of 2-deschloro-2-hydroxy-A80915C to A80915C[13] and the series of napyradiomycins from *Chainia rubra* MG802AF1[14] (Appendix Table 2A.1 and Figure 2A.5).

2.3.8: Proposed biosynthesis of the chlorinated dihydroquinones

Expression of the *nap* cluster in *S. albus* unequivocally confirmed that all the genes required for the production of the 7-methylnapyradiomycin family of chlorinated dihydroquinones were contained on the cosmid clone pJW6F11. A biosynthetic scheme for the production of napyradiomycins A80915C, 2-deschloro-A80915C, and 3"-hydroxy-7-methylnapyradiomycin B2 was proposed on the basis of the molecular logic of the *nap* cluster (Figure 2.12). As in furaquinocin[19] and furanonaphthoquinone I[18] biosynthesis, assembly of the dihydroquinone core is catalyzed by the type III polyketide synthase homologous THNS NapB1, which condenses five malonly-CoA molecules to THN. The monooxygenase NapB2 putatively oxidizes THN to a dihydroquinone intermediate, which is then methylated by the methyltransferase NapB5. Attachment of the first isoprene unit, using dimethylallyl pyrophosphate as the substrate, occurs through a nucleophilic attack involving one of the two prenyltransferases (NapT8/T9). Hydrogenation or chlorination at C-2 by the $FADH_2$-dependent halogenase NapH2 may facilitate the second prenylation reaction at C-3 with geranyl pyrophosphate by the second *nap* prenyltransferase

to yield the diprenylated intermediate SF2415B1[12]. Cyclization of the hemiterpene subunit via a chloronium ion is putatively catalyzed by one of the three *nap* V-ClPOs (NapH1, H3, H4) giving rise to the 7-methyl derivative of napyradiomycin A1. The monoterpene subunit of 7-methylnapyradiomycin A1 putatively undergoes a related V-ClPO-facilitated cyclization to form A80915C and 2-deschloro-A80915C, in which a molecule of water is incorporated into the cyclohexanol moiety. Further dechlorination of A80915C likely gives rise to 3”-hydroxy-7-methylnapyradiomycin B2 (Figure 2.12). Although the specifics of the biosynthetic reaction sequence have yet to be confirmed, the successful heterologous expression of the *nap* cluster confirms that all of the genes required for biosynthesis are present.

Figure 2.12: Proposed biosynthetic pathway of the chlorinated dihydroquinones. The numbering scheme for the napyradiomycin analogs has been adopted from Reference 12.

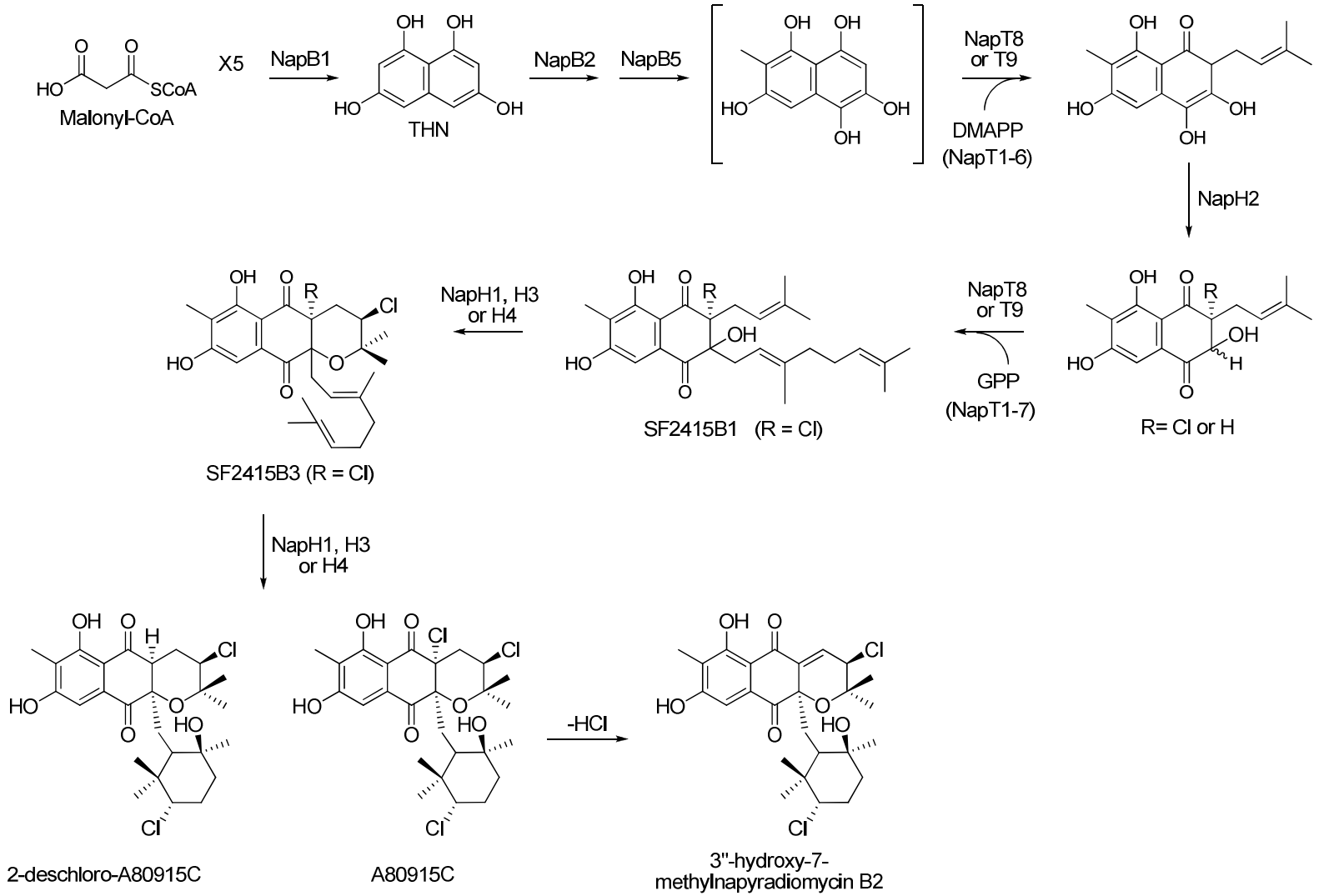
Malonyl-CoA
X5
NapB1
THN
NapB2
NapB5
NapT8
or T9
DMAPP
(NapT1-6)
NapH2
R= Cl or H
NapT8
or T9
GPP
(NapT1-7)
SF2415B1 (R = Cl)
NapH1, H3
or H4
SF2415B3 (R = Cl)
NapH1, H3
or H4
2-deschloro-A80915C
A80915C
-HCl
3''-hydroxy-7-
methylnapyradiomycin B2

2.4: Conclusion

Structural inspection of the bacterial meroterpenoid antibiotics belonging to the napyradiomycin family of chlorinated dihydroquinones suggests that the biosynthetic cyclization of their terpenoid subunits is initiated via a chloronium ion. The cloning and sequencing analysis of the 43-kb napyradiomycin biosynthetic cluster from *S. aculeolatus* NRRL 18422 and from the undescribed marine sediment-derived *S.* sp. CNQ-525 revealed 33 open reading frames, three of which putatively encode V-ClPOs. Heterologous expression of the CNQ-525 based *nap* biosynthetic cluster in *S. albus* produced at least seven napyradiomycins, including the new analog 2-deschloro-2-hydroxy-A80915C. It is proposed that the putative V-ClPOs may be responsible for the chlorination and cyclization of SF2415B1 to A80915C in a manner reminiscent of that of snyderol biosynthesis in *Corallina officinalis*.

To date, V-BrPOs are the only characterized haloperoxidase that demonstrate the ability to facilitate bromonium ion induced cyclization of terpenes *in vitro.*[1] While this study established the likely role of V-BrPOs in the biosynthesis of brominated cyclic sesquiterpenes from marine red algae, conventional wisdom still suggests that V-HPOs lack substrate specificity and regioselectivity because the natural substrates and final products of these enzymes are unknown. Unfortunately, because all characterized V-HPOs have been identified from fungi and marine algae, their biosynthetic roles *in vivo* have not been elucidated due to the inability to identify and isolate all of the

corresponding genes required for the assembly of a natural product. Thus, the *nap* biosynthetic cluster not only provides an opportunity to probe the *in vitro* biochemistry associated with the three *nap*- V-ClPOs, but also provides a tractable biological system for exploring the role of these enzymes *in vivo.*

Unfortunately, the *nap* gene cluster did not reveal an obvious mechanism for diazo synthesis and rearrangement nor did its heterologous expression yield nitrogenated napyradiomycin analogues. The only gene that may encode a diazo biosynthetic enzyme is napB3, which codes for a putative aminotransferase and may facilitate the transamination to the aminodihydroquinone intermediate. The *nap* cluster furthermore harbors a number of oxygenases whose functions have not yet been clarified that may be involved in the nitrogen biochemistry of azamerone. It is, however, quite likely that some of the encoding genes are extraneous to the *nap* locus and may reside elsewhere in the *S.* sp. CNQ-525 genome, given that the expression of the cluster only yielded non-nitrogenated napyradiomycins.

2.5: Appendix

A.

A1 Media	
Starch	10 g
Yeast Extract	4 g
Bacto-peptone	2 g
Natural sea water	1 L

B.

M1 Media	
Glucose	10 g
Molasses	20 g
Bacto-peptone	5 g
$CaCO_3$	2 g
KCl	0.2 g
$MgSO_4$ $7H_2O$	0.2 g
$FeSO_4$ $7H_2O$	0.004 g
dd H_2O	1 L
Adjust to pH 7.0 before autoclaving	

C.

Luria-Bertani Media	
Tryptone	10 g
Yeast Extract	5 g
NaCl	10 g
dd H_2O	1 L
Adjust pH to 7.0 before autoclaving	

D.

Luria-Bertani Agar	
Tryptone	10 g
Yeast Extract	5 g
NaCl	10 g
Agar	8 g
dd H_2O	1 L
Adjust pH to 7.0 before autoclaving	

Figure 2A.1: Media components. A) A1 growth media.[11] B) M1 media.[10] C) LB media.[28] D) LB agar.[28]

A.

R2YE Media	
Sucrose	103 g
K_2SO_4	0.25 g
$MgCl_2$ $6H_2O$	10.12 g
Glucose	10 g
Casaminoacids	0.1 g
Milli-Q H_2O	800 ml
Pour 80 mL in a 250 mL flask and autoclave	
For R2YE agar, add 2.5 g of agar to the flask before autoclaving	
To the 80 mL's add:	
KH_2PO_4 (0.5%)	1 ml
$CaCl_2$ $2H_2O$ (3.68%)	8 ml
L-proline (20%)	1.5 ml
TES buffer (5.73%, pH 7.2)	10 ml
Trace element solution*	0.2 ml
NaOH (1N)	0.5 ml
Yeast extract (10%)	5 ml

B.

***Trace element solution**	
$ZnCl_2$	40 mg
$FeCl_3$ 6 H_2O	200 mg
$CuCl_2$ $2H_2O$	10 mg
$MnCl_2$ $4H_2O$	10 mg
$Na_2B_4O_7$ $10H_2O$	10 mg
$(NH_4)_6Mo_7O_{24}$ $4H_2O$	10 mg
Milli-Q H_2O	1 L

Figure 2A.2: Media components II. A) R2YE media. B) Trace elements solution.[28]

A.

Lysis Buffer	
Sucrose	15 %
Tris-HCl pH 8.0	25 mM
EDTA	25 mM

B.

Phage Dilution Buffer	
10 mM Tris-HCl pH 8.3	100 mL
NaCl	100 mM
$MgCl_2$	10 mM

C.

TE Buffer	
Tris-HCl pH 8.0	10 mM
EDTA	1 mM

D.

20 X SSC	
NaCl	175.3 g
Na Citrate	88.2 g
Milli-Q H_2O	800 mL
Adjust pH to 7.0	
Add Milli-Q H_2O to 1L	

E.

P1 Buffer	
PEG 4000	60% (w/v)
Tris-HCl pH 7.5	10 mM
$CaCl_2$	50 mM

F.

EB Buffer	
Tris-HCl pH 8.5	10 mM

Figure 2A.3: Buffer components. A) Lysis buffer; B) Phage dilution buffer; C) TE buffer; D) 20X SSC; E) P1 buffer; F) EB buffer.

Table 2A.1: NMR data for 2-deschloro-2-hydroxy-A80915C

Carbon[a]	δ_C (ppm)[b]	δ_H (ppm)[b] (J, Hz)	Me-HSQC[a]	$^1H-^{13}C$-HMBC[a]	NOESY[a]	J_{cc} (Hz) [1,2-$^{13}C_2$]acetate[e]
1	199.01	-	-	-	-	57, 40
2	79.21	-	-	-	-	40[d]
3	84.47	-	-	-	-	40[d]
4	192.50	-	-	-	-	51, 40
4a	132.80	-	-	-	-	63, 51
5	108.65	7.58 (s)	CH	C4, C7, C8a	-	63[f]
6	164.17	-	-	-	-	69, 63
7	119.73	-	-	-	-	69[f]
8	162.35	-	-	-	-	69, 63
8a	106.97	-	-	-	-	63, 57
9	8.28	2.23 (s)	CH_3	C7, C8	OH on C8	-
1'	42.15	2.15 (d,d) (6.9, 2.4)	CH_2	C2, C3, C2', C3'	H2'	35
2'	58.00	4.47 (d,d) (9.46, 6.8)	CH	C1', C4', C5'	H1', H5'	35
3'	80.84	-	-	-	-	40
4'	21.96	1.29 (s)	CH_3	C2', C3', C5'	-	40
5'	28.97	1.53 (s)	CH_3	C2', C3', C4'	-	S[g]
1"	34.35	a) 1.34 (m)	CH_2	C2, C2", C3", C7"	-	
		b) 2.54 (m)		C3, C4, C2", C3"	-	36
2"	50.89	1.51 (d) (8.8)[c]	CH	C3, C1", C3", C4", C7", C8", C9"	H6"	36
3"	71.72	-	-	-	-	39
4"	40.78[c]	a) 1.89 (m)[c]	CH_2	C2", C3"	-	S[g]
		b) 1.50 (d) (8.8)[c]		C3", C10"	-	
5"	30.15	a) 1.90 (m)[c]	CH_2	C3"	-	35
		b) 1.75 (m)		-	-	
6"	71.12	3.55 (d,d) (12.2, 3.5)	CH	-	H2", H4"a, H8"	35
7"	40.78[c]	-	-	-	-	37
8"	28.62	0.39 (s)	CH_3	C2", C6", C7", C9"	H6"	S[g]
9"	15.85	0.71 (s)	CH_3	C2", C6", C7", C8"	H1"a	37
10"	24.37	1.25 (s)	CH_3	C2", C3", C4"	-	39

Figure 2A.4: ^{1}H NMR spectrum (500 MHz) of 2-deschloro-2-hydroxy-A80915C in $CDCl_3$.

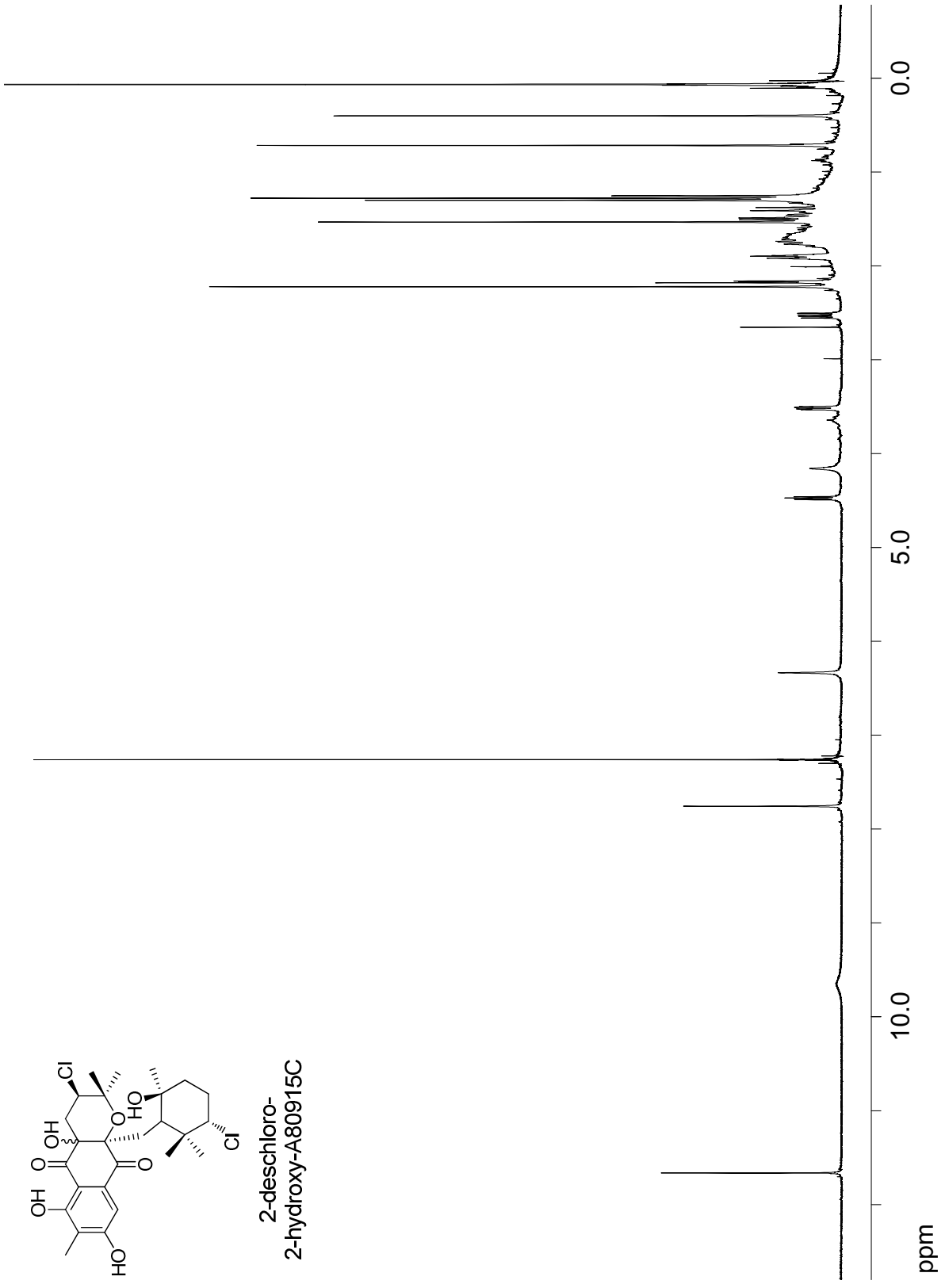
0.0
5.0
10.0
ppm
2-deschloro-
2-hydroxy-A80915C

Figure 2A.5: ^{13}C NMR spectrum (125 MHz) 2-deschloro-2-hydroxy-A80915C enriched with [1,2-$^{13}C_2$]acetate in $CDCl_3$.

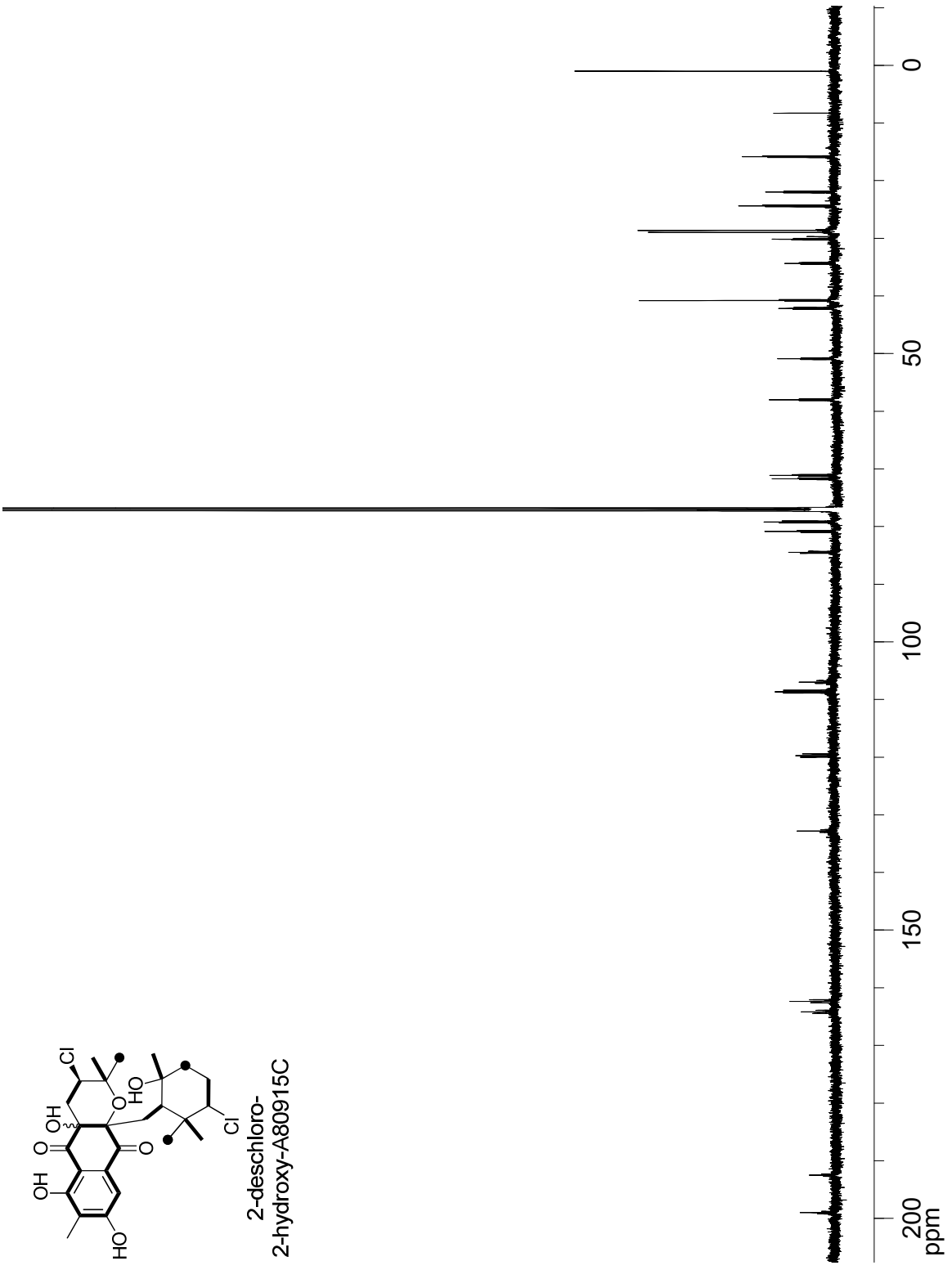
Cl
OH
O
O
OH
HO
O
HO
Cl
2-deschloro-
2-hydroxy-A80915C
0
50
100
150
200
ppm

Figure 2A.6: gHMBC NMR spectrum of 2-deschloro-2-hydroxy-A80915C in $CDCl_3$.

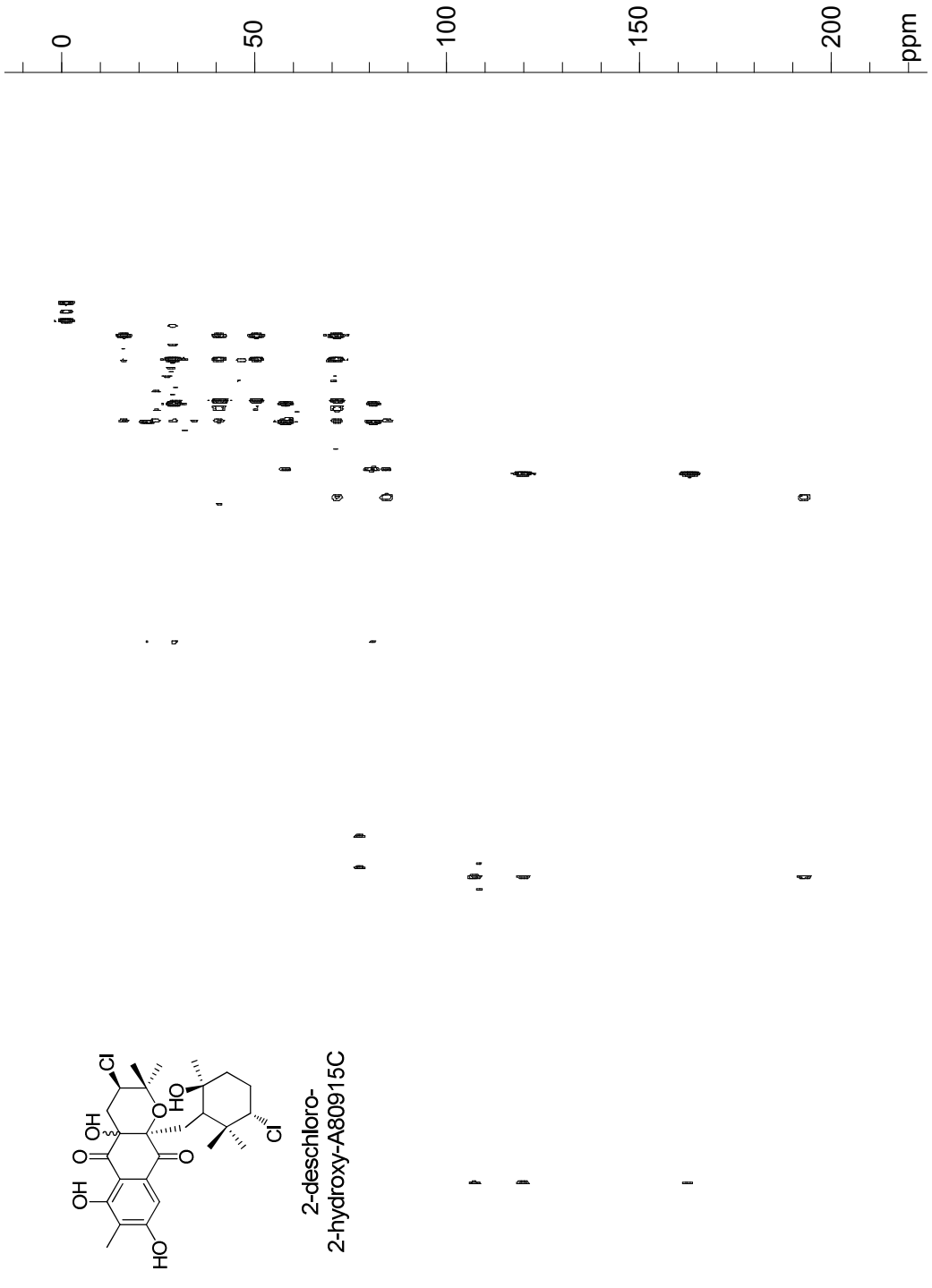
0
50
100
150
200
ppm
0.0
5.0
10.0
ppm
2-deschloro-
2-hydroxy-A80915C

Figure 2A.7: gHSQC NMR spectrum of 2-deschloro-2-hydroxy-A80915C in $CDCl_3$.

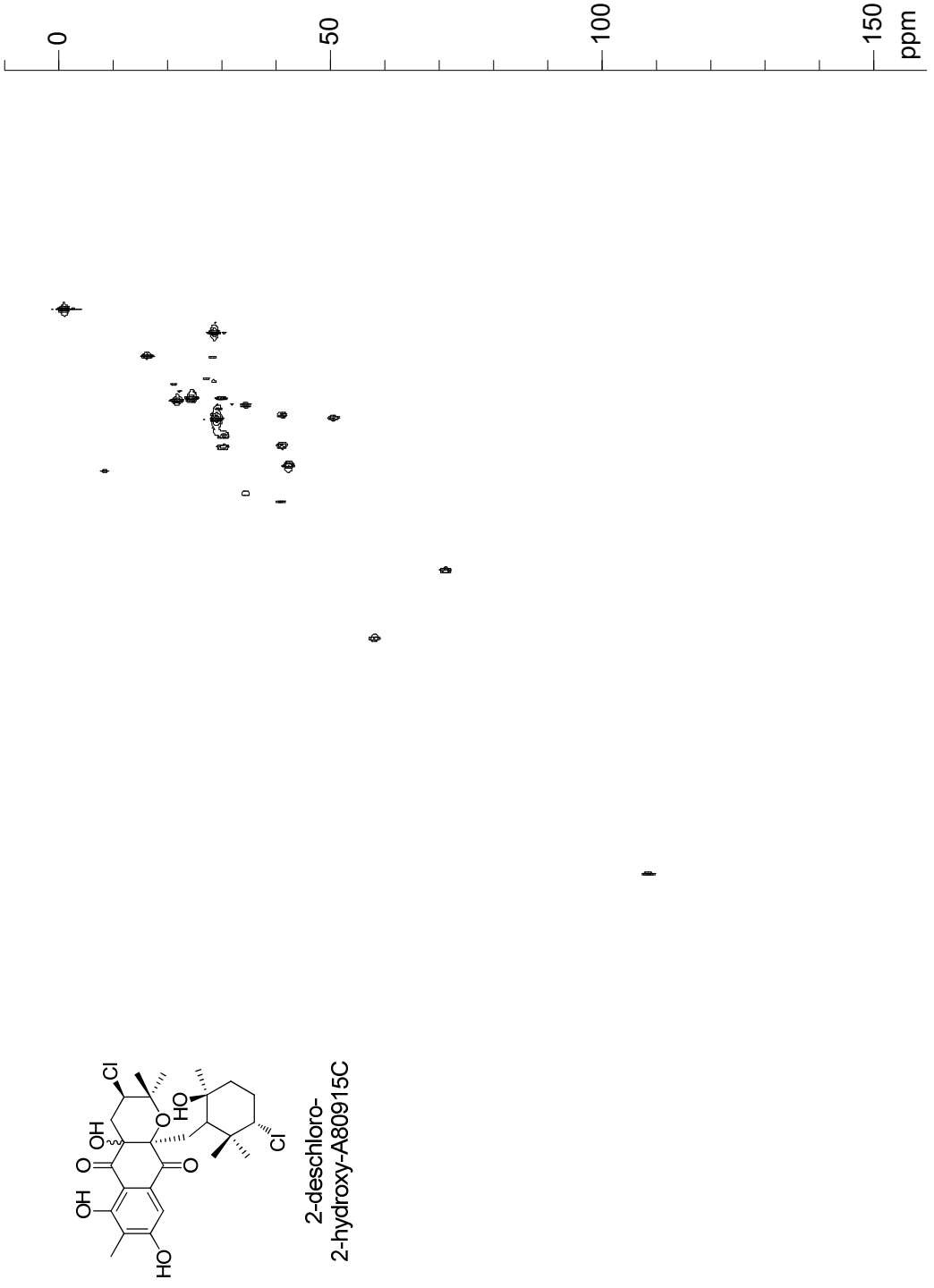
0
50
100
150
ppm
0.0
5.0
10.0
ppm
Cl
O
HO
OH
O
O
OH
HO
Cl
2-deschloro-
2-hydroxy-A80915C

Figure 2A.8: NOESY NMR spectrum of 2-deschloro-2-hydroxy-A80915C in $CDCl_3$.

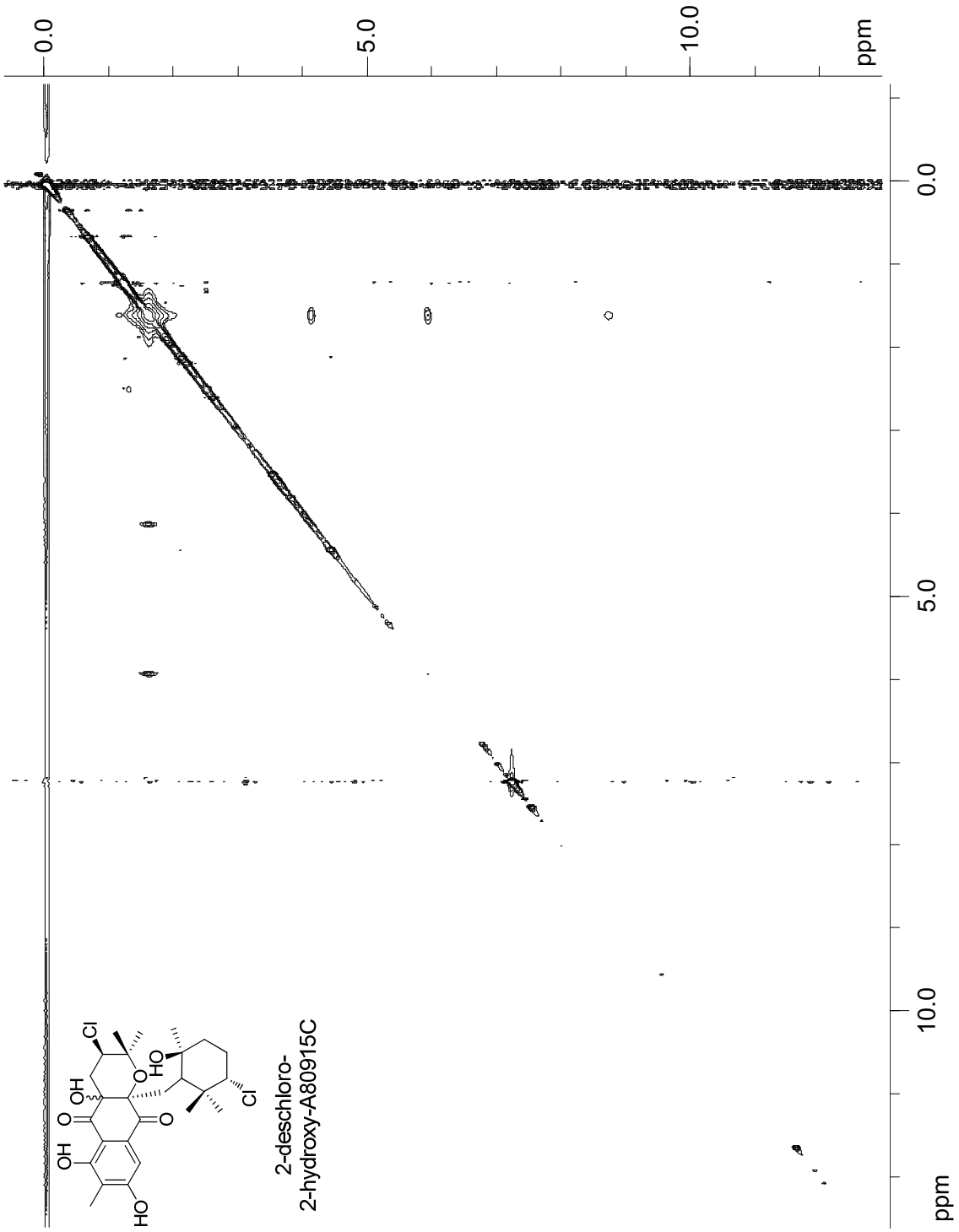
0.0
5.0
10.0
ppm
0.0
5.0
10.0
ppm
Cl
HO
OH
O
O
OH
HO
Cl
2-deschloro-
2-hydroxy-A80915C

2.6: References

1. Butler, A.; Carter-Franklin, J. N., The role of vanadium bromoperoxidase in the biosynthesis of halogenated marine natural products. *Nat. Prod. Rep.* **2004,** 21, 180-88.

2. Moore, B. S., Biosynthesis of marine natural products: macroorganisms (Part B). *Nat. Prod. Rep.* **2006,** 23, 615-29.

3. vanPee, K. H.; Unversucht, S., Biological dehalogenation and halogenation reactions. *Chemosphere* **2003,** 52, 299-12.

4. Renirie, R.; Hemrika, W.; Wever, R., Peroxidase and phosphatase activity of active-site mutants of vanadium chloroperoxidase from the fungus *Curvularia inaequalis*. Implications for the catalytic mechanisms. *J. Biol. Chem.* **2000,** 275, 11650-57.

5. Littlechild, J.; Garcia-Rodriguez, E.; Dalby, A.; Isupov, M., Structural and functional comparisons between vanadium haloperoxidase and acid phosphatase enzymes. *J. Mol. Recognit.* **2002,** 15, 291-96.

6. Hofrichter, M.; Ullrich, R., Heme-thiolate haloperoxidases: versatile biocatalysts with biotechnological and environmental significance. *Appl. Microbiol. Biotechnol.* **2006,** 71, 276-88.

7. vanPee, K. H., Biosynthesis of halogenated metabolites by bacteria. *Annu. Rev. Microbiol.* **1996,** 50, 375-99.

8. Shiomi, K.; Nakamura, H.; Iinuma, H.; Naganawa, H.; Isshiki, K.; Takeuchi, T.; Umezawa, H.; Iitaka, Y., Structures of new antibiotics napyradiomycins. *J. Antibiot.* **1986,** 39, 494-01.

9. Shiomi, K.; Nakamura, H.; Iinuma, H.; Naganawa, H.; Takeuchi, T.; Umezawa, H.; Iitaka, Y., New antibiotic napyradiomycins A2 and B4 and stereochemistry of napyradiomycins. *J. Antibiot.* **1987,** 40, 1213-19.

10. Fukuda, D. S.; Mynderse, J. S.; Baker, P. J.; Berry, D. M.; Boeck, L. D.; Counter, L. D.; Ensminger, P. W.; Allen, N. E.; Alborn, W. E.; Hobbs, J. N., A80915, a new antibiotic complex produced by *Streptomyces aculeolatus*. Discovery, taxonomy, fermentation, isolation, characterization, and antibacterial evaluation. *J. Antibiot.* **1989,** 63, 623-33.

11. Soria-Mercado, I. E.; Prieto-Davo, A.; Jensen, P. R.; Fenical, W., Antibiotic terpenoid chloro-dihydroquinones from a new marine actinomycete. *J. Nat. Prod.* **2005,** 68, 904-10.

12. Gomi, S.; Ohuchi, S.; Sasaki, T.; Itoh, J.; Sezaki, M., Studies on new antibiotics SF2415. II. The structural elucidation. *J. Antibiot.* **1987,** 40, 740-49.

13. Winter, J. M.; Jansma, A. L.; Handel, T. M.; Moore, B. S., Formation of the pyridazine natural product azamerone by biosynthetic rearrangement of an aryl diazoketone. *Angew. Chem. Int. Ed. Engl.* **2009,** 48, 767-70.

14. Shiomi, K.; Iinuma, H.; Naganawa, H.; Isshiki, K.; Takeuchi, T.; Umezawa, H., Biosynthesis of napyradiomycins. *J. Antibiot.* **1987,** 40, 1740-45.

15. Shin-Ya, K.; Furihata, K.; Hayakawa, Y.; Seto, H., Biosynthetic studies of naphterpin, a terpenoid metabolite of *Streptomyces*. *Tetrahedron Lett.* **1990,** 31, 6025-26.

16. Funayama, S.; Ishibashi, M.; Komiyama, K.; Omura, S., Biosynthesis of furaquinocin-A and furaquinocin-B. *J. Org. Chem.* **1990,** 55, 1132-33.

17. Kalaitzis, J. A.; Hamano, Y.; Nilsen, G.; Moore, B. S., Biosynthesis and structural revision of neomarinone. *Org. Lett.* **2003,** 5, 4449-52.

18. Haagen, Y.; Glueck, K.; Fay, K.; Kammerer, B.; Gust, B.; Heide, L., A gene cluster for prenylated naphthoquinone and prenylated phenazine biosynthesis in *Streptomyces cinnamonensis* DSM 1042. *Chembiochem* **2006,** 7, 2016-27.

19. Kawasaki, T.; Hayashi, Y.; Kuzuyama, T.; Furihata, K.; Itoh, N.; Seto, H.; Dairi, T., Biosynthesis of a natural polyketide-isoprenoid hybrid compound, furaquinocin A: identification and heterologous expression of the gene cluster. *J. Bacteriol.* **2006,** 188, 1236-44.

20. Dairi, T., Studies on biosynthetic genes and enzymes of isoprenoids produced by actinomycetes. *J. Antibiot.* **2005,** 58, 227-43.

21. Kawasaki, T.; Kuzuyama, T.; Furihata, K.; Itoh, N.; Seto, H.; Dairi, T., A relationship between the mevalonate pathway and isoprenoid production in actinomycetes. *J. Antibiot.* **2003,** 56, 957-66.

22. Dairi, T.; Hamano, Y.; Kuzuyama, T.; Itoh, N.; Furihata, K.; Seto, H., Eubacterial diterpene cyclase genes essential for production of the isoprenoid antibiotic terpentecin. *J. Bacteriol.* **2001,** 183, 6085-94.

23. Bierman, M.; Logan, R.; O'Brien, K.; Seno, E. T.; Rao, R. N.; Schoner, B. E., Plasmid cloning vectors for the conjugal transfer of DNA from *Escherichia coli* to *Streptomyces* spp. *Gene* **1992,** 116, 43-49.

24. Sambrook, J.; Fritsch, E. F.; Maniatis, T., *Molecular Cloning, a Laboratory Manual,* 2nd ed.; Cold spring Harbor Laboratory: Cold Spring Harbor, NY, 1989.

25. Altschul, S. F.; Gish, W.; Miller, W.; Myers, E. W.; Lipman, D. J., Basic local alignment search tool. *J. Mol. Biol.* **1990,** 215, 403-10.

26. Banskota, A. H.; McAlpine, J. B.; Sorensen, D.; Aouidate, M.; Piraee, M.; Alarco, A. M.; Omura, S.; Shiomi, K.; Farnet, C. M.; Zazopoulos, E., Isolation and identification of three new 5-alkenyl-3,3(2H)-furanones from two *Streptomyces* species using a genomic screening approach. *J. Antibiot.* **2006,** 59, 168-76.

27. Ishikawa, J.; Hotta, K., FramePlot: a new implementation of the frame analysis for predicting protein-coding regions in bacterial DNA with a high G + C content. *FEMS Microbiol. Lett.* **1999,** 174, 251-53.

28. Kieser, T.; Bibb, M. J.; Buttner, M. J.; Chater, K. F.; Hopwood, D. A., *Practical Streptomyces Genetics*. The John Innes Foundation: Norwich, 2000.

29. Moffit, M. C.; Moore, B. S., *unpublished data*.

30. Austin, M. B.; Izumikawa, M.; Bowman, M. E.; Udwary, D. W.; Ferrer, J. L.; Moore, B. S.; Noel, J. P., Crystal structure of a bacterial type III polyketide synthase and enzymatic control of reactive polyketide intermediates. *J. Biol. Chem.* **2004,** 279, 45162-74.

31. Kuzuyama, T.; Noel, J. P.; Richard, S. B., Structural basis for the promiscuous biosynthetic prenylation of aromatic natural products. *Nature* **2005,** 435, 983-87.

32. Botta, B.; Delle Monache, G.; Menendez, P.; Boffi, A., Novel prenyltransferase enzymes as a tool for flavonoid prenylation. *Trends Pharmacol. Sci.* **2005,** 26, 606-68.

33. Comte, G.; Daskiewicz, J. B.; Bayet, C.; Conseil, G.; Viornery-Vanier, A.; Dumontet, C.; Di Pietro, A.; Barron, D., C-Isoprenylation of flavonoids enhances binding affinity toward P-glycoprotein and modulation of cancer cell chemoresistance. *J. Med. Chem.* **2001,** 44, 763-68.

34. Fenical, W., Halogenation in Rhodophyta - Review. *J. Phycol.* **1975,** 11, 245-59.

35. Lombo, F.; Velasco, A.; Castro, A.; de la Calle, F.; Brana, A. F.; Sanchez-Puelles, J. M.; Mendez, C.; Salas, J. A., Deciphering the biosynthesis pathway of the antitumor thiocoraline from a marine actinomycete and its expression in two *Streptomyces* species. *Chembiochem* **2006,** 7, 366-76.

36. Bringmann, G.; Haagen, Y.; Gulder, T. A. M.; Gulder, T.; Heide, L., Biosynthesis of the isoprenoid moieties of furanonaphthoquinone I and endophenazine A in *Streptomyces cinnamonensis* DSM 1042. *J. Org. Chem.* **2007,** 72, 4198-04.

37. Soria-Mercado, I. E.; Jensen, P. R.; Fenical, W.; Kassel, S.; Golen, J., 3,4a-dichloro-10a-(3-chloro-6-hydroxy-2,2,6-trimethylcyclohexylmethyl)-6,8-dihydroxy-2,2,7-trimethyl-3,4,4a,10a-tetrhydro-2H-benzo[g]chromene-5,10-dione. *Acta Crystallogr., Sect. E* **2004,** 60, 1627-29.

2.7: Acknowledgement

Chapter 2, in full, is a reprint of the material as it appears in Molecular Basis for Chloronium-mediated Meroterpene Cyclization: Cloning, Sequencing, and Heterologous Expression of the Napyradiomycin Biosynthetic Gene Cluster (2007). Winter, Jaclyn M; Moffitt, Michelle; Zazopoulos Emmanuel; McAlpine James; Dorrestein, Pieter C.; Moore, Bradley S., Journal of Biological Chemistry, 282, 16362–68. The dissertation author was the primary investigator and author of this paper.

Chapter 3

Towards the Characterization of Recombinant Vanadium-Dependent Chloroperoxidases from the Napyradiomycin Biosynthetic Cluster by In vitro Expression Experiments and X-Ray Crystallography

3.1: Introduction

3.1.1: Biological Halogenation

Halogens are an abundant component of the Earth's biosphere, so it is of little surprise that nature produces a profuse number of organohalogens.[1] Halogenated natural products possess diverse biological activities of pharmacological interest, including antifungal, antibacterial, antiviral, and anti-inflammatory activities.[2] Clinically important halogenated natural products include the antibiotics vancomycin,[3] chlortetracycline,[4] and chloramphenicol[5] as well as the anticancer agents rebeccamycin[6] and salinosporamide A[7] (Figure 3.1).[8, 9] To

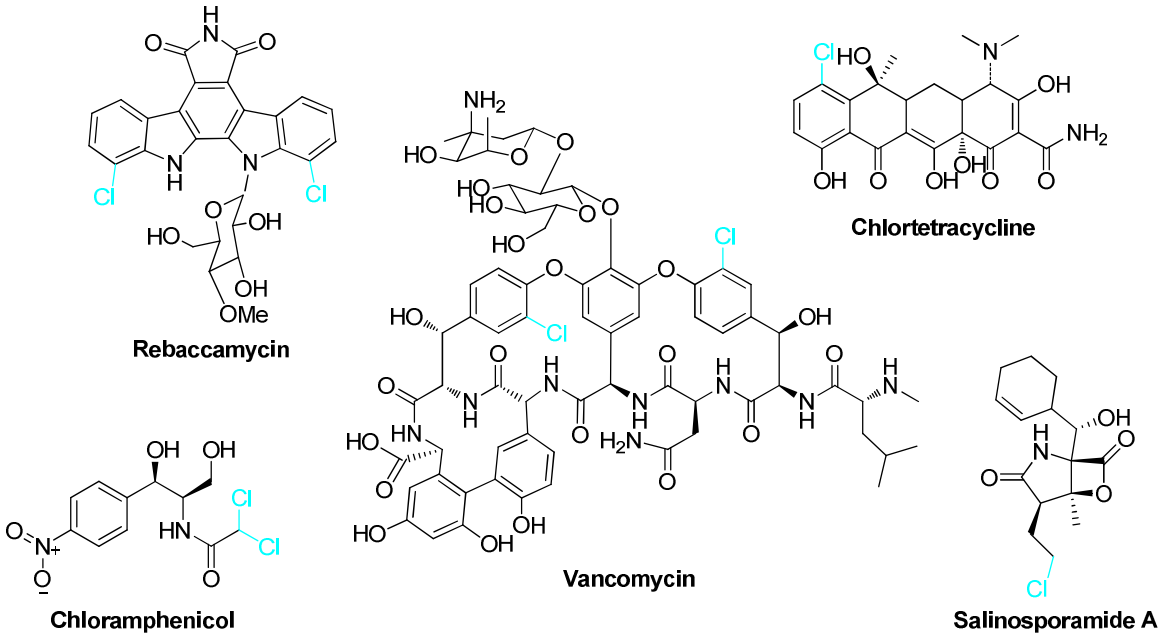

Figure 3.1: Chlorinated natural products with biological activity.

date, there have been more than 4,000 distinct natural organohalogens discovered, and as of July 2004 the breakdown of these halogenated compounds

was approximately 2,300 organochlorines, 2,050 organobromines, 110 organoiodines, and 30 organofluorines.[1] In addition to their therapeutic potential for human health, halogenated natural products have important biological functions for the producing organism, ranging from chemical defense to signaling molecules. However, the position, number, and/or type of halogen atom is often detrimental for its affinity, selectivity, and reactivity toward a biological target.

Nature has developed an exquisite array of methods to introduce halogen atoms into organic compounds. Most of these enzymes are oxidative and require either hydrogen peroxide or molecular oxygen as co-factors to generate a reactive halogen atom for catalysis. During the past 40 years, four classes of oxidative halogenating enzymes have been characterized and include the heme-dependent haloperoxidases and vanadium-dependent haloperoxidases (V-HPOs), which require H_2O_2 as an oxidant, and the flavin-dependent halogenases and non-heme iron-dependent halogenases, which require molecular oxygen as the oxidant (Table 3.1).[10-12]

Table 3.1: The four classes of oxidative halogenating enzymes with their cofactors and cosubstrates.

Enzyme Type	Redox Cofactor	Oxidant	Cosubstrates
Haloperoxidase	Heme iron	H_2O_2	Halide
Haloperoxidase	Vanadium	H_2O_2	Halide
Halogenase	$FADH_2$	O_2	Halide
Halogenase	Non-heme iron	O_2	Halide and α-ketoglutarate

3.1.2: Vanadium haloperoxidases

V-HPOs have a large distribution in nature where they are present in macroalgae, fungi, and bacteria.[2, 13, 14] Together with the heme-dependent haloperoxidases, V-HPOs utilize hydrogen peroxide to convert a halide ion (X^-) to a hypohalite (–OX) intermediate that is chemically equivalent to an electrophilic "X^+". These enzymes, which contain a ligated vanadate ion, oxidize halide ions to their corresponding hypohalous acids at the expense of hydrogen peroxide and are classified by the most electronegative halide they oxidize. Thus, vanadium chloroperoxidases (V-ClPOs) oxidize chloride, bromide, and iodide, whereas vanadium-bromoperoxidases (V-BrPOs) oxidize only bromide and iodide. However, unlike the heme enzyme, there is no change in the oxidation state of the V-HPO metal center during the synthesis of the halogenating agent. Hence, V-HPOs do not suffer from oxidative inactivation during turnover and have received increasing attention as biocatalysts for pharmaceutical applications given their tolerance for organic solvents and high temperatures,[15, 16] their ability to halogenate a range of organic compounds in a regio- and stereospecific manner,[2, 17, 18] and their ability to oxidize organic sulfides in the absence of halides.[19, 20]

The majority of naturally occurring organohalogens are of marine origin, and nearly all brominated natural products are produced by marine organisms.[1] Some of the most frequently reported halometabolites are produced by marine red algae (Rhodophyceae) and include halogenated indoles, terpenes, acetylenes, phenols, and volatile hydrocarbons.[1, 2, 17, 21, 22] Among the red,

brown, and green algae, Rhydophyta are the richest in bromoperoxidase activity, with the genus *Corallina* possessing the highest activity.[23, 24] Vanadium bromoperoxidases (V-BrPOs) are proposed to be responsible for the halogenations of natural products produced by marine algae,[17, 21] and the first V-HPO to be isolated and characterized was the V-BrPO from the brown alga *Ascophyllum nodosum* in 1984.[25] To date, V-BrPOs have been characterized from all major classes of marine algae[15, 26-30] as well as terrestrial lichen.[31] Their proposed role in the biosynthesis of brominated cyclic sesquiterpenes from marine red algae was established through *in vitro* chemoenzymatic conversion of (*E*)-(+)-nerolidol to yield the marine natural products α-snyderol, β -snyderol, and γ-snyderol (Figure 3.2).[17]

Fungi belonging to the dematiaceous hyphomycetes were discovered to produce haloperoxidases distinct from the heme haloperoxidases that could function at elevated pH and temperature.[32] A non-heme chloroperoxidases was identified from the fungus *Curvularia inaequalis* in 1987[33] and six years later was characterized as a V-ClPO.[34] A second V-ClPO was later isolated from the fungus *Embellisia didymospora;*[35] however, no halogenated metabolites have been reported to date from either source. Rather, fungal V-ClPOs are suggested to function physiologically in the generation of hypochlorous acid to facilitate the oxidative degradation of plant cell wall lignocelluloses to allow for fungal hyphen penetration.[14] A related *in vivo* role has been proposed for some macroalgal V-HPOs that are present on the plant surface in which the hypohalous acids function as anti-fouling agents against opportunistic bacteria.[14] A recent study

analyzing gene expression in the brown alga *Laminaria digitata* has shed light on how V-BrPOs and vanadium-dependent iodoperoxidases are up-regulated upon defense elicitation.[36]

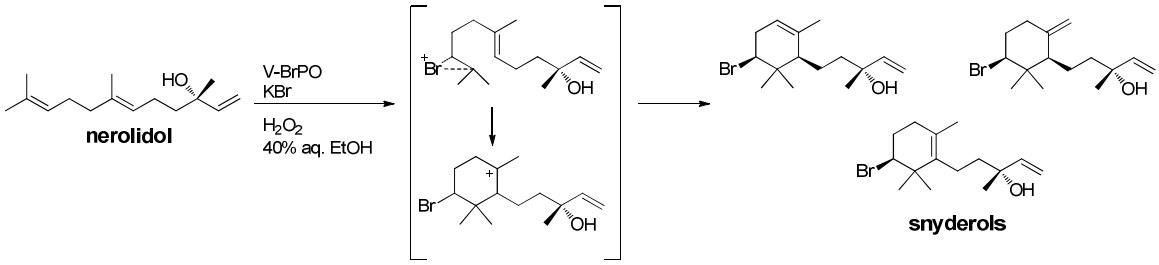

Figure 3.2: Chemoenzymatic cyclization of nerolidol to form the brominated snyderol series of compounds using the V-BrPO from *Corallina officinalis*.

3.1.3: Structure Relationships

Crystal structures are available for three vanadium-dependent haloperoxidases, namely V-ClPO from the fungus *C. inaequalis*,[37-39] V-BrPO from the brown alga *A. nodosum*,[40] and V-BrPO from the red alga *C. officinalis*[41]. At the primary level, the proteins share less than 30% sequence identity, and differ dramatically in reported monomeric state. The V-ClPO from *C. inaequalis* is a monomeric protein, while the V-BrPO from *A. nodosum* is a homo-dimer. Interestingly, the V-BrPO from *C. officinalis,* which is associated with snyderol biosynthesis (Figure 3.2), is a homo-dodecameric protein arranged in a 23-point group symmetry.[41] Differences in monomeric states between the V-HPOs may be indicative of their biological function. Each protein, however, shares a core structure consisting of mainly α-helices with two four-helix bundles as the main

tertiary structural motif[37-39, 41] and has an identical arrangement of amino acid residues at the vanadium active site itself.

The vanadium-binding site lies at the bottom of a 15–20 Å deep funnel-shaped channel located at the core of the four-helix bundle.[2, 39-41] Vanadium is present as a vanadate(V) ion and is ligated to the imidazole ring of a conserved histidine residue that anchors the cofactor in a trigonal bipyrimidal fashion (Figure 3.3).[39-41] Three oxygen atoms of the cofactor are located in the equatorial plane, and the negative charges are compensated by an extensive hydrogen bonding network with protonated amino acid residues in the conserved active site. Through quantum mechanics/molecular mechanics, ^{51}V solid-state NMR, and UV-Visible spectroscopy studies, the resting state of the enzyme likely contains at least one hydroxyl group in the apical position.[42-44] An axial water molecule is putatively incorporated at this position and stabilized through a hydrogen bond with a side chain His imidazole.[43]

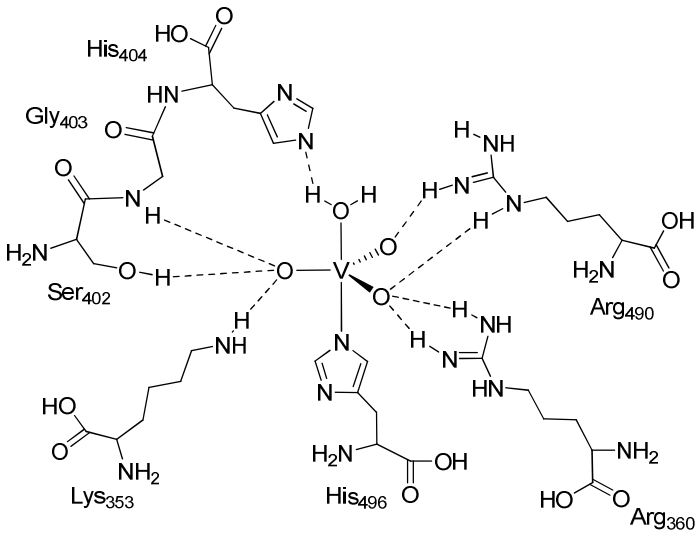

Figure 3.3: Vanadium site of native V-ClPO from *Curvularia inaequalis*. Possible hydrogen bonds are drawn as dashed lines (adapted from references [37, 39, 43]).

3.1.4: Catalytic Cycle

Active site mutagenesis experiments and steady-state kinetics on recombinant V-ClPO from *C. inaequalis* have shed light on the catalytic mechanism of the V-HPOs (Figure 3.4).[14, 45, 46] Alanine scanning mutagenesis of the active site residues Lys353, His404, Arg360, Arg490, and His496 (numbering from *C. inaequalis*) yielded mutant enzymes unable to oxidize chloride. However, the modified enzymes could still function as bromoperoxidases, albeit with decreased activity compared to native V-BrPOs.[41, 45, 46] The H496A mutant lost the ability to bind vanadate and could no longer function as a V-HPO, while the H404A mutation was shown to have a reduced affinity for the cofactor.[45]

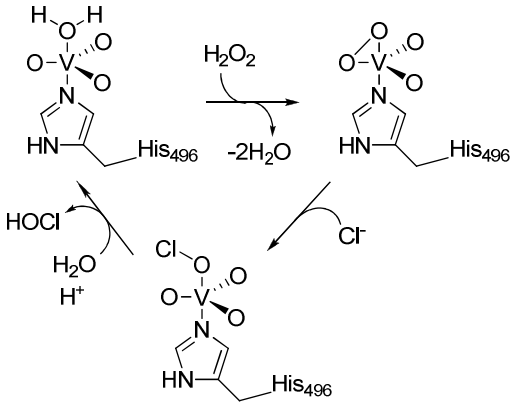

Figure 3.4: Proposed catalytic scheme of a V-ClPO (adapted from references [37, 45, 46]).

Steady-state kinetics show that V-HPOs catalyze the two-electron oxidation of halides in a substrate-inhibited bi-bi ping-pong mechanism.[2, 14, 47] Coordination of hydrogen peroxide to the vanadium center is the first step in catalysis, and the His404 residue, which activates the axial water molecule, must

be deprotonated for H_2O_2 to bind.[34] A crystal structure of the peroxo-V-ClPO shows that peroxide is coordinated in a side-on manner in the equatorial plane and distorts the vanadium site to a tetragonal bipyramidal geometry.[37] After the binding of peroxide, His404 is no longer hydrogen-bonded to any oxygen atoms of the cofactor and Lys353 makes direct contact with one of the oxygen atoms of the bound peroxide, further activating the bound peroxide through charge separation.

A halide ion is the second substrate that binds to the enzyme through a nucleophilic attack on the partially positive oxygen atom (Figure 3.4). This binding breaks the peroxide bond and creates the nucleophilic OX^- group, which leaves the coordination sphere as hypohalous acid after protonation by an incoming water molecule.[46] If an appropriate nucleophile is present, the generated hypohalous acid intermediate will react with the organic substrate giving rise to a halogenated compound. If not, the oxidized halogen intermediate will react with another equivalent of hydrogen peroxide to generate dioxygen in the singlet state and the halide.[2] A new fluorescence microscopy-based method, which uses a fluorogenic derivative to monitor the formation and migration of HOBr from a V-BrPO active site, will shed light over where the actual halogenation of organic substrates occurs.[48]

Active site residues assisting with the selection and binding of the halide are still being elucidated. On the basis of crystal structure analysis, residues Phe397 and Trp350 (numbering from *C. inaequalis*) may participate in halide binding through their $\delta+$ ring edge.[49] V-BrPOs alternatively contain His and Arg

residues at these positions, respectively.[49] Recently, chlorinating activity was created in the *C. pilulifera* V-BrPO through a single amino acid substitution.[48] The substitution of the Arg residue at position 350 to Trp or Phe increased V-BrPO's affinity for chloride.[50] The native V-BrPO from *A. nodosum* also contains a Trp residue corresponding to position 350, and it too was shown to exhibit chloroperoxidases activity.[51] Therefore, this Trp residue is believed to participate in chloride binding.

Additional mutagenesis experiments on the His residue corresponding to Phe397 showed the importance of the residue in the oxidation of halides.[52] The His residue was mutated to Ala on the V-BrPO from *C. officinalis*, which resulted in the enzyme's inability to efficiently oxidize bromide, however, the mutant could still oxidize iodide.[52] Interestingly, like the V-BrPOs, the three putative V-ClPOs from the napyradiomycin biosynthetic cluster also contain a His residue in the position corresponding to Phe397,[53] and this residue may also play a role in substrate binding or selectivity.

3.1.5: Relationship to phosphatases

Sequence alignment of V-ClPO from *C. inaequalis* and V-BrPOs from *A. nodosum* and *Corallina officinalis* and analysis of their high-resolution crystal structures revealed that the amino acid residues required for binding the vanadate cofactor share homology with a family of acid phosphatases.[13, 14, 54] Many of these enzymes are membrane-bound and include type 2 phosphatidic

acid phosphatase, bacterial non-specific acid phosphatases and mammalian glucose-6-phosphatases.[13, 14, 47, 54] Studies with vanadium-substituted bacterial class A non-specific acid phosphatases from *Shigella flexneri* and *Salmonella enterica* ser. *Typhimurium*, which catalyze the hydrolysis of phosphomonoesters, showed that these enzymes also exhibit bromoperoxidase activity.[55] Conversely, recombinant apo-chloroperoxidase from *C. inaequalis* possesses phosphatase activity using the substrate para-nitrophenyl phosphate,[45, 54] and its crystal structure was recently solved with a trapped phosphohistidine intermediate.[56] Together, these data suggest an evolutionary relationship between the acid phosphatases and V-HPOs.

3.1.6: Chemoenzymatic biotransformations

While the biological function of fungal V-ClPOs has yet to be confirmed, marine algal V-BrPOs have been shown through *in vitro* chemoenzymatic conversions to catalyze the bromonium-assisted cyclization of terpenes and ethers.[2, 17] Initial studies on the enzymatic halogenation of anisole and prochiral aromatic compounds by the *C. pilulifera* V-BrPO failed to show any regio- or stereospecificity suggesting that the hypobromite intermediate was freely diffusible to facilitate the molecular bromination reaction outside of the enzyme's active site.[2, 12] However, more recent studies have convincingly shown that various V-BrPOs isolated from marine red algae (e.g., *Corallina officinalis*, *Laurencia pacifica*, and *Plocamium cartilagineum*) catalyze the asymmetric

bromination/cyclization reactions of the sesquiterpene nerolidol to the snyderol family of marine natural products (Figure 3.2).[17] Single diasteromers of β- and γ-snyderol were produced in the enzyme reaction, whereas, in the synthetic reaction, two diasteromers of each were formed. This study established the likely role of V-BrPOs in the biosynthesis of brominated cyclic sesquiterpenes from marine red algae and further implies that other marine algal brominated natural products may similarly be constructed.

3.1.7: Specific aim

The unprecedented discovery of three V-ClPOs within the napyradiomycin biosynthetic cluster was a significant discovery as these enzymes are not only rare in nature but have never before been characterized from prokaryotes.[35] To date, V-BrPOs are the only characterized haloperoxidases that demonstrate the ability to facilitate bromonium ion induced cyclization of terpenes *in vitro*.[2] The genes for each of the V-ClPOs (*nap*H1, *nap*H3 and *nap*H4), as well as the $FADH_2$ dependent halogenase *nap*H2, will be expressed and subjected to a variety of assays to test their ability to halogenate substrates under various conditions. Soluble recombinant proteins will also be used in crystallographic studies in hopes of solving their three-dimensional structure. Through structure and functional analysis, it is known which amino acids are required for halogenating activity and which residues are required for halide selectivity. However, it is know known which amino acids located in the channel leading to

the active site are required for substrate specificity. The final products produced by many of these enzymes are still not known so their natural substrate still remains a mystery. The discovery of the *nap* biosynthetic operon does not only provide unique halogenating enzymes, but also provides unique halogenated secondary metabolites that can be used to elucidate natural substrate preference for each of the V-ClPOs.

3.2: Materials and Methods

3.2.1: Bacterial strains

Streptomyces sp. CNQ-525 was a gift from Professors William Fenical and Paul R. Jensen (University of California at San Diego).[57] *Escherichia coli* cultures (Table 3.2) were grown in Luria Bertani (LB) broth (Appendix Figure 2A.1) at 37 ^{o}C in 15 ml conical tubes for 16 hours at constant shaking. When selecting *E. coli* harboring plasmids, the cultures were grown with the appropriate antibiotics.

Table 3.2: *E. coli* strains used and their corresponding genotypes

***E. Coli* strain**	**Genotype**	**Source**
Subcloning efficiency DH5-α competent cells	F- φ80*lac*ZΔM15 Δ(*lac*ZYA-*arg*F)U169 *rec*A1 *end*A1 *hsd*R17(rk-, mk+) *pho*A*sup*E44 *thi*-1 *gyr*A96 *rel*A1 λ-	Invitrogen, USA
BL21(DE3) competent cells	*E. coli* B F^- dcmompT hsdS(r_B^- m_B^-) gal λ(DE3)	Stratagene, USA
ArcticExpress™ (DE3) competent cells	*E. coli B* F^- *ompT hsdS*(r_B^- m_B^-) *dcm*$^+$ *Tet*^{r} *gal λ(DE3) endA Hte [cpn10cpn60 Gent*^{r}*]*	Stratagene, USA

3.2.2: Autoinduction

Expression of halogenases from the napyradiomycin biosynthetic cluster were performed using an autoinduction method.[58] This procedure used a defined media, which allows for the expression of recombinant proteins under the T7

polymerase without the need to add inducers. Components for the media can be purchased from Novagen (Overnight Express™ Autoinduction System 1) or can be prepared using recipes from the Altman laboratory website (Appendix Figure 3A.1).[59]

3.2.3: Preparation of expression vectors

3.2.3.1: pHIS8

The expression vector pHIS8[60] was used in the expression of NapH1, NapH2, NapH3 and NapH4 and transformed into DH5-α cells for amplification according to standard procedures.[61] To create the ligation site for *nap*H1 or *nap*H3, 6 µg of expression vector was doubly digested with 2.5 µl of NcoI (New England Biolabs, 10,000 U/ml) and 2.5 µl NotI (New England Biolabs, 10,000 U/ml) in a 50 µl reaction containing 0.5 µl BSA (New England Biolabs, 10 mg/ml), 5 µl of NEBuffer 3 (New England Biolabs) and 9.5 µl of Milli-Q water. The reaction was incubated for two hours at 37 ^{o}C and the DNA was purified with a QIAGEN gel elution kit according to manufacturer's instructions. DNA was eluted off the column with 40 µl EB buffer and stored at –20 ^{o}C. To create the ligation site for *nap*H2 or *nap*H4, 6 µg of expression vector was doubly digested with 2.5 µl of EcoR1 (New England Biolabs, 20,000 U/ml) and 2.5 µl HindIII (New England Biolabs, 20,000 U/ml) in a 50 µl reaction containing 5 µl of NEBuffer EcoR1 (New England Biolabs) and 10 µl of Milli-Q water. The reaction was incubated for two hours at 37 ^{o}C and the DNA was purified with a QIAGEN gel

elution kit according to manufacturer's instructions. DNA was eluted off the column with 40 µl EB buffer (Appendix Figure 2A.3) and stored at –20 ^{o}C.

3.2.3.2: pGS-21a

The expression vector GS-21a (GenScript) was used in the expression of NapH4 and transformed into DH5-α cells for amplification according to standard procedures.[61] To create the ligation site for *nap*H4, 3 µg of expression vector was doubly digested with 1.5 µl of EcoR1 (New England Biolabs, 20,000 U/ml) and 1.5 µl HindIII (New England Biolabs, 20,000 U/ml) in a 25 µl reaction containing 2.5 µl of NEBuffer EcoR1 (New England Biolabs) and 4.5 µl of Milli-Q water. The reaction was incubated for two hours at 37 ^{o}C and the DNA was purified with a QIAGEN gel elution kit according to manufacturer's instructions. DNA was eluted off the column with 20 µl EB buffer (Appendix Figure 2A.3) and stored at –20 ^{o}C.

3.2.4: Expression and purification of NapH1

3.2.4.1: Amplification of *nap*H1

Using total genomic DNA from *S.* sp. CNQ-525 (see Section 2.2.2.1), *nap*H1 was amplified by PCR using the primers NapH1p Fwd and NapH1p Rev (Table 3.3). NapH1p Fwd contains a NcoI restriction site whereas NapH1p Rev contains a NotI site. Both primers were diluted with Milli-Q water to a final concentration of 20 µM. For a 50 µl PCR reaction, 1µl of gDNA DNA (22 ng/µl)

was mixed with 0.5 µl pfu turbo (2.5 U/µl, Stratagene), 5 µl pfu 10 X buffer, 1 µl NapH1p Fwd (10 pmol/µl), 1 µl of NapH1p Rev (10pmol/µl), 1 µl dNTPs (10 mM), 2.5 µl DMSO and 38 µl Milli-Q water. PCR conditions were 96 ^{o}C for five minutes; 25 cycles of 96 ^{o}C for one minute, 56 ^{o}C for one minute and 72 ^{o}C for 90 seconds, followed by an extra ten minutes at 72 ^{o}C. Following amplification, the PCR reaction was desalted using a QIAGEN gel purification kit according to manufacturer's instructions. DNA was eluted off the column with 30 µl of EB buffer (Appendix Tabe 2A.3) and doubly digested with 2.5 µl of NcoI (New England Biolabs, 10,000 U/ml), 2.5 µl NotI (New England Biolabs, 10,000 U/ml), 0.5 µl BSA (New England Biolabs, 10 mg/mL), 5 µl of NEBuffer 3 (New England Biolabs), and 9.5 µl of Milli-Q water. The reaction was incubated for two hours at 37 ^{o}C and the DNA was purified with a QIAGEN gel elution kit according to manufacturer's instructions. DNA was eluted off the column with 20 µl EB buffer.

Doubly digested DNA was ligated into a NcoI/NotI digested pHIS8 vector in a 10 µl reaction containing 1 µl vector, 6 µl DNA (5 ng/µl), 1µl 10X ligation buffer, 1 µl T4 DNA ligase (400,000 U/ml, New England Biolabs), and 1 µl Milli-Q water. The ligation reaction was incubated overnight at 16 ^{o}C. After which, 2 µl of the ligation reaction was transformed into DH5-α cells (Invitrogen) according to manufacturer's instructions. A 50 µl aliquot was plated on LB agar (Appendix Figure 2A.1) containing kanamycin (50 µg/ml) and incubated overnight at 37 ^{o}C. Colonies were picked and grown overnight by constant shaking at 37 ^{o}C in 5 ml LB (Appendix Figure 2A.1) containing kanamycin (50 µg/ml). Plasmid DNA was extracted according to section 2.2.2.2, eluted off the QIAGEN column with 50 µl

EB buffer, and sequenced using the T7 promoter and T7 teminator sites on the vector (Table 3.4).

Table 3.3: Primer sequences used to amplify the four *nap* halogenases from *S.* sp. CNQ-525

Primer Name	Primer Sequence (5' to 3')	Target Gene	Tm (°C)
NapH1p Fwd	GCACTGGCCATGGCATGACGACGTCCG GA	V-ClPO	75
NapH1p Rev	GACGGACGGCGGCCGCTCAGTCCTTGA CGTC	V-ClPO	78
NapH2p Fwd	GACAGCGAGGAATTCATGTCGTCCAAC GTT	$FADH_2$ Halogenase	69
NapH2p Rev	GTAGCGGGAAGCTTTCAGCTATCGGCG GG	$FADH_2$ Halogenase	73
NapH3p Fwd	GCATGCCAGCCATGGCGTGACGACATC CGCC	V-ClPO	77
NapH3p Rev	GACGGACGGCGGCCGCTCAGTCCTTGA CGTC	V-ClPO	78
NapH4p Fwd	GACCGAGCGAATTCATGACGACATCCG GA	V-ClPO	70
NapH4p Rev	GACTCGGGAAGCTTTCAGCCGTCGCCC TC	V-ClPO	75
NapH4 Fwd for GST	GACCGAGCGAATTCATGACGACATCCG GA	V-ClPO	81
NapH4 Rev for GST	GACTCGGGAAGCTTTCAGCCGTCGCCC TC	V-ClPO	83

Restriction sites are underlines

Table 3.4: Primer sequences used to verify insertion of *nap* halogenases in the pHIS8 vector

Primer Name	Primer Sequence (5' to 3')
T7 promoter	TAATACGACTCACTATAGGG
T7 terminator	GCTAGTTATTGCTCAGCGG

3.2.4.2: Expression of *nap*H1

The pHIS8 vector containing *nap*H1 was transformed into BL21(DE3) chemically competent cells (Stratagene) according to manufacturer's instructions. A 50 µl aliquot was plated on LB agar (Appendix Figure 2A.1) containing kanamycin (50 µg/ml) and incubated overnight at 37 ^{o}C. A single colony was used to inoculate 25 ml Terrific Broth (TB) (Appendix Figure 3A.1) plus kanamycin (50µg/ml) and grown overnight at 37^{o} C with constant shaking in a 250 ml Erlenmeyer flask. A 12.5 ml aliquot of the seed culture was used to inoculate 200 ml TB plus kanamycin (50µg/ml) and shaken overnight at 37 ^{o}C in a 500 ml Erlenmeyer flask. For expression of *nap*H1 using autoinduction media,[59] a 25 ml aliquot of the 200 ml seed culture was used to inoculate 500 ml TB plus kanamycin (50µg/ml) in a 2.8 L Fernbach flask. At the time of inoculation, 500 µl of 1M $MgSO_4$, 10 ml 50 x 5052 (Appendix Figure 3A.1), and 25 ml 20 x NPS (Appendix Figure 3A.1) were added to each 500 ml culture. The cultures were grown at 20 ^{o}C with constant shaking for 27 hours. After the 27 hour induction, the cultures were harvested by centrifugation at 5,600 x g for ten minutes at 4 ^{o}C (Beckman Coulter Avanti J–E using a F-10.1 rotor), and the pellet was stored at -20 ^{o}C. This was repeated until a total of 10 L were expressed.

3.2.4.3: Purification of NapH1

The cell pellet from 10 L's was resuspended in 400 ml of lysis buffer (Appendix Figure 3A.2) and sonicated in 10 second intervals at until

homogeneous using a Sonic Dismembrator (Model 100, Fisher Scientific). Soluble protein was isolated by centrifuging the homogeneous mixture at 39,191 x g for 25 minutes at 4 ^{o}C (Beckman Coulter Avanti J–E using a JA-20 rotor). The supernatant was decanted and split in half. To each 200 ml fraction, 0.75 ml of Ni-NTA (Invitrogen, USA), which was washed two times with 10 ml lysis buffer, was added. On ice, the soluble protein was incubated with the Ni-NTA for one hour with constant stirring. To a 5 ml column, the soluble fractions containing Ni-NTA were added and allowed to flow-through. The column was washed two times with 10 ml wash buffer (Appendix Figure 3A.2), and His-tagged protein was eluted off the column with 7 x 5 ml aliquots of elution buffer (Appendix Figure 3A.2). A NanoDrop (NanoDrop Technologies) was used to determine which of the seven fractions contained protein. Those containing protein were combined and stored overnight at 4 ^{o}C, and a 5 µl aliquot was run on a NuPAGE gel according to Section 3.2.8.

Thrombin cleavage was used to remove the His-tag from the protein. To a two inch piece of 12–14K molecular weight cut-off dialysis tubing (Spectrum Labs), the 17 mg of protein was incubated with 34 µl of thrombin (0.5 mg/ml, Sigma Aldrich) and incubated overnight at 4 ^{o}C in 2 L dialysis buffer (Appendix Figure 3A.2). Benzamidine sepharose 4 fast flow (GE) was used to remove the thrombin. To a 20 ml plastic column, 2 ml of the benzamidine sepharose slurry was added. The flow-through was allowed to pass and the resin was washed with 10 ml of dialysis buffer. After the resin was washed, the protein was added and the flow-through was collected.

Ni-NTA was used to remove proteins with His-tags that were not removed during thrombin cleavage. To a 20 ml plastic column, 2 ml of Ni-NTA slurry was added. The flow-through was allowed to pass through and the resin was washed with 10 ml of dialysis buffer. After the washing, the protein fraction from above was added to the column and the flow-through was collected. This fraction was concentrated to 8 ml using a 10K molecular weight cut-off concentrator (Thermo Scientific). NapH1 was purified on a FPLC (Akta, Amersham) using a size exclusion column (Hiload 16/60 Superdex 200 prep grade) and an isocratic buffer (Appendix Figure 3A.2). Fractions containing NapH1 were combined and concentrated to ~10 mg/ml with a 10 K molecular weight cut-off concentrator. Aliquots of 50–100 µl were dispensed and stored at -80 ^{o}C.

3.2.5: Expression and purification of NapH2

3.2.5.1: Amplification of *nap*H2

Using total genomic DNA from *S.* sp. CNQ-525 (see Section 2.2.2.1), *nap*H2 was amplified by PCR using the primers NapH2p Fwd and NapH2p Rev (Table 3.3). NapH2p Fwd contains an EcoR1 restriction site whereas NapH2p Rev contains a HindIII site. Both primers were diluted with Milli-Q water to a final concentration of 20 µM. For a 50 µl PCR reaction, 1µl of gDNA DNA (22 ng/µl) was mixed with 0.5 µl pfu turbo (2.5 U/µl, Stratagene), 5 µl pfu 10 X buffer, 1 µl NapH2p Fwd (10 pmol/µl), 1 µl of NapH2p Rev (10pmol/µl), 1 µl dNTPs (10 mM), 2.5 µl DMSO and 38 µl Milli-Q water. PCR conditions were 96 ^{o}C for five

minutes; 25 cycles of 96 ^{o}C for one minute, 56 ^{o}C for one minute and 72 ^{o}C for 90 seconds, followed by an extra ten minutes at 72 ^{o}C. Following amplification, the PCR reaction was desalted using a QIAGEN gel purification kit according to manufacturer's instructions. DNA was eluted off the column with 30 µl of EB buffer (Appendix Tabe 2A.3) and doubly digested with 2.5 µl of EcoR1 (New England Biolabs, 20,000 U/ml), 2.5 µl HindIII (New England Biolabs, 20,000 U/ml), 5 µl of NEBuffer EcoR1 (New England Biolabs), and 10 µl of Milli-Q water. The reaction was incubated for two hours at 37 ^{o}C and the DNA was purified with a QIAGEN gel elution kit according to manufacturer's instructions. DNA was eluted off the column with 20 µl EB buffer.

Doubly digested DNA was ligated into an EcoR1/HindIII digested pHIS8 vector in a 10 µl reaction containing 1 µl vector, 6 µl DNA (5 ng/µl), 1µl 10X ligation buffer, 1 µl T4 DNA ligase (400,000 U/ml, New England Biolabs), and 1 µl Milli-Q water. The ligation was incubated overnight at 16 ^{o}C. After which, 2 µl of the ligation reaction was transformed into DH5-α cells (Invitrogen) according to manufacturer's instructions. A 50 µl aliquot was plated on LB agar (Appendix Figure 2A.1) containing kanamycin (50 µg/ml) and incubated overnight at 37 ^{o}C. Colonies were picked and grown overnight by constant shaking at 37 ^{o}C in 5 ml LB (Appendix Figure 2A.1) containing kanamycin (50 µg/ml). Plasmid DNA was extracted according to Section 2.2.2.2, eluted off the QIAGEN column with 50 µl EB buffer, and sequenced using the T7 promoter and T7 teminator sites on the vector (Table 3.4).

3.2.5.2: Expression of *nap*H2

The pHIS8 vector containing *nap*H2 was transformed into BL21(DE3) chemically competent cells (Stratagene) according to manufacturer's instructions. A 50 µl aliquot was plated on LB agar (Appendix Figure 2A.1) containing kanamycin (50 µg/ml) and incubated overnight at 37 ^{o}C. A single colony was used to inoculate 25 ml TB (Appendix Figure 3A.1) plus kanamycin (50 µg/ml) and grown overnight at 37 ^{o}C with constant shaking in a 250 ml Erlenmeyer flask. A 12.5 ml aliquot of the seed culture was used to inoculate 200 ml TB plus kanamycin (50 µg/ml) and shaken overnight at 37 ^{o}C in a 500 ml Erlenmeyer flask. For expression of *nap*H2 using autoinduction media,[59] a 25 ml aliquot of this seed culture was used to inoculate 500 ml TB plus kanamycin (50 µg/ml) in a 2.8 L Fernbach flask. To each 500 ml culture, 500 µl of 1M $MgSO_4$, 10 ml 50 x 5052 (Appendix Figure 3A.1), and 25 ml 20 x NPS (Appendix Figure 3A.1) were added at the time of inoculation. The cultures were grown at 25 ^{o}C with constant shaking for 16 hours. After the 16 hour induction, the cultures were harvested by centrifugation at 5,500 x g for ten minutes at 4 ^{o}C (Beckman Coulter Avanti J–E using a F-10.1 rotor) and the pellet was stored at -20 ^{o}C. This was repeated until a total of 2 L were expressed.

3.2.5.3: Purification of NapH2

The cell pellet from 2 L's of culture was resuspended in 200 ml lysis buffer (Appendix Figure 3A.2) and sonicated in 10 second intervals until homogeneous. Soluble protein was isolated by centrifuging the homogeneous mixture at 39,191

x g for 25 minutes at 4 ^{o}C (Beckman Coulter Avanti J–E using a JA-20 rotor). The supernatant was decanted and 1.5 ml of Ni-NTA (Invitrogen, USA), which was washed two times with10 ml lysis buffer, was added. On ice, the soluble protein was incubated with the Ni-NTA for one hour with constant stirring. To a 5 ml column, the soluble fractions containing Ni-NTA were added and allowed to flow-through. The column was washed two times with 10 ml wash buffer (Appendix Figure 3A.2), and His-tagged protein was eluted off the column with 2 x 3.5 ml aliquots of elution buffer (Appendix Figure 3A.2). A 10 K molecular weight cut-off concentrator (Thermo Scientific) was used to concentration the fraction to ~1.5 ml and its concentration was taken using a NanoDrop. Glycerol was added to NapH2 to a final concentration of 50%, a 5 µl aliquot was run on a NuPAGE gel according to Section 3.2.8, and the sample was stored at -80 ^{o}C.

3.2.6: Expression and purification of NapH3

3.2.6.1: Amplification of *nap*H3

Using total genomic DNA from *S.* sp. CNQ-525 (see Section 2.2.2.1), *nap*H3 was amplified by PCR using the primers NapH3p Fwd and NapH3p Rev (Table 3.3). NapH3p Fwd contains a NcoI restriction site whereas NapH3p Rev contains a NotI site. Both primers were diluted with Milli-Q water to a final concentration of 20 µM. For a 50 µl PCR reaction, 1µl of gDNA DNA (22 ng/µl) was mixed with 0.5 µl pfu turbo (2.5 U/µl, Stratagene), 5 µl pfu 10 X buffer, 1 µl NapH3p Fwd (10 pmol/µl), 1 µl of NapH3p Rev (10pmol/µl), 1 µl dNTPs (10 mM),

2.5 µl DMSO and 38 µl Milli-Q water. PCR conditions were 96 ^{o}C for five minutes; 25 cycles of 96 ^{o}C for one minute, 56 ^{o}C for one minute and 72 ^{o}C for 90 seconds, followed by an extra ten minutes at 72 ^{o}C. Following amplification, the PCR reaction was desalted using a QIAGEN gel purification kit according to manufacturer's procedures. DNA was eluted off the column with 30 µl of EB buffer (Appendix Tabe 2A.3) and doubly digested with 2.5 µl of NcoI (New England Biolabs, 10,000 U/ml), 2.5 µl NotI (New England Biolabs, 10,000 U/ml), 0.5 µl BSA (New England Biolabs, 10 mg/ml), 5 µl of NEBuffer 3 (New England Biolabs), and 9.5 µl of Milli-Q water. The reaction was incubated for two hours at 37 ^{o}C and the DNA was purified with a QIAGEN gel elution kit according to manufacturer's instructions. DNA was eluted off the column with 20 µl EB buffer.

Doubly digested DNA was ligated into a NcoI/NotI digested pHIS8 vector in a 10 µl reaction containing 1 µl vector, 6 µl DNA (5 ng/µl), 1µl 10X ligation buffer, 1 µl T4 DNA ligase (400,000 U/ml, New England Biolabs), and 1 µl Milli-Q water. The ligation reaction was incubated overnight at 16 ^{o}C. After which, 2 µl of the ligation reaction was transformed into DH5-α cells (Invitrogen) according to manufacturer's instructions. A 50 µl aliquot was plated on LB agar (Appendix Figure 2A.1) containing kanamycin (50 µg/ml) and incubated overnight at 37 ^{o}C. Colonies were picked and grown overnight by constant shaking at 37 ^{o}C in 5 ml LB (Appendix Figure 2A.1) containing kanamycin (50 µg/ml). Plasmid DNA was extracted according to Section 2.2.2.2, eluted off the QIAGEN column with 50 µl EB buffer, and sequenced using the T7 promoter and T7 teminator sites on the vector (Table 3.4).

3.2.6.2: Expression of *nap*H3

The pHIS8 vector containing *nap*H3 was transformed into BL21(DE3) chemically competent cells (Stratagene) according to manufacturer's instructions. A 50 µl aliquot was plated on LB agar (Appendix Figure 2A.1) containing kanamycin (50 µg/ml) and incubated overnight at 37 ^{o}C. A single colony was used to inoculate 25 ml TB (Appendix Figure 3A.1) plus kanamycin (50 µg/ml) and grown overnight at 37 ^{o}C with constant shaking in a 250 ml Erlenmeyer flask. A 12.5 ml aliquot of the seed culture was used to inoculate 200 ml TB plus kanamycin (50 µg/mL) and shaken overnight at 37 ^{o}C in a 500 ml Erlenmeyer flask. For expression of *nap*H3, a 25 ml aliquot of the 200 ml seed culture was used to inoculate 500 ml TB plus kanamycin (50 µg/ml) in a 2.8 L Fernbach flask. At the time of inoculation, 500 µl of 1M $MgSO_4$, 10 ml 50 x 5052 (Appendix Figure 3A.1), and 25 ml 20 x NPS (Appendix Figure 3A.1) were added to each 500 ml culture. The cultures were grown at 20 ^{o}C with constant shaking for 24 hours. After the 24 hour induction, the cultures were harvested by centrifugation at 5,600 x g for ten minutes at 4 ^{o}C (Beckman Coulter Avanti J–E using a F-10.1 rotor), and the pellet was stored at -20 ^{o}C. A total of 1 L was expressed.

3.2.6.3: Purification of NapH3

The cell pellet was resuspended in 100 ml of lysis buffer (Appendix Figure 3A.2) and sonicated in 10 second intervals until homogeneous. Soluble protein was isolated by centrifuging the homogeneous mixture at 39,191 x g for 25 minutes at 4 ^{o}C (Beckman Coulter Avanti J–E using a JA-20 rotor). The supernatant was decanted and 1.75 ml of Ni-NTA (Invitrogen, USA), which was washed two times with 10 ml lysis buffer, was added. On ice, the Ni-NTA was incubated with the soluble protein for one hour with constant stirring. To a 5 ml column, the soluble fraction containing Ni-NTA was added and allowed to flow-through. The column was washed two times with 10 ml wash buffer (Appendix Figure 3A.2), and His-tagged protein was eluted off the column with 7 x 5 ml aliquots of elution buffer (Appendix Figure 3A.2). A NanoDrop (NanoDrop Technologies) was used to determine which of the seven fractions contained protein, and those containing protein were combined and stored overnight at 4 ^{o}C. A 5 µl aliquot was run on a NuPAGE gel according to Section 3.2.8.

Thrombin cleavage was used to remove the His-tag from the protein. To a two inch piece of 12–14K molecular weight cut-off dialysis tubing (Spectrum Labs), the 60 mg of protein was incubated with 120 µl of thrombin (0.5 mg/ml, Sigma Aldrich) and incubated overnight at 4 ^{o}C in 2 L dialysis buffer (Appendix Figure 3A.2). Benzamidine sepharose 4 fast flow (GE) was used to remove the thrombin. To a 20 ml plastic column, 2 ml of the benzamidine sepharose slurry was added. The flow-through was allowed to pass and the resin was washed

with 10 ml of dialysis buffer. After the resin was washed, the protein was added and the flow-through was collected.

Ni-NTA was used to remove proteins with His-tags that were not removed during thrombin cleavage. To a 20 ml plastic column, 2 ml of Ni-NTA slurry was added. The flow-through was allowed to pass through and the resin was washed with 10 ml of dialysis buffer. After the washing, the protein fraction that was passed over benzamidine was added to the column and the flow-through was collected. This fraction was concentrated to 10 ml using a 10K molecular weight cut-off concentrator (Thermo Scientific). NapH3 was purified on a FPLC (Akta, Amersham) using a size exclusion column (Hiload 16/60 Superdex 200 prep grade) and an isocratic buffer (Appendix Figure 3A.2). Fractions containing NapH3 were combined and concentrated to ~10 mg/ml with a 10 K molecular weight cut-off concentrator. Aliquots of 100-300 µl were dispensed and stored at -80 ^{o}C.

3.2.7: Expression of NapH4

3.2.7.1: Amplification of *nap*H4

Using total genomic DNA from *S.* sp. CNQ-525 (see Section 2.2.2.1), *nap*H4 was amplified by PCR using the primers NapH4p Fwd and NapH4p Rev or NapH4 Fwd for GST and NapH4 Rev for GST (Table 3.3). Both NapH4 forward primers contain an EcoR1 restriction site whereas both reverse primers contain a HindIII site. Both primers were diluted with Milli-Q water to a final

concentration of 20 µM. For a 50 µl PCR reaction, 1µl of gDNA DNA (22 ng/µl) was mixed with 0.5 µl pfu turbo (2.5 U/µl, Stratagene), 5 µl pfu 10 X buffer, 1 µl of forward primer (10 pmol/µl), 1 µl of reverse primer (10pmol/µl), 1 µl dNTPs (10 mM), 2.5 µl DMSO and 38 µl Milli-Q water. PCR conditions were 96 ^{o}C for five minutes; 25 cycles of 96 ^{o}C for one minute, 56 ^{o}C for one minute and 72 ^{o}C for 90 seconds, followed by an extra ten minutes at 72 ^{o}C. Following amplification, the PCR reaction was desalted using a QIAGEN gel purification kit according to manufacturer's procedures. DNA was eluted off the column with 30 µl of EB buffer (Appendix Tabe 2A.3) and doubly digested with 2.5 µl of EcoR1 (New England Biolabs, 20,000 U/ml), 2.5 µl HindIII (New England Biolabs, 20,000 U/ml), 5 µl of NEBuffer EcoR1 (New England Biolabs), and 10 µl of Milli-Q water. The reaction was incubated for two hours at 37 ^{o}C and the DNA was purified with a QIAGEN gel elution kit according to manufacturer's instructions. DNA was eluted off the column with 20 µl EB buffer.

Doubly digested DNA was ligated into an EcoR1/HindIII digested pHIS8 or pGS-21a vector in a 10 µl reaction containing 1 µl vector, 6 µl DNA (5 ng/µl), 1µl 10X ligation buffer, 1 µl T4 DNA ligase (400,000 U/ml, New England Biolabs), and 1 µl Milli-Q water. The ligation reaction was incubated overnight at 16 ^{o}C. After which, 2 µl of the ligation reaction was transformed into DH5-α cells (Invitrogen) according to manufacturer's instructions. A 50 µl aliquot was plated on LB agar (Appendix Figure 2A.1) containing kanamycin (50 µg/ml) and incubated overnight at 37 ^{o}C. Colonies were picked and grown overnight by constant shaking at 37 ^{o}C in 5 ml LB (Appendix Figure 2A.1) containing

kanamycin (50 µg/ml). Plasmid DNA was extracted according to Section 2.2.2.2, eluted off the QIAGEN column with 50 µl EB buffer, and sequenced using the T7 promoter and T7 teminator sites on the vectors (Table 3.4).

3.2.7.2: Expression of *nap*H4

The pHIS8 and pGS-21a vectors containing *nap*H4 were transformed into BL21(DE3) chemically competent cells (Stratagene) according to manufacturer's instructions. A 50 µl aliquot was plated on LB agar (Appendix Figure 2A.1) containing kanamycin (50 µg/ml) and incubated overnight at 37 ^{o}C. Single colonies were used to inoculate 25 ml TB (Appendix Figure 3A.1) plus kanamycin (50 µg/ml) and grown overnight at 37 ^{o}C with constant shaking in a 250 ml Erlenmeyer flask. A 2.5 ml aliquot of the seed culture was used to inoculate 50 ml TB plus kanamycin (50 µg/mL). For expression of *nap*H4, 25 µl of 1M $MgSO_4$, 0.5 ml 50 x 5052 (Appendix Figure 3A.1), and 1.25 ml 20 x NPS (Appendix Figure 3A.1) were added to each 50 ml culture at the time of inoculation. The cultures were grown at 16–37 ^{o}C with constant shaking for 20–30 hours. After the induction, the cultures were harvested by centrifugation at 5,600 x g for ten minutes at 4 ^{o}C (Beckman Coulter Avanti J–E using a F-10.1 rotor), and the pellet was stored at -20 ^{o}C.

The pHIS8 vector containing *nap*H4 was transformed into ArcticExpress (DE3) chemically competent cells (Stratagene) according to manufacturer's instructions. A 50 µl aliquot was plated on LB agar plus kanamycin (50 µg/ml)

and incubated overnight at 37 ^{o}C. Single colonies were used to inoculate 25 ml TB plus kanamycin (50 µg/ml) and grown overnight at 37 ^{o}C with constant shaking in a 250 ml Erlenmeyer flask. A 2.5 ml aliquot of the seed culture was used to inoculate 50 ml TB plus kanamycin (50 µg/mL). For expression of *nap*H4, 25 µl of 1M $MgSO_4$, 0.5 ml 50 x 5052, and 1.25 ml 20 x NPS were added to each 50 ml culture at the time of inoculation. The cultures were grown at 4 ^{o}C with constant shaking for 36 hours. After the induction, the cultures were harvested by centrifugation at 5,600 x g for ten minutes at 4 ^{o}C (Beckman Coulter Avanti J–E using a F-10.1 rotor), and the pellet was stored at -20 ^{o}C.

The cell pellet was resuspended in 10 ml of lysis buffer (Appendix Figure 3A.2) and sonicated in 10 second intervals until homogeneous. A soluble fraction was isolated by centrifuging the homogeneous mixture at 39,191 x g for 25 minutes at 4 ^{o}C (Beckman Coulter Avanti J–E using a JA-20 rotor). The supernatant was decanted and 0.5 ml of Ni-NTA (Invitrogen, USA), which was washed two times with 10 ml lysis buffer, was added. On ice, the Ni-NTA was incubated with the soluble fraction for one hour with constant stirring. To a 5 ml column, the soluble fraction containing Ni-NTA was added and allowed to flow-through. The column was washed two times with 10 ml wash buffer (Appendix Figure 3A.2), and His-tagged protein was eluted off the column with 2 x 3.5 ml aliquots of elution buffer (Appendix Figure 3A.2). A 25 µl aliquot was run on a NuPAGE gel according to Section 3.2.8.

With pHIS8 as the expression vector, expression of *nap*H4 was attempted in *E. coli* BL21 (DE3) cells as previoiusly described using isopropyl-β-D-1-

thiogalactopyranoside (IPTG) as the inducer.[60] In attempts to generate soluble NapH4, growth temperature, A_{600} values before induction, concentration of IPTG, and length of induction (Table 3.5) were modified and evaluated. Harvesting the cells and isolating soluble His-tagged protein were performed as described above.

Table 3.5: Expression conditions tested for generation of soluble NapH4

A_{600}	IPTG concentration (mM)	Temperature of induction (°C)	Time induced (h)
0.391	1	37	3
0.513	0.2	37	2
0.520	0.2	37	4
0.535	0.5	37	4
0.417	0.5	30	8
0.416	1	30	8
0.731	0.2	27	19
0.868	0.2	20	21
0.929	0.1	20	21
0.973	0.05	20	21
0.526	0.5	15	19
0.472	1	15	19

3.2.8: Polyacrylamide gel electrophoresis (PAGE)

After eluting off of Ni-NTA, an aliquot of the soluble protein was mixed with 4X loading buffer (Invitrogen) and boiled for 10 minutes. The entire sample was

loaded onto a NuPAGE 4–12% Bis-Tris gel (Invitrogen) and run at 104 V for 1-2 hours in 1X MOPS buffer (Invitrogen). To visualize protein bands, the gel was soaked in coomassie brillant blue for 10 hours–overnight at room temperature. After the incubation, excess stain was removed by soaking the gel in destainer (45:45:10 methanol:water:acetic acid) for 6–16 hours at room temperature.

3.2.9: Biochemical characterization with the phenol red assay

To a 30 ml culture of *S.* sp. CNQ-525 grown in A1 growth media (Appendix Figure 2A.1) for 7 days at 30 ^{o}C by shaking at 250 revolutions/min, 15 ml of the phenol red reagent mix (40 ml of 0.2% phenol red in 95% ethanol, 0.3 M potassium phosphate buffer pH 7.0, and 0.05 M potassium bromide per liter of Milli-Q water) was added. A control experiment using 30 ml of A1 growth media without cells was tested under the same conditions. At room temperature, the reaction was initiated by adding 5 µl of 0.3% hydrogen peroxide to each flask. After an hour incubation at room temperature, another 5 µl of hydrogen peroxide was added to each flask. Additional hydrogen peroxide was added after 2, 3 and 4 hours. After the final addition, the flasks were incubated at room temperature for five days without shaking.

3.2.10: Biochemical characterization with the monochlorodimedone assay

In a 10 mm QS quartz cuvette, 2 µg of protein was mixed with 982 µl 50 mM citrate buffer (pH 3–6), 5 µl 5 mM KCl and 1 µl 1 mM Na_3VO_4 and incubated at room temperature for five minutes. After the incubation, 10 µl of 5 mM monochlorodimedone (MCD), which was dissolved in 100% ethanol, was added to the reaction and the cuvette was inverted three times to mix. The cuvette was placed in a Cary 50 Conc UV-Visible spectrophotometer (Varian) and 1.64 µl of 15% hydrogen peroxide was added. Immediately after the addition of hydrogen peroxide, the A_{290} was measured every 0.5 seconds for one minute.

3.2.11: Biochemical characterization of NapH1 and NapH3 using lapachol as a substrate

Lapachol was purchased from Sigma Aldrich and was of analytical grade. For a 1 ml reaction, 23 nM of protein was mixed with 40 µl of 40 mM KCl, 100 µl of 0.5 mM lapachol, 391 ul of 50 mM citrate buffer pH 4.5, 10 µl of 10 mM Na_3VO_4, and 400 µl of 100 % ethanol in a 5 ml glass vial. To start the reaction 56 µl of 0.5 mM hydrogen peroxide was added and the reaction was incubated for three hours at room temperature. After the incubation, the reaction was extracted with three equal volumes of hexanes, dried over $MgSO_4$ and concentrated *in vacuo*. Extracts were analyzed in positive and negative mode on a Hewlett Packard 1100 series high performance liquid chromatography system linked to an Agilent ESI-1100 MSD mass spectrometer (gas flow set to 13

ml/min, drying temperature set to 350 ^{o}C, capillary voltage set to 4500 V, and nebulizing pressure set to 40 pounds/square inch).

3.2.12: Crystallization of NapH1 and data collection

Crystals were obtained for recombinant apo-NapH1 by vapor diffusion at 4 ^{o}C. On a cover slip, 1 µl of 8.75 mg/ml NapH1 was mixed with 1 µl of crystallization buffer (7% w/v PEG 8,000, 0.3M NH_4OAc, 100mM HEPES pH 7.5, and 2 mM DTT). The 1:1 mixture was equilibrated over a 500 µl reservoir of the same crystal solution for three days at 4 ^{o}C.

Suitable crystals for data collection were obtained by microseeding using the same conditions mentioned above. However, the hanging drop was only equilibrated for one day at 4 ^{o}C and only six out of 24 wells in the tray were used. After the 24 hour incubation, 6-1.5 ml tubes were placed on ice. To tube 1, 100 µl of the crystallization buffer (without 2 mM DTT) was added, whereas 50 µl was added to tubes 2–6. At 4 ^{o}C, 2 µl of the crystallization buffer was added to a cover slip. Using a 1 mM microloop (Hampton Research), a small corner of the NapH1 crystal was transferred to the 2 µl drop of crystallization buffer. The crystal was broken up in the droplet and pipetted to mix thoroughly. The entire droplet was transferred to tube one and mixed. A 50 µl aliquot was transferred from tube one to tube two and mixed. After mixing, a 50 µl aliquot from tube two was transferred to tube three and so on until all six tubes were mixed. From

each tube, 0.3 µl was transferred to its corresponding hanging drop and allowed to equilibrate for an additional two days at 4 ^{o}C.

Crystals were stabilized for data collection by soaking in a cryoprotectant solution containing 9% (w/v) PEG 8,000, 0.3M NH_4OAc, 100 mM HEPES pH 7.5, and 17% ethylene glycol for 30 seconds. Individual crystals were transferred to a 2 µl drop of cryoprotectant using a microloop (Hampton Research), soaked, and flash frozen to the microloop using liquid nitrogen. Diffraction data was collected on BL 8.2.2 at the Advanced Light Source (Berkeley, California). Image files were processed using iMosfilm and molecules/unit cell was calculated using Matthews probabilities.[62] Phase determination was attempted by molecular replacement using MOLREP[63] and PHASER, which are part of the CCP4i Suite.[64]

3.3: Results and Discussion

3.3.1: Phylogenetic analysis of the *nap*-VClPOs

To determine how homologous the *nap*-VClPOs (NapH1, NapH3 and NapH4) (Appendix Figure 3A.3) were to each other, the amino acid sequences were aligned using a pairwise BLAST alignment.[65] Results from the alignments showed that NapH1 and NapH4 were more similar to each other than either enzyme was to NapH3 (Table 3.6). Phylogenetic analysis of the three *nap* V-ClPOs with characterized V-ClPOs, V-BrPOs, and bacterial non-specific acid phosphatases revealed that the enzymes form clades based on proposed enzymatic function (Figure 3.5). However, the three putative V-ClPOs from the bacterium *Streptomyces* sp. CNQ-525 do not cluster with the fungal or other postulated bacterial-derived V-ClPOs, which is consistent with their proposed role in natural product biosynthesis in contrast to the other known V-ClPOs.

Table 3.6: Results from the pairwise alignments of the three *nap*-based V-ClPOs

Alignment	Percent Identity	Percent Similarity
NapH1:NapH3	51%	65%
NapH1:NapH4	72%	85%
NapH3:NapH4	50%	65%

Figure 3.5: Relatedness of V-BrPOs, V-ClPOs, and acid phosphatases identified in fungi, algae, and bacteria and some of their associated chemistry. Phylogenetic analysis was performed using Clustal W,[66] and the unrooted neighbor-joining tree was visualized by TreeView. The *scale bar* indicates 0.1 changes per amino acid. Sequence identification codes include Ci_VClPO from *Curvularia inaequalis* (accession number CAA59686); hypothetical Rb_VClPO from *Rhodopirellula baltica* SH1 (CAD72609); Ed_VClPO from *Embellisia didymospora* (CAA72622); hypothetical Ss1_VClPO from *Streptomyces* sp. CNQ-525 (ABS50486); hypothetical Ss3_VClPO from *Streptomyces* sp. CNQ-525 (ABS50491); hypothetical Ss4_VClPO from *Streptomyces* sp. CNQ-525 (ABS50492); hypothetical Cs_VClPO from *Cellulophaga* sp. MED134 (ZP_01050453); An_VBrPO from *Ascophyllum nodosum* (P81701); Co_VBrPO from *Corallina officinalis* (AAM46061); Cp1_VBrPO from *Corallina pilulifera* (BAA31261); Cp2_VBrPO from *Corallina pilulifera* (BAA31262); hypothetical Sys_VBrPO from *Synechococcus* sp. CC9311 (YP_731869); Fd_VBrPO from *Fucus distichus* (AAC35279); Ld1_VBrPO from *Laminaria digitata* (CAD37191); Ld2_VBrPO from *Laminaria digitata* (CAD37192); Pi_ACP acid phosphatase from *Prevotella intermedia* (AB017537); Kp_ACP acid phosphatase from *Klebsiella pneumonia* (AJ250377); St_ACP acid phosphatase from *Salmonella typhimurium* (X63599); Ps_ACP acid phosphatase from *Providencia stuarti* (X64820); and Eb_ACP acid phosphatase from *Escherichia blattae* (AB020481). Halogenated natural products: α-snyderol, β-snyderol, γ-snyderol, and A80915C. Proposed substrates for V-HPOs: (*E*)-(+)-nerolidol and SF2415B1.

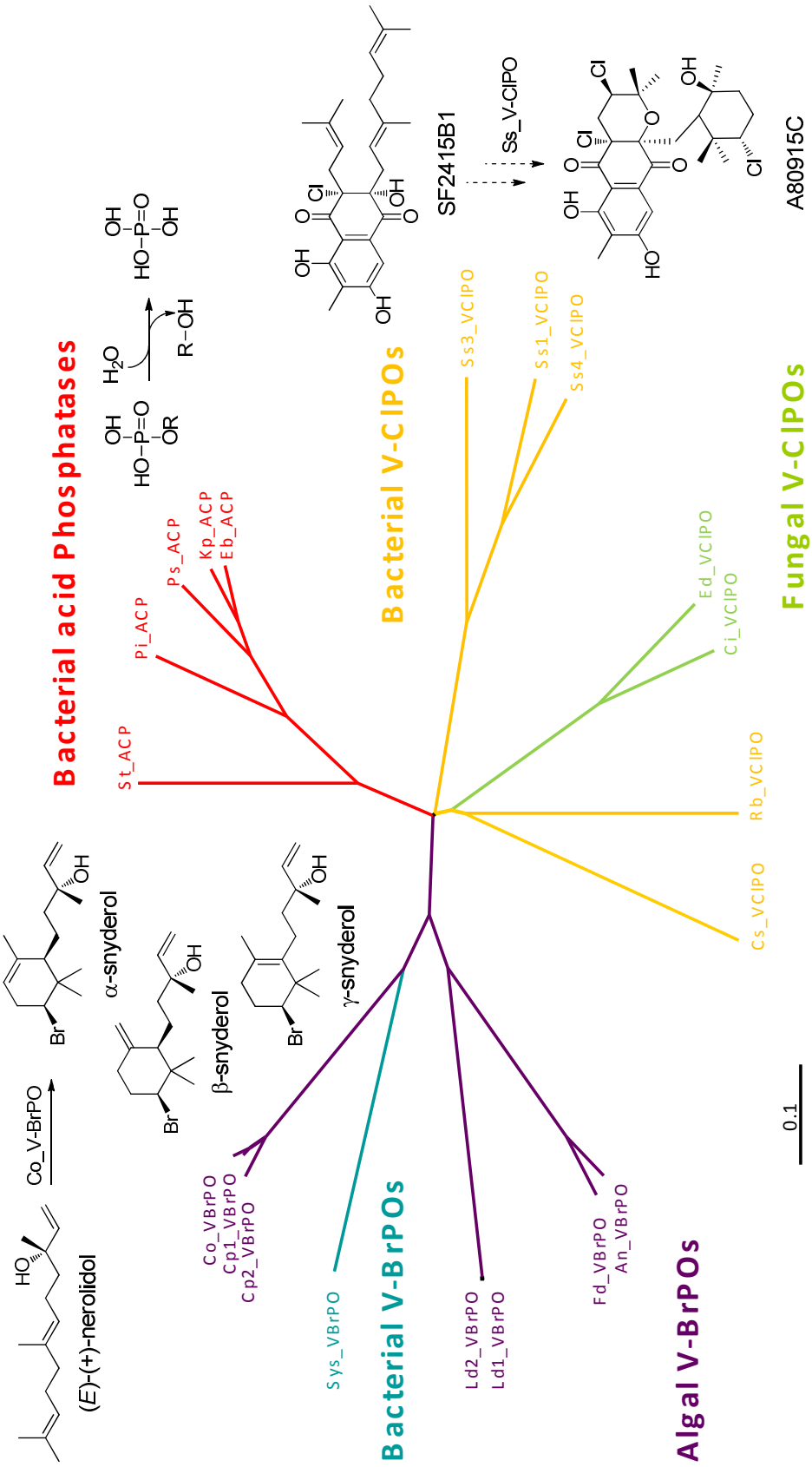
(E)-(+)-nerolidol
Co_V-BrPO
α-snyderol
β-snyderol
γ-snyderol
Bacterial acid Phosphatases
St_ACP
Pi_ACP
Ps_ACP
Kp_ACP
Eb_ACP
Bacterial V-ClPOs
Ss3_VClPO
Ss1_VClPO
Ss4_VClPO
Ed_VClPO
Ci_VClPO
Rb_VClPO
Cs_VClPO
Fungal V-ClPOs
SF2415B1
Ss_V-ClPO
A80915C
Co_VBrPO
Cp1_VBrPO
Cp2_VBrPO
Sys_VBrPO
Bacterial V-BrPOs
Ld2_VBrPO
Ld1_VBrPO
Fd_VBrPO
An_VBrPO
Algal V-BrPOs
0.1

A multiple sequence alignment using amino acid sequences from characterized V-ClPOs, V-BrPOs, acid phosphatases, and the three *nap*-V-ClPOs was constructed using ClustalW (Figure 3.6).[66] Inspection of the amino acid residues in the active sites of the vanadium haloperoxidases suggests that NapH3 may not be directly involved in the chlorination and cyclization of the terpene units and may instead act as a hydroxylase. Structural and functional comparisons of vanadium haloperoxidases from eukaryotic organisms have shown that seven amino acids are required for halogenating activity.[13, 35, 44, 45] All three *nap* enzymes contain His-496 (which covalently binds to the vanadate co-factor) and five of the six residues that participate in hydrogen bonding, Lys-353, Arg-360, Ser-402, Gly-403, and Arg-490. Conserved residue His-404, which is proposed to form a hydrogen bond to the apical oxygen of the co-factor,[45] is replaced with Ser (as seen in NapH1 and NapH4) or Phe (as seen in NapH3). Mutagenesis studies have shown that the V-ClPO mutant H404A from *C. inaequalis* loses chlorinating activity,[45] and a similar natural exchange is observed in NapH3. Hence, NapH3 may not be involved in halogenation but rather may be used to hydrate aliphatic carbons to produce such compounds as 7-methylnapyradiomycin A2.[67] NapH1 and NapH4, on the other hand, contain a hydrophilic Ser residue at this position and are therefore predicted to catalyze the chloronium-induced cyclization of the two terpene units.

```
                          *       *
Ss1_VClPO 365 LIAAWHHKTRFD-AVRPVTAI 384
Ss3_VClPO 315 LIAAWHHKRAYD-TVRPFSAV 334
Ss4_VClPO 360 LIAAWGYKRKYE-AVRPITAV 379
Ci_VClPO  346 GIFSWKEKWEFE-FWRPLSGV 365
Ed_VClPO  342 GIFAWKEKWEFE-FWRPLSGV 361
Rb_VClPO  463 GVVAWTTKFGEE-LWRPVTAI 482
Cs_VClPO  329 AVSTWADKYEYM-VMRPSVYI 348
An_VBrPO  334 QRSSWYQKWQVHRFARPEALG 353
Cp1_VBrPO 393 LKAVRYQKFNIHRRLRPEATG 412
Cp2_VBrPO 391 LKAVRYQKFNIHRRLRPEATG 410
Co_VBrPO  393 LKAVRYQKFNIHRRLRPEATG 412
Fd_VBrPO  453 QRASCYQKWQVHRFARPEALG 472
Sys_VBrPO 372 LKAVRYQKFNNHLRLRPEALA 391
Ld1_VBrPO 366 TRHAWYAKWQVHRMLRPEAYG 385
Ld2_VBrPO 402 TRHAWYAKWQVHRMLRPEAYG 421
Pi_ACP    128 DLATRSAKDHYMR-------- 140
Kp_ACP    126 DLATRSAKEKYMR-------- 138
St_ACP    116 YYATASAKKYYMR-------- 128
Ps_ACP    126 DLATRSAKEKYMR-------- 138
Eb_ACP    126 DLATRSAKDHYMR-------- 138
```

Figure 3.6: Multiple sequence alignment of V-BrPOs, V-ClPOs, and acid phosphatases identified in fungi, algae, and bacteria. Phylogenetic analysis was performed using ClustalW (Ref Thompson 1994). Sequence identification codes include Ci_VClPO from *Curvularia inaequalis* (accession number CAA59686); hypothetical Rb_VClPO from *Rhodopirellula baltica* SH1 (CAD72609); Ed_VClPO from *Embellisia didymospora* (CAA72622); hypothetical Ss1_VClPO from *Streptomyces* sp. CNQ-525 (ABS50486); hypothetical Ss3_VClPO from *Streptomyces* sp. CNQ-525 (ABS50491); hypothetical Ss4_VClPO from *Streptomyces* sp. CNQ-525 (ABS50492); hypothetical Cs_VClPO from *Cellulophaga* sp. MED134 (ZP_01050453); An_VBrPO from *Ascophyllum nodosum* (P81701); Co_VBrPO from *Corallina officinalis* (AAM46061); Cp1_VBrPO from *Corallina pilulifera* (BAA31261); Cp2_VBrPO from *Corallina pilulifera* (BAA31262); hypothetical Sys_VBrPO from *Synechococcus* sp. CC9311 (YP_731869); Fd_VBrPO from *Fucus distichus* (AAC35279); Ld1_VBrPO from *Laminaria digitata* (CAD37191); Ld2_VBrPO from *Laminaria digitata* (CAD37192); Pi_ACP acid phosphatase from *Prevotella intermedia* (AB017537); Kp_ACP acid phosphatase from *Klebsiella pneumonia* (AJ250377); St_ACP acid phosphatase from *Salmonella typhimurium* (X63599); Ps_ACP acid phosphatase from *Providencia stuarti* (X64820); and Eb_ACP acid phosphatase from *Escherichia blattae* (AB020481). Conserved residues are in bold and active site residues are marked with an asterisk.

```
                                          ***
Ss1_VClPO 399 -VGMGTVD-IRASEWSSYLPVGDHPEYPSGSTSLCSATSQAARRYF 442
Ss3_VClPO 349 -PGKGTVESIPADEWTGYLPVGNHPEYPSGFTTLIAAQAQAARSFL 393
Ss4_VClPO 394 -VGMGTVDDIPANEWAGYLPVGDHPEYPSGSTTVGSAASQAARRFF 438
Ci_VlPO   375 -DPFWLTLGAPATNTNDIPFKPPFPAYPSGHATFGGAVFQMVRRYY 419
Ed_VClPO  377 AIHSGLASAPQLQNSDEAPFKPPFPAYPSGHATFGAAAFQMVRKYY 422
Rb_VClPO  495 GDADWTALGAPDGGDDIVGFTPQFPTYISGHATFGGALFGTLQEFY 540
Cs_VClPO  355 -------TYETNLYRFINWPNPSFPGYPSGHSAFASAAAGVFIGAF 393
An_VBrPO  392 ----PNNEVTYLLPQAIQEGSPTHPSYPSGHATQNGAFATVLKALI 433
Cp1_VBrPO 457 ADGDPDPDPSFLLPMAFAEGSPFHPSYGSGHAVVAGACVTILKAFF 502
Cp2_VBrPO 456 ADGIVSPDKSFLLPMAFAEGSPFHPSYGSGHAVVAGACVTILKAFF 501
Co_VBrPO  457 ADGDPDPDPSFLLPQAFAEGSPFHPSYGSGHAVVAGACVTILKAFF 502
Fd_VBrPO  511 ----PNNEVTYLLPQAIQVGSPTHPSYPSGHATQNGAFATVLKALI 552
Sys_VBrPO 432 SLAG---EATALLPMAFAEGSPMHPAYGAGHATVAGACVTILKAFF 474
Ld1_VBrPO 424 ----PDGEKTFLLPMAAAQGSPTHPAYPSGHAINNGAYITALKAFL 465
Ld2_VBrPO 460 ----PDGEKTFLLPMAAAQGSPTHPAYPSGHAINNGAYITALKAFL 501
Pi_ACP    141 -VRPFAFYNEMTCNPEQQQELSTNGSYPSGHTAIGWATALVLSEIN 185
Kp_ACP    139 -IRPFAFYGVSTCNTTEQDKLAKNGSYPSGHTSIGWATALVLAEIN 183
St_ACP    129 -TRPFVLFNHSTCRPEDENTLRKNGSYPSGHTAYGTLLALVLSEAR 173
Ps_ACP    139 -IRPFAFYGVATCNTKDQDKLSKNGSYPSGHTAIGWASALVLSEIN 183
Eb_ACP    139 -IRPFAFYGVSTCNTTEQDKLSKNGSYPSGHTSIGWATALVLAEIN 183

                                        *     *
Ss1_VClPO 475 -------PTWTDFTRTCATSRVWGGVHFQTTVDR-------- 501
Ss3_VClPO 426 -------ATWTDFENDCATSRVWAGAHFTKTAET-------- 452
Ss4_VClPO 471 -------PTWTDFNKRCAYSRLDGGVHFKKTVER-------- 497
Ci_VClPO  470 TRIVRHFDSAWELMFENAISRIFLGVHWRFDAAAARDILIPT 511
Ed_VClPO  473 TRMPRRFSSCWEMMFENAVSRIFLGVHWRFDAAAGQDILIPT 514
Rb_VClPO  572 DDAERTFSSFSEAMAENGRSRVYLGIHFDFDDLVGQEVGQSI 613
Cs_VClPO  413 --APRQFTSFTDMAQENGYSRIPLGVHIEMDCTEGLR----- 447
An_VBrPO  461 -SCLTFEGEINKLAVNVAFGRQMLGIHYRFDGIQGL------ 495
Cp1_VBrPO 529 --TLTVAGELNKLADNIAIGRNMAGVHYFSDQFESL------ 562
Cp2_VBrPO 528 --TLTVAGELNKLADNVAIGRNMAGVHYFSDQFESL------ 561
Co_VBrPO  529 --TLTVAGELNKLADNIAIGRNMAGVHYFSDQFESI------ 562
Fd_VBrPO  580 -ACLTYEGEINKLAVNVAFGRQMLGIHYRFDGIQGL------ 614
Sys_VBrPO 547 CCPLTLEGELNKLAANISIGRNMAGVHYFSDYYDSL------ 582
Ld1_VBrPO 509 VEGLTYEGELNKISANVLLGRSHIGVHWRMDGVYGA------ 544
Ld2_VBrPO 545 VEGLTYEGELNKISANVLLGRSHIGVHWRMDGVYGA------ 580
Pi_ACP    186 ---IDRQNEILERGYQMGQSRVICGYHWQSDVDAAR------ 218
Kp_ACP    184 ---PQRQNEILKRGYELGESRVICGYHWQSDVDAAR------ 216
St_ACP    174 ---PERAQELARRGWEFGQSRVICGAHWQSDVDAGR------ 206
Ps_ACP    184 ---PENQDKILKRGYELGQSRVICGYHWQSDVDAAR------ 216
Eb_ACP    184 ---PQRQNEILKRGYELGQSRVICGYHWQSDVDAAR------ 216
```

Figure 3.6: Continued.

3.3.2: Phenol red assay

Phenol red, also known as phenolsulfonphthalein, is a pH indicator and is a component of a qualitative assay used to identify organisms producing active haloperoxidases (Figure 3.7).[32] At pH below 6.8, the ketone in phenolsulfonphthalein is protonated resulting in a yellow compound. As the pH increases, the extra proton on the ketone group is lost, which causes a red-orange colored compound, and further increase in pH causes deprotonation of the hydroxyl group resulting in a red colored compound. In the phenol red assay, phenol red, which is dissolved in a phosphate buffer at pH 7, is added to a culture along with the substrate KBr and the oxidant H_2O_2. If halopeoxidases are produced by the organism, the phenol red reagent will become brominated and a color change of red-orange to blue-violet will be observed.

When the phenol red substrate reagent mix was incubated with *S.* sp. CNQ-525 cultured in A1 growth media, a red-orange to blue-violet color change was observed. This color change implied that phenol red was brominated and indicated that active haloperoxidases produced by *S.* sp. CNQ-525 were responible for the reaction. Interestingly, when the phenol red substrate reagent mix was added to A1 growth media without *S.* sp. CNQ-525, a red to yellow color change occurred indicating a decrease in pH. Together, these results indicated that *S.* sp. CNQ-525 produces active haloperoxidases and efforts were taken to express recombinant *nap*-halogenases (NapH1, NapH2, NapH3, NapH4) to delineate their functions and specificities.

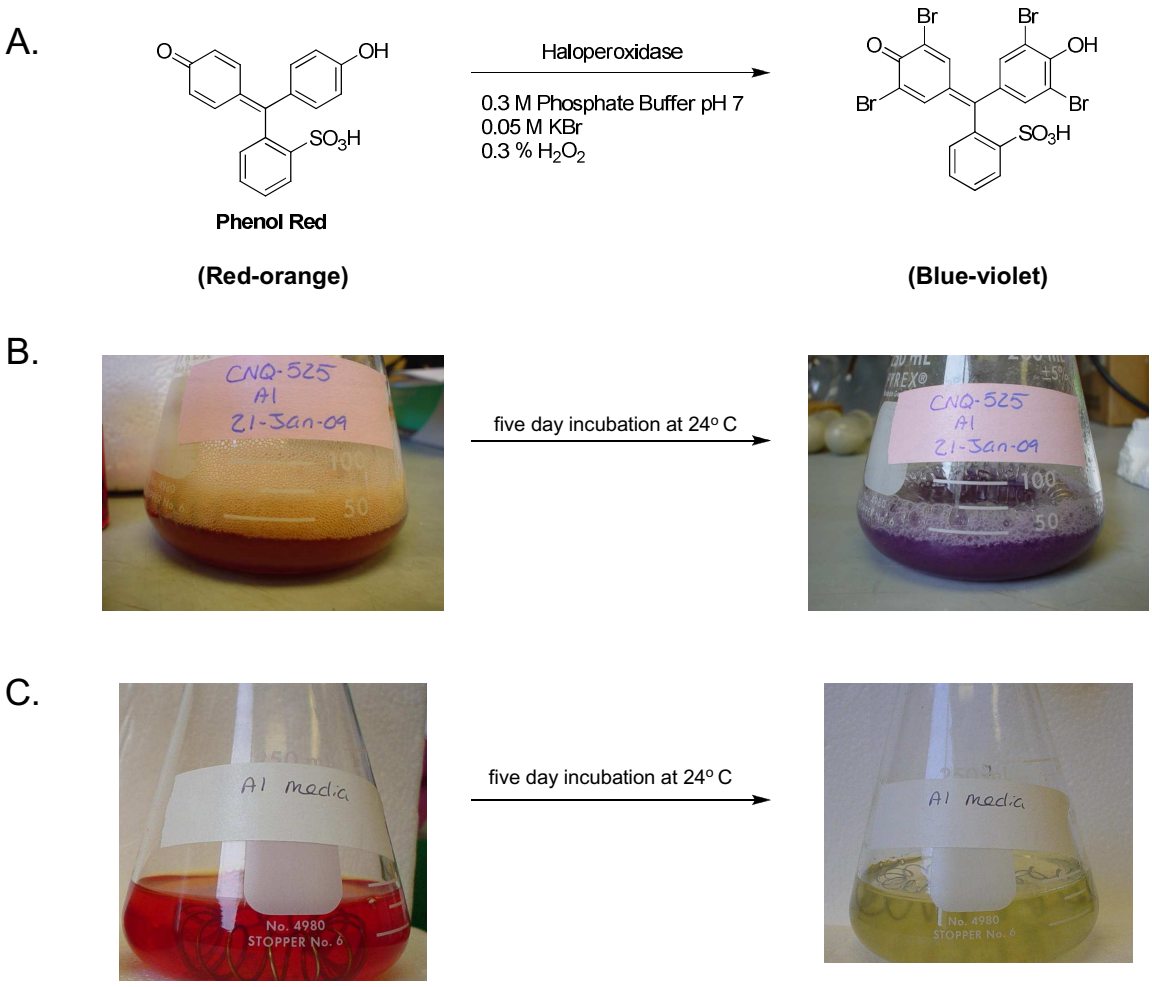

Figure 3.7: Phenol red assay. A) Color change observed after the bromination of phenol red by haloperoxidases. B) Phenol red reagent mix incubated for five days with *S.* sp. CNQ-525 cultured in A1 growth media. C) Phenol red reagent mix incubated for five days with A1 growth media without *S.* sp. CNQ-525.

3.3.3: Expressing recombinant *nap*-halogenating enzymes

All four halogenating enzymes from the napyradiomycin biosynthetic cluster wre PCR amplified, sequence verified, and cloned into the expression vector pHIS8.[60] The pHIS8 vector is a derivative of the pET-28(+) plasmid (Novagen) and encodes and N-terminal His_8 tag followed by a thrombin cleavage

site for removal of the polyhistidyl-containing segment from expressed proteins. Successful expression and purification of recombinant NapH1, NapH2 and NapH3 as octahistidyl-tagged proteins was achieved in *E. coli* BL21(DE3) cells using an autoinduction method (Table 3.7).[58] This procedure allows for the expression of recombinant proteins under the T7 polymerase without the need to add inducers. Bacteria are grown in a defined buffered media, which automatically induces the T7 polymerase during late log-phase. As the cell density reaches saturation and carbon sources become depleted, lactose, which is the remaining carbon source, enters the cells and induces transcription of the T7 RNA polymerase. In most cases, the tight regulation of cell growth and late log-phase transcription of the T7 polymerase allows for a greater yield in soluble protein. This approach yielded 1–2 mg/L soluble NapH1, 2 mg/L soluble NapH2 and 60 mg/L soluble NapH3 (Figure 3.8). Unfortunately, this method did not yield any measureable amounts of soluble NapH4. The gene coding for NapH4 was then cloned into the expression vector GS-21a (GenScript). This vector encodes a N-terminal His_6 tag fused to a glutathione S-transferase (GST) followed by an enterokinase cleavage site for removal of the 6xHis-GST complex from expressed protein. The presence of the highly soluble GST fused to the N-terminal region of the targeted protein is supposed to increase its solubility. Yet, no soluble NapH4 was detected after expressing the vector in *E. coli* BL21(DE3) cells using the autoinduction method. A variety of conditions (i.e., induction temperature, amount of IPTG, OD_{600}, and time of induction) were then tested and altered (Table 3.5) in hopes of expressing soluble NapH4 in *E. coli* BL21(DE3)

cells using the pHIS8 expression vector, but no soluble protein was detected. A minuscule amount of soluble NapH4, 0.2 µg/L, was finally detected when the pHIS8 vector containing the gene coding for NapH4 was expressed at 4 °C in ArcticExpress (DE3) chemically competent cells (Stratagene) using the autoinduction method (Table 3.7). However, this value is most likely not attributed to soluble NapH4, but instead due to *E. coli* chaperone proteins that were co-purified with the targeted protein.

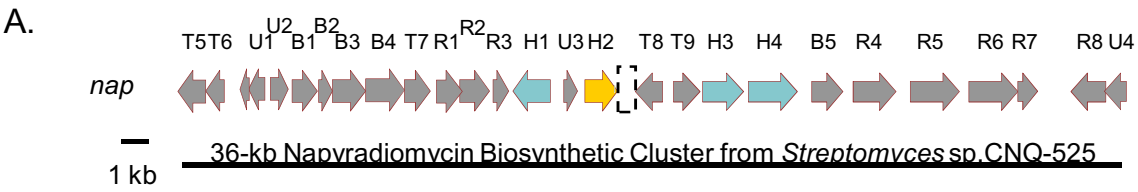

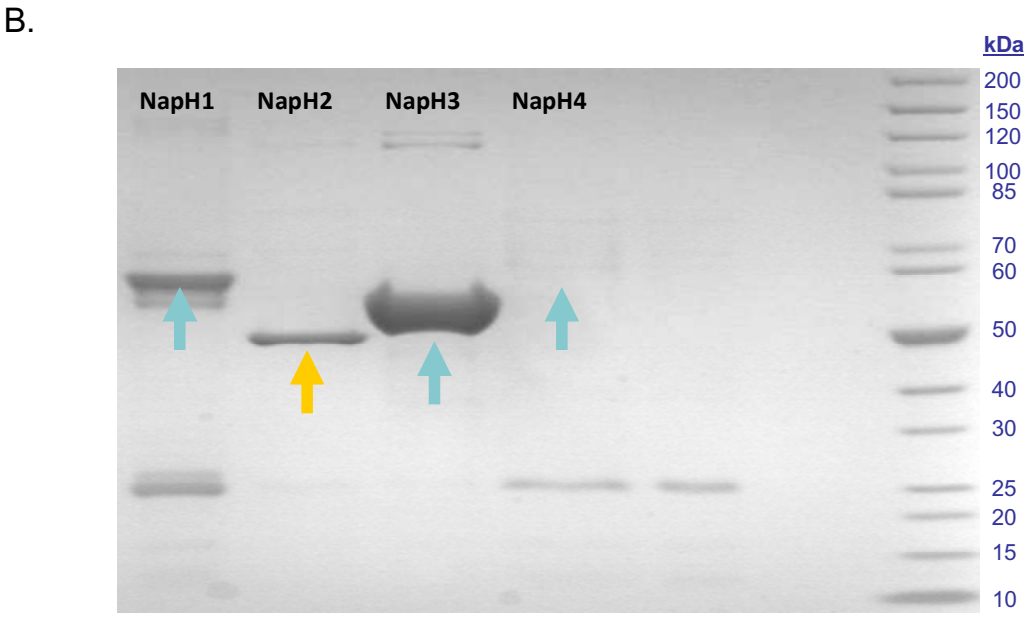

Figure 3.8: Soluble *nap*-halogenating enzymes. A) *nap* biosynthetic cluster highlighting the *nap*-halogenating enzymes targeted for expression. The three V-ClPOs (*nap*H1, *nap*H3 and *nap*H4) are highlighted in blue and the $FADH_2$ dependent halogenase, *nap*H2, is highlighted in yellow. B) A NuPAGE 4–12% Bis-Tris gel stained with coomassie brillant blue showing soluble fractions of denatured octahistidyl-tagged recombinant NapH1, NapH2, NapH3, and NapH4. The arrows indicate which bands on the gel correspond to soluble recombinant protein.

Table 3.7: *nap*-halogenating enzymes and the amount of soluble protein generated.

Enzyme	Amino Acids	Molecular Weight (kDa)	Amount of Soluble Protein
NapH1	527	58	1–2 mg/L
NapH2	425	47	2 mg/L
NapH3	478	52	60 mg/L
NapH4	523	57	200 µg/L

3.3.4: Biochemical characterization of NapH1 and NapH3 as haloperoxidases

As octahistidyl-tagged proteins, recombinant NapH1 and NapH3 were characterized as chloroperoxidases through the monochlorodimedone assay. Although the *nap* biosynthetic cluster contains a fourth halogenating enzyme, the $FADH_2$ -dependent halogenase NapH2, it is believe that this enzyme is responsible for the chlorination of the naphthoquinone ring (Figure 2.11) as seen and extensively characterized with other related microbial systems[12] and was not characterized by this assay.

The monochlorodimedone assay indirectly measures the conversion of monochlorodimedone to dichlorodimedone by the loss of absorbance at 290 nm (Figure 3.9) and was originally used for detecting haloperoxidases from fungi and algae.[68] Monochlorodimedone is a synthetic compound with structural similarity to 2-chloro-1,3-cyclopentanedione, which is a late intermediate in the biosynthesis of the natural product caldariomycin and is believed to be the

natural substrate of the heme-dependent chloroperoxidase isolated from *Caldariomyces fumago* (Figure 3.9).[68, 69] Unlike 2-chloro-1,3-cycloopentanedione, monochlorodimedone is more readily available and is therefore used as the substrate in the assay.

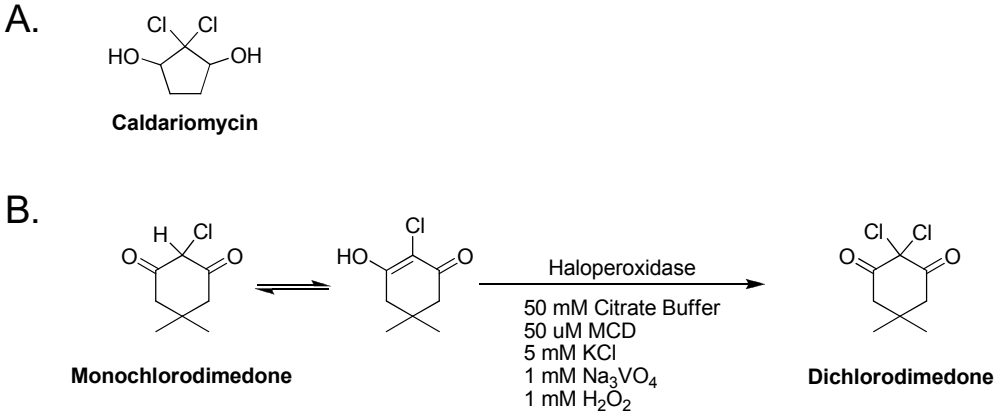

Figure 3.9: Haloperoxidase assay. A) The natural product caldariomycin isolated from *Caldariomyces fumago.* B) The monochlorodimedone assay and conditions used to characterize NapH1 and NapH3.

pH optimas for recombinant NapH1 and NapH3 were calculated from the monochlorodimedone assay, and a pH optima of 3.5–4.5 was determined for recombinant NapH1 (Figure 3.10), whereas recombinant NapH3 had two distinct optimas at pH 3.5 and pH 4.5 (Figure 3.11). Nonetheless, both recombinant enzymes have pH optimas that fall within the reported ranges for V-ClPOs characterized from fungi (pH 4.5–5.5).[34, 35, 37, 46, 49] It was also observed that when either the redox cofactor vanadate, the substrate KCl, or the oxidant H_2O_2 were omitted from the reaction, no loss of A_{290} could be measured with recombinant NapH1 or NapH3. These results indicate that both NapH1 and

NapH3 are V-ClPOs, which require vanadate, KCl and H_2O_2 for halogenating activity.

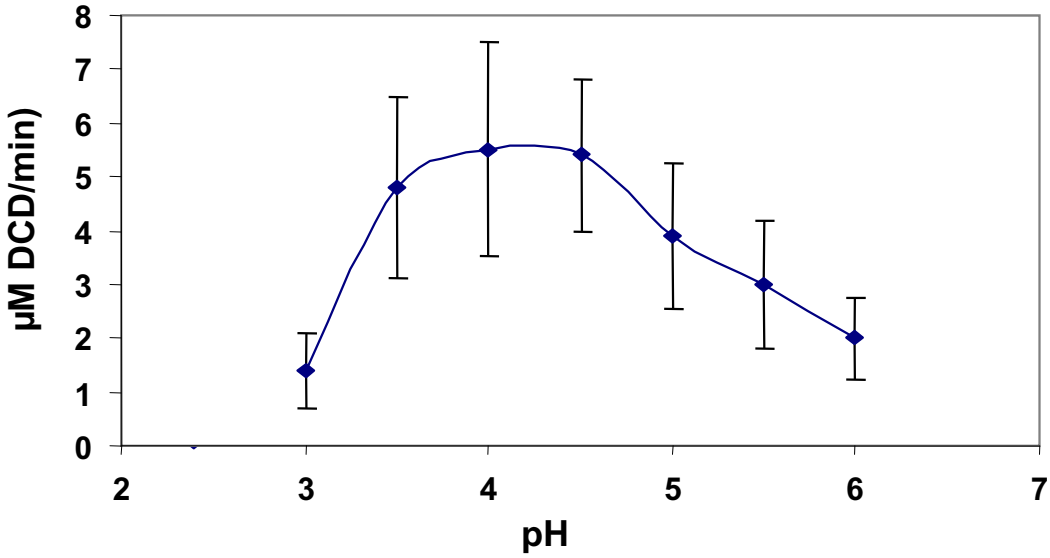

Figure 3.10: pH curve established for recombinant NapH1 through the monochlorodimedone assay.

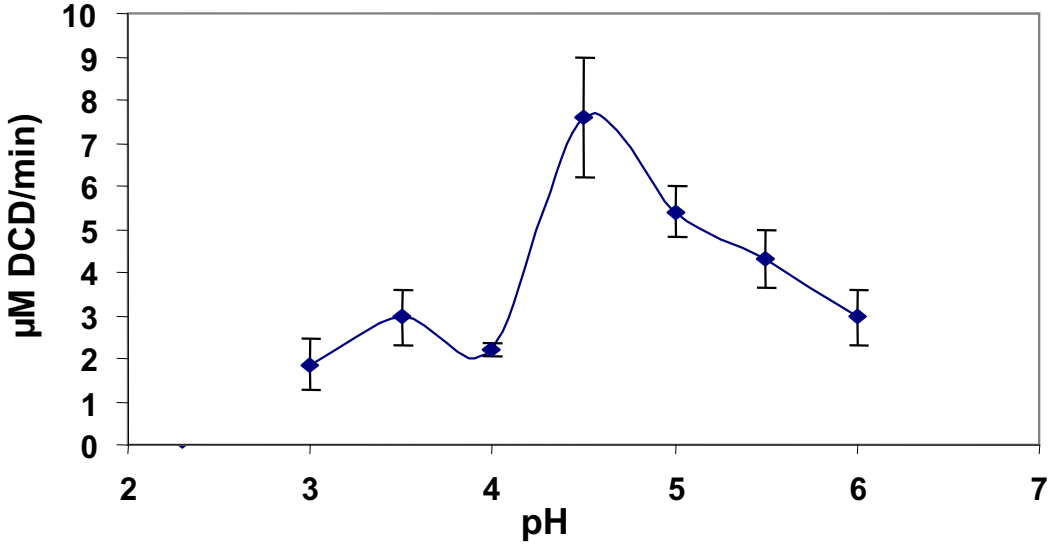

Figure 3.11: pH curve established for recombinant NapH3 through the monochlorodimedone assay.

To test the regio- and stereospecific halogenating ability of NapH1 and NapH3, a more napyradiomycin substrate specific assay was employed using the molecule lapachol (Figure 3.12). It was proposed that a chemoenzymatic conversion similar to the reaction observed with nerolidol would occur (Figures 3.2 and 3.12). A pH of 4.5, which was calculated as the pH optimum for both NapH1 and NapH3, was used in the assay as well as all the same substrate and cofactor concentrations employed in the monochlorodimedone assay. Sadly, no halogenated products were detected by *m*/*z* after incubating lapachol with recombinant His_8 tagged NapH1 or NapH3.

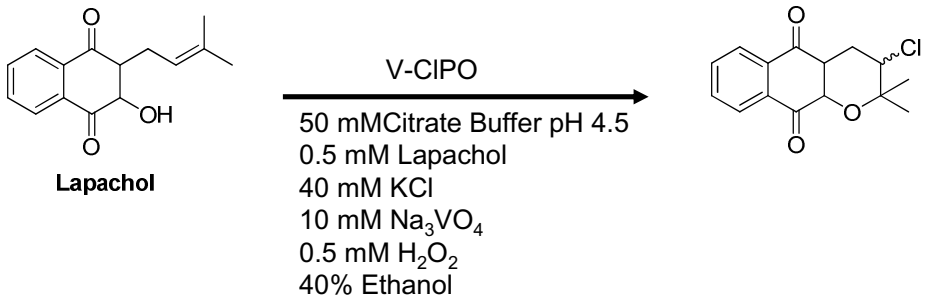

Figure 3.12: Chemoenzymatic cyclization and chlorination of lapachol by a V-ClPO.

3.3.5: Crystal studies

To date, the V-ClPO from *C. inaequalis* is the only V-ClPO whose three-dimensional structure has been solved,[37-39] and its structure differs dramatically to the structure of the V-BrPO from *C. officinalis*, which is associated with snyderol biosynthesis.[41] Differences in monomeric states between the V-HPOs may be indicative of their biological functions so efforts were made to solve the

three-dimensional structures of NapH1 and NapH3. The successful expression of the *nap* biosynthetic cluster in a serrogate host demonstrated that genes contained within the biosynthetic cluster were responsible for the oxidative cyclization and halogenation of the terpenoid subunits. It is believed that NapH1 and/or NapH3 is responsible for the novel natural product chemistry associated with the napyradiomycin class of bacterial antibiotics, but both soluble NapH1 and NapH3 behave as monomeric proteins, as seen with the V-ClPO from *C. inaequalis*,[37-39] when purified from *E. coli* BL21(DE3). This data suggests that the monomeric state of the V-HPOs is not indicative of their biological function.

After removal of the N-terminal His_8 tag, apo-NapH1 was crystallized by vapor diffusion at 4 ^{o}C using a crystallization buffer of 7% w/v PEG 8,000, 0.3 M NH_4OAc, 100 mM HEPES pH 7.5, and 2 mM DTT. Unfortunately, no crystals have yet to be obtained for apo-NapH3 despite an extensive screening process (Appendix Table 3A.1). The crystals obtained for apo-Nap1 were clear rectangular plates ranging in size from 380-420 μm (Figure 3.13), and diffraction data of 2.5 angstrom (Å) resolution was collected on the BL8.2.2 beam line at the Advanced Light Source (Berkeley, California). Apo-NapH1 crystallized in the orthorhombic space group $P2_12_12_1$ with unit cell dimension of a= 59.67 Å, b= 137.26 Å , c=156.35 Å, $\alpha = \beta = \gamma = 90^{o}$, with two molecules/unit cell. Molecular replacement using the published structure of V-ClPO from *C. inaequalis* with a H404A mutation (PDB accession number 1VNG) was used for phase determination. Due to a 29% similarity between the two enzymes, molecular

replacement was unsuccessful at phasing the diffraction data collected for apo-NapH1.

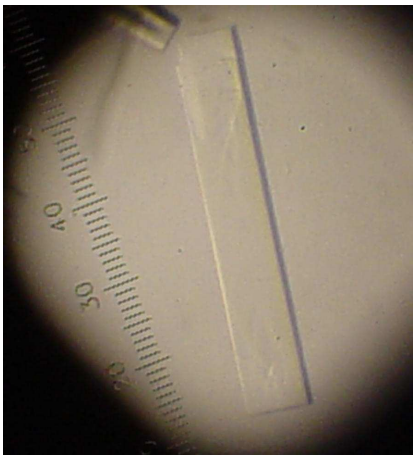

Figure 3.13: A crystal of NapH1

3.4: Conclusion

To date, V-HPOs have been identified in most branches of life, but have been characterized exlusively in eukaryotes. Although their biological roles have not yet been fully elucidated, the discovery of three V-ClPOs within the *nap* biosynthetic cluster, NapH1, NapH3 and NapH4, was a significant discovery as these enzymes are not only rare in nature, but had never before been characterized from prokaryotes. The successful expression of soluble NapH1 and NapH3 represented the first time a V-ClPO was expressed from a marine organism and the first time a V-HPO was expressed from a prokaryote. It is proposed that the V-ClPOs from the *nap* cluster are responsible for the natural product chemistry associated with the napyradiomycin class of antibiotics, in which they catalyze the oxidative cyclization and halogenation of terpenoid units, and both recombinant NapH1 and NapH3 exhibited halogenating activity in the monochlorodimedone assay. However, in the lapachol assay, neither NapH1 or NapH3 was able to cyclize and halogenate the terpenoid unit of lapachol. This suggests that the enzymes have a high substrate specificity or another enzyme, NapH4, is responsible for the cyclization of the 5-carbon terpene unit.

The crystallization of NapH1 represents the first time a V-HPO from a prokaryote has been crystallized. Because molecular replacement was unsuccessful at solving the three-dimensional structure of NapH1, heavy atom derivatives will be constructed by soaking the crystals and/or co-crystallizing NapH1 with heavy atoms acquired from Hampton Research including mercury

acetate, mercury chloride, sodium tungstate dihydrate, and ammonium tetrathiotungstate. Once a three-dimensional structure has been solved, NapH1 will be soaked with napyradiomycin analogs and precursors to determine which residues surrounding the active site are required for substrate selectivity.

3.5: Appendix

A.

Terrific Broth	
Starch	10 g
Yeast Extract	4 g
Bacto-peptone	2 g
Sea H_2O	1 L

B.

50 X 5052	
glycerol	250 g
α-lactose	10 mM
Glucose	25 g
Milli-Q H_2O	730 ml

C.

20 X NPS	
$(NH_4)_2SO_4$	66 g
KH_2PO_4	136 g
Na_2HPO_4	142 g
Milli-Q H_2O	900 ml

Figure 3A.1: Media used for protein expression. A) Terrific Broth. B) Autoinduction component 50 X 5052. C) Autoinduction component 20 X NPS.

A.

Lysis Buffer	
NaCl	500 mM
Imidazole	10 mM
Tris-HCl pH 8.0	50 mM
Glycerol	10%
β-Mercaptoethanol	5 mM
Tween 20	0.1%

B.

Wash Buffer	
NaCl	500 mM
Imidazole	20 mM
Tris-HCl pH 8.0	50 mM
Glycerol	10%

C.

Elution Buffer	
NaCl	500 mM
Imidazole	250 mM
Tris-HCl pH 8.0	50 mM
Glycerol	10%

D.

Dialysis Buffer	
NaCl	500 mM
Tris-HCl pH 8.0	50 mM
β-Mercaptoethanol	10 mM

E.

FPLC Isocratic Buffer	
NaCl	500 mM
Tris-HCl pH 8.0	50 mM
DTT	2 mM

Figure 3A.2: Buffers used for protein purification. A) Lysis buffer. B) Wash buffer. C) Elution buffer. D) Dialysis buffer. E) Fast protein liquid chromatography buffer.

A.

```
  1 MTTSGHTSFSDYSPRRRSMLLGGLGGAAALSAAGFTGMASASPRGSAGSK
 51 AAAIEFDLDKDNYIKWAQPTDENAGQSPTLAILGPMDVTVFLWINRVVWL
101 AAFDALAPYHETAVGVYSQIPRRPSSESATNRNLNIAALHAQHGVWKRVL
151 PQQVDQLRELMTALGLDPSDETENLSSPVGIGNVAAKNAFNALKNDGMNF
201 LGYEGRKYNPRPWADYTGYEPVNTAFKVNNPSRWQPQLQAHNARRAGGGP
251 GDLGIYVTQHFVTPQTARTKAHIFRDPSRFRIPRPEFSDHTNTRAYKRSV
301 DEIIDASANLNDERKALAEIMENKLWGIGHSSIVIANKYDQNNEMGVHGW
351 CHWMLAHVLATFEPLIAAWHHKTRFDAVRPVTAIRHVYGNRKIRAWGGVG
401 MGTVDIRASEWSSYLPVGDHPEYPSGSTSLCSATSQAARRYFDSDELDWT
451 INYPAGSTVVEPGITPGKDLSIHIPTWTDFTRTCATSRVWGGVHFQTTVD
501 RTIDFGEQFGDLAHEFVQRHVKGDVKD
```

B.

```
  1 MSSNVVGFSGDFDVIVIGGGPAGATTAALLSKRGRRVLVLDRERFPRYHV
 51 GESLIPGVMVPMEELGLKERMEAKGFERKYGGTLVWGNNEVPWNFSFSTG
101 GRIPYAFHTRRADLDALVLDRARELGAFVVEDATVKDTIEEDGRVVGVRY
151 ALRGLGGTQEARASLVIDASGQARVIGRKYTEVNWNEQLRNVAVWTYFDN
201 CHRLPGDEWSNILIEGTSDGWFWGIPIDKGVFSVGYVTRSELATESGKSL
251 EDLFQSEIASTTKLKELLKDATQAAGYRSARDWSYTNDRFYGKGWALVGD
301 AAAFVDPLFSTGVALATLAGSTLSKVVDQILQYPAIEEKALDRYSNAYQE
351 FFHDIRKFVEGFYDRSKTKGFYFNMAQEMVDPEKENAAEVDFVKLVSGLS
401 GRQGGLFELNVDDLIEDAKSTPADS
```

C.

```
  1 VTTSAPAQQIPFDFDNGNFIRDLITTHGGGGYPPADAMAPGDVSSYTWVT
 51 HLLQTSWFDALAPYHPTAVGVYSRIPRRPAEESATNRNKNIAGLYAMFQV
101 VKAAFTERVPVLRQALGALGLDPDDESQDLSTAVGIGNTAGKAVAAARMG
151 DGMNALGGKDRTHNGQPYEDYTGYRPVNTADELVDPSRWQPAVEPHRRRT
201 DGGPGDKGIFTAQRFATPQLGLVAPQTYRDPARFKLAAPDHLDHNDAGAY
251 RQAVDEVLAASAGLTDEQKVKAEFFEHTPLSVTLSPRAAAMAHDLDLDGW
301 AQLFLVCSTARFDSLIAAWHHKRAYDTVRPFSAVRHVYGSKPVTAWGGPG
351 KGTVESIPADEWTGYLPVGNHPEYPSGFTTLIAAQAQAARSFLGDDVLNW
401 THAFPAGSGQREPGAVPASDLELTWATWTDFENDCATSRVWAGAHFTKTA
451 ETSLAFGTQFGDLAHTFVQRHINGDVKD
```

D.

```
  1 MTTSGHTSVSDFSLGRRSLLVGGASAASLSMLSLSRPAAAATGDEPPELP
 51 DLDKDNYIKWAQPTGARTGQSASDAFIGSMDVTLILFMNRAAMLALFDAL
101 APYHETAVGIHSQIPRRPSSESATNRNMNIACIHAQNAIWSRLLPPIVAG
151 LRELMVALGLDPDDKSEDVTTPVGIGNVAAKAVWNVLKNDGMNVLGHEGG
201 RKYNPRPWADYTGYVPTNTAFKLNNPSRWQPQLQAHNGRRAGGGPGDLGI
251 YVTQHFVTPQIAVTLPHIFKDPTAFPLPRPDFTDHTDRRAYKRSVDEIIE
301 ASAALDDERKALAEIMENKLWGIGHSSIEIGLKNDQNNELGVHGWAQWML
351 QHILATFDTLIAAWGYKRKYEAVRPITAVRHVYGNRKIRAWGGVGMGTVD
401 DIPANEWAGYLPVGDHPEYPSGSTTVGSAASQAARRFFDSDDLNWEFDFE
451 VGKSIVEPGITPVENVRVSFPTWTDFNKRCAYSRLDGGVHFKKTVERSMA
501 FGEQFGDLAHDFIQRHVKGEGDG
```

Figure 3A.3: Amino acid sequences of the *nap*-halogenating enzymes. A) Amino acid sequence of V-ClPO; NapH1. B) Amino acid sequence of $FADH_2$ halogenase; NapH2. C) Amino acid sequence of V-ClPO; NapH3. D) Amino acid sequence of V-ClPO; NapH4.

Table 3A.1: NapH3 crystal screen.

Buffer	Salt	Precipitant
0.1 M sodium acetate pH 4.5	0.3 M ammonium sulfate	PEG 17,500 (5, 11, 17, and 23 % w/v)
0.1 M sodium succinate pH 5.5	0.3 M ammonium sulfate	PEG 17,500 (5, 11, 17, and 23 % w/v)
0.1 M sodium PIPES pH 6.5	0.3 M ammonium sulfate	PEG 17,500 (5, 11, 17, and 23 % w/v)
0.1 M sodium MOPSO pH 7.0	0.3 M ammonium sulfate	PEG 17,500 (5, 11, 17, and 23 % w/v)
0.1 M sodium HEPES pH 7.5	0.3 M ammonium sulfate	PEG 17,500 (5, 11, 17, and 23 % w/v)
0.1 M sodium TAPS pH 8.5	0.3 M ammonium sulfate	PEG 17,500 (5, 11, 17, and 23 % w/v)
0.1 M sodium acetate pH 4.5	2.50 M lithium nitrate	PEG 10,000 (7, 14, 21, and 28 % w/v)
0.1 M sodium succinate pH 5.5	2.50 M lithium nitrate	PEG 10,000 (7, 14, 21, and 28 % w/v)
0.1 M sodium PIPES pH 6.5	2.50 M lithium nitrate	PEG 10,000 (7, 14, 21, and 28 % w/v)
0.1 M sodium MOPSO pH 7.0	2.50 M lithium nitrate	PEG 10,000 (7, 14, 21, and 28 % w/v)
0.1 M sodium HEPES pH 7.5	2.50 M lithium nitrate	PEG 10,000 (7, 14, 21, and 28 % w/v)
0.1 M sodium TAPS pH 8.5	2.50 M lithium nitrate	PEG 10,000 (7, 14, 21, and 28 % w/v)
0.1 M sodium acetate pH 4.5	none	PEG 8,000 (7, 14, 21, and 28 % w/v)
0.1 M sodium succinate pH 5.5	none	PEG 8,000 (7, 14, 21, and 28 % w/v)
0.1 M sodium PIPES pH 6.5	none	PEG 8,000 (7, 14, 21, and 28 % w/v)
0.1 M sodium MOPSO pH 7.0	none	PEG 8,000 (7, 14, 21, and 28 % w/v)
0.1 M sodium HEPES pH 7.5	none	PEG 8,000 (7, 14, 21, and 28 % w/v)
0.1 M sodium TAPS pH 8.5	none	PEG 8,000 (7, 14, 21, and 28 % w/v)
0.1 M sodium acetate pH 4.5	0.3 M ammonium acetate	PEG 8,000 (7, 14, 21, and 28 % w/v)
0.1 M sodium succinate pH 5.5	0.3 M ammonium acetate	PEG 8,000 (7, 14, 21, and 28 % w/v)

Table 3A.1 continued.

Buffer	Salt	Precipitant
0.1 M sodium PIPES pH 6.5	0.3 M ammonium acetate	PEG 8,000 (7, 14, 21, and 28 % w/v)
0.1 M sodium MOPSO pH 7.0	0.3 M ammonium acetate	PEG 8,000 (7, 14, 21, and 28 % w/v)
0.1 M sodium HEPES pH 7.5	0.3 M ammonium acetate	PEG 8,000 (7, 14, 21, and 28 % w/v)
0.1 M sodium TAPS pH 8.5	0.3 M ammonium acetate	PEG 8,000 (7, 14, 21, and 28 % w/v)
0.1 M sodium acetate pH 4.5	0.2 M magnesium chloride	PEG 8,000 (7, 14, 21, and 28 % w/v)
0.1 M sodium succinate pH 5.5	0.2 M magnesium chloride	PEG 8,000 (7, 14, 21, and 28 % w/v)
0.1 M sodium PIPES pH 6.5	0.2 M magnesium chloride	PEG 8,000 (7, 14, 21, and 28 % w/v)
0.1 M sodium MOPSO pH 7.0	0.2 M magnesium chloride	PEG 8,000 (7, 14, 21, and 28 % w/v)
0.1 M sodium HEPES pH 7.5	0.2 M magnesium chloride	PEG 8,000 (7, 14, 21, and 28 % w/v)
0.1 M sodium TAPS pH 8.5	0.2 M magnesium chloride	PEG 8,000 (7, 14, 21, and 28 % w/v)
0.1 M sodium acetate pH 4.5	0.25 M lithium sulfate	PEG 8,000 (7, 14, 21, and 28 % w/v)
0.1 M sodium succinate pH 5.5	0.25 M lithium sulfate	PEG 8,000 (7, 14, 21, and 28 % w/v)
0.1 M sodium PIPES pH 6.5	0.25 M lithium sulfate	PEG 8,000 (7, 14, 21, and 28 % w/v)
0.1 M sodium MOPSO pH 7.0	0.25 M lithium sulfate	PEG 8,000 (7, 14, 21, and 28 % w/v)
0.1 M sodium HEPES pH 7.5	0.25 M lithium sulfate	PEG 8,000 (7, 14, 21, and 28 % w/v)
0.1 M sodium TAPS pH 8.5	0.25 M lithium sulfate	PEG 8,000 (7, 14, 21, and 28 % w/v)
0.1 M sodium acetate pH 4.5	0.2 M calcium acetate	PEG 8,000 (7, 14, 21, and 28 % w/v)
0.1 M sodium succinate pH 5.5	0.2 M calcium acetate	PEG 8,000 (7, 14, 21, and 28 % w/v)
0.1 M sodium PIPES pH 6.5	0.2 M calcium acetate	PEG 8,000 (7, 14, 21, and 28 % w/v)
0.1 M sodium MOPSO pH 7.0	0.2 M calcium acetate	PEG 8,000 (7, 14, 21, and 28 % w/v)
0.1 M sodium HEPES	0.2 M calcium acetate	PEG 8,000 (7, 14, 21, and

Table 3A.1 continued.

Buffer	Salt	Precipitant
pH 7.5		28 % w/v)
0.1 M sodium TAPS pH 8.5	0.2 M calcium acetate	PEG 8,000 (7, 14, 21, and 28 % w/v)
0.1 M sodium acetate pH 4.5	0.3 M magnesium nitrate	PEG 4,000 (7, 14, 21, and 28 % w/v)
0.1 M sodium succinate pH 5.5	0.3 M magnesium nitrate	PEG 4,000 (7, 14, 21, and 28 % w/v)
0.1 M sodium PIPES pH 6.5	0.3 M magnesium nitrate	PEG 4,000 (7, 14, 21, and 28 % w/v)
0.1 M sodium MOPSO pH 7.0	0.3 M magnesium nitrate	PEG 4,000 (7, 14, 21, and 28 % w/v)
0.1 M sodium HEPES pH 7.5	0.3 M magnesium nitrate	PEG 4,000 (7, 14, 21, and 28 % w/v)
0.1 M sodium TAPS pH 8.5	0.3 M magnesium nitrate	PEG 4,000 (7, 14, 21, and 28 % w/v)
0.1 M sodium acetate pH 4.5	0.3 M potassium chloride	PEG 3,350 (7, 14, 21, and 28 % w/v)
0.1 M sodium succinate pH 5.5	0.3 M potassium chloride	PEG 3,350 (7, 14, 21, and 28 % w/v)
0.1 M sodium PIPES pH 6.5	0.3 M potassium chloride	PEG 3,350 (7, 14, 21, and 28 % w/v)
0.1 M sodium MOPSO pH 7.0	0.3 M potassium chloride	PEG 3,350 (7, 14, 21, and 28 % w/v)
0.1 M sodium HEPES pH 7.5	0.3 M potassium chloride	PEG 3,350 (7, 14, 21, and 28 % w/v)
0.1 M sodium TAPS pH 8.5	0.3 M potassium chloride	PEG 3,350 (7, 14, 21, and 28 % w/v)
0.1 M sodium acetate pH 4.5	0.3 M potassium nitrate	PEGMME 5,000 (7, 14, 21, and 28 % w/v)
0.1 M sodium succinate pH 5.5	0.3 M potassium nitrate	PEGMME 5,000 (7, 14, 21, and 28 % w/v)
0.1 M sodium PIPES pH 6.5	0.3 M potassium nitrate	PEGMME 5,000 (7, 14, 21, and 28 % w/v)
0.1 M sodium MOPSO pH 7.0	0.3 M potassium nitrate	PEGMME 5,000 (7, 14, 21, and 28 % w/v)
0.1 M sodium HEPES pH 7.5	0.3 M potassium nitrate	PEGMME 5,000 (7, 14, 21, and 28 % w/v)
0.1 M sodium TAPS pH 8.5	0.3 M potassium nitrate	PEGMME 5,000 (7, 14, 21, and 28 % w/v)
0.1 M sodium acetate pH 4.5	0.5 M ammonium bromide	PEGMME 2,000 (10, 20, 40, and 40 % w/v)

Table 3A.1 continued.

Buffer	Salt	Precipitant
0.1 M sodium succinate pH 5.5	0.5 M ammonium bromide	PEGMME 2,000 (10, 20, 40, and 40 % w/v)
0.1 M sodium PIPES pH 6.5	0.5 M ammonium bromide	PEGMME 2,000 (10, 20, 40, and 40 % w/v)
0.1 M sodium MOPSO pH 7.0	0.5 M ammonium bromide	PEGMME 2,000 (10, 20, 40, and 40 % w/v)
0.1 M sodium HEPES pH 7.5	0.5 M ammonium bromide	PEGMME 2,000 (10, 20, 40, and 40 % w/v)
0.1 M sodium TAPS pH 8.5	0.5 M ammonium bromide	PEGMME 2,000 (10, 20, 40, and 40 % w/v)
0.1 M sodium acetate pH 4.5		1.5, 2.0, 2.5, and 3.0 M ammonium sulfate
0.1 M sodium succinate pH 5.5		1.5, 2.0, 2.5, and 3.0 M ammonium sulfate
0.1 M sodium PIPES pH 6.5		1.5, 2.0, 2.5, and 3.0 M ammonium sulfate
0.1 M sodium MOPSO pH 7.0		1.5, 2.0, 2.5, and 3.0 M ammonium sulfate
0.1 M sodium HEPES pH 7.5		1.5, 2.0, 2.5, and 3.0 M ammonium sulfate
0.1 M sodium TAPS pH 8.5		1.5, 2.0, 2.5, and 3.0 M ammonium sulfate
0.1 M sodium acetate pH 4.5	0.2 M ammonium sulfate	PEE 797 (15, 22, 29, and 36 % w/v)
0.1 M sodium succinate pH 5.5	0.2 M ammonium sulfate	PEE 797 (15, 22, 29, and 36 % w/v)
0.1 M sodium PIPES pH 6.5	0.2 M ammonium sulfate	PEE 797 (15, 22, 29, and 36 % w/v)
0.1 M sodium MOPSO pH 7.0	0.2 M ammonium sulfate	PEE 797 (15, 22, 29, and 36 % w/v)
0.1 M sodium HEPES pH 7.5	0.2 M ammonium sulfate	PEE 797 (15, 22, 29, and 36 % w/v)
0.1 M sodium TAPS pH 8.5	0.2 M ammonium sulfate	PEE 797 (15, 22, 29, and 36 % w/v)

PEG= polyethylene glycol; PEGMME= polyethylene glycol monomethylethers

3.6: References

1. Gribble, G. W., Amazing organohalogens. *Am. Sci.* **2004,** 92, 342-49.

2. Butler, A.; Carter-Franklin, J. N., The role of vanadium bromoperoxidase in the biosynthesis of halogenated marine natural products. *Nat. Prod. Rep.* **2004,** 21, 180-88.

3. McCormick, M. H.; McGuire, J. M.; Pittenger, G. E.; Pittenger, R. C.; Stark, W. M., Vancomycin, a new antibiotic. I. Chemical and biological properties. *Antibiot. Annu.* **1955,** 3, 606-11.

4. Raistrick, H., Aureomycin, a new antibiotic. *Nature* **1949,** 163, 159.

5. Bartz, Q. R., Isolation and characterization of chlormycetin. *J. Biol. Chem.* **1948,** 172, 445-50.

6. Bush, J. A.; Long, B. H.; Catino, J. J.; Bradner, W. T.; Tomita, K., Production and biological activity of rebeccamycin, a novel antitumor agent. *J. Antibiot.* **1987,** 40, 668-78.

7. Feling, R. H.; Buchanan, G. O.; Mincer, T. J.; Kauffman, C. A.; Jensen, P. R.; Fenical, W., Salinosporamide A: A highly cytotoxic proteasome inhibitor from a novel microbial source, a marine bacterium of the new genus *Salinospora*. *Angew. Chem. Int. Ed. Engl.* **2003,** 42, 355-57.

8. Nogami, T.; Shigihara, Y.; Matsuda, N.; Takahashi, Y.; Naganawa, H.; Hamada, M.; Muraoka, Y.; Takita, T.; Iitaka, Y.; Takeuchi, T., Neopyrrolomycin, a new chlorinated phenylpyrrole antibiotic. *J. Antibiot.* **1987,** 53, 1192-94.

9. Blunt, J.; Copp, B. R.; Munro, M. G. H.; Northcote, P. T.; Prinsep, M. R., Marine natural products. *Nat. Prod. Rep.* **2005,** 22, 15-61.

10. Vaillancourt, F. H.; Yeh, E.; Vosburg, D. A.; Garneau-Tsodikova, S.; Walsh, C. T., Nature's inventory of halogenation catalysts: oxidative strategies predominate. *Chem. Rev.* **2006,** 106, 3364-78.

11. Neumann, C. S.; Fujimori, D. G.; Walsh, C. T., Halogenation strategies in natural product biosynthesis. *Chem. Biol.* **2008,** 15, 99-09.

12. Chen, X.; van Pee, K. H., Catalytic mechanisms, basic roles, and biotechnological and environmental significance of halogenating enzymes. *Acta Biochim. Biophys. Sin. (Shanghai)* **2008,** 40, 183-93.

13. Littlechild, J.; Garcia-Rodriguez, E.; Dalby, A.; Isupov, M., Structural and functional comparisons between vanadium haloperoxidase and acid phosphatase enzymes. *J. Mol. Recognit.* **2002,** 15, 291-96.

14. Wever, R.; Hemrika, W., *Handbook of Metalloproteins*. John Wiley & Sons Ltd.: Chichester, United Kingdom, 2001.

15. de Boer, E.; Plat, H.; Tromp, M. G.; Wever, R.; Franssen, M. C.; van der Plas, H. C.; Meijer, E. M.; Schoemaker, H. E., Vanadium containing bromoperoxidase: an example of an oxidoreductase with high operational stability in aqueous and organic media. *Biotechnol. Bioeng.* **1987,** 30, 607-10.

16. Coupe, E. E.; Smyth, M. G.; Fosberry, A. P.; Hall, R. M.; Littlechild, J. A., The dodecameric vanadium-dependent haloperoxidase from the marine algae *Corallina officinalis*: cloning, expression, and refolding of the recombinant enzyme. *Protein Expr. Purif.* **2007,** 52, 265-72.

17. Carter-Franklin, J. N.; Butler, A., Vanadium bromoperoxidase-catalyzed biosynthesis of halogenated marine natural products. *J. Am. Chem. Soc.* **2004,** 126, 15060-66.

18. Itoh, N.; Hasan, A. K.; Izumi, Y.; Yamada, H., Substrate specificity, regiospecificity and stereospecificity of halogenation reactions catalyzed by non-heme-type bromoperoxidase of *Corallina pilulifera*. *Eur. J. Biochem.* **1988,** 172, 477-84.

19. Andersson, M.; Willetts, A.; Allenmark, S., Asymmetric sulfoxidation catalyzed by a vanadium-containing bromoperoxidase. *J. Org. Chem.* **1997,** 62, 8455-58.

20. ten Brink, H. B.; Dekker, H. L.; Schoemaker, H. E.; Wever, R., Oxidation reactions catalyzed by vanadium chloroperoxidase from *Curvularia inaequalis*. *J. Inorg. Biochem.* **2000,** 80, 91-8.

21. Fenical, W., Halogenation in Rhodophyta - Review. *J. Phycol.* **1975,** 11, 245-59.

22. Kladi, M.; Vagias, C.; Roussis, V., Volatile halogenated metabolites from marine red algae. *Phytochem. Rev.* **2004,** 3, 337-66.

23. Yamada, H.; Itoh, N.; Murakami, S.; Izumi, Y., New bromoperoxidase from Coralline algae that brominates phenol compounds. *Agricultural Biological and Chemistry* **1985,** 49, 2961-67.

24. Hewson, W. D.; Hager, L. P., Bromoperoxidases and halogenated lipids in marine algae. *J. Phycol.* **1980,** 16, 340-45.

25. Vitler, H., Peroxidases from Phaeophyceae: a vanadium(V)-dependent peroxidase from *Ascophyllum nodosum*. *Phytochemistry* **1984,** 23, 1387-90.

26. Colin, C.; Leblanc, C.; Wagner, E.; Delage, L.; Leize-Wagner, E.; Van Dorsselaer, A.; Kloareg, B.; Potin, P., The brown algal kelp *Laminaria digitata* features distinct bromoperoxidase and iodoperoxidase activities. *J. Biol. Chem.* **2003,** 278, 23545-52.

27. Ohshiro, T.; Nakano, S.; Takahashi, Y.; Suzuki, M.; Izumi, Y., Occurrence of bromoperoxidase in the marine green macro-alga, *Ulvella lens*, and emission of volatile brominated methane by the enzyme. *Phytochemistry* **1999,** 52, 1211-15.

28. Sheffield, D. J.; Harry, T.; Smith, A. J.; Rogers, L. J., Purification and characterization of the vanadium bromoperoxidase from the macroalga *Corallina officinalis*. *Phytochemistry* **1993,** 32, 21-26.

29. Itoh, N.; Izumi, Y.; Yamada, H., Purification of bromoperoxidase from *Corallina pilulifera*. *Biochem. Biophys. Res. Commun.* **1985,** 131, 428-35.

30. Shimonishi, M.; Kuwamoto, S.; Inoue, H.; Wever, R.; Ohshiro, T.; Izumi, Y.; Tanabe, T., Cloning and expression of the gene for a vanadium-dependent bromoperoxidase from a marine macro-alga, *Corallina pilulifera*. *FEBS Lett.* **1998,** 428, 105-10.

31. Plat, H.; Krenn, B. E.; Wever, R., The bromoperoxidase from the lichen *Xanthoria parietina* is a novel vanadium enzyme. *Biochem. J.* **1987,** 248, 277-79.

32. Hunter-Cevera, C. J.; Sotos, L., Screening for a “new” enzyme in nature: haloperoxidase production by Death Valley dematiaceous hyphomycetes. *Microb. Ecol.* **1986,** 12, 121-27.

33. Liu, T. N.; M'Timkulu, T.; Geigert, J.; Wolf, B.; Neidleman, S. L.; Silva, D.; Hunter-Cevera, J. C., Isolation and characterization of a novel nonheme chloroperoxidase. *Biochem. Biophys. Res. Commun.* **1987,** 142, 329-33.

34. van Schijndel, J. W.; Vollenbroek, E. G.; Wever, R., The chloroperoxidase from the fungus *Curvularia inaequalis*; a novel vanadium enzyme. *Biochim. Biophys. Acta* **1993,** 1161, 249-56.

35. Barnett, P.; Hemrika, W.; Dekker, H. L.; Muijsers, A. O.; Renirie, R.; Wever, R., Isolation, characterization, and primary structure of the vanadium chloroperoxidase from the fungus *Embellisia didymospora*. *J. Biol. Chem.* **1998,** 273, 23381-87.

36. Cosse, A.; Potin, P.; Leblanc, C., Patterns of gene expression induced by oligoguluronates reveal conserved and environment-specific molecular defense responses in the brown alga *Laminaria digitata*. *New Phytol.* **2009,** 182, 239-50.

37. Macedo-Ribeiro, S.; Hemrika, W.; Renirie, R.; Wever, R.; Messerschmidt, A., X-ray crystal structures of active site mutants of the vanadium-containing chloroperoxidase from the fungus *Curvularia inaequalis*. *J. Biol. Inorg. Chem.* **1999,** 4, 209-19.

38. Messerschmidt, A.; Prade, L.; Wever, R., Implications for the catalytic mechanism of the vanadium-containing enzyme chloroperoxidase from the fungus *Curvularia inaequalis* by X-ray structures of the native and peroxide form. *Biol. Chem.* **1997,** 378, 309-15.

39. Messerschmidt, A.; Wever, R., X-ray structure of a vanadium-containing enzyme: chloroperoxidase from the fungus *Curvularia inaequalis*. *Proc. Natl. Acad. Sci. USA* **1996,** 93, 392-96.

40. Weyand, M.; Hecht, H. J.; Kiess, M.; Liaud, M. F.; Vilter, H.; Schomburg, D., X-ray structure determination of a vanadium-dependent haloperoxidase from *Ascophyllum nodosum* at 2.0 angstrom resolution. *J. Mol. Biol.* **1999,** 293, 595-11.

41. Isupov, M. N.; Dalby, A. R.; Brindley, A. A.; Izumi, Y.; Tanabe, T.; Murshudov, G. N.; Littlechild, J. A., Crystal structure of dodecameric vanadium-dependent bromoperoxidase from the red algae *Corallina officinalis*. *J. Mol. Biol.* **2000,** 299, 1035-49.

42. Pooransingh-Margolis, N.; Renirie, R.; Hasan, Z.; Wever, R.; Vega, A. J.; Polenova, T., 51V solid-state magic angle spinning NMR spectroscopy of vanadium chloroperoxidase. *J. Am. Chem. Soc.* **2006,** 128, 5190-08.

43. Zhang, Y.; Gascon, J. A., QM/MM investigation of structure and spectroscopic properties of a vanadium-containing peroxidase. *J. Inorg. Biochem.* **2008,** 102, 1684-90.

44. Raugei, S.; Carloni, P., Structure and function of vanadium haloperoxidases. *J. Phys. Chem. B* **2006,** 110, 3747-58.

45. Renirie, R.; Hemrika, W.; Wever, R., Peroxidase and phosphatase activity of active-site mutants of vanadium chloroperoxidase from the fungus *Curvularia inaequalis*. Implications for the catalytic mechanisms. *J. Biol. Chem.* **2000,** 275, 11650-57.

46. Hemrika, W.; Renirie, R.; Macedo-Ribeiro, S.; Messerschmidt, A.; Wever, R., Heterologous expression of the vanadium-containing chloroperoxidase from *Curvularia inaequalis* in *Saccharomyces cerevisiae* and site-directed mutagenesis of the active site residues His(496), Lys(353), Arg(360), and Arg(490). *J. Biol. Chem.* **1999,** 274, 23820-27.

47. Butler, A.; Carter, J. N.; Simpson, M. T., *Handbook of Metalloproteins*. Marcel Dekker Inc.: New York, 2001.

48. Martinez, V. M.; De Cremer, G.; Roeffaers, M. B.; Sliwa, M.; Baruah, M.; De Vos, D. E.; Hofkens, J.; Sels, B. F., Exploration of single molecule events in a haloperoxidase and its biomimic: localization of halogenation activity. *J. Am. Chem. Soc.* **2008,** 130, 13192-93.

49. Hasan, Z.; Renirie, R.; Kerkman, R.; Ruijssenaars, H. J.; Hartog, A. F.; Wever, R., Laboratory-evolved vanadium chloroperoxidase exhibits 100-fold higher halogenating activity at alkaline pH: catalytic effects from first and second coordination sphere mutations. *J. Biol. Chem.* **2006,** 281, 9738-44.

50. Ohshiro, T.; Littlechild, J.; Garcia-Rodriguez, E.; Isupov, M. N.; Iida, Y.; Kobayashi, T.; Izumi, Y., Modification of halogen specificity of a vanadium-dependent bromoperoxidase. *Protein Sci.* **2004,** 13, 1566-71.

51. Soedjak, H. S.; Butler, A., Chlorination catalyzed by vanadium bromoperoxidase. *Inorg. Chem.* **1990,** 29, 5015-17.

52. Carter, J. N.; Beatty, K. E.; Simpson, M. T.; Butler, A., Reactivity of recombinant and mutant vanadium bromoperoxidase from the red alga *Corallina officinalis*. *J. Inorg. Biochem.* **2002,** 91, 59-69.

53. Winter, J. M.; Moffitt, M. C.; Zazopoulos, E.; McAlpine, J. B.; Dorrestein, P. C.; Moore, B. S., Molecular basis for chloronium-mediated meroterpene cyclization: cloning, sequencing, and heterologous expression of the napyradiomycin biosynthetic gene cluster. *J. Biol. Chem.* **2007,** 282, 16362-68.

54. Hemrika, W.; Renirie, R.; Dekker, H. L.; Barnett, P.; Wever, R., From phosphatases to vanadium peroxidases: a similar architecture of the active site. *Proc. Natl. Acad. Sci. USA* **1997,** 94, 2145-49.

55. Tanaka, N.; Dumay, V.; Liao, Q.; Lange, A. J.; Wever, R., Bromoperoxidase activity of vanadate-substituted acid phosphatases from *Shigella flexneri* and *Salmonella enterica ser. typhimurium*. *Eur. J. Biochem.* **2002,** 269, 2162-67.

56. de Macedo-Ribeiro, S.; Renirie, R.; Wever, R.; Messerschmidt, A., Crystal structure of a trapped phosphate intermediate in vanadium apochloroperoxidase catalyzing a dephosphorylation reaction. *Biochemistry* **2008,** 47, 929-34.

57. Soria-Mercado, I. E.; Prieto-Davo, A.; Jensen, P. R.; Fenical, W., Antibiotic terpenoid chloro-dihydroquinones from a new marine actinomycete. *J. Nat. Prod.* **2005,** 68, 904-10.

58. Studier, F. W., Protein production by auto-induction in high density shaking cultures. *Protein Expr. Purif.* **2005,** 41, 207-34.

59. Altman, J. Altman laboratory home page. http://www.microbiology.emory.edu/altman/jdaWebSite_v3/p_tet_autoInduction.shtml

60. Jez, J. M.; Ferrer, J. L.; Bowman, M. E.; Dixon, R. A.; Noel, J. P., Dissection of malonyl-coenzyme A decarboxylation from polyketide formation in the reaction mechanism of a plant polyketide synthase. *Biochemistry* **2000,** 39, 890-02.

61. Sambrook, J.; Fritsch, E. F.; Maniatis, T., *Molecular Cloning, a Laboratory Manual,* . 2nd ed.; Cold spring Harbor Laboratory: Cold Spring Harbor, NY, 1989.

62. Matthews probabilities. http://ruppweb.dyndns.org/mattprob/

63. Vagin, A. A.; Isupov, M. N., Spherically averaged phased translation function and its application to the search for molecules and fragments in electron-density maps. *Acta Crystallogr. D Biol. Crystallogr.* **2001,** 57, (Pt 10), 1451-6.

64. The CCP4 suite: programs for protein crystallography. *Acta Crystallogr. D Biol. Crystallogr.* **1994,** 50, (Pt 5), 760-3.

65. NCBI Blast Home Page. <http://www.ncbi.nlm.nih.gov/BLAST/> (March 2007).

66. Thompson, J. D.; Higgins, D. G.; Gibson, T. J., CLUSTAL W: improving the sensitivity of progressive multiple sequence alignment through sequence weighting, position-specific gap penalties and weight matrix choice. *Nucleic Acids Res.* **1994,** 22, 4673-80.

67. Shiomi, K.; Iinuma, H.; Naganawa, H.; Isshiki, K.; Takeuchi, T.; Umezawa, H., Biosynthesis of napyradiomycins. *J. Antibiot.* **1987,** 40, 1740-45.

68. Hager, L. P.; Morris, D. R.; Brown, F. S.; Eberwein, H., Chloroperoxidase. II. Utilization of halogen anions. *J. Biol. Chem.* **1966,** 241, 1769-77.

69. Morris, D. R.; Hager, L. P., Chloroperoxidase. I. Isolation and properties of the crystalline glycoprotein. . *J. Biol. Chem.* **1966,** 241, 1763-68.

3.7: Acknowledgement

Chapter 3, in full, is a reprint of the material as it appears in Exploring the Chemistry and Biology of Vanadium-Dependent Haloperoxidases. (2009). Winter, Jaclyn M.; Moore, Bradley S., Journal of Biological Chemistry, 284, 18577–81. The dissertation was the primary investigator and author of this material.

Chapter 4

Functional Characterization of Halogenating enzymes from the Napyradiomycin Biosynthetic Cluster by *In vivo* Mutagenesis Experiments

4.1: Introduction

4.1.1: Vanadium haloperoxidases

Vanadium-dependent haloperoxidases (V-HPOs) are enzymes that catalyze the oxidation of halides to their corresponding hypohalous acids at the expense of hydrogen peroxide and are named after the most electronegative halide they are able to oxidize.[1] These enzymes have received increasing attention due to their ability to halogenate a range of organic compounds and because they have the capability to do so in a regio- and stereospecific manner.[2] Vanadium bromoperoxidases (V-BrPOs) are widely distributed in marine algae, while vanadium chloroperoxidases (V-ClPOs) have been primarily isolated from dematiaceous hyphomycete fungi.[3] To date, all known V-HPOs have only been characterized *in vitro* from eukaryotic systems. While the biological function of V-ClPOs has yet to be elucidated, marine algal V-BrPOs have been shown through *in vitro* chemoenzymatic conversions to catalyze the cyclization of terpenes and ethers via a bromonium ion (Figure 4.1).

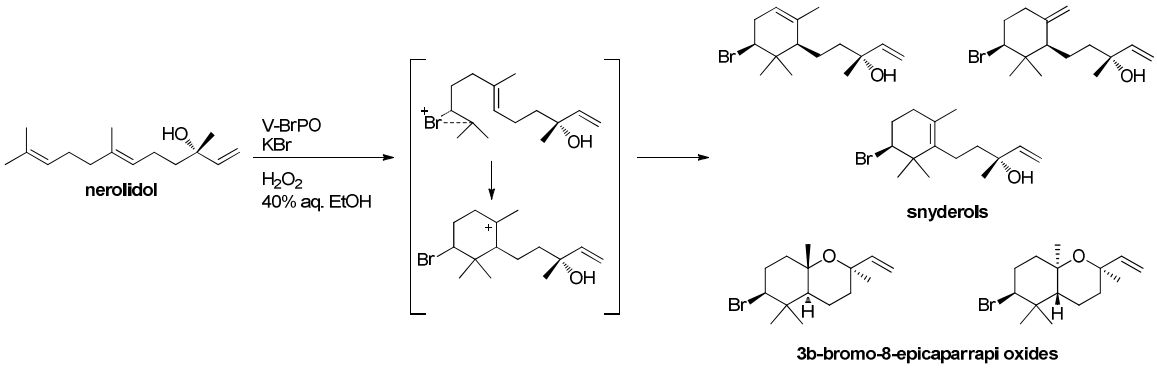

Figure 4.1: V-BrPO chemoenzymatic cyclization of nerolidol to brominated algal natural products using the V-BrPO from *Corallina officinalis*.

4.1.2: Specific Aim

V-HPOs have a large distribution in nature, where they are present in macroalgae, fungi, and bacteria, but have been exclusively characterized in eukaryotes. V-BrPOs are the only V-HPOs characterized that demonstrates the ability to facilitate bromonium ion induced cyclization of terpenes *in vitro.*[3] While this study established the likely role of V-BrPOs in the biosynthesis of brominated cyclic sesquiterpenes from marine red algae, conventional wisdom still suggests that V-HPOs lack substrate specificity and regioselectivity because the natural substrates and final products of these enzymes are unknown. Because all characterized V-HPOs to date have been identified from fungi and marine algae, their biosynthetic roles *in vivo* have not been yet elucidated due to the inability to identify and clone all of the corresponding genes required for the assembly of a natural product.

The cloning and sequencing of the 46-kb napyradiomycin biosynthetic gene cluster from the marine-derived *Streptomyces* sp. CNQ-525 revealed three homologous V-ClPO genes, which represented the first time V-HPO genes were identified in prokaryotes.[4] Through heterologous expression in a surrogate bacterial host, the napyradiomycin biosynthetic gene cluster from *S.* sp. CNQ-525 was shown to be wholly responsible for the synthesis of the chlorinated meroterpenoids. It is proposed that the V-ClPOs from this cluster are responsible for the novel natural product chemistry associated with the napyradiomycin class of antibiotics in which they catalyze the oxidative cyclization and halogenation of terpenoid units in a manner reminiscent of that of

snyderol biosynthesis in *Corallina officinalis* (Figure 4.2). Therefore, the *nap* biosynthetic cluster provides a tractable system for elucidating the role of V-HPOs *in vivo*.

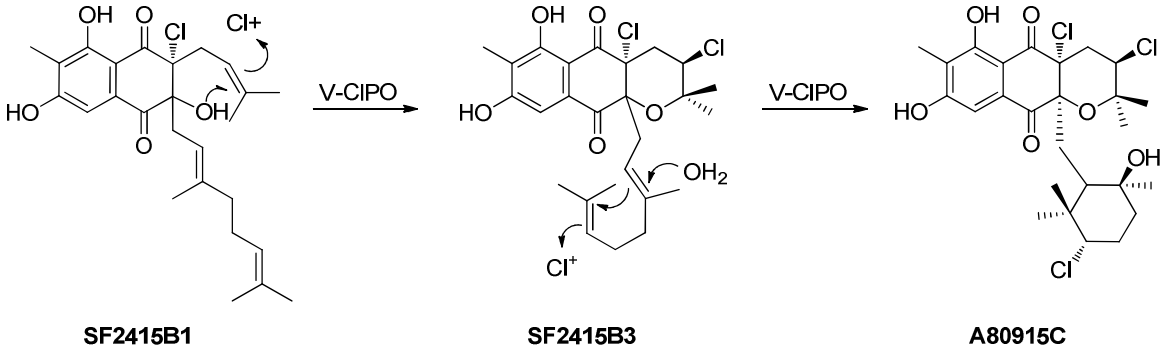

SF2415B1 **SF2415B3** **A80915C**

Figure 4.2: V-ClPO catalyzed cyclization of chlorinated dihydroquinones using *nap* derived V-ClPOs from *S.* sp. CNQ-525.

4.2: Materials and Methods

4.2.1: Bacterial strains and cultural conditions

Streptomyces sp. CNQ-525 was a gift from Professors William Fenical and Paul R. Jensen (University of California at San Diego).[5] Cultures were grown in 50 ml of A1 growth media (Appendix Figure 2A.1) for nine days at 30 ^{o}C with shaking at 250 revolutions/min. *Escherichia coli* cultures (Table 4.1) were grown in Luria Bertani (LB) broth (Appendix Figure 2A.1) at 37 ^{o}C in 15 ml conical tubes for 16 hours at constant shaking, unless otherwise specified. When selecting *E. coli* harboring plasmids, the cultures were grown with the appropriate antibiotics.

Table 4.1: *E. coli* strains used and their corresponding genotypes

***E. Coli* strain**	**Genotype**	**Source**
XL1-Blue MRF' Supercompetent cells	Δ(*mcrA*)*183* Δ(*mcrCB-hsdSMR-mrr*)*173 endA1 supE44 thi-1 recA1 gyrA96 relA1 lac* (F´*roAB lacIqZ*Δ*M15*Tn*10* (Tetr))	Stratagene, USA
TOPO One Shot Top10 competent cells	F- *mcr*A Δ(*mrr-hsd*RMS-*mcr*BC) Φ80*lac*ZΔM15 Δ*lac*X74 *rec*A1 *ara*D139 Δ(*araleu*)7697 *gal*U *gal*K *rps*L (StrR) *end*A1 *nup*G	Invitrogen, USA
Subcloning efficiency DH5-α competent cells	F- φ80*lac*ZΔM15 Δ(*lac*ZYA-*arg*F)U169 *rec*A1 *end*A1 *hsd*R17(rk-, mk+) *pho*A*sup*E44 *thi*-1 *gyr*A96 *rel*A1 λ-	Invitrogen, USA
BW25113/pIJ790	Δ(*araD-araB*)567, Δ*lacZ*4787(::*rrnB-4*), *lacIp-4000*(lacI^{Q}), λ^{-}, *rpoS369* (Am), *rph-1*, Δ(*rhaD-rhaB*) 568, *hsdR514*	Plant Biosciences Limited, UK
S17-1	*recA pro hsdR RP4-2-Tc::Mu-Km::Tn7*	American Type Culture Collection
ET12567/pUZ8002	*Dam-13*:::*Tn9*, *dcm-6*, *hsdM*	Plant Biosciences Limited, UK

4.2.2: Transcription analysis of the napyradiomycin biosynthetic cluster

4.2.2.1: Sample preparation

A 1% aliquot from a seven day old seed culture of *S.* sp. CNQ-525 was used to inoculate 50 ml of A1 growth media (Appendix Figure 2A.1) in a 250 Erlenmeyer flask containing a spring. At 24 hours, day 3, day 5, day 7 and day 10, a 2 ml aliquot was extracted from the 50 ml culture and placed into a cryovial. Cells were pelleted from the aliquot by centrifuging at 15,700 g for five minutes at room temperature (Eppendorf 5415 R centrifuge). After the first centrifugation, the vial was rotated 180^{o} and centrifuged for an additional five minutes. The pellet was flash frozen in liquid nitrogen and immediately stored at -80 ^{o}C.

4.2.2.2: RNA extraction

RNA was isolated from the five *S.* sp. CNQ-525 samples using a RiboPure Bacteria kit (Ambion) according to the manufacturer's protocol. Cells were disrupted using Zirconia beads supplied with the kit. A phenol/chloroform extraction of the lysate yielded RNA, which was passed through a column with a silca filter. This filter bound the RNA, which was then eluted with 50 µl low ionic strength solution supplied with the kit. All extracted RNA was kept on ice until reverse-transcription PCR (RT-PCR) was performed. After RT-PCR, all samples were stored at -20 ^{o}C.

4.2.2.3: Reverse-transcription PCR

To remove trace amounts of gDNA from the samples, 5.5 µl of 10 x DNase buffer (Invitrogen) and 4 µl DNAaseI(2 U/µl) was added to each 50µl aliquot of extracted RNA. The reactions were incubated at 37 ^{o}C for five hours, and then 10 µl DNase inactivation reagent (Invitrogen) was added. The reaction was stored at room temperature for two minutes, flicked two times to mix, and centrifuged at 15,700 g for ten minutes at 4 ^{o}C (Eppendorf 5415 R centrifuge). The supernatant was transferred to a clean DNA-free microcentrifuge tube and a NanoDrop (NanoDrop Technologies) was used to measure the RNA concentration.

A SuperScript III First Strand Synthesis System for RT-PCR (Invitrogen) was used to synthesize first-strand complementary DNA (cDNA) from total RNA according to the manufacturer's protocol. The cDNA strand was created from 1 µg of extracted RNA using random hexamer primers and reverse transcriptase supplied with the kit. Specific primers that targeted regions genes within the *nap* biosynthetic cluster were designed by Frodowhitehead (Table 4.2) and PCR was used to amplify targeted regions of cDNA. In a 25 µl reaction, 2 µl of cDNA was mixed with 12.5 µl Taq 2X Master Mix (New England Biolabs), 1.25 µl DMSO, 0.5 µl forward primer (10 pmol/µl), 0.5 µl of reverse primer (10pmol/µl), and 8.25 µl Milli-Q water. PCR conditions were 95 ^{o}C for two minutes; 25 cycles of 96 ^{o}C for 45 seconds, 55 ^{o}C for 45 seconds and 72 ^{o}C for 45 seconds, followed by an extra five minutes at 72 ^{o}C. The entire 25 µl reaction was analyzed on a 0.8% agarose gel.

Table 4.2: Primers used to amplify sections of cDNA of target genes

Primer Name	Primer Sequence (5' to 3')	Target Gene	Tm (°C)
NapB1 Fwd	ACCGAGATGTTCAGGTGGTC	Type III PKS	64
NapB1 Rev	TCAAGGAGGTTCCATGAAGG	Type III PKS	64
NapH1 Fwd	TTCGTCGGAGTCGAAGTAGC	V-ClPO	64
NapH1 Rev	ACCACAAGACCAGGTTCGAC	V-ClPO	64
NapH2 Fwd	GACTGGTCGTACACCAACGA	$FADH_2$ Halogenase	64
NapH2 Rev	TGGAAGAACTCCTGGTACGC	$FADH_2$ Halogenase	64
NapH3 Fwd	CTTTACGCCATGTTCCAGGT	V-ClPO	64
NapH3 Rev	AGCCGGTGTAGTCCTCGTAG	V-ClPO	63
NapH4 Fwd	TACAAGCGCAAGTACGAAGC	V-ClPO	63
NapH4 Rev	TCGAACTCCCAGTTCAGGTC	V-ClPO	64
RT_RP_16SrRNA	GTCTCCCCTACCGAACTCTA	16S rRNA	54
RT_FP_16SrRNA	GACGGTACCTGCAGAAGA	16S rRNA	53

4.2.3: Cosmid library construction in SuperCos 1

4.2.3.1: Preparing the vector

The vector SuperCos 1 (Stratagene) was used for library construction and was transformed into DH5-α cells for amplification according to standard procedures.[6] To linearize the vector, 16 ug of SuperCos1 was digested with 1.5 µl XbaI (New England Biolabs, 20,000 U/ml) in a 100 µl reaction containing 10 µl of NEBuffer 2 (New England Biolabs), 1 µl BSA (New England Biolabs, 10 mg/ml) and 20.5 µl Milli-Q water and incubated at 37 ^{o}C for one hour. After the digest, 1 µl of calf intestinal phosphatase (Invitrogen, 1,000 U/ml) was added to the digest to de-phosphorylate the ends of the linearized cosmid and the reaction was incubated for an additional hour at 37 ^{o}C. A QIAGEN gel purification kit was

used according to manufacturer's procedures to change the buffer and salt concentrations of the reaction. The digest was split between two columns and the DNA was eluted off each column with 30 µl of EB buffer (Appendix Tabe 2A.3). A second digest with 4 µl of BamH1 (New England Biolabs, 20,000 U/ml), 2 µl bovine serum albumin (BSA) (New England Biolabs, 10 mg/ml), 20 µl of NEBuffer 2 (New England Biolabs), 114 µl of Milli-Q water, and 50 µl of the eluted de-phosphorylated DNA created the site for the *S.* sp. CNQ-525 genomic DNA insert. The reaction was incubated for one hour at 37 ^{o}C and the DNA was purified with a QIAGEN gel elution kit (QIAGEN) according to manufacturer's instructions. DNA was eluted off the column with 50 µl EB buffer (Appendix Figure 2A.3) and was cleaned by ethanol precipitation to remove any remaining salt (Section 2.2.3.1).

4.2.3.2: Preparing the genomic DNA insert

S. sp. CNQ-525's genomic DNA was isolated (Section 2.2.2.1) and partially digested with the restriction enzyme Sau3AI. A serial dilution of the enzyme was used to find optimal conditions required to digest the genomic DNA into fragments of ≥ 35 kilobases (kb), which is the desired size for the bacteria phage packaging reaction. In a 700 µl reaction, 39 µg of genomic DNA was incubated with 70 µl NEBbuffer 4 (New England Biolabs), 7 µl BSA (New England Biolabs, 10 mg/ml) and 473 µl Milli-Q water for an hour at room temperature. Microcentrifuge tubes were placed on ice, and 120 µl of the

genomic DNA mixture was added to tube one while 60 µl of the reaction was added to tubes 2–10. Using a cut-off pipet tip, a 4 µl aliquot of Sau3AI (New England Biolabs, 4,000 U/ml) was added to tube one, mixed, and a 60 µl aliquot was transferred to tube two. After mixing, a 60 µl aliquot was transferred to tube three and so on until tubes 1–9 contained Sau3AI. All reactions were incubated at 37 ^{o}C for one hour, heated to 70 ^{o}C for 15 mintues to inactivate the enzyme, and iced for ten minutes. DNA fragments between 35 and 40 kb were isolated by agarose gel electrophoresis (0.6 % agarose gel run at 100 V) and purified for ligation using a QIAEX II kit (QIAGEN) according to manufacturer's standards.

4.2.3.3: Ligating genomic DNA into SuperCos 1

A ligation reaction was carried out in a 20 µl reaction using ~100 ng of genomic DNA, 40 ng of doubly digested SuperCos 1, 1 µl T4 ligase (New England Biolabs, 400,000 U/ml), 2 µl T4 10X ligase buffer (New England Biolabs), and 5 µl Milli-Q water. Before adding the ligase, the mixture containing plasmid and genomic DNA was incubated at 50 ^{o}C for five mintues and then placed on ice for five mintues. Ligation was carried out overnight at 16 ^{o}C.

4.2.3.4: Packaging and titration

Packaging and titration reactions were performed using MaxPlax λ packaging extracts (Epicenter) and XL1-Blue MRF' supercompetent cells (Stratagene). On ice, 10 µl of the ligation reaction was added to 25 µl of a packaging extract and incubated for 90 minutes at 30 ^{o}C. Following the 90

minute incubation, 25 µl of the remaining packaging extract was added to the reaction and incubated for another 90 minutes at 30 ^{o}C. After the second 90 minute incubation, 500 µl of phage dilution buffer (Appendix Figure 2A.3) was added to the reaction and gently vortexed. A 25 µl aliquot of chloroform was added and the entire reaction was stored at 4 ^{o}C.

XL1-Blue MRF' cells were prepared according to the manufacturer's instructions. A 1:5 dilution of the packaging reaction was prepared with Milli-Q water and brought to a final volume of 50 µl with phage dilution buffer (Appendix Figure 2A.3). A 50 µl aliquot of the XL1-Blue MRF' cells (OD_{600} = 0.5) was added to the diluted packaging reaction and incubated at room temperature for 30 minutes. After 30 minutes, 200 µl of LB (Appendix Figure 2A.1) was added to the reaction. Incubation was carried out at 37 ^{o}C for an hour and the microcentrifuge tube was gently inverted every 15 minutes to mix the packaging reaction with the XL1-Blue MRF' cells. After the incubation, 300 µl of the reaction was plated on LB agar (Appendix Figure 2A.1) with kanamycin (50 µg/ml) and incubated overnight at 37 ^{o}C. To determine if the ligation of genomic DNA into SuperCos 1 was successful, 10 colonies were grown in 3 ml of LB with kanamycin (50 µg/ml) and grown overnight at 37 ^{o}C by constant shaking. The DNA was isolated according to section 2.2.2.2 and digested with PvuII in a 10 µl reaction containing 4 µl of DNA, 0.2 µl PvuII (10 U/µl, New England Biolabs), 1 µl NEBuffer 2 and 4.8 µl Milli-Q water. The digest was incubated at 37 ^{o}C for one hour and the entire digest was analyzed on a 0.8% agarose gel. When it was verified that the 10 cosmids contained genomic DNA inserts that gave different

banding patterns after digestion with PvuII, a 2,000 colony library was picked and incubated overnight at 37 ^{o}C in 96-welled plates containing 100 µl LB and kanamycin (50 µg/ml).

4.2.4: Designing nucleic acid probes for cosmid library screening

4.2.4.1: Vanadium-dependent chloroperoxidase *nap*H1

The pHIS8 vector transformed in DH5-α cells containing *nap*H1 (from Section 3.2.4.1) was used as a source for the probe. A double digest containing NcoI and NotI was used to excise *nap*H1 from the vector. In a 50 µl reaction, 20 µl of DNA (300 ng/µl) was mixed with 1.5 µl NcoI (10 U/µl, New England Biolabs), 1.5 µl NotI (10 U/µl, New England Biolabs), 5 µl NEBuffer 3, 0.5 µl BSA (New England Biolabs, 10 mg/ml), and 21.5 µl Milli-Q water and incubated at 37 ^{o}C for two hours. The entire digest was run on a 0.8% agarose gel, and the fragment was excised out of the gel and eluted using a QIAGEN gel extraction kit (QIAGEN) according to manufacturer's instructions. Eluted DNA was cleaned by ethanol precipitation (section 2.2.3.1), resuspended in 15 µl Milli-Q water and stored at -20 ^{o}C.

4.2.5: Screening the cosmid library

The 2,000 cosmid library was screened using the *nap*H1 gene from the napyradiomycin biosynthetic cluster. A DIG High Prime DNA Labeling and

Detection Starter Kit (Roche Applied Science) was used for the labeling and detection of positive cosmid clones by an enzyme immunoassay according to the manufacturer's instructions. *nap*H1 was labeled with digoxigenin-dUTP and hybridized to DNA, which was bound to a positively charged nylon membrane (see Sections 2.2.5 and 2.2.6). The membrane was first incubated with anti-digoxigenin-alkaline phosphatase conjugate and then incubated with a solution containing nitroblue tetrazolium chloride and 5-bromo-4-chloro-3-indolyl-phosphate, which is a substrate for alkaline phosphatase. Cleavage of the phosphate group results in a blue color, which can be visualized on the nylon membrane.

4.2.6: Partially sequencing cosmid clone scJW7F6

After screening the library with the *nap*H1 probe, three cosmid clones were sent off for end sequencing using the T7 and T3 promoter sites on the vector (Table 4.3). A BLASTP analysis[7] was conducted on the sequence data and cosmid clone scJW7F6's sequencing results showed homology to the efflux protein NapR6 from the *nap* biosynthetic cluster. scJW7F6 was digested with BamH1 in 40 µl reaction containing 20 µl DNA (200 ng/µl), 2 µl BamH1 (20 U/µl, New England Biolabs), 4 µl NEBuffer 2, 0.4 µl BSA (New England Biolabs, 10 mg/ml) and 13.6 µl Milli-Q water. The reaction was incubated for an hour at 37 ^{o}C and analyzed on a 0.8% agarose gel. Two bands were excised from the gel (~6.5 and 3.0 kb) and DNA was eluted using a QIAGEN gel extraction kit

(QIAGEN) according to manufacturer's instructions. All four fragments were cloned into the pGEM-3Z easy clone vector (Promega) according to manufacturer's instructions and sequenced using the T7 promoter and SP6 promoter sites on the vector (Table 4.3).

Table 4.3: Primer sequences used to analyze subcloned fragments from cosmid clone pJW6F11

Primer Name	Primer Sequence (5' to 3')
T7 Promoter	GTA ATA CGA CTC ACT ATA GGG
T3 Promoter	ATT AAC CCT CAC TAA AGG
SP6 promoter	ATTTAGGTGACACTATAGAA

4.2.7: Antibiotic sensitivity tests

To choose a suitable resistance marker for mutagenesis experiments, antibiotic sensitivity tests with *S.* sp. CNQ-525 were conducted. A 50 ml seed culture of *S.* sp. CNQ-525 was grown in A1 growth media (Appendix Figure 2A.1) as mentioned in Section 4.2.1. After nine days, 100 µl aliquots from the seed culture were streaked on 25 ml A1 agar (Table 4A.1) containing either apramycin (50 µg/ml, 100 µg/ml, 150 µg/ml, 200 µg/ml, 250 µg/ml, or 300 µg/ml), kanamycin (100 µg/ml, 150 µg/ml, 200 µg/ml, 300 µg/ml, 400 µg/ml, 500 µg/ml, or 600 µg/ml), or nalidixic acid (25 µg/ml, 50 µg/ml, 75 µg/ml, 100 µg/ml, 150 µg/ml, or 200 µg/ml). All plates were replica streaked and incubated for one month at 30 ^{o}C.

4.2.8: PCR targeted mutagenesis

Inactivation of *nap*H1, *nap*H2, *nap*H3, and *nap*H4 was attempted using the PCR targeting system.[8] Within cosmid scJW7F6 (SuperCos 1-based) containing the napyradiomycin biosynthetic cluster, *nap*H1, *nap*H2, *nap*H3, and *nap*H4 were independently replaced by an *aac(3)IV*/*oriT* cassette. PCR was used to generate the eight independent *aac(3)IV*/*oriT* cassettes using the primer pairs in Table 4.4.

Cosmid clone scJW7F6 was transformed into the *E. coli* strain BW25113/pIJ790 according to standard procedures[6, 8] and each gene was independently disrupted with its corresponding *aac(3)IV*/*oriT* cassette. PCR analysis was used to confirm the correct genotype in BW25113/pIJ790 using the primers in Table 4.5. A restriction digest was also implemented to confirm the correct geneotype of *nap*H1, *nap*H2, *nap*H3 and *nap*H4 gene distruptions. In a 20 µl reaction, 10 µl of DNA from the verification PCR reaction was digested with 1 µl XbaI (20 U/ml, New England Biolabs), 2 µl NEBuffer 2, 0.2 µl BSA (10 mg/ml, New England Biolabs), and 6.8 µl Milli-Q water. The reaction was incubated at 37 ^{o}C for two hours and analyzed on a 0.8% agarose gel.

Table 4.4: PCR primers used to generate the *aac(3)IV*/*oriT* cassettes for gene replacements

Primer Name	Primer Sequence (5' to 3')	Target Gene	Tm (°C)
napH1m Fwd	ACCGCGGAGCCCCCTCCTTAGAAAG GAACACGCGCATGATTCCGGGGATC CGTCGACC	V-ClPO	82
napH1m Rev	CGCTCCCCGGCTGTTTCCCGGGACC GGGGACGAGGATCATGTAGGCTGG AGCTGCTTC	V-ClPO	84
napH2m Fwd	GCGTGGTGCGGCCGCATCGGAACT GGAAGGTCCTATATGATTCCGGGGA TCCGTCGACC	$FADH_2$ halogenase	82
napH2m Rev	CCTGTGTCCTGCGGTGCGCCGGCC GGCGCCCGTGCCTCATGTAGGCTG GAGCTGCTTC	$FADH_2$ halogenase	86
napH3m Fwd	ACCACGCACGGTGGCGGAGGTTAC CCGCCGGCGGATGCGATTCCGGGG ATCCGTCGACC	V-ClPO	81
napH3m Rev	CGGTGCCGGCGTCGGCATCGTGGC AGGGAAGACGGTCATGTAGGCTGGA GCTGCTTC	V-ClPO	84
napH4m Fwd	CCAAGCCCCTCCCTGCTGAGAATAA GGAAGACGATCATGATTGGCGGGAT CCGTCGACC	V-ClPO	80
napH4m Rev	TCAAAAGGCCCCCTTCTGCTGCTTC GGGCAGGGCCGTCATGTAGGCTGG AGCTGCTTC	V-ClPO	82

Underlined letters in the primer sequence represents 39-nucleotide extensions with sequence identity to upstream and downstream regions of the targeted gene that will attach to the *aac(3)IV*/*oriT* cassette.

Table 4.5: Primers used to confirm gene replacement in cosmid clone scJW7F6.

Primer Name	Primer Sequence (5' to 3')	Target Gene	Tm (°C)
napH1 ver Fwd	CCCGCTCTTATGGAAGCG	V-ClPO	62
napH1 ver Rev	GGCACGGCGAAGGGCAGG	V-ClPO	75
napH2 ver II rev	CCTGTGTCCTGCGGTGCGCC	$FADH_2$ halogenase	71
napH2 ver Fwd	CGCCGCACGGTCCCGGTGGA	$FADH_2$ halogenase	73
napH3 ver Rev	GGGAGGGGCTTGGAGGAGAA	V-ClPO	67
napH3 ver Fwd	GTTCCTGCGGGCCACGCCGC	V-ClPO	73
napH4 ver Fwd	GACGCCGGCACCGCGACCCG	V-ClPO	75
napH4 ver Rev	CCCTGGCGGTGCCGGACCGT	V-ClPO	73

Mutated scJW7F6 cosmids were transformed into the *E. coli* strains S17-1 and ET12567 carrying the non-transmissible pUZ8002 plasmid according to standard procedures.[8] Introduction of cosmid DNA into wild-type *S.* sp. CNQ-525 was attempted by conjugation. Exoconjugants resistant to apramycin and sensitive to kanamycin were grown in 5 ml A1 growth media (Appendix Figure 2A.1) containing 250 µg/ml apramycin at 30 ^{o}C for 7–10 days with shaking at 250 revolutions/min. gDNA was extracted according to Section 2.2.2.1 and PCR using the primers from Table 4.5 was used to analyze the genotypes.

4.2.9: Single-crossover inactivation experiments

4.2.9.1: Vector preparation

The non-replicating E. coli plasmid pKC1132, which is a derivative of pOJ260,[9] was used as the vector for insertional inactivation of genes within the napyradiomycin biosynthetic cluster. The vector was transformed into DH5-α cells for amplification according to standard procedures.[6] To create the ligation site for the internal DNA fragments of *nap*H1, *nap*H2, or *nap*H4, 6 µg of pKC1132 was doubly digested with 2.5 µl of EcoR1 (New England Biolabs, 20 U/µl) and 2.5 µl HindIII (New England Biolabs, 20 U/µl) in a 50 µl reaction containing 5 µl of EcoR1 Buffer (New England Biolabs) and 10 µl of Milli-Q water. The reaction was incubated for one hour at 37 ^{o}C and the DNA was purified with a QIAGEN gel elution kit (QIAGEN) according to manufacturer's instructions. DNA was eluted off the column with 50 µl EB buffer and stored at –20 ^{o}C.

4.2.9.2: Construction and ligation of the DNA insert

A 1 kb internal fragment of *nap*H1, a 900 bp internal fragment of *nap*H2, and a 1 kb internal fragment of *nap*H4 were amplified by PCR using the primers listed in Table 4.6. All forward primers were designed to contain a HindIII site, whereas all reverse primers were designed to contain an EcoR1 restriction site. All primers were diluted with Milli-Q water to a final concentration of 20 µM. For a 50 µl PCR reaction, 1µl of gDNA (23 ng/µl) from wild-type *S.* sp. CNQ-525 was mixed with 0.5 µl pfu turbo (2.5 U/µl, Stratagene), 5 µl pfu 10 X buffer, 1 µl forward primer (10 pmol/µl), 1 µl of reverse primer (10pmol/µl), 2.5 µl DMSO, 1 µl dNTPs (10 mM), and 38 µl Milli-Q water. PCR conditions were 95 ^{o}C for five minutes; 25 cycles of 95 ^{o}C for 45 seconds, 55 ^{o}C for 45 seconds and 72 ^{o}C for 90 seconds, followed by an extra ten minutes at 72 ^{o}C.

Table 4.6: Primers used to amplify internal fragments for insertional inactivation of genes.

Primer Name	Primer Sequence (5' to 3')	Target Gene	Tm (^{o}C)
napH1 single X over Fwd	GGCGAAGCTTTGTGGCTCGCGGCGT	V-ClPO	83
napH1 single X over Rev	GGCGGAATTCCACAGGCTGGTGGAG	V-ClPO	79
napH2 single X over Fwd	GGCGAAGCTTGAACTCGGGCTGAAG	$FADH_2$ halogenase	76
napH2 single X over Rev	GGCGGAATTCGTAGAACCCCTCCAC	$FADH_2$ halogenase	75
napH4 single X over Fwd	GGCGAAGCTTTGTTCGACGCGCTGG	V-ClPO	81
napH4 single X over Rev	GGCGGAATTCCGGTGGTAGAGCCCG	V-ClPO	80

Underlined letters indicates restriction sites.

A 2 µl aliquot of the PCR reaction was analyzed on a 0.8% agarose gel,and the PCR reaction was desalted using a QIAGEN gel purification kit according to manufacturer's instructions. DNA was eluted off the column with 20 µl of EB buffer (Appendix Tabe 2A.3) and 15 µl of DNA was doubly digested with 1 µl of HindIII (New England Biolabs, 20 U/µl) and 1 µl EcoR1 (New England Biolabs, 20 U/µl) in a 25 µl reaction containing 2.5 µl of EcoR1 Buffer (New England Biolabs), and 5.5 µl of Milli-Q water. The reaction was incubated for two hours at 37 ^{o}C and the DNA was purified with a QIAGEN gel elution kit according to manufacturer's instructions. DNA was eluted off the column with 10 µl EB buffer. Doubly digested DNA was ligated into a HindIII/EcoR1 digested pKC1132 in a 10 µl reaction containing 1 µl vector, 3–5 µl DNA (5 ng/µl), 1µl 10X ligation buffer, 0.5 µl T4 DNA ligase (400,000 U/ml, New England Biolabs), and 2.5–4.5 µl Milli-Q water. The ligation reaction was incubated overnight at 16 ^{o}C. A 2 µl aliquot of the ligation reaction was transformed into DH5-α cells (Invitrogen) according to manufacturer's instructions. A 50 µl aliquot and 100 µl aliquot was plated on LB agar (Appendix Figure 2A.1) containing apraymycin (50 µg/ml) and incubated overnight at 37 ^{o}C. Colonies were picked and grown overnight by constant shaking at 37 ^{o}C in 5 ml LB containing apramycin (50 µg/ml). Plasmid DNA was extracted according to section 2.2.2.2, eluted off the QIAGEN column with 40 µl EB buffer, and sequenced using the M13 forward site on the vector (5'-TGTAAAACGACGGCCAGT-3').

4.2.9.3: Introduction of "suicide vectors" into wild-type *S.* sp. CNQ-525

pKC1132 vectors containing internal fragments of *nap*H1, *nap*H2, or *nap*H4 were introduced into wild-type *S.* sp. CNQ-525 by conjugation from the *E. coli* strain ET12567, which carries the driver plasmid pUZ8002. Electrocompetent ET12567/pUZ8002 cells were prepared as described by Gust et al.,[8] and the pKC1132 vectors containing DNA inserts were introduced into the electrocompetents cells according to standard procedures.[6] For each conjugation reaction, a 500 µl aliquot from a 50 ml culture of *S.* sp. CNQ-525, which was shaken at 30 ^{o}C for four days in A1 growth media (Appendix 2A.1) , was centrifuged at 5,000 rpm for five minutes at room temperature. The samples were decanted and resuspended in 500 µl of fresh A1 growth media. A 500 µl suspension of *E. coli* ET12567/pUZ8002 carrying the pKC1132 vectors with gene fragments was mixed with the 500 µl mycelium extract of *S.* sp. CNQ-525. Immediately after mixing, 50–200 µl aliquots were plated on A1 agar (Appendix Table 4A.1). After incubating at 30 ^{o}C for 18 hours, the plates were overlaid with 1 ml water containing 2 mg nalidixic acid and 6.25 mg apramycin and incubated for an additional 5–8 days at 30 ^{o}C.

4.2.9.4: Inactivation of *nap*H1 in *S.* sp. CNQ-525

Exoconjugates resistant to apramycin were grown in 5 ml A1 growth media (Appendix Figure 2A.1) with 250 µg/ml apramycin at 30 ^{o}C for 7–10 days with shaking at 250 revolutions/min. gDNA was extracted according to Section 2.2.2.1 and digested with BamH1. In a 25 µl reaction, 1 µg of gDNA was mixed

with 2 µl BamH1 (New England Biolabs, 20,000 U/ml), 0.25 µl BSA (New England Biolabs, 10 mg/ml), 2.5 µl of NEBuffer 2 (New England Biolabs), Milli-Q water. After incubating at 37 ^{o}C for 18 hours, a 15 µl aliquot of the digest was analyzed on a 0.8% agarose gel. Digested gDNA was transferred to a positively charged nylon membrane (see Section 2.2.6) and Southern hybridization using NapH1 as the probe (see Section 4.2.4) was used to characterize the genotype of *S.* sp. CNQ-525/*nap*H1^{-}.

4.2.10: HPLC analysis of *S.* sp. CNQ-525/*nap*H1^{-}

For analysis of chlorinated dihydroquinones, *S.* sp. CNQ-525/*nap*H1^{-} was grown in 50 ml A1 growth media (Appendix Figure 2A.1) containing apramycin (250 µg/ml) and cultured as described in Section 4.2.1. Cultures were extracted with ethyl acetate, dried over anhydrous $MgSO_4$ and concentrated *in vacuo*. Crude extracts were analyzed in positive and negative mode on a Hewlett Packard 1100 series high performance liquid chromatography system linked to an Agilent ESI-1100 MSD mass spectrometer (gas flow set to 13 ml/min, drying temperature set to 350 ^{o}C, capillary voltage set to 4500 V, and nebulizing pressure set to 40 pounds/square inch).

4.2.11: Chemical complementation of *S.* sp. CNQ-525/*nap*H1^{-}

[9-^{13}C]SF2415A3 was biosynthetically prepared from a fermentation of *S.* sp. CNQ-525 supplemented with 100 mg L-[methyl-^{13}C]methionine and purified as described in section 1.2.8. Feeding studies with [9-^{13}C]SF2415A3 were carried out in 50 ml A1 growth media (Appendix Figure 2A.1) in 250 ml Erlenmeyer flasks at 30 ^{o}C at 200 rpm for 15 days. At days 3, 5, 7, and 10, 1 mg of [9-^{13}C]SF2415A3 dissolved in 200 µl of DMSO was administered to the 50 ml culture of *S.* sp. CNQ-525/*nap*H1^{-}. For analysis of secondary metabolites, the culture was extracted and analyzed as described in Section 4.2.9.

4.3: Results and Discussion

4.3.1: Phylogenetic analysis

Phylogenetic analysis of V-BrPOs, V-ClPOs, and bacterial non-specific acid phosphatases shows that the enzymes form clades based on proposed enzymatic function (Figure 3.5). However, the three putative V-ClPOs from the bacterium *Streptomyces* sp. CNQ-525 do not cluster with the fungal or other postulated bacterial-derived V-ClPOs, which is consistent with their proposed role in natural product biosynthesis. In contrast to the known fungal V-ClPOs whose biological function is to produce hypohalous acids as antimicrobial agents, the V-ClPOs from the *nap* biosynthetic cluster appear to be responsible for the novel regio- and stereospecific chlorination chemistry associated with meroterpenoid biosynthesis.

4.3.2: Transcription analysis of the halogenating enzymes from the *nap* cluster

Semiquantitative RT-PCR analysis was used to analyze the transcription levels of the V-ClPOs *nap*H1, *nap*H3, and *nap*H4; the $FADH_2$-dependent halogenase *nap*H2; the type III PKS THNS *nap*B1 and the 16S rRNA housekeeping gene from *S.* sp. CNQ-525. The 16S housekeeping gene was used in the study as a positive control because the gene is transcribed at a relatively constant level during cell growth. Analysis of the type III PKS THNS

*nap*B1 gene was used for comparative purposes to the putative halogenating genes, *nap*H1–*nap*H4, because it is known that the enzyme is responsible for the biosynthesis of the naphthoquinone core of the chlorinated dihydroquinones. RNA concentrations were also analyzed over the ten day period and compared to transcription levels of the targeted genes. It was observed that the RNA concentrations increased significantly between 24 hours and the day three time point, peaked at day three, and dropped-off during days 5–10 (Table 4.7). Coincidentally, the genes proposed to be involved with the biosynthesis of the chlorinated dihydroquinones (*nap*B1, *nap*H1, *nap*H2, *nap*H3, and *nap*H4) are first transcribed on day three and remain transcribed through day five before they all disappear at day seven (Figure 4.3). Interestingly, these results coincide with the natural product chemistry associated with *S.* sp. CNQ-525 in which the chlorinated dihydroquinones are first detected in culture at day three and peak at days 5–7.

Table 4.7: RNA concentrations from *S.* sp. CNQ-525.

Sample	ng/µl	A_{260}	A_{280}	A_{260}/A_{280}
24 hours	88	1.76	0.86	2.04
3 Days	263	5.25	2.50	2.10
5 Days	194	3.88	1.85	2.10
7 Days	52	1.05	0.54	1.95
10 Days	70	1.40	0.69	2.02

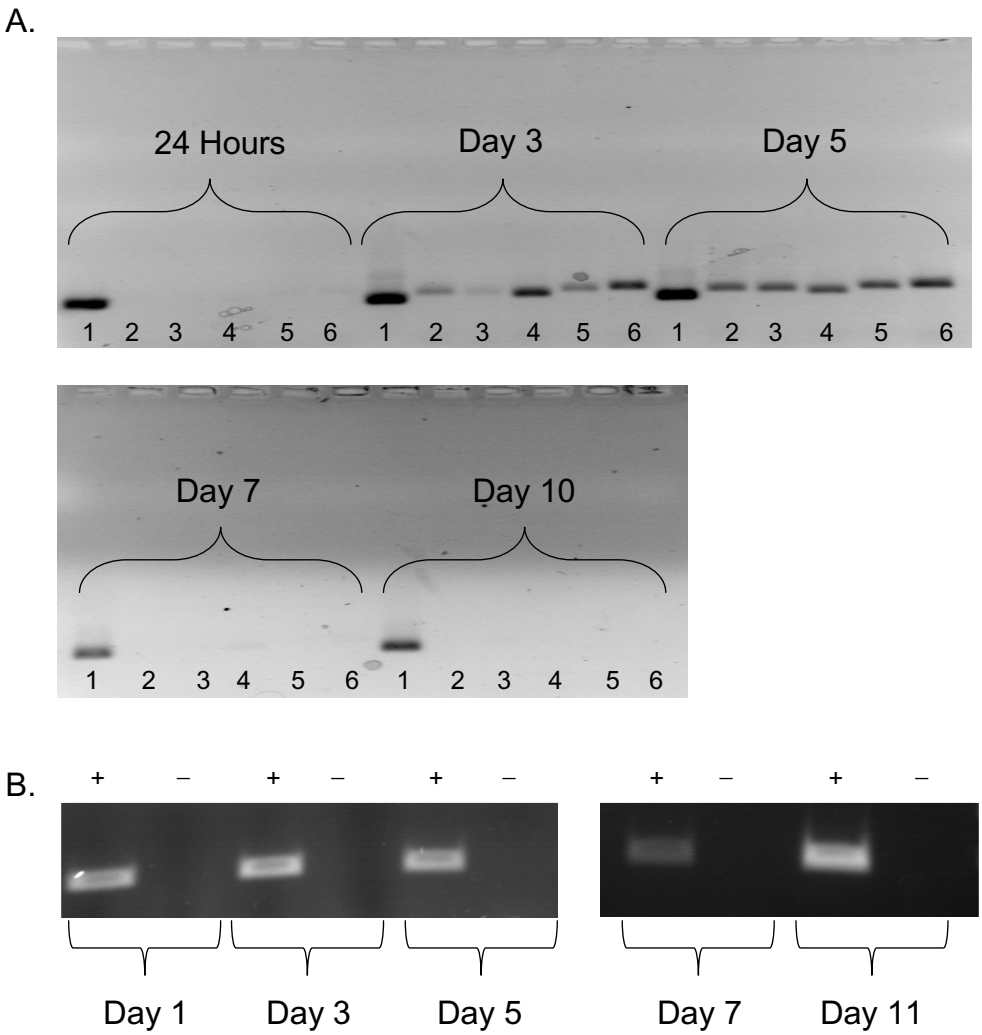

Figure 4.3: Transcription analysis of *nap*H1, *nap*H2, *nap*H3, *nap*H4, *nap*B1 and the 16S housekeeping gene from *S.* sp. CNQ-525. A) Analysis of PCR amplification from cDNA by agarose gel electrophoresis. 1= 16S transcript, 2 = *nap*B1 transcript, 3 = *nap*H1 transcript, 4 = *nap*H2 transcript, 5 = *nap*H3 transcript, 6 = *nap*H4 transcript. B) Analysis of gDNA contamination in the RNA fractions by agarose gel electrophoresis. "+" indicates the RNA extract spiked with *S.* sp. CNQ-525 gDNA and "-" indicates the RNA extract used to prepare cDNA without contaminating DNA.

4.3.3: PCR-based mutagenesis

Based on preliminary data, it is proposed that the three *nap* V-ClPOs catalyze the oxidative cyclization and halogenation of terpenoid units. A PCR-based mutagenesis technique was implemented to elucidate the role each enzyme has in the production of the chlorinated dihydroquinones. The classical approach to inactive a gene in a *Streptomyces* sp. involves a single or double homologous recombination crossover event using a suicide vector.[10] These procedures are very time consuming, and are not ideal for multiple gene inactivation experiments. The PCR-mutagenesis approach is very quick and allows for immediate screening of mutants by PCR.

The strategy for PCR-targeting for mutagenesis of actinomycetes is to replace a chromosomal sequence within a library clone by a selectable marker that has been generated by PCR using primers with 39 nt homology extensions (Figure 4.4).[8] Recombination of these short homologous sequences with the cosmid DNA contained in *E. coli* is promoted by the λ Red functions (*gam, bet, exo*). *Gam* inhibits *E. coli* exonucleases, which would otherwise degrade linear DNA, while *bet* and *exo* promote recombination. The inclusion of *oriT* in the disruption cassette allows conjugation to be used to introduce the targeted cosmid DNA into *S.* sp. CNQ-525. Once in the actinomycete, the vector used for the library construction does not replicate autonomously, but the long regions of sequence identity in the inserts promote efficient integration by homologous recombination, thus creating gene replacements. Unfortunately, the original cosmid clone library, from which the *nap* biosynthetic cluster was identified, was

constructed in the shuttle vector pOJ446. This shuttle vector is not compatible with the PCR-based mutageneis technique, so a new comid clone library was constructed using the vector SuperCos 1 (Stratagene).

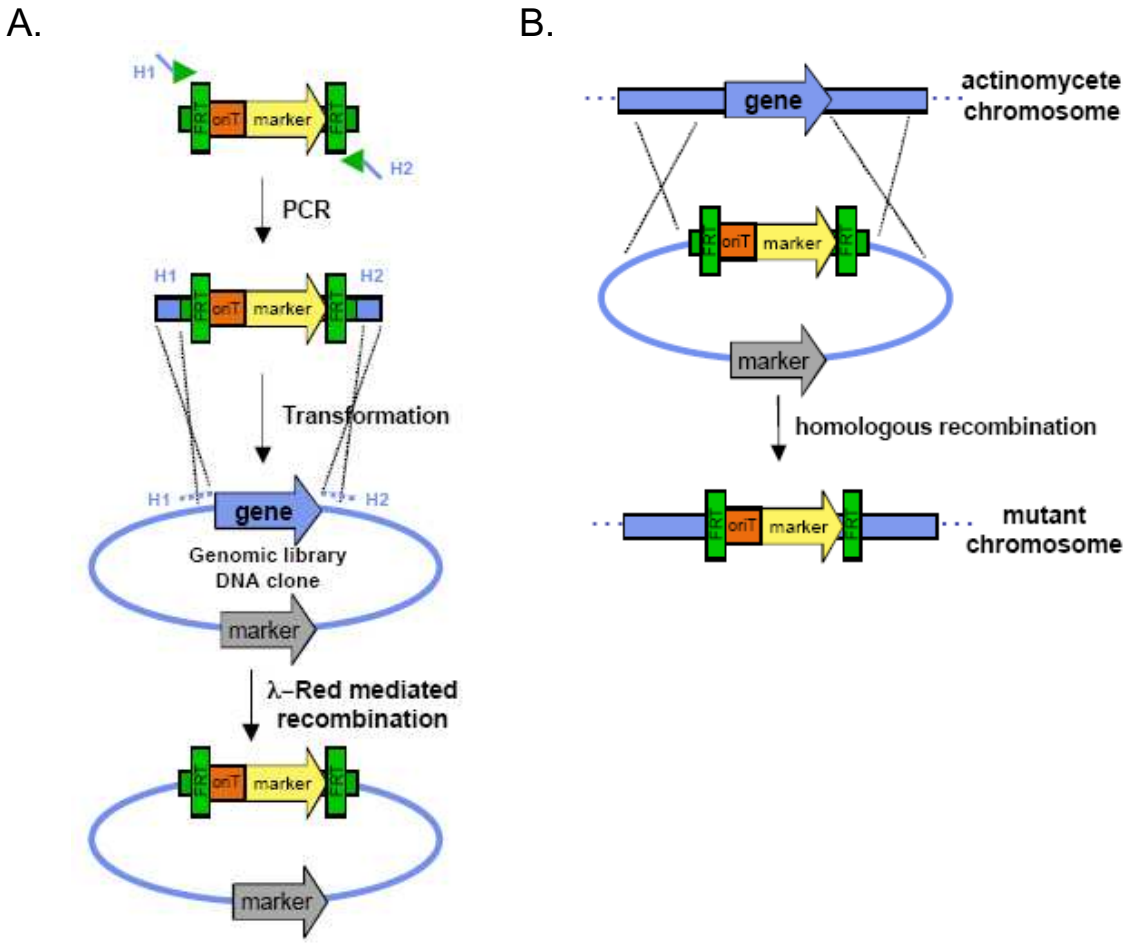

Figure 4.4: PCR-targeting strategy. A) amplification of a resistance cassette using primers containing 39-nt 5' homology extensions (H1 and H2) corresponding to regions flanking the target gene. The PCR product is transformed into a λ-Red expressing *E. coli* strain that contains the targeted gene in a genomic library DNA clone. Potential transformants are selected based on antibiotic resistance and are confirmed by PCR and restriction analysis. B) The targeted DNA clone can be introduced into an actinomycetes by conjugation from *E. coli* using the *oriT* in the cassette.

4.3.3.1: Selecting a cosmid clone for PCR-based mutagenesis experiments

Based on the equation N = (CG)/L, where N = the number of colonies, C = the desired coverage, G = the size of the genome and L = length of gDNA insert, a 2,000 colony library was selected to ensure at least a 5–10X coverage of *S.* sp. CNQ-525's ~8 Mb genome. Screening the library with the V-ClPO *nap*H1 as a heterologous probe yielded three colonies that were sent out for end squencing. Analysis of cosmid clone scJW7F6's sequencing results showed homology to the efflux protein NapR6 from the *nap* biosynthetic cluster. The two gene fragments from scJW7F6 (6.5 and 3.0 kb) were subcloned and end sequenced. Sequence data from one end of the 6.5 kb fragment was homologous to the phosphomevalonate kinase NapT4, while the other end produced data that was homologous to the type III PKS THNS NapB1. End sequencing of the 3.0 kb fragment showed homology to the transporter NapR4 and the efflux protein NapR5. Based on the sequencing results, it was predicted that the gDNA insert in cosmid clone scJW7F6 contained most of the genes for the *nap* biosynthetic cluster (*nap*T1 through *nap*R6) (Figure 4.5).

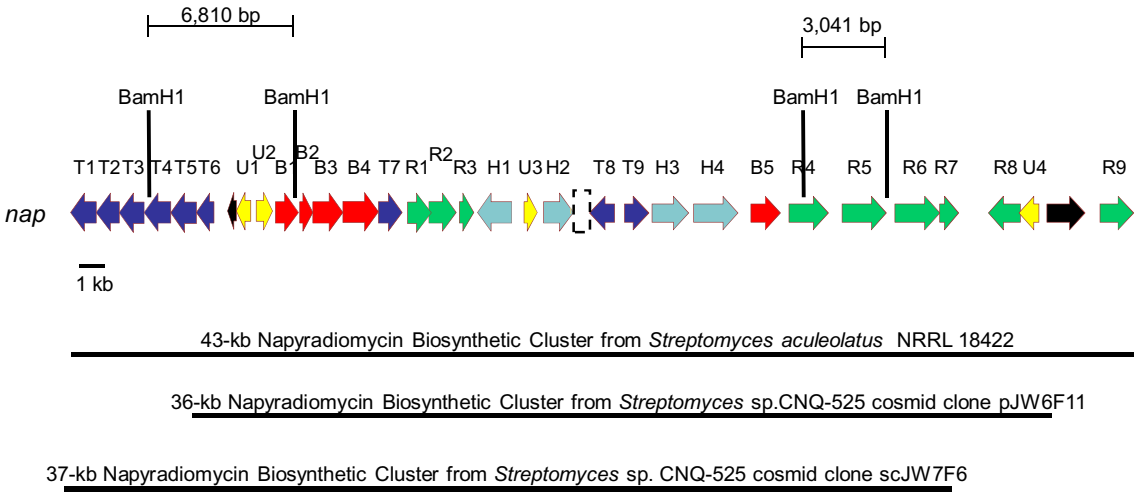

Figure 4.5: The size of the napyradiomycin biosynthetic gene cluster identified in *S. aculeolatus* NRRL 18422, *S.* sp. CNQ-525 cosmid clone pJW6F11 and *S.* sp. CNQ-525 cosmid clone scJW7F6. BamH1 sites and the size of the fragments subcloned and end sequenced from cosmid clone scJW7F6 are shown.

4.3.3.2: Attempts to inactivate the *nap* halogenating enzymes by PCR-based mutagenesis

Inactivation of *nap*H1, *nap*H2, *nap*H3 and *nap*H4 was attempted using the PCR-targeting system (Figure 4.6).[8] The *aac(3)IV* apramycin resistance cassette from pIJ773 was PCR amplified using the primers from Table 4.4. After amplification, each extended cassette was independently introduced into the λ-Red expressing *E. coli* BW25113/pIJ790 containing cosmid clone scJW7F6, which harbored the *nap* biosynthetic cluster. After gene replacements with the extended *aac(3)IV* resistance cassette was confirmed by PCR and restriction analysis, each mutant cosmid was introduced into *S.* sp. CNQ-525 by conjugation from *E. coli* ET12567/pUZ8002. Exoconjugants exhibiting apramycin

resistance were analyzed by PCR, restriction digest and Southern blot analysis, but all “mutants” were confirmed by genotype to be wild-type.

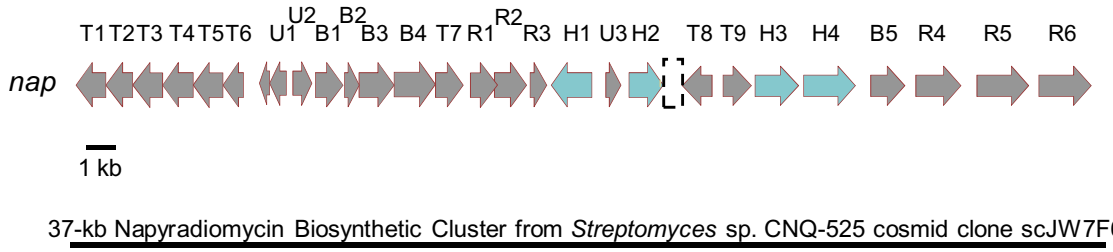

Figure 4.6: Napyradiomycin biosynthetic cluster in cosmid clone scJW7F6 and the genes targeted for inactivation by PCR-based mutagenesis. *nap*H1 = V-ClPO, *nap*H2 = $FADH_2$-dependent halogenase, *nap*H3 = V-ClPO, and *nap*H4 = V-ClPO.

Typically, over 10% of the transformants harboring apramycin resistance undergo double crossover events and the desired gene replacement in the actinomycetes can be obtained directly after conjugation. Unfortunately, after screening >100 exoconjugants for each of the targeted gene inactivations by PCR, restriction digest and/or Southern hybridization, no single crossover or double crossover events were detected in any of the transformants harboring apramycin resistance. Therefore, a more classical homologous deletion technique using a suicide vector was implemented to inactive the halogenating genes from the *nap* biosynthetic cluster.

4.3.4: Single crossover inactivation experiment

*nap*H1, *nap*H2 and *nap*H4 were target for inactivation by homologous recombination via a single cross-over (Figure 4.7). With this approach, an

internal DNA fragment of a target gene is cloned into a vector which can be integrated into the chromosome by a single homologous crossover event resulting in an integrated copy of the vector and two disrupted copies of the target gene; one copy will be truncated at the 3' end and the other at the 5' end (Figure 4.8).[10] When selecting genes to inactivate, it is necessary to analyze the location and orientation of the target gene to other genes within the cluster. As a result, polar effects on the expression of genes downstream of the targeted gene, which are co-transcribed with it, can occur with disruption of the target gene. Therefore, the resulting phenotype of the disruption may not be directly attributed to loss of function of the target gene. In the napyradiomycin biosynthetic cluster, *nap*H1, *nap*H2, and *nap*H4 were selected for gene disruption because all three genes are on the ends of transcripts and are believed to have no polar effects on downstream genes (Figure 4.7). Unfortunately, the *nap*H3 gene that codes for a V-ClPO is on the same transcript as *nap*H4 and disruption of this gene would give rise to undesired effects.

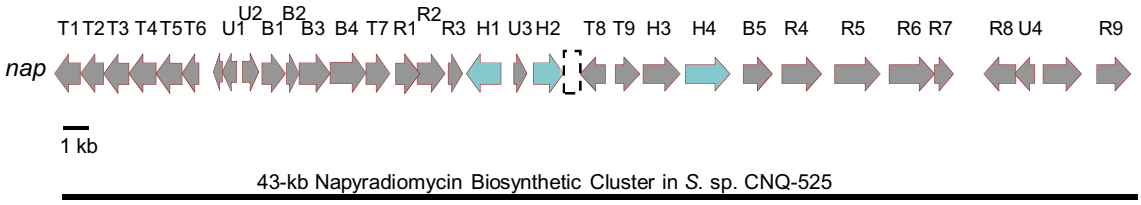

Figure 4.7: Organization of the napyradiomycin biosynthetic cluster in *S.* sp. CNQ-525 and the genes targeted for inactivation by homologous recombination via a single cross-over. *nap*H1 = V-ClPO, *nap*H2 = $FADH_2$- dependent halogenase, *nap*H3 = V-ClPO, and *nap*H4 = V-ClPO.

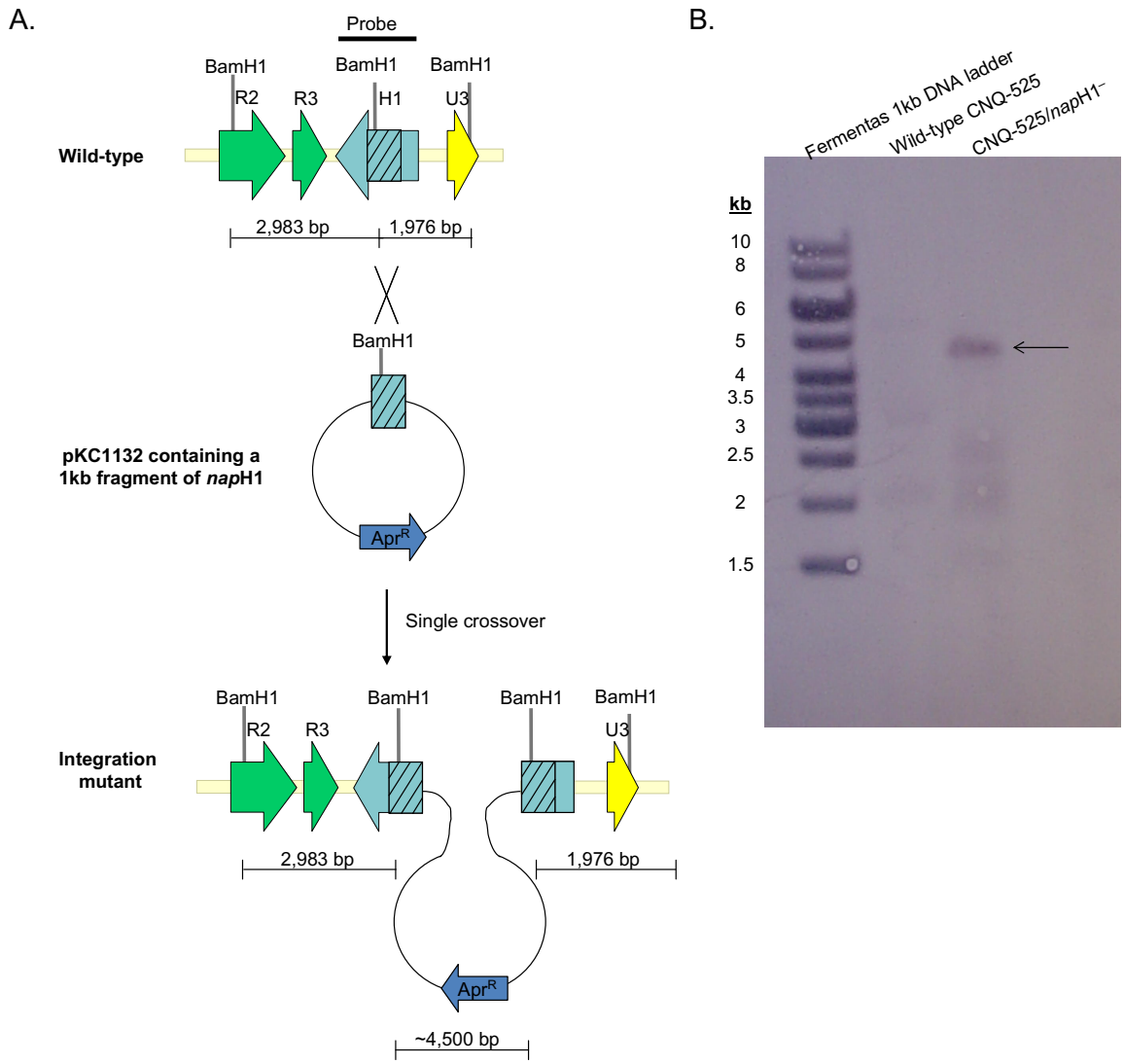

Figure 4.8: Inactivation of a gene by homologous recombination through a single cross-over event. A) Inactivation of the *nap*H1 gene in *S.* sp. CNQ-525. B) Southern blot analysis of BamH1 digested gDNA from the wild-type *S.* sp. CNQ-525 and gDNA from the *nap*H1^{-} mutant using the entire *nap*H1 gene as a probe. The arrow points the 4.5 kb DNA fragment in the mutant that is attributed to the integration of the suicide vector into *S.* sp. CNQ-525's chromosome.

4.3.4.1: Inactivation of *nap*H1 and chemical complementation of the mutant

Out of the targeted genes, only *nap*H1 was inactivated by homologous recombination through a single cross-over event after introducing the pKC1132 vector containing an internal 1 kb fragment of *nap*H1 into *S.* sp. CNQ-525 by conjugation from *E. coli* ET12567/pUZ8002. The gene inactivation was confirmed by Southern blot analysis using the entire *nap*H1 gene as a heterologous probe (Figure 4.8). Inactivation of *nap*H1 led to the total abolishment of chlorinated dihydroquinone production in *S.* sp. CNQ-525 (Figure 4.9). [9-^{13}C]SF2415A3 was biosynthetically prepared from L-methyl-^{13}C]methionine and administered to the *nap*H1^{-} mutant. Production of the chlorinated dihydroquinones along with the diazonaphthoquinone A80915D were analyzed by HPLC-MS (Figure 4.10).

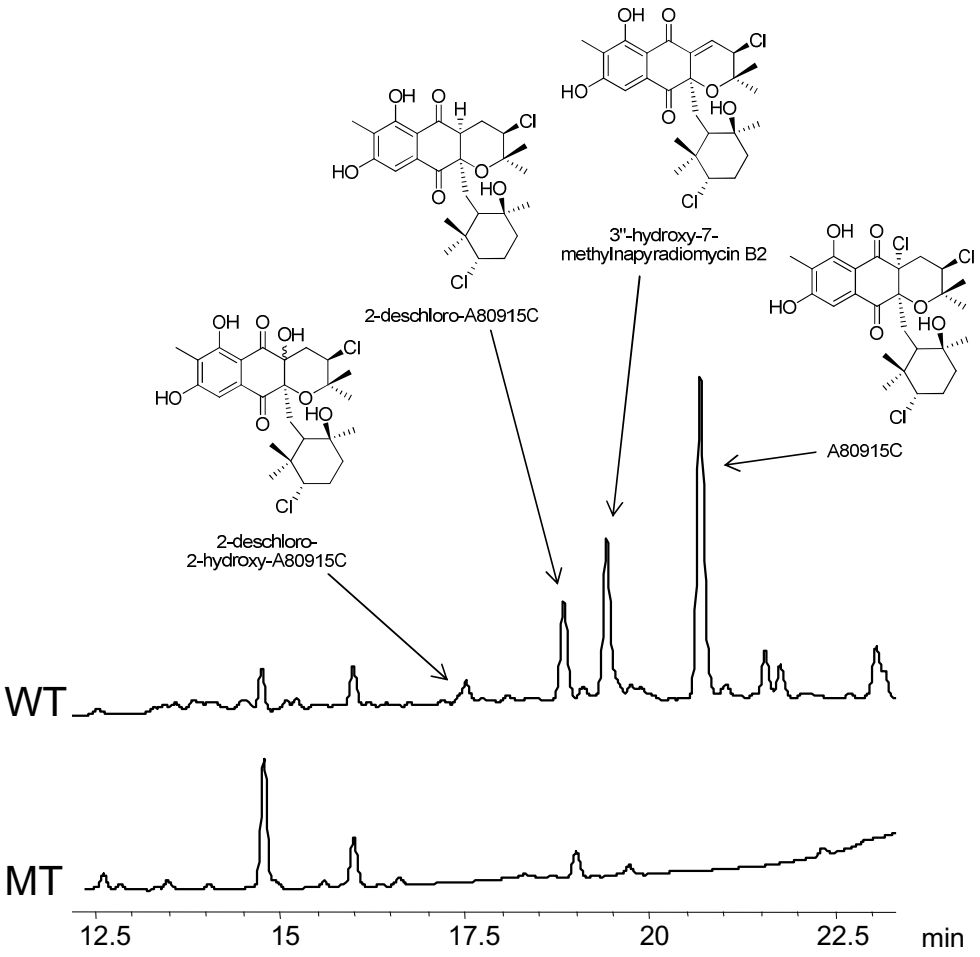

Figure 4.9: Inactivation of the V-ClPO gene *nap*H1 abolishes napyradiomycin production. LC-MS chromatogram of the culture extract showing the napyradiomycin fraction of the *nap*H1^{-} mutant (MT) and *S.* sp. CNQ-525 wild-type (WT). UV detection was carried out at 210 nm.

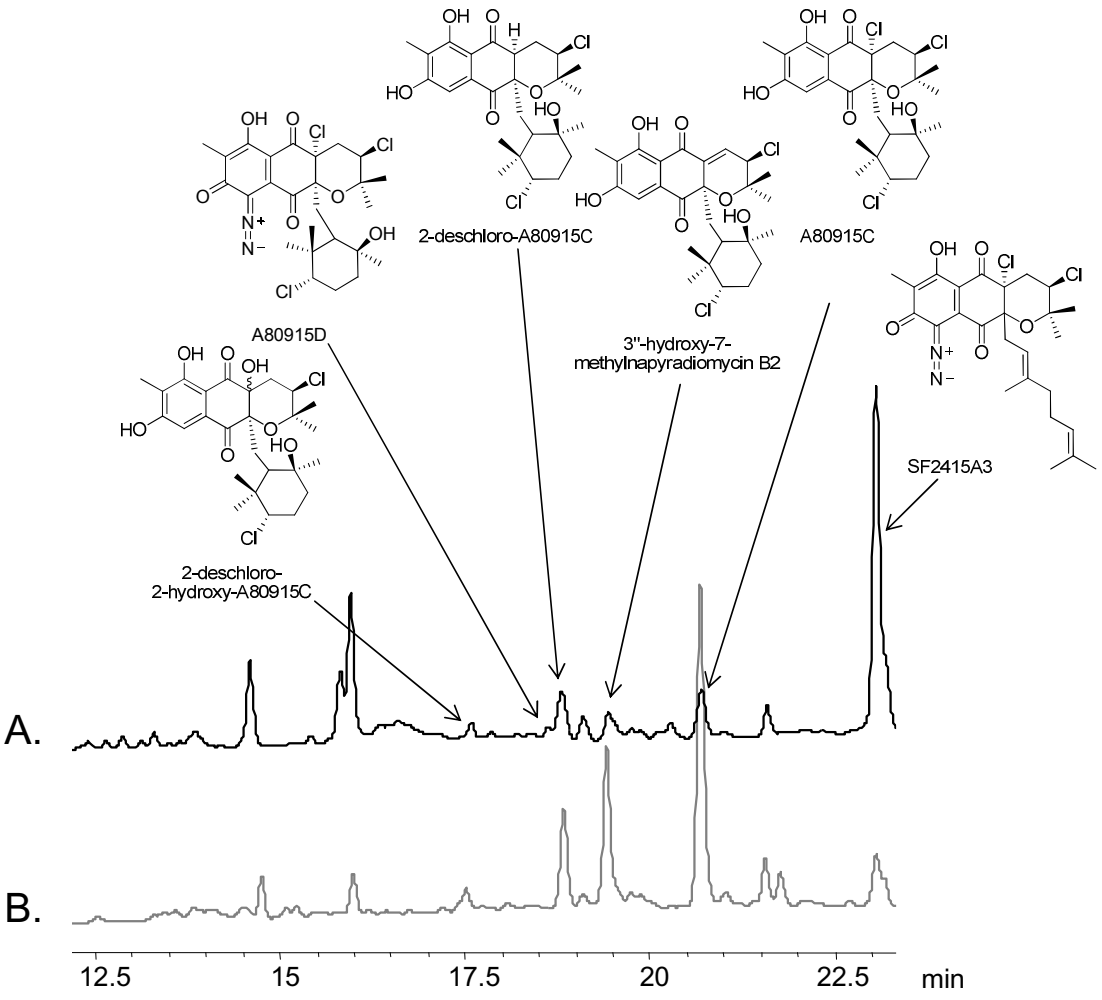

Figure 4.10: Chemical complementation of the *nap*H1^{-} mutant with [9-^{13}C]SF2415A3 restores production of the chlorinated dihydroquinones. A) LC-MS chromatogram of the napyradiomycin fraction of the *nap*H1^{-} mutant fed [9-^{13}C]SF2415A3. B) LC-MS chromatogram of the napyradiomycin fraction of wild-type *S.* sp. CNQ-525. UV light detection was carried out at 210 nm.

The diazo containing meroterpenoid SF2415A3 was able to restore production of the chlorinated dihydroquinones in the *nap*H1^{-} mutant, which supports the theory that either NapH3 or NapH4 from the *nap* cluster is responsible for the cyclization reaction of the monoterpene subunit via a chloronium ion (Scheme 4.1 and 4.2). HPLC-MS analysis of the chlorinated

dihydroquinone analogs and the diazonaphthoquinone A80915D showed a single enrichment without isotopic dilution indicating that SF2415A3 was biotransformed into these analogs (Scheme 4.1).[11] This restoration supports the hypothesis that NapH1 is responsible for the cyclization of the hemiterpene subunit via a chloronium ion giving rise to SF2415B3 (Scheme 4.2). However, inspection of the crude extract from the *nap*H1^{-} mutant did not yield any compound resembling SF2415B1 or any predicted monoprenylated precursors.

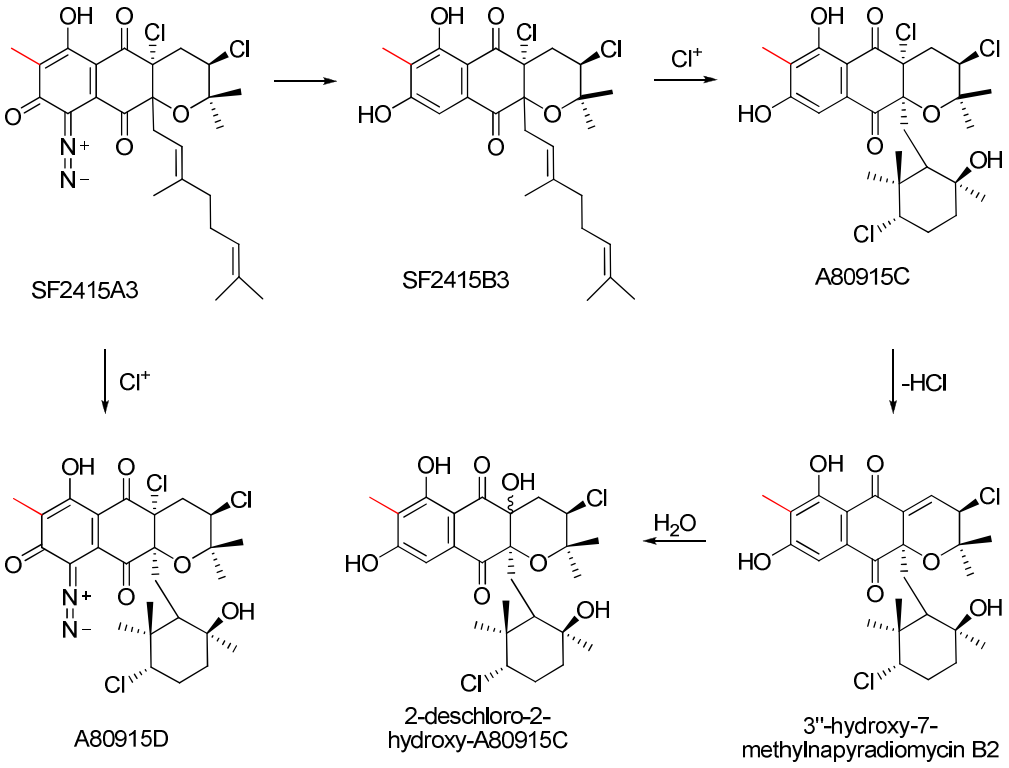

Scheme 4.1: Biotransformation of the diazomeroterpenoid SF2415A3 into A80915D and the related chlorinated dihydroquinones after loss of the diazo functional group. Isotopically labeled carbon atoms from [9-^{13}C]SF2415A3 are shown in red.

Scheme 4.2: Proposed biosynthetic pathway of the chlorinated dihydroquinones. NapH1 is highlighted in red.

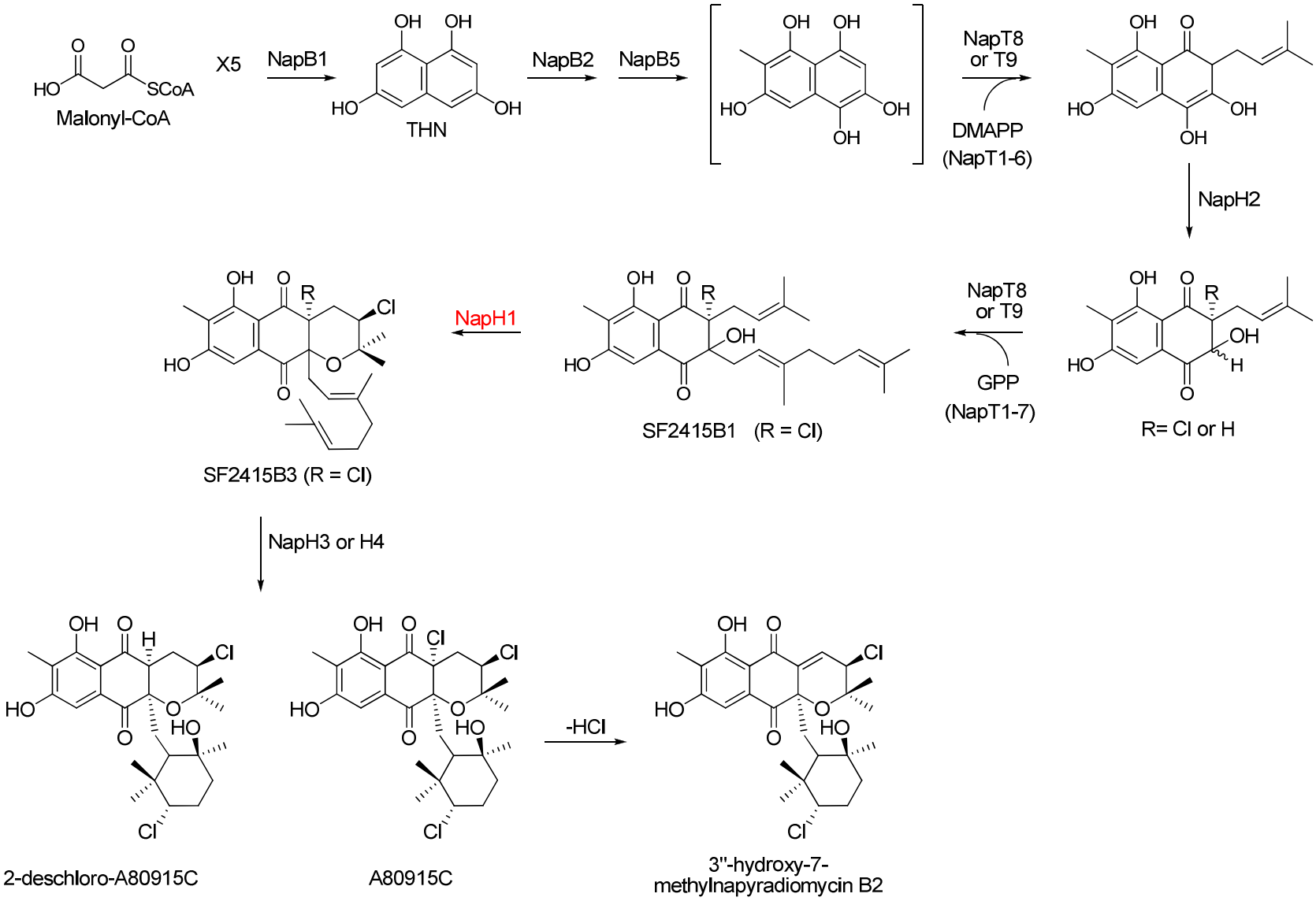
Malonyl-CoA
X5
NapB1
THN
NapB2
NapB5
NapT8
or T9
DMAPP
(NapT1-6)
NapH2
R= Cl or H
NapT8
or T9
GPP
(NapT1-7)
SF2415B1 (R = Cl)
NapH1
SF2415B3 (R = Cl)
NapH3 or H4
-HCl
2-deschloro-A80915C
A80915C
3''-hydroxy-7-
methylnapyradiomycin B2

4.4: Conclusion

V-HPOs have been identified in most branches of life, but have been characterized exclusively in eukaryotes. To date, V-BrPOs are the only characterized haloperoxidase that demonstrate the ability to facilitate bromonium ion induced cyclization of terpenes *in vitro.*[3] While this study established the likely role of V-BrPOs in the biosynthesis of brominated cyclic sesquiterpenes from marine red algae*,* conventional wisdom still suggests that V-HPOs lack substrate specificity and regioselectivity because the natural substrates and final products of these enzymes are unknown. Unfortunately, because all characterized V-HPOs have been identified from fungi and marine algae, their biosynthetic roles *in vivo* have not been elucidated due to the inability to identify and isolate all of the corresponding genes required for the assembly of a natural product.

The 36-kb napyradiomycin biosynthetic cluster identified from the marine sediment-derived *Streptomyces* sp. CNQ-525, which produces a suite of chlorinated dihydroquinones, contained three putative genes coding for V-ClPOs. Successful heterologous expression of *nap* cluster in a surrogate host proved that all the genes required for the biosynthesis of the chlorinated dihydroquinones were contained in the cluster. Thus, the *nap* biosynthetic cluster provided a tractable system for exploring the role of V-HPOs *in vivo.*

Inactivation of the V-ClPO *nap*H1 was accomplished through homologous recombination by a single cross-over using the non-replicating *E. coli* plasmid

pKC1132. *nap*H1 inactivation completely abolished production of all chlorinated dihydroquinones produced by *S.* sp. CNQ-525 suggesting the enzymes early role in the biosynthesis of the napyradiomycin analogs. Production of di-cyclized chlorinated dihydroquinones A80915C, 2-deschloro-2-hydroxy-A80915C, 2-deschloro-A80915C, 3"-hydroxy-7-methylnapyradiomycin B2, and the diazomeroterpenoid A80915D were rescued after administering [9-^{13}C]SF2415A3 to the mutant. Based on this result, it is proposed that NapH1 catalyzes the cyclization of the hemiterpenoid subunit via a chloronium ion, which occurs early in the pathway, and a second V-ClPO from the *nap* biosynthetic cluster, perhaps NapH3 or NapH4, is responsible for the cyclization and halogenation of the monoterpene subunit.

The successful inactivation of the V-ClPO *nap*H1 from the napyradiomycin biosynthetic cluster represents the first time a V-HPO has been characterized *in vivo*. This study established the enzymes early role in the biosynthesis of the chlorinated dihydroquinones, in which it is purposed to catalyze the selective cyclization and chlorination of the hemiterpenoid subunit. To unequivocally confirm the biological function of NapH1, the *nap*H1^{-} mutant will be genetically complemented with the wild-type *nap*H1 V-ClPO gene to restore activity, and napyradiomycin precursors produced by the *nap*H1^{-} mutant will be used as substrates for *in vitro* characterization experiments with NapH1.

4.5: Appendix

Table 4A.1: Components of A1 agar.[5]

A1 agar	
Starch	10 g
Yeast Extract	4 g
Bacto-peptone	2 g
Agar	8 g
Natural sea water	1 L

4.6: References

1. Renirie, R.; Hemrika, W.; Wever, R., Peroxidase and phosphatase activity of active-site mutants of vanadium chloroperoxidase from the fungus *Curvularia inaequalis*. Implications for the catalytic mechanisms. *J. Biol. Chem.* **2000,** 275, 11650-7.

2. Littlechild, J.; Garcia-Rodriguez, E.; Dalby, A.; Isupov, M., Structural and functional comparisons between vanadium haloperoxidase and acid phosphatase enzymes. *J. Mol. Recognit.* **2002,** 15, 291-6.

3. Butler, A.; Carter-Franklin, J. N., The role of vanadium bromoperoxidase in the biosynthesis of halogenated marine natural products. *Nat. Prod. Rep.* **2004,** 21, 180-8.

4. Winter, J. M.; Moffitt, M. C.; Zazopoulos, E.; McAlpine, J. B.; Dorrestein, P. C.; Moore, B. S., Molecular basis for chloronium-mediated meroterpene cyclization: cloning, sequencing, and heterologous expression of the napyradiomycin biosynthetic gene cluster. *J. Biol. Chem.* **2007,** 282, 16362-8.

5. Soria-Mercado, I. E.; Prieto-Davo, A.; Jensen, P. R.; Fenical, W., Antibiotic terpenoid chloro-dihydroquinones from a new marine actinomycete. *J. Nat. Prod.* **2005,** 68, 904-10.

6. Sambrook, J.; Fritsch, E. F.; Maniatis, T., *Molecular Cloning, a Laboratory Manual,* 2nd ed.; Cold spring Harbor Laboratory: Cold Spring Harbor, NY, 1989.

7. Altschul, S. F.; Gish, W.; Miller, W.; Myers, E. W.; Lipman, D. J., Basic local alignment search tool. *J. Mol. Biol.* **1990,** 215, 403-10.

8. Gust, B.; Challis, G. L.; Fowler, K.; Kieser, T.; Chater, K. F., PCR-targeted *Streptomyces* gene replacement identifies a protein domain needed for biosynthesis of the sesquiterpene soil odor geosmin. *Proc. Natl. Acad. Sci. USA* **2003,** 100, 1541-6.

9. Bierman, M.; Logan, R.; O'Brien, K.; Seno, E. T.; Rao, R. N.; Schoner, B. E., Plasmid cloning vectors for the conjugal transfer of DNA from *Escherichia coli* to *Streptomyces* spp. *Gene* **1992,** 116, 43-9.

10. Kieser, T.; Bibb, M. J.; Buttner, M. J.; Chater, K. F.; Hopwood, D. A., *Practical Streptomyces Genetics*. The John Innes Foundation: Norwich, 2000.

11. Biemann, K., *Mass Spectrometry: Organic Chemical Applications*. McGraw-Hill: Ney York, 1962; Vol. 2.

Conclusion

Many biologically active natural products that benefit human health are chlorinated, and it is now known that the introduction of a chlorine atom into one or more specific positions of a molecule may substantially improve, or be required for, biological activity. Although synthetic chemistry has been successful at introducing halogen atoms into specific locations on molecules, the harsh conditions used to do so and the low yields of compounds can make this approach costly and environmentally unfriendly. For this reason, there is a great need for new efforts to introduce chlorine atoms into specific locations on existing molecules. One possible solution is using enzymes as biocatalysts. The advantage of this approach over traditional chemical synthesis is that biocatalysts are renewable and environmentally friendly. Therefore, the discovery and characterization of new halogenating enzymes is an important step in making these enzymes available as biocatalysts.

Recently, Professors William Fenical and Paul R. Jensen (University of California at San Diego) identified and characterized a phylogenetically distinct group of marine sediment-derived actinomycetes belonging to the group MAR4, which is related to the genus *Streptomyces*. Although hybrid isoprenoids are uncommon actinomycetes natural products, actinomycetes strains belonging to the MAR4 group predominantly produce hybrid isoprenoids, including prenylated pyrroles, prenylated phenazines, and meroterpenoids. In particular, *S.* spp. CNQ-525 and CNQ-766 are prolific producers of meroterpenoids, which include the family of chlorinated napyradiomycin analogs, the diazo chlorinated dihydroquinones, and the phthalazinone containing chlorinated meroterpenoid

azamerone. Structural inspection of these chlorinated meroterpenoids suggests that the biosynthetic cyclization of their terpenoid subunits is initiated via a chloronium ion. The vanadium-dependent haloperoxidases that are known to catalyze such reactions are distributed in fungi and marine algae and have yet to be characterized from bacteria. Therefore, understanding how the chlorinated meroterpenoids produced by *S.* spp. CNQ-525 and CNQ-766 are assembled will help facilitate the identification of unique biosynthetic enzymes with unique halogenating capabilities, which in turn can be used to generate new secondary metabolite diversity and enhance the inherent biological activity of natural products.

The MAR4 strain *S.* sp. CNQ-525 was used as a source for identifying novel halogenating enzymes. The cloning and sequence analysis of the 43-kb napyradiomycin biosynthetic cluster from *S. aculeolatus* NRRL and from the marine sediment-derived *S.* sp. CNQ-525 revealed 33 open reading frames, three of which putatively code for V-ClPOs. Heterologous expression of the *S.* sp. CNQ-525-based napyradiomycin biosynthetic cluster in the surrogate host *S. albus* produced at least seven napyradiomycins, including A80915C, 2-deschloro-A80915C, 3”-hydroxy-7-methylnapyradiomycin B2, and the newly elucidated analog 2-deschloro-2-hydroxy-A80915C. These data revealed the molecular basis behind the biosynthesis of these novel meroterpenoid natural products, and also resulted in the first identification of vanadium-dependent haloperoxidases from a prokaryote.

To date, V-BrPOs are the only characterized haloperoxidases that demonstrate the ability to facilitate bromonium ion induced cyclization of terpenes *in vitro*. While this study established the likely role of V-BrPOs in the biosynthesis of brominated cyclic sesquiterpenes from marine red algae, conventional wisdom still suggests that V-HPOs lack substrate specificity and regioselectivity because natural substrates and final products of these enzymes are unknown. Because all characterized V-HPOs have been identified from fungi and marine algae, their biosynthetic roles *in vivo* have not been elucidated due to the inability to identify and isolate all of the corresponding genes required for the assembly of a natural product. It is proposed that the three putative V-ClPOs from the napyradiomycin biosynthetic cluster catalyze the oxidative cyclization and chlorination of the terpenoid units associated with the napyradiomycin class of bacterial antibiotics in a manner reminiscent to the biochemically characterized V-BrPOs. Thus, the napyradiomycin biosynthetic cluster not only provides an opportunity to probe the *in vitro* biochemistry associated with the three *nap*-V-ClPOs, but also provides a tractable biological system for exploring the role of these enzymes *in vivo*.

Phylogenetic analysis of the three napyradiomycin-based V-ClPOs with characterized V-ClPOs, V-BrPOs and bacterial non-specific acid phosphatases revealed that the enzymes form clades based on proposed enzymatic function. The three putative V-ClPOs from the bacterium *S.* sp. CNQ-525 do not cluster with the fungal or other postulated bacterial-derived V-ClPOs, which is consistent with their proposed role in natural product biosynthesis in contrast to other known

V-ClPOs. Inspection of the amino acid residues in the active sites of the V-HPOs suggests that NapH3 may not be directly involved in the chlorination and cyclization of the terpene units and may instead act as a hydroxylase. Structural and functional comparisons of V-HPOS from eukaryotic organisms have shown that six amino acids are required for halogenating activity. All three *nap*-V-ClPOs enzymes contain His-496 (which covalently binds to the vanadate co-factor) and five of the six residues that participate in hydrogen bonding, Lys-353, Arg-360, Ser-402, Gly-403, and Arg-490. Conserved residue His-404, which is proposed to form a hydrogen bond to the apical oxygen of the co-factor, is replaced with Ser (as seen in NapH1 and NapH4) or Phe (as in NapH3). Mutagenesis studies have shown that the V-ClPO mutant H404A from *C. inaequalis* loses chlorinating activity, and a similar natural exchange is observed in NapH3. Hence, NapH3 may not be involved in halogenation but rather may be used to hydrate aliphatic carbons. NapH1 and NapH4, on the other hand, contain a hydrophilic Ser residue at this position and are therefore predicted to catalyze the chloronium-induced cyclization of the two terpene units.

The successful expression of soluble NapH1 and NapH3 represented the first time a V-ClPO was expressed from a marine organism and the first time a V-HPO was expressed from a prokaryote. It is proposed that the V-ClPOs from the napyradiomycin biosynthetic cluster are responsible for the natural product chemistry associated with the napyradiomycin class of antibiotics, and both recombinant NapH1 and NapH3 exhibited halogenating activity in the monochlorodimedone assay, which is an assay used to detect haloperoxidases

from fungi and algae. Because recombinant NapH3 demonstrated halogenating activity in the monochlorodimedone assay, it is predicted that His-404 may not be required for halogenating activity in the bacterial V-ClPOs. However, a three-dimensional structure of a bacterial V-ClPO would shed light on which active site residues are required for halogenating activity, and the crystallization of NapH1 represents the first time a V-HPO from a prokaryote has been crystallized. Unfortunately, molecular replacement was unsuccessful at solving the three-dimensional structure of NapH1. Therefore, isomorphous replacement will be used to solve the structure of NapH1 and heavy atom derivatives are being constructed by soaking the crystals and/or co-crystallizing NapH1 with mercury acetate, mercury chloride, sodium tungstate dehydrate, and ammonium tetrathiotungstate.

In addition to probing the *in vitro* biochemistry associated with the *nap*-V-ClPOs, the napyradiomycin biosynthetic cluster also provides a tractable biological system for exploring the role of these enzymes *in vivo*. Inactivation of the V-ClPO *nap*H1 was accomplished through homologous recombination by a single cross-over using a non-replicating *E. coli* plasmid and represents the first time a V-HPO has been characterized *in vivo*. Inactivation of *nap*H1 completely abolished production of all chlorinated dihydroquinones produced by *S.* sp. CNQ-525 suggesting the enzymes early role in the biosynthesis of the napyradiomycin analogs. Administering biosynthetically prepared [9-^{13}C]SF2415A3 to the mutant restored production of the di-cyclized chlorinated dihydroquinones A80915C, 2-deschloro-2-hydroxy-A80915C, 2-deschloro-A80915C, 3”-hydroxy-7-

methylnapyradiomycin B2, and the diazomeroterpenoid A80915D. Based on this result and the activity observed in the monochlorodimedone assay, it is proposed that NapH1 catalyzes the cyclization of the hemiterpenoid subunit via a chloronium ion, which occurs early in the pathway. To unequivocally confirm the biological function of NapH1, the *nap*H1^{-} mutant will be genetically complemented with the wild-type *nap*H1 V-ClPO gene to restore activity, and napyradiomycin precursors produced by the *nap*H1^{-} mutant will be identified and used as substrates for *in vitro* characterization experiments. Completely characterizing NapH1 is an important step in making this enzyme available as a biochemical catalyst.

Given the structural novelty of azamerone and its relation to the chlorinated meroterpenoids, a variety of feeding experiments with ^{13}C- and ^{15}N-labeled molecules were used to explore the formation of its phthalazinone core. From the ^{15}N enrichment studies, it was established that *S.* sp. CNQ-766 contains unique enzymes capable of assimilating both oxidized and reduced forms of nitrogen into natural products. Results from the ^{15}N enrichment studies also confirmed that the diazo group in the diazomeroterpenoids SF2415A3 and A80915D was derived from the sequential addition of two nitrogen atoms. The ^{15}N labeling studies indirectly supported that the diazo group, such as those in SF2415A3 and A80915D, is a biosynthetic precursor to the pyridazine unit in azamerone based on their similar isotope characteristics. To unequivocally link the aryl diazoketones to azamerone, [2-^{15}N, 9-^{13}C]SF2415A3 was biosynthetically prepared and administered to *S.* sp. CNQ-766. HPLC-MS

analysis and NMR spectroscopy indicated that SF2415A3 was converted into A80915D and azamerone, and the diazo N2 atom in SF2415A3 is biosynthetically equivalent with N2 of the pyridazine group in azamerone. These stable isotope experiments link azamerone to the napyradiomycin family of chlorinated meroterpenoids. The aryl diazoketone undergoes a novel rearrangement wherein the aromatic ring is oxidatively cleaved to allow for its rearomatization with a dinitrogen group to give the unique phthalazinone core of azamerone. The unprecedented nitrogen biochemistry observed in *S.* sp. CNQ-766 extends the limited knowledge of the biosynthesis of natural products containing N–N bonds and opens the door to exploring and exploiting its molecular basis at the biochemical and genetic levels.